Bioprocess Intensification: Production of α-amylase by immobilised *Bacillus subtilis* in porous polymeric PolyHIPE

A thesis submitted to the Newcastle University for the degree of Doctor of Philosophy by

Dzun Noraini Jimat

School of Chemical Engineering and Advanced Materials
Newcastle University

Author's Declaration

This thesis is submitted in fulfilment of the requirements for the degree of Doctor of Philosophy at University of Newcastle, United Kingdom. All the studies described within are solely my work unless expressly stated otherwise, and were undertaken at the School of Chemical Engineering and Advanced Materials under the guidance and supervision of Professor Galip Akay and Prof Colin R. Harwood between November 2006 and December 2010.

I certify that none of the material offered in this thesis has been previously submitted for a degree or any other qualification at the above or any other university or institute.

Neither the author nor the University of Newcastle upon Tyne accepts any liability for the contents of this document.

Abstract

The microcellular polymer known as polyHIPE polymer (PHP), with modified physico-chemical characteristics, was developed as a cell matrix for the immobilization of the starch-degrading bacterium, *Bacillus subtilis*. Initially, a suspension of *B. subtilis spores* were inoculated *in situ* into a synthesized PHP matrix which had pore and interconnect sizes of 20μm and 5μm respectively. These inoculated spores were activated by supplying continuously well-aerated culture medium (LB medium) and placed in a 37^0C room for 24h incubation. On many occasions the PHP emulsions failed to polymerize in the presence of the spores and, when they did, the germination frequency of the spores was low. Since, the *in situ* entrapment of spores into synthesized PHP was unsuccessful, the immobilization technique was changed to the adsorption of spores onto the PHP matrix. This was performed by forced-flow inoculation of a suspension of pre-germinated spores onto PHP matrices sealed in a PTFE microchamber. Culture medium was pumped continuously through the matrix at a flow rate of 1.0ml/min for 24h and samples collected at various time intervals for the determination of the number of cells released from the PHP matrix and for α-amylase productivity.

Two different of chemically structured of PHPs were used; vinyl-pyridine PHP (TVP) and sulphonated PHPs (SPHPs). The growth and enzyme productivity data were evaluated and compared. Three different pore and interconnect sizes of SPHPs were evaluated; 42.0±0.61μm, 36.0±0.50μm and 30.0±0.64 μm. The collected samples obtained from the 24h cultivation were used to determine α-amylase productivity and the loss of cells from the matrices. The data showed that sulphonated PHP had a better performance as a cell matrix compared to vinyl-pyridine PHP.

The morphology, viability and proliferation of the immobilized cells on PHP matrices were observed by scanning electron microscopy (SEM). The SPHP with a pore size of 36.0μm performed better with respect to the production of α-amylase and the penetration of cells through the whole matrix compared to other SPHPs. Consequently, this matrix was selected and three different concentrations of LB medium (0.5x, 0.75x and 2x) and three different concentrations of cell loading (2 x 10^8/ml, 2 x 10^7/ml and 2 x 10^6/ml) were used to establish the

relationships between yield, cell numbers, cell loading concentrations and media concentration. These results were compared with planktonic batch cell culture.

The data showed that the total productivity of α-amylase enzyme produced by immobilized cells (on the basis of SPHP volume) was 7.6-fold higher than the planktonic batch culture. However, if productivity was determined on the basis of total volume of nutrient medium used, that of the immobilised cells was relatively low compared to planktonic batch culture. The effect of increasing the concentration of individual components of LB medium (tryptone /NaCl/ yeast extract) on the productivity of α-amylase and loss of cells from the matrices was also evaluated. Results showed that medium with double the yeast extract (D7) had the most significant impact on α-amylase production by *B. subtilis* cells for both systems; immobilized cells and planktonic batch cell culture. The overall yield of α-amylase by immobilized cell cultures was relatively low (<1) compared to planktonic batch cultures. However, the work from this thesis shows that the developed SPHP matrix could be used as a cell matrix but further studies are required to improve its productivity with respect to enzyme production.

Acknowledgment

I would like to express my sincere appreciation especially to Professor Colin R Harwood for his supervision, support, advice and in-depth knowledge in guiding and helping me during my studies. His encourgement and kind words really helped me to go through hard times along my studies. I am also thankful to Professor Galip Akay for his supports and advice as well as to Professor Alan Ward for his lessons and assistance in my project.

My gratitude goes to my officemates, Rozita, Hasni, Steve and especially Salwanis for being good colleagues for sharing their knowledge, experiences as well as moral support. Thanks are also due to the academic and support staff at the department, especially all the technicians for their help in the laboratory.

Thanks are also due to my sponsors: Ministry of Higher Education, Malaysia and International Islamic University Malaysia (IIUM) for their financial support.

My full gratitude is also dedicated to my beloved husband, Mohd Khairizal Mahat and my lovely son, Zuhair Luqman for their love, patience and understanding. I wholeheartedly would like to express my thankfulness to my parents, Zakiah Hj Abd Aziz and Jimat Hassan and my family in-law for their sacrifice and encouragement, without them it is impossible for me to finish my studies.

Abbreviation

AFM	atomic force microscopy
AIBN	azobisisobutyronitrile
AIBN	α,α'-azoisobutyronitrile
BA	butyl acrylate
BET	Brunaeur, Emmet and Teller (BET)
BATH	bacterial cell adhesion to hydrocarbon
CB	chlorobenzene
CDW	cell dry weight
CEB	2-chloroethylbenzene
CMC	sodium carboxylmethyl cellulose
D_f	OD_{440nm} of aqueous phase
D_i	OD_{440nm} of initial bacterial suspension
DNA	deoxyribonucleic acid
DPA	dipicolinic acid
DSM	Difco sporulation medium
DVB	divinylbenzene
2-EHA	2-ethyl hexyl acrylate
EHMA	methacrylate
FTIR	Fourier transform-infrared spectroscopy
GRAS	Generally Recognized as Safe
HIPE	high internal phase emulsion
HLB	hydrophilic-lipophilic-balance
IBA	isobornyl acrylate
IPTG	isopropyl-β-D-thiogalactosidase
LB	Luria-Bertani
LTA	lipoteichoic acid
O/W	oil in water
W/O	water in oil
PBS	phosphate buffered saline
PEG	polyethylene glycol

PEO	polyethylene oxide (PEO)
PGA	poly(glycolide)
PLA	poly(lactic acid)
PHP	polyHIPE polymer
PIM	process intensification-miniaturization
PU	polyurethanes
SASP	acid-soluble spore proteins
SEM	scanning electron microscopy
SPAN 80	sorbitan monooleate
THF	tetrahydrofuron
TVP-PHPs	vinylpyridine polyHIPE polymers
VBC	4-vinylbenzyl chloride
4-VBC	4-vinylbenzyl chloride
2-VP	2-vinyl pyridine
W_f	final weight of PHPs
W_i	initial weight of PHPs

Nomenclature

d	interconnect size (μm)
D	pore sizes (μm)
D_0	diameter of the batch mixer
D_1	diameter of the impellers
R_D	dosing rate (min^{-1})
R_M	mixing rate (min^{-1})
t	total mixing time (min.)
t_D	dosing time (min.)
td	doubling time
t_H	homogenization time (min.)
V_0	volume of the oil phase
V_A	volume of aqueous phase
σ^B	sigma factor
Φ	internal phase volume ratio
Ω	rotational speed of the impellers
μ	specific growth rate (h^{-1})

List of figures

Chapter 1

Chapter 2

Chapter 3

Chapter 4

Chapter 5

Chapter 6

Chapter 7

Chapter 8

Chapter 9

List of tables

Chapter 1

Chapter 2

Chapter 3

Chapter 5

Chapter 6

Chapter 8

Chapter 9

Introduction

Enzymes are biological products that can act as catalysts. Owing to their specific, effective and versatile features, they tend to exhibit much higher reaction rates as compared to reactions catalyzed by chemical catalysts. They can be categorized into three sections of industrial applications: technical enzymes, food enzymes and animal feed enzymes. The enzymes used in the food processing industry currently represent approximately 20% of the enzyme market. Additionally, the sales of enzyme for the baking industry have increased in recent years due to the demand for healthier baked goods. On the other hand, the technical enzymes which including hydrolytic enzymes such as proteases and amylases, are mainly used for detergent, textiles and pulp and paper. These hydrolases are also used in the processing of starch materials from crops such as corn, wheat, potato and tapioca, breaking down this polymer into short-chain polymeric carbohydrates. Enzymes are also used in the biodegradation of agricultural waste (e.g. straw), containing of lignocellulose, into shorter metabolizable intermediates. Lignocellulosic materials are composed of cellulose, hemicellulose, pectin and lignin which can be degraded by many enzymes such as cellulases, xylanases and pectinases. Moreover, the degradation of these biomass wastes by enzymes produces simple sugars that can be used in industrial fermentors to generate biofuels such as ethanol and biogas. The production of biofuel through this route provides an alternative to fossil-based fuels, but can only compete if improved enzymes and strains are used to increase the cost-effectiveness of the processes. Enzymes are also used for the production of fine chemicals such as amino acids (e.g. hydroxyproline), sweeteners (e.g. aspartame) and non-natural monosaccharides (e.g. L-ribose and L-xylose). The use of recombinant organisms in the production of industrial enzymes has improved the capacity to produce huge amounts of enzymes with the desired activities. Additionally, the emergence of technologies to engineer enzymes has led to the development of enzymes with high specificity and rates. As a result, microbial enzymes are used as biocatalyst in a great variety of manufacturing processes, including processes that were originally driven by chemical catalysts. The global

enzyme market is expected to reach $2.7 billion by 2012 (reported by Business Communication Co. Research, Jan. 2008). Moreover, reactions catalyzed by biocatalysts can be carried out under mild conditions and are significantly less polluting than chemical catalysts, which often involve the use of harsh and hazardous conditions. Reactions catalyzed by chemical are more likely to produce unwanted products or toxic by-products due to their lack of specificity and that can subsequently lead to poor product yields and increased waste disposal costs. Biocatalysts may not require specially designed equipment and control systems, which are expensive both to manufacture and run.

One of the world's largest industrial enzyme producers is Novozymes (Denmark), which is involved in the development, production and distribution of microbial enzymes. These enzymes are produced from genetically modified microorganisms, indicating that microbial fermentation is the major route for the production of industrial enzymes. There is a need to explore novel processes that could improve the production systems to meet the anticipated increased demand for industrial enzymes. Currently, the production of enzymes is through conventional batch or fed-batch fermentation. This involves high capital and operating costs due to the continual start up and shut down nature of such processes. Moreover, this system involves the routine batch process of "fill and shut" which can lead to culture contamination and the need for long fermentation times. On the other hand, the use of continuous culture processes have the potential to reduce operating costs and energy requirements as it allows the almost complete utilisation of expensive substrates. However, continuous cultures have the limitations of maintaining high cell concentrations in the bioreactor and in some cases this is associated with low volumetric productivities and requires even longer fermentation times. They can also lead to genetic instabilities among the strains being used.

The application of immobilized cell technology can improve bioreactor productivity by maintaining high cell concentrations as well as operational stability. Additionally, immobilized cell technology can reduce processing time and down-stream processing as it can act as a biomass separator. The selection of the materials used for the matrices is of the utmost importance because it determines their characteristics. Currently, most of the support matrices used for cell immobilisation are derived from natural sources such as alginate,

carrageenan, gelatine and chitosan. These natural matrices lack mechanical rigidity and stability and are therefore prone to damage during long processing conditions. This is due to the impact of rapidly growing colonies on the outer surface of the matrix and subsequently leads to the release of cells into the medium. Additionally, the concentration of cells in the interior of these matrices is inconsistent because some treatments allow significant numbers of cells to escape. This means that more cells are observed growing on the outer surface rather than migrating deeper into the matrix. As a result, the efficiency of immobilization is compromised, affecting the final output of the bioreactor. The main factor that causes these problems is the limited mass transfer rates for nutrients, products or waste to and from the immobilized matrix. Thus there is a need to improve the characteristics of the immobilized matrices used as cell supports. The matrix of the immobilized cell support must be porous enough to provide easy access for nutrients and waste but to retain most or all of the bacteria. In this study, a polymeric material known as polyHIPE polymer (PHP) was used to immobilise the starch-degrading bacterium, *Bacillus subtilis*. This polyHIPE matrix is synthesized through the high internal phase (HIPE) route and its physico-chemical properties can be modified as desired. This type of polymeric matrix has a highly interconnected porous structure and is mechanically durable in the presence of harsh conditions such as high temperature, pH and toxic chemicals. Therefore, it can be sterilized and used for long-operating conditions without significant physical or chemical degradation.

The microstructure of the matrix with respect to its physico-chemical characteristics, which include appropriate pore and interconnect sizes as well as surface chemistry (i.e. hydrophobic, hydrophilic), are very important with respect to the flow of nutrients and waste material and also for cell migration. The polyHIPE matrix used in this study was chemically modified and located in a PTFE chamber where it performed like a miniature monolith microreactor. Such a system has been used for the *in vitro* growth of osteoblast-like cells in which the polyHIPE matrix was able to promote cell growth, maturation and bone-like tissue production (Akay *et al*., 2004, Bokhari *et al*., 2005). Similar observations have been made for *Pseudomonas syringae,* a phenol degrading bacterium immobilized on the monolithic form of PHP (Akay *et al*., 2005d, Akay *et al*., 2005a).

In the current study a polyHIPE matrix was sealed in a PTFE chamber, inoculated with a strain of *Bacillus subtilis* and supplied with a nutrient medium that was continuously aerated to provide both the required nutrients and sufficient oxygen. The impact of the matrix on the characteristics and behaviour of the immobilized cells was determined with respect to growth, viability, proliferation and metabolic activity. The results showed that the behavior of the immobilized cells was dependent on the microenvironment provided by the supporting matrix.

The used of a polyHIPE polymer matrix in the developed system was designed to improve the production of α-amylase by *B. subtilis*. The confined microenvironment was designed to promote the growth and metabolic activity of this bacterium. Moreover, the applied forced-flow seeding technique yielded a more uniform distribution of cells within the polymeric support, which also helps to improve nutrient transport. This also prevents significant growth of cells around the outer surface of matrix, which often restricts mass transfer into the interior area of the matrix. Adjusting the porosity of the polyHIPE matrix helps to retain the producer cells without any clogging the matrix, as is often reported in previous studies (Akay *et al*., 2005a, Erhan *et al*., 2004). As a resulting intensified microreactor system is developed is partly due to a reduction in mass transfer restrictions, and partly due to the miniaturization of the bioreactor. Thus, the developed system has implemented the process intensification-miniaturization (PIM), which is an essential approach for a design strategy in biotechnology industry. The implementation of this approach may offer several advantages over conventional systems, such as a reduction of process volume, invention of novel product, reduction of energy, capital and operating cost and a platform for other technologies. This approach is essential in the area of bioprocess development specifically for microbial fermentations which are laborious and typically performed in expensive, complex apparatus. The results of these studies may provide a platform for developing microreactors with sufficient mass transfer capacities, to complete with traditional fermentors.

1 PolyHIPE polymers (PHPs)

1.1 Introduction

PolyHIPE polymers (PHPs) are micro-porous materials of different chemical compositions (see Section 1.1.2) that are generated via high internal phase emulsions (HIPE). Polymerization via HIPE results in the dispersion of a large internal (or dispersed) phase volume in a continuous (or monomer) phase. The internal phase volume ratio (Φ) is designed to be 0.74 or greater, but can, if necessary, exceed 0.99. Several types of polyHIPE-based materials have been developed including a number of biocompatible polymers (Busby *et al*., 2001, Busby *et al*., 2002, Hayman *et al*., 2004, Hayman *et al*., 2005, Bokhari *et al*., 2003, Bokhari *et al*., 2005, Akay *et al*., 2004, Barbetta *et al*., 2005b, Christenson *et al*., 2007, Krajnc *et al*., 2005, Stefanec and Krajnc, 2005), crystallisable side-chain polymers (Livshin and Silverstein, 2007, Livshin and Silverstein, 2008a, Livshin and Silverstein, 2008b), hydrogel (using oil in water HIPE) (Gitli and Silverstein, 2008, Kulygin and Silverstein, 2007), copolymers (Sergienko *et al*., 2002, Sergienko *et al*., 2004), interpenetrating polymer networks (IPNs) (Tai *et al*., 2001), organic-inorganic hybrids (Silverstein *et al*., 2005, Tai *et al*., 2001) and composites (Normatov and Silverstein, 2007, Haibach et al., 2006, Menner *et al*., 2006a, Menner *et al*., 2006b). The main definable physical parameters of these polymers are their average pore sizes (D), interconnect sizes (d) and the distribution of pores and the total surface area of the matrix. Each of these physical parameters can be controlled through the phase compositions, processing conditions (e.g. dosing and mixing time), and emulsification temperature. Furthermore, it is also possible to modify the chemical and mechanical properties of the generic polymers, as and when required. The physical and chemical characteristics of the PHPs strongly influence their efficiency as a support material.

The most extensively studied polyHIPE polymer material, polystyrene-divinylbenzene polyHIPE polymer, was originally discovered by researchers at Unilever. This porous polymeric material can be generated with smaller and more

highly interconnected pores than conventional gas-blown polystyrene foams. The pore sizes of this PHP can range from 5 to 100μm, depending on the operational conditions used in its preparation. On the other hand, larger pores (above ~ 200μm) can be obtained through the coalescence polymerization route (Akay *et al*., 2005a, Akay *et al*., 2005b). Because it can be used as a porous polymer monolith support, polystyrene-divinylbenzene can replace classical bead-based polymer supports prepared by suspension polymerization. Monolith supports have the advantage of retaining porosity and do not compress significantly at high liquid flow rates.

1.1.1 Composition of PolyHIPE polymers (PHPs)

PolyHIPE polymers are composed of a continuous phase containing monomer(s), cross-linking agent, surfactant, an aqueous phase with water-phase soluble polymerization initiator and in some cases, an oil-phase soluble polymerization initiator. Commonly, the oil phase comprises 78% monomer (styrene), 14% surfactant (Span 80 or sorbitan monooleate) and 8% crosslinking agent (divinyl benzene). In some cases, 1% of an oil soluble initiator, (lauroyl peroxide) is included, in which case the percentage of styrene is decreased to 77%. The aqueous phase initiator is 1% potassium persulfate (Williams *et al*., 1990) and the PHP produced by this initiator is 50% stiffer than that produced by the oil initiator. The produced polyHIPE polymers can have a rigid physical structure, however, the addition of 2-ethyl hexyl acrylate (2-EHA) to the emulsion, can produce an elastomeric polymer. Figure 1.1 shows the polymerization reaction between styrene and divinylbenzene.

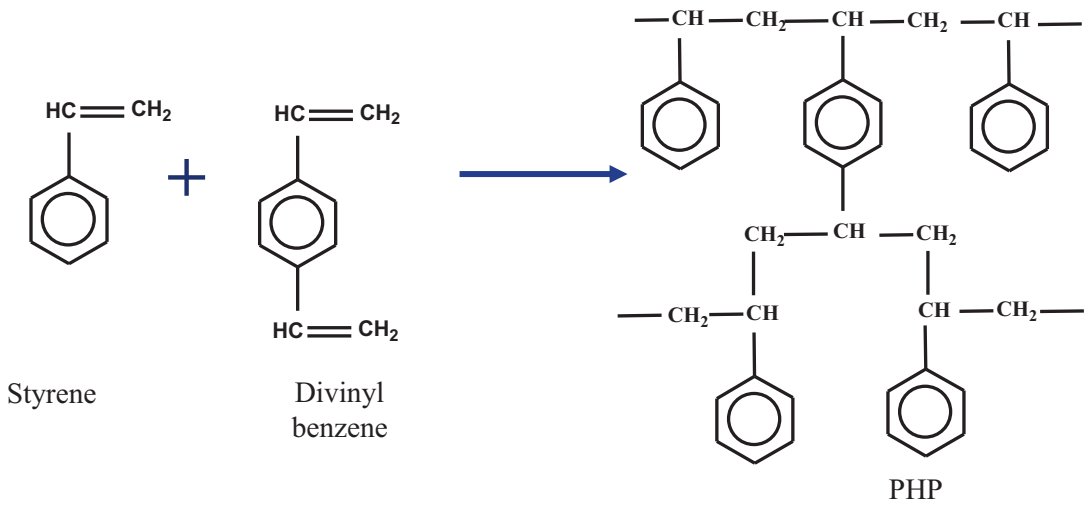

Figure 1.1: Polymerization reaction between styrene and divinylbenzene, producing the rigid form of PHP

In the production of PHP, styrene is used as a monomer in water-in-oil (w/o) HIPE and it is immiscible with water. Other researchers have attempted to use other hydrophobic monomers, such as 2-ethylhexyl acrylate methacrylate (EHMA), butyl acrylate (BA) or isobornyl acrylate (IBA), to alter the physical or chemical characteristics of PHP.

A cross-linking agent such as divinyl benzene (DVB) is required in the manufacture of PHP as without it the polymer structure would collapse. Furthermore, its absence would limit the polymer structure from swelling when it is exposed to solvents that dissolve the linear non-cross-linked polymer. Previous studies have shown that increasing the DVB content decreases the pore size (Williams *et al*., 1990). Replacing DVB with 4-vinylbenzyl chloride (VBC) results in a lower interfacial tension and a more stable emulsion (Barbetta *et al*., 2005a).

One or more surfactants are required to stabilize the structure of the polymers. The most useful approach to selecting surfactants is to apply the hydrophilic-lipophilic-balance (HLB) concept (Kirk-Othmer, 2007). HLB confers a measure of the relative hydrophobicity of a non-ionic on a scale ranging from 0 (very hydrophobic) to 20 (very hydrophilic). Surfactants with a high HLB number are used as oil-in-water (O/W) emulsifiers because they have more active hydrophilic groups. Surfactants with a low HLB number are used as water-in-oil (W/O) emulsifiers as they have more active lyphophilic groups and are oil soluble. For O/W emulsions, the HLB range is 8-18, whereas for the W/O

emulsions, the range is 3 – 6 (Kirk-Othmer, 2007). The surfactants used in styrene/divinylbenzene W/O emulsions having values ranging from 2 to 6. Span 80 (also known as sorbitan monooleate), used as surfactant and emulsifier in the production of PHP, is a non-ionic surfactant with a HLB value of 4.3.

The appropriate amount of surfactant in an emulsion is important as it determines the microstructures of the PHP. Increasing the surfactant concentration increases the interconnect size until, at surfactant concentration of 80% content, the polymer collapses due to the disappearance of the connected monolithic material. This is likely to be due to the retraction of the thin oil layer that separates the individual droplets in the emulsion (Williams *et al*., 1990). Therefore, surfactant concentration influences the polymer morphology as a result of its effect on the thickness of the film separating emulsion droplets (Cameron, 2005). The thinner separation films also produce larger interconnecting holes between voids (Carnachan *et al*., 2006).

The surfactant molecules form a separate phase at the interface region between the polymerizing monomer and the internal aqueous phase of the HIPE and do not become part of the polymer chain itself. The tail group of the surfactant (monooleate) is hydrophobic while the head group (sorbitan ring) is hydrophilic (Figure 1.2). The tail groups of surfactant molecules that are opposite each other (Figure 1.3a) sterically attract each other and agglomerate into a separate phase (Figure 1.3b). Any excess surfactant that does not occupy a place at the interface exists as micellular droplets in the oil phase and therefore will also become part of the separate surfactant phase. The agglomerated surfactant molecules form areas in the external phase that exclude the polymerized material; once the surfactant is removed, these areas become the pores between the cells. However, if too great a surfactant concentration is used, the surfactant agglomerates begin to attach to each other, breaking up the wall-like structure and causing the collapse of the PHP (Bhumgara, 1995b).

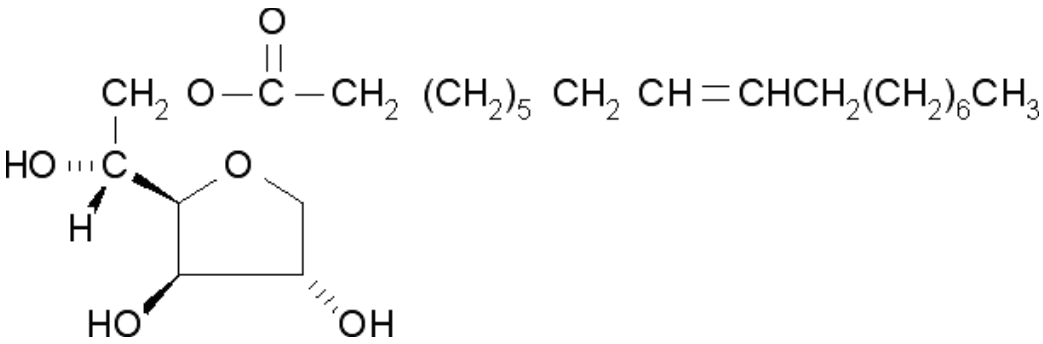

Figure 1.2: Chemical structure of Span 80 (sorbitan monooleate)

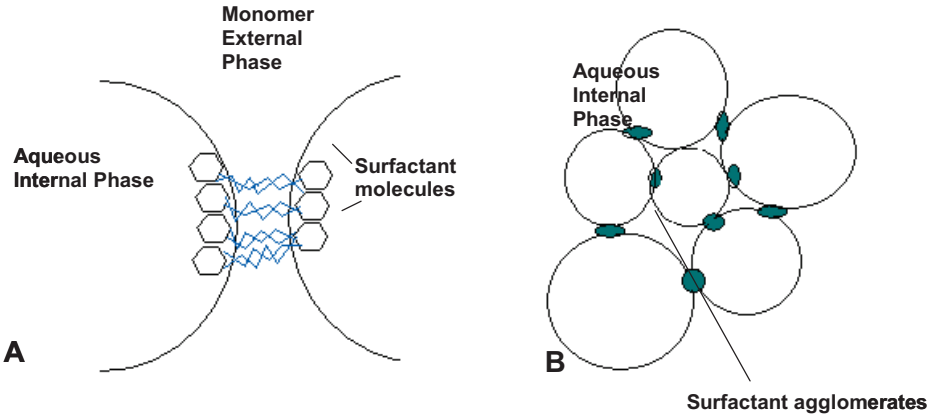

Figure 1.3: Schematic diagram of the formation of pores in PHP by the surfactant molecules (Adapted from (Bhumgara, 1995b))

1.1.2 Preparation of high-internal-phase emulsions (HIPE)

High internal phase emulsions (HIPE) lead to the deformation of the spheroidal droplets in the dispersed phase of the emulsion into polyhedra, resulting in a network of thin films that surround these droplets (Figure 1.4). Inversion of the emulsion may occur if the optimal HIPE stability is not achieved, leading to the formation of a layer of liquid above or below the foam and, in severe cases, the disappearance of the foam.

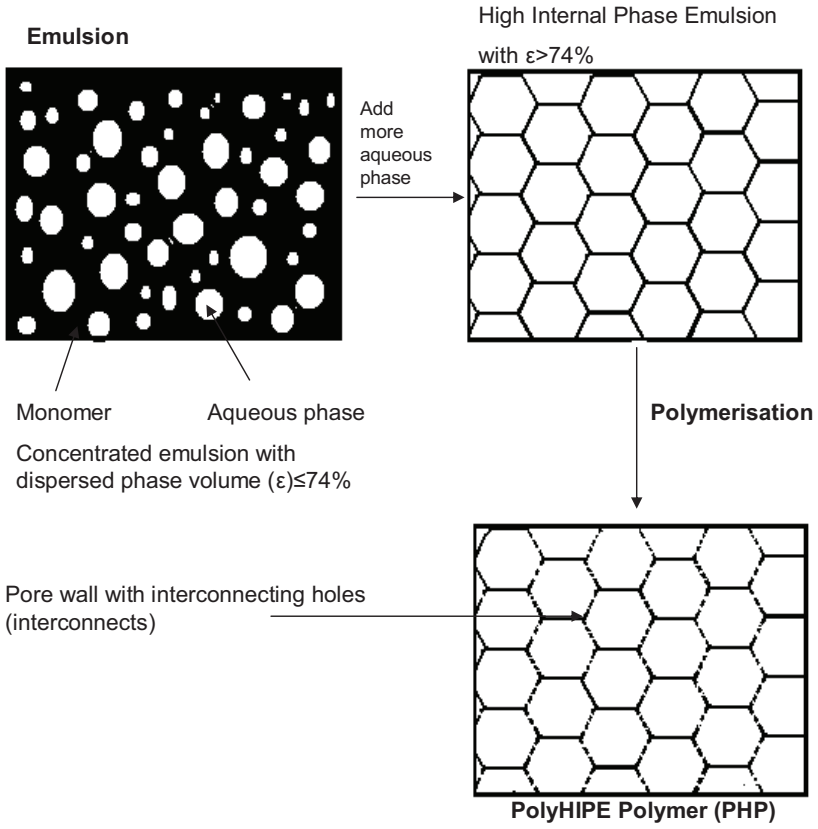

Figure 1.4: Schematic diagram of PHP formation (Adapted from (Byron, 2000))

There are two stages involved in the preparation of PolyHIPE. The first stage involves the preparation of emulsion; the dosing of the dispersed (aqueous) phase (consisting of distilled water with initiator) into the continuous phase (containing monomer, crosslinker and surfactant) (Figure 1.5), followed by the mixing stage.

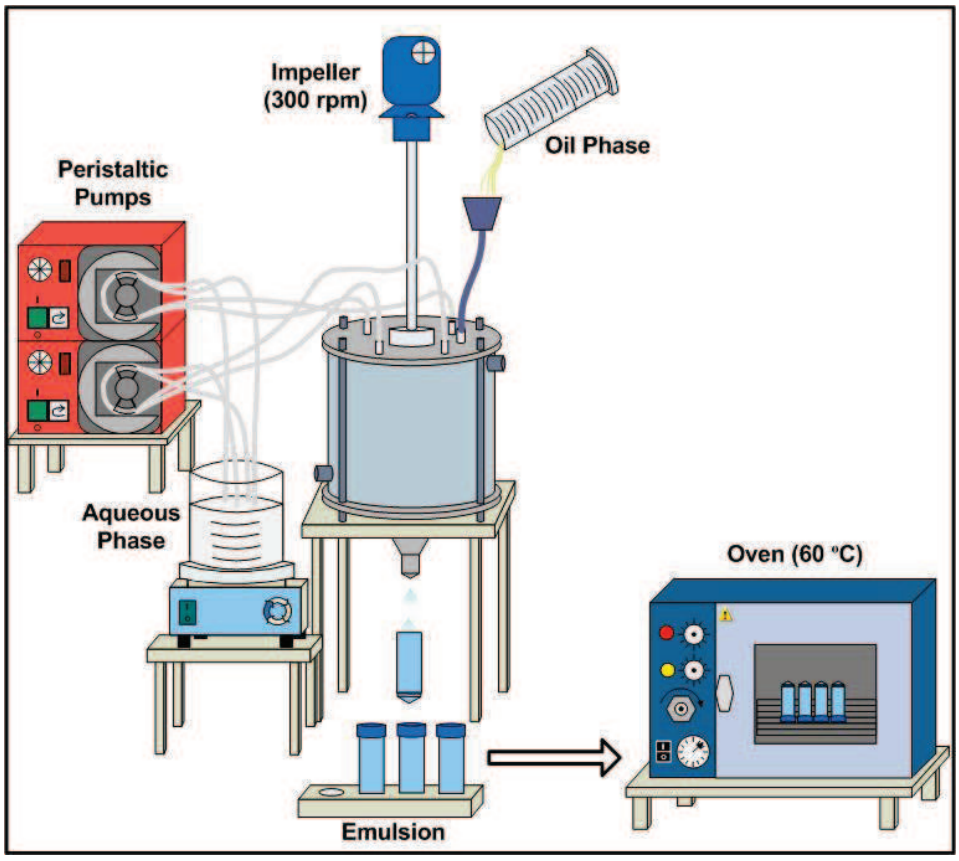

Figure 1.5*:* Schematic diagram of the equipment and process for the production of polyHIPE polymer.

Once the dosing process is completed, the second stage involves reducing the size of the aqueous phase droplets to both reduce the pore size of the resulting polymer and to improve the pore size distribution. This is achieved by prolonging the mixing. Finally, the prepared emulsion is transferred to plastic containers with an internal diameter 2.8cm, and polymerized at 60^0C for at least 8 hours. Finally, the polymer is washed extensively to eliminate residue chemicals. Under these conditions the phase volume ranges from 80% to 95%.

1.1.2.1 Operating variables of preparation PolyHIPE polymer

There are several operating variables that can be varied in order to modulate the properties of the PHP. These include mixing time, dosing rate and emulsification temperature.

Dosing rate. The population of pore diameters is more uniform when the dosing rate is high. When the dosing rate is slow, a smaller average droplet diameter is obtained due to the need for a substantially longer mixing time. If the dosing rate is very high and the mixing rate is low, the HIPE does not form, but a dilute (low) internal oil-in-water emulsion is obtained (Akay *et al*., 2005b). The following equation is used to determine the dosing rate of the aqueous phase.

$$R_D = \frac{V_A}{t_D V_o} \qquad \text{Equation 1.1}$$

where V_A is the volume of aqueous phase added over a period of time, t_D, and V_0 is the volume of the oil phase placed in the batch mixer.

Mixing time. The size of the pores within the PHP can be reduced by extending the mixing phase, as this results in the breakdown of droplets. Mixing inputs energy to the droplets, allowing them to exist at a higher energy state which, in turn, results in the formation of smaller droplets. The average pore diameter is similar for different void fraction. However, when the void volume increases, the size and the number of interconnecting holes increase as well. As the volume of the dispersed phase increases the continuous phase preferentially occupies the position of lowest energy, namely in the voids between droplets, leaving a thinner layer between the droplets. On polymerization, the oil phase contracts producing interconnecting holes. The thinner the initial layer the larger the interconnecting hole. The equation below is used to define the total mixing time *t* as follows:

$$t = t_D + t_M \qquad \text{Equation 1.2}$$

where t_M is the mixing time.

The mixing rate is represented by the following:

$$R_M = \frac{D_1}{D_0}\Omega \qquad \text{Equation 1.3}$$

where D_0 is the diameter of the batch mixer, D_1 is the diameter of the impellers and Ω is the rotational speed of the impellers.

It has been reported that with increased mixing time, there is a reduction in water cavity size and an increase in the number of windows resulting in a more open micro-structure size (Walsh *et al*., 1996). However, continuous mixing would result in the droplets coalescing and this would reduce the stability of the emulsion and, ultimately, increase the pore size.

*Emulsification temperature***.** Large pores within the PHPs can be obtained by increasing the temperature (Figure 1.6b) and this provides another means for controlling the pore size, especially when large pores are required. Several techniques are available to control the interconnect size (d) (Akay *et al*., 2002b).

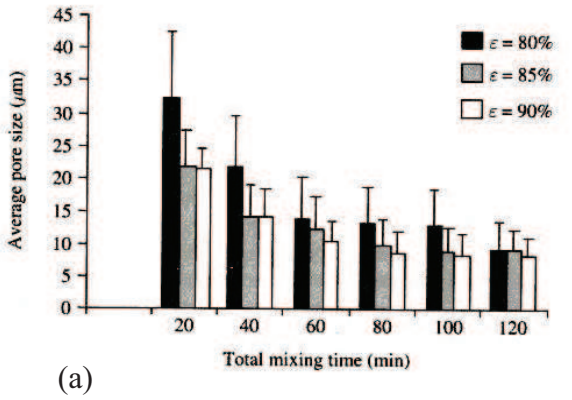

(a)

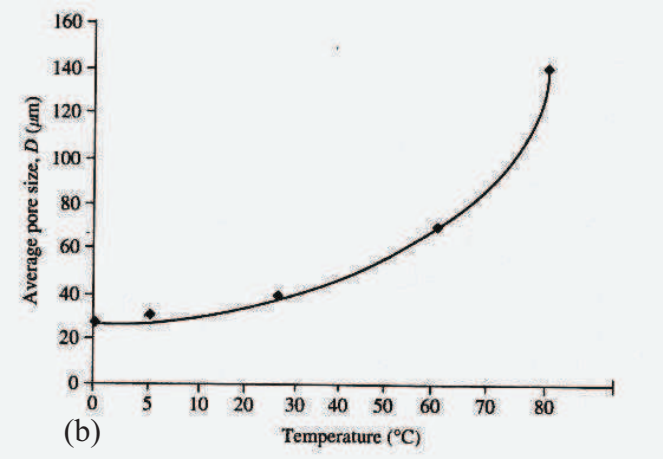

(b)

Figure 1.6 (a) Variation of average pore size (D) with total mixing time (t) as a function of dispersed phase volume fraction (ε). Dosing time = 10 min, impeller speed Ω = 300 rpm, emulsification temperature T = 25ºC. Pore size is determined from scanning electron micrographs of the polymers (b) Variation of average pore size with emulsification temperature when dosing time = 40 s, total mixing time = 100 s, impeller speed = 300rpm, phase volume = 90 % (Akay, 2005).

1.1.3 Morphology of PolyHIPE polymer

Williams and colleagues observed that the cellular structure and morphology of the polyHIPE polymer is highly dependent on the concentrations of surfactant and salt used in the polymerization reaction (Williams *et al*., 1990). Initially, they identified that the cellular nature of PHP was influenced by the internal phase volume ratio (Φ). Previous studies have shown that a closed-cell styrene/DVB polyHIPE polymer could be generated with a phase volume (Φ) of 97% by employing a relatively low concentration of surfactant relative to monomer phase. In addition, increasing the DVB: styrene ratio in a styrene/DVB

HIPE from 0% to 100% DVB, yielded a small but significant decrease in average pore diameter, from 15 to 5μm (Williams *et al*., 1990). The resulting increased emulsion stability causes a smaller average droplet size due, presumably, to a lower interfacial tension, which allows a larger interfacial area. Furthermore, they also showed a 10-fold reduction of pore size when the K_2SO_4 concentration in the aqueous solution was increased up to 10g/100ml (with azobisisobutyronitrile (AIBN) used as initiator and inclusion of 5% DVB in the oil phase).

A larger PHP average pore and interconnect size can be obtained by increasing the aqueous phase temperature prior to emulsification (Carnachan *et al*., 2006). This is from droplet coalescence with increased droplet collision and/or surfactant solubility in the organic phase. The presence of additives or co-solvents in the aqueous phase can also lead to a PHP with a higher average pore and interconnect size. The greatest effect was seen when tetrahydrofuron (THF), polyethylene glycol (PEG) and methanol were used as additives. The pore structures observed in PHPs are illustrated in Figure 1.7.

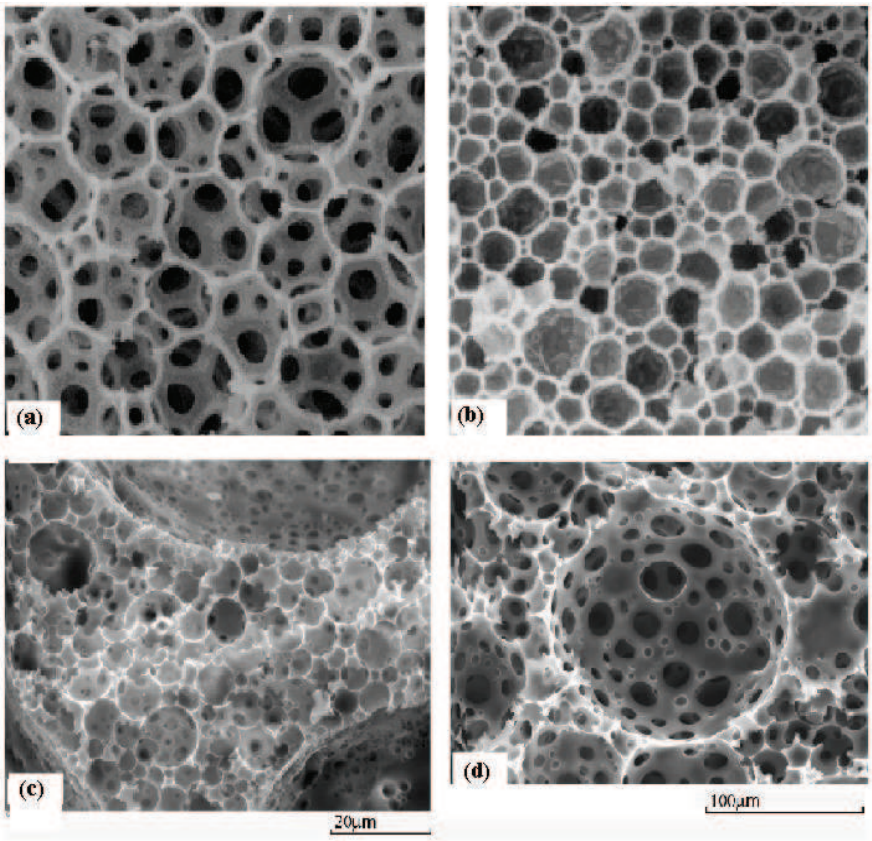

Figure 1.7: Basic polyHIPE polymer structures: (a) primary pores with large interconnecting holes; (b) primary pores with nano-sized interconnecting holes: (c) large coalescence pores (three such pores are partially shown) dispersed into the primary pores in the process of coalescence ; and (d) detail of the coalescence pores (Akay et al., 2005b).

1.1.4 Properties of PolyHIPE polymer

The properties of PolyHIPE polymers can be modified before or after they are prepared. PHP usually has less than 5 m^2/g of BET surface area, as reported in previous studies (Cameron and Sherrington, 1996). Other studies reported that the surface areas of PHP are within the range of 3 – 30m^2/g and they have significantly higher porosity (Hainey *et al.*, 1991). However, the inclusion of a porogenic solvent into the monomeric oil phase of the concentrated emulsion, can lead to a much higher surface area. The surface area can be increased up to 350m^2/g by altering the oil composition of the PHP.

Typically, a clean dry PHP material has a Young's modulus of 11 MN/m^2 (Bhumgara, 1995b). Other studies found that polymers with thin-film cell wall structures have the maximum crush strength and Young's modulus, unlike for

those polymers with completely closed cells, thick walls or have struts (Williams and Wrobleski, 1988). These authors observed that the stiffest, most crush-resistant polymers at any density were obtained from an emulsion with an optimal amount of surfactant. Other studies showed reinforcing the polymer phase with nano-sized silica particles could dramatically increase the Young's modulus and the crush strength of PHPs (Haibach *et al*., 2006). Nevertheless, the surface areas (ranges from 3.6 to 7.6m^2/g) and the pores size (ranges from 3 to 30μm) of these specific materials are similar to those of typical PHP.

1.1.5 Chemical modification of PHPs

It has been shown that functionalization by chemical modification can change the characteristics of PHP. This can be achieved by modifying the chemical composition of the aqueous and/or oil phases or by chemical treatment following the polymerization stage. In respect of first approach, the addition of co-monomers such as 2-vinyl pyridine (C_7H_7N) into the oil phase of PHP can enhance the hydrophilicity of the resulting PHP. This is due to the presence of pyridinic nitrogen atoms that may hydrogen bond with styrene groups. The poly-2-vinylpyridine is preferentially exposed to the aqueous solution due to its polar nature and therefore the use of this chemical will alter the chemically structure of PHP which is normally dominated by the non-polar nature of polystyrene. Consequently, this chemical can be used to generate PHPs with improved hydrophilicity properties.

Initially, these generic microporous materials are hydrophobic, preferring to absorb oil-based liquids rather than aqueous ones through capillary action. However, chemical modification of this material, for example via sulphonation (Figure 1.8), can change its hydrophilicity. The amount of sulphonation is expressed as a percentage of available benzene rings (those associated with the styrene part of the polymer) producing $–SO_3$ groups. Other agents, such as acetyl and lauroyl sulphate (Cameron *et al*., 1996), chlorosulfonic acid in chlorinated solvents (Chakravorty *et al*., 1989) and acetyl sulphate (Thaler, 1983) can also be used to change the surface properties of the polymer.

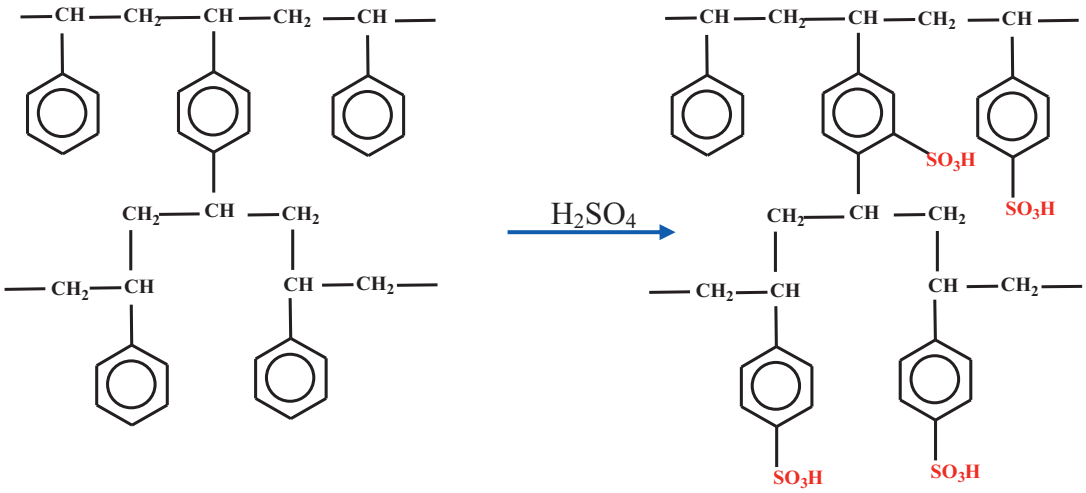

Figure 1.8: Chemical modification of PHP via sulphonation

The sulphonation treatment of PHP was discovered by Unilever researchers (Haq, 1985) who described two different methods of sulphonation. Firstly, the washed PHPs discs were soaking in various concentrations of sulphuric acid (25%, 50%, 75% and 98%) at room temperature for a set period. Following treatment, the sulphuric acid is removed from the samples by washing with water and dried at 40^{O}C. The second method involved the treatment of dried PHPs discs with 98% sulphuric acid at 95^{0}C. Again, the rate of sulphonation depends on the length of the treatment. After treatment, the PHPs samples are washed to remove the excess acid and then dried at 80^{0}C.

In the current study, the chemical modification of PHPs via sulphonation was carried out using methods developed by Akay and co-workers (Akay *et al*., 2005c). In the first method, sulphuric acid is added to the aqueous phase during the preparation of the PHP. Following polymerisation, PHP discs are incubated in a pre-heated oven (40^{0}C) for various lengths of time for sulphonation to take place. The rate of sulphonation increases with increasing temperature as well as with the concentration of the acid within the polymer pores. The amount of sulphuric acid added into the aqueous phase can be varied from 10 to 25% wt./vol. In the second method, the PHPs discs are dried overnight in an oven before soaking in concentrated sulphuric acid for 3 hours. Drying the PHPs prior to sulphonation treatment may help to increase the rate of sulphuric acid

migration within the PHPs. Following incubation, the PHPs samples are microwaved in a 1 kW microwave oven for 30 seconds, repeated five times, in a fume cupboard. The PHPs samples are then washed with deionized water and neutralized with ammonium hydroxide. Finally, the discs are dried overnight in a fume cupboard and washed using the Soxhlet system. The degree of hydrophilicity of the PHPs is dependant on the sulphonation conditions. In the current study the second method was used as the microwave treatment increases the overall efficiency of the sulphonation process as well as reducing the processing time. It should be noted, however, that when the degree of sulphonation is too high, the polymer can break into pieces due to the internal stress caused by the intensive thermal treatment and the swelling of the polymer as it absorbs water.

1.1.6 Application of PHP as an immobilized cell matrix or tissue cell scaffold

The styrene monomer used in the manufacture of PHPs is toxic to cells. However, once it is polymerized it becomes non-toxic. Table 1.1 shows a list of studies that have employed micro-porous polyHIPE polymers and the other types of polyHIPE that have been used as immobilized microbial cell matrices or as a scaffolds for tissue cells.

Table 1.1: Studies that used porous polymeric polyHIPE as matrices for immobilized cells or scaffold for tissue cells

	Organism/Tissue cells culture	Characteristics of PHP	Observations	References
Hydroxyapatite-modified polystyrene-DVB PHP	Osteoblastic cells	Pore size (D): 40 -100μm Interconnect size (d): 15 – 30 μm Surface area: 4.8 – 8.6 m^2/g	Capable of supporting in vitro growth and maturation of osteoblast-like cells over a period of 35 days	(Akay *et al*., 2004)
Hydroxyapatite-modified polystyrene-DVB PHP with incorporated RAD16-I peptide hydrogel	Osteoblastic cells	Pore size (D): 100μm Void volume: 95%	Significantly increased the osteoblast activity and bone formation in vitro compared to hydroxyapatite modified Polystyrene-DVB alone	(Bokhari *et al*., 2005)
Polystyrene-DVB PHP (in a fixed-bed column bioreactor)	*Pseudomonas syringae,* phenol-degrading bacterium	Void volume: 85%	Biofilm formation on the surface of the support particle after 120 days of continuous operation	(Erhan *et al*., 2004)
Polystyrene-DVB PHP coated with aqueous-based solutions including poly-D-lysine and laminin	Human stem-derived cells	Addition of around 1% (v/v) of tetrahydrofuran to the aqueous phase resulted in foams with void diameters in the range 50–100 μm	The seeded cell adhered, remained viable and showed significant cell differentiation within the interior section of the scaffold	(Hayman *et al*., 2005)

Polystyrene-DVB PHP (in monolith form)	*Pseudomonas syringae,* phenol-degrading bacterium	Pore size (D): 25-100μm Interconnect size (d): 5 – 20 μm Surface area: 6.2 m^2/g Void volume: 85% - 90%	Volumetric utilization rate of the developed system is achieved at least 20-fold more efficient than the packed bed depending on the flow rate of the substrate solution	(Akay *et al*., 2005d)
Dextran-based polyHIPE	Neural cell type derived from mouse primary retinal culture		Preliminary observation: the cells surrounding the scaffold maintain their morphology without showing modification or signs of cell damage	(Barbetta *et al*., 2005b)
Polystyrene-DVB PHP (in packed-bed reactor)	*Saccharomyces cerevisiae* for ethanol production from glucose	Void volume: 90%	The efficiency of reactor reached 83.69% when medium containing 50g/l glucose with a flow rate of 1ml/min	(Karagöz *et al*., 2009)
Polystyrene-DVB PHP	MG63 osteoblast-like cells	Void volume: 90% Sectioning porous polystyrene into 120μm thin membrane	The performance of cells on 3-D porous polystyrene was significantly enhanced compared to functional activity of cells grown on 2-D surface cultures	(Bokhari *et al*., 2007b)
Polystyrene-DVB PHP	HepG2 liver cells	Void volume: 90% Sectioning porous polystyrene into 120μm thin membrane	The 3-D porous polystyrene capable to support the cell growth up to 35 days, producing complex arrangements of cells interacting with one another	(Bokhari *et al*., 2007a)

In order to use PHPs as an immobilized cells matrix, the following characteristics need to be considered:

i) It must be porous enough to allow the accessibility of nutrients and oxygen to, and waste materials from, the cells in the immobilization system
ii) It must have a high surface area to provide sites for the attachment of cells
iii) It must be relatively homogeneous to ensure the even distribution of the cells within the system
iv) It must have appropriately sized pores and interconnects to avoid passage of cells across the material supports

These conditions not only ensure a permissive environment that promotes the viability, proliferation and functionality (metabolic activity) of living cells, but also help maintain their morphology and phenotype.

1.2 Cells immobilization

1.2.0 Introduction

The immobilization of the diverse types of microbial species in various bioprocesses that they are currently applied to (e.g. wastewater treatment, production of enzymes and solvents etc) has shown that this cultivation system offers a number of advantages over conventional free cells (planktonic) cultures. The advantages of this system include high cell concentrations and high productivity for metabolites and proteins, the maintenance of plasmid stability, the ease of biomass removal from the bulk liquid and a reduction in cell washout associated with high dilution rates. The careful selection of immobilization technique, as well as the matrix material used, is essential for ensuring the efficiency of the system and the minimalization of problems such as cell leakage and restricted substrate diffusion.

Cell immobilization can be defined as the physical confinement or localization of viable microbial cells to a defined region of space in such a way as to exhibit hydrodynamic characteristics which differ from those of the surrounding environment (Karel *et al*., 1985a). There are three components that can be differentiated in the immobilized cell systems, (Figure 1.9a). These are cells; the support which may be solid or a gel; and the solution that fills the remainder of the space in the aggregate (Karel *et al*., 1985a). On the other hand, the immobilized cells in the porous material can be illustrated as shown in Figure 1.9b.

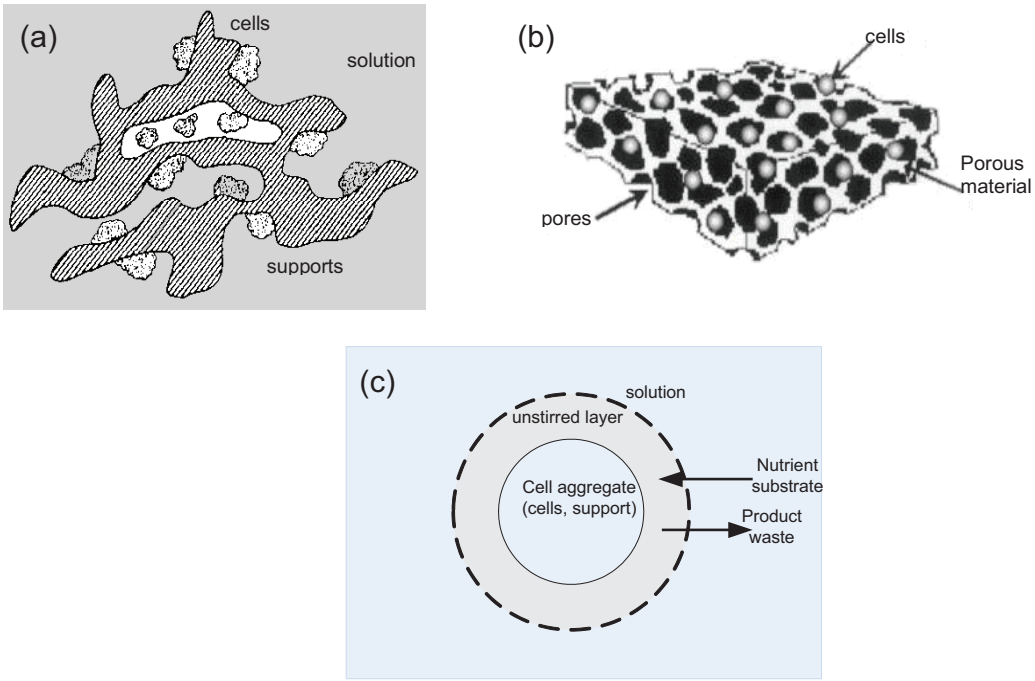

Figure 1.9 (a) The immobilized cell systems consists of three phases which are: cells, cell support, interstitial fluid (b) macroporous matrix with cells (Riddle and Mooney, 2004) and (c) an engineering representation of an immobilized cell system (Karel *et al*., 1985a).

The success of the immobilized cells system is dependent on the applied cell immobilization technique and as well as the immobilized matrix materials used. Since, a number of different techniques and immobilized matrix materials are available, the selection of the right combination is essential to ensure the efficiency exceeds that of conventional free-cell systems. This is also important for the subsequent implementation of this system to large-scale industrial level processes.

1.2.1 Methods of cells immobilisation

Cells immobilisation can be categorized into four major groups: (1) attachment to a surface, (2) entrapment within a porous matrix, (3) containment behind a barrier and (4) self-aggregation (Figure 1.10). However, this discussion will focus on the first two categories. The entrapment of cells within a porous matrix can be performed by two techniques. In the first the cells are allowed to migrate into the preformed porous matrix. These cells then become trapped as their movement is restricted as they begin to grow due to the presence of other cells in the matrix. In the second, the porous matrix is manufactured *in situ* around the cells to be immobilized (Karel *et al*., 1985a). In this case the cells are entrapped either in-gel type matrices such as alginate, κ-carrageenan and acrylamide or pre-formed porous matrices such as polyethylene terephthalate, polystyrene and polyurethane foam. The latter was used in this study in which micro-porous PHP was synthesized *in situ* with spore suspensions of *B. subtilis*.

Another method of cell entrapment, known as encapsulation, uses microspheres that are made from different types of polymer such as nylon, collodion, polystyrene, acrylate, polylysine-alginate hydrogel, cellulose acetate-ethyl cellulose and polyester membranes. Microspheres are hollow, spherical particles bound by semipermeable membranes or entrap the cell within them. This method has the advantage that more cells can be packed per unit volume of support material into capsules and intraparticle diffusion restrictions are slightly reduced due to the presence of liquid cell suspension in the intracapsule space (Shuler and Kargi, 2001). The selection of the appropriate polymer membranes, with different compositions and molecular size cutoffs, is crucial for the specific application. This is because the capsules will retain some high-MW products and serve only for the passage of low-MW nutrients and products.

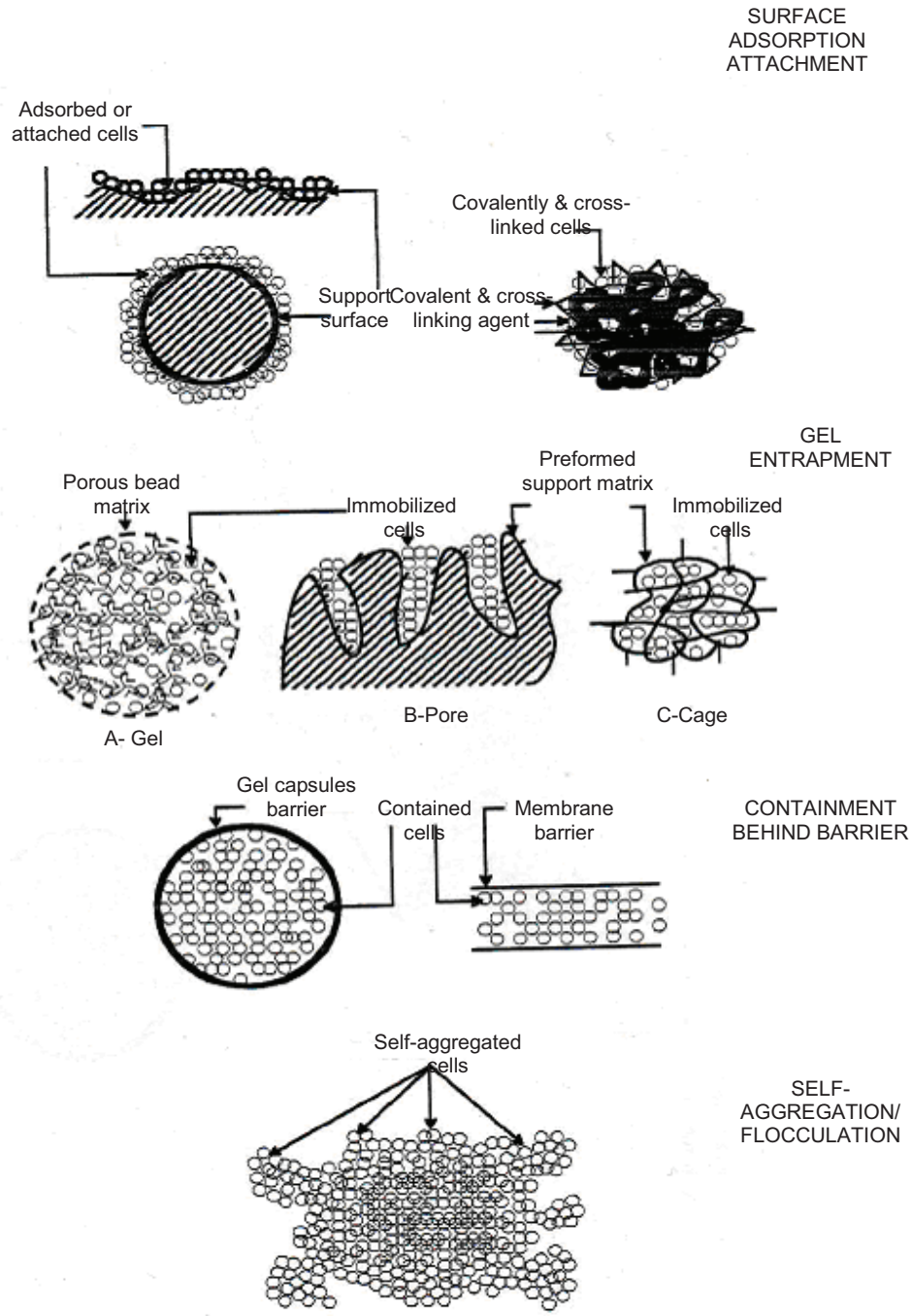

Figure 1.10: Basic immobilized cell systems which is categorized into four major groups (Adapted from (Dervakos and Webb, 1991)).

The cell immobilization by the attachment onto non-porous or porous solid matrix can be achieved by adsorption of cells to a matrix by electrostatic interactions, covalent bonding or using cross-linking agents. Naturally, the cells will be colonized on to any surface that is in contact with nutrient medium due to cell adsorption. However, these cells are easily detached from the surface due to high shear forces generated by the flow of fluids over the matrix. There are several factors that influence the adsorption of cells onto solid surfaces. They include the particle size, porosity, and charge of the type of matrix used. The physico-chemical of microorganism such as its surface charge or hydrophobic/hydrophilic ratio as well as environmental conditions (temperature, pH, fluid flow rate, composition) also affect to the adsorption of cell.

1.2.2 Characteristics of immobilized cells supports/matrices

Several factors need to be considered when selecting a suitable matrix for the immobilization of living cells. Firstly, porosity and pore size needs to be adequate to allow nutrients and wastes to pass into and out of the matrix, as well as allowing the cells to migrate throughout the matrix. The pores size distribution needs to be relatively homogeneous to allow individual cells to behave similarly within the entire population. Secondly, the matrix needs to be mechanically durable and resistant to other chemical substances as well as not reacting with substrates, nutrients or products. This is particularly important for long-term operational conditions. Thirdly, the matrix should have a high surface-to-volume area to provide space for cell attachment. Fourthly, the surface chemistry of matrix, whether hydrophilic, hydrophobic or ligand-complexed will determine the strength of the interaction between the immobilized cells and the matrix. All of these characteristics influence system performance with respect to product formation. Other matrix characteristics that are important are the ease of handling, lack of general toxicity, consistency and reasonable cost.

Previous studies have shown that the above characteristics do in fact influence the efficiency of immobilized cell systems. In respect to the matrix pore size, when osteoblast-like cells were grown in a polyHIPE matrix/scaffold, more cells were observed in the layers below the surface of the 40 μm pore-sized PHP

compared to both 60 and 100 μm (Akay *et al*., 2004). The authors also reported that the architecture of PHP appears to aid the inteaction of the osteoblasts with the surface and permit their migration. On the other hand, the largest pore sized polymer (100 μm) showed the most rapid cell penetration through the matrix, although they concluded that this was a more passive migration. Other studies showed that monolayers of *Pseudomonas syringae* cells were observed in a 25 μm pore-sized PHP without any apparent cell debris during a 30-day continuous experimental period compared in contrast to PHP with a 100 μm pore size (Akay *et al*., 2005d).

Natural polymer matrices such as alginate beads, carrageenan and gelatine are often not substantial enough for long-processes due to their low mechanical durability. These type of matrices were often damaged due to the pressure exerted by growing colonies closed to their surface and this leads to the released of cell into the medium. This has been observed in several studies, such as the immobilization of *B. subtilis* cells on polyacrylamide gels (Kokubu *et al*., 1978) and κ-carrageenan beads (Duran-Paramo et al., 2000).

Previous studies have shown that the production of α-amylase by membrane-immobilized cells was significantly affected by the type of reactive chemical groups used for immobilisation and the size of the spacer molecule (Dobreva *et al*., 1998). These authors found that the larger spaces between the membrane surface and the cells resulted in a decrease in α -amylase yield and operational stability. This was probably due to weak cell attachment, and this was confirmed by the higher numbers of released cells. Similar observations were made during a study of immobilization of *Pseudomonas syringae,* phenol-degrading bacteria on polyHIPE matrix. This study showed that the relatively high resistance to washout was due to the strong adhesion between the bacteria and the hydrophobic surface of the polyHIPE matrix (Erhan *et al*., 2004).

1.2.2.1 Materials used for making matrices

Various matrices are available for cell immobilization, made either from natural or synthetic polymers. The natural polymers include alginate or calcium alginate, carrageenan, gelatin, polyacrylamide and chitosan which are attractive because they are generally biocompatible and non-toxic. Additionally, they exhibit a broad range of physical properties that offer unique characteristics for cell encapsulation technologies (Riddle and Mooney, 2004). However, some natural polymers such as collagen are expensive due to high purification costs. Others, such as alginate and carrageenan are less-expensive. Nevertheless, natural polymers lack mechanical rigidity especially for long-run operating process and can be degraded by certain chemicals and enzymes. For example calcium alginate, is reported to loose its mechanical stability in the presence of phosphate used in culture medium. The loss of interactions between calcium and alginate subsequently causes the beads to swell. The stability of calcium alginate beads can be improved by coating with high molecular weight cationic polymers such as polyethyleneimine, although this treatment can inhibit the respiration of entrapped cells. On the other hand, synthetic polymers such as poly(glycolide) (PGA), poly(lactide) (PLA), polyanhydrides, poly(ethylene oxide) (PEO) and poly(ethylene glycol) (PEG) can be synthesized by ring opening polymerization, melt polycondensation or anionic or cationic polymerization of ethylene oxide. A degradable and hydrophilic polymer can be formed through co-polymerized PEG with poly(lactic acid) (PLA) and this modified polymer can be used as a hydrogel for cell immobilization. Hydrogels contains a high water content that, to some extent, resembles the environment that promotes the regeneration of tissues. Besides these polymers, the pre-formed porous polymer matrices such as polyurethanes (PU) and polyvinyl can be also used for cell immobilization. These matrices, which can be purchased from commercial suppliers (e.g. PPL Polyurethane Products Ltd. Retford, UK, Polymer Ltd., Cardiff, UK, Kanebo Kasei Co., Japan), are widely used as supports for a variety of living cell types. For example, the immobilization of *Dictyostelium discoideum* in a rotating polyurethane foam-bed reactor produced a high cell densities and is reported to improve its productivity of recombinant proteins (Wei *et al*., 2010).

1.2.3 Effect of initial cell loading and flow rate on the cell immobilization process

Mass transport of substrates and products in immobilized cells systems can be achieved by molecular diffusion as well as convection by suitable matrix design and appropriately applied external flow. This requires the cells to colonize the porous matrix while retaining some free space for the flow of liquids. However, in some cases, cells self-aggregate and are retained in dead-end pockets within the matrix material. This occurs when the cells do not adhered strongly to the matrix material and the applied external flow is high enough to reversibly remove them from the matrix. Therefore, an optimum flow rate is required to prevent these problems as well as to minimize the mass transfer limitations that frequently occur in immobilized cell systems.

The initial cell concentration used in an immobilization experiment can influence the overall performance of the system. A higher initial cell concentration can result in a lower retention rate and increased immobilization time (Baron and Willaert, 2004). While higher final cell counts can be obtained at higher cell loads, growth rate is often more rapid at lower initial cell loads (Mamo and Gessesse, 1997). The authors have suggested that the faster growth rate is the result of reduced competition. As the number of immobilized cells increases, the movement of free cells from interstitial spaces of matrix into the interior section of matrix is increasingly restricted. This can affect the product production rate, as shown in a previous study (Konsoula and Liakopoulou-Kyriakides, 2006). For example, the rate of α-amylase production increased two-fold when the cell content in the gel capsules increased from 0.32 to 1.92% (w/v) wet weight. However, no significant increase in the amylase yield was observed at higher initial biomass concentration.

The applied external fluid flow rate also influences the productivity of the system because of its role in the diffusive transport and distribution of substrates and products, and the stability of the immobilized cells. A slower rate of flow of fluid might make it difficult for cells to enter the interior of the porous matrix with the result that they colonize the outer surface of the matrix. Too low a rate of fluid flow rate can also lead to the clogging of the matrix pores as more cells are deposited on the top surface. A higher flow rate may enhance intraparticle fluid

velocities, allowing cells to penetrate further into the matrix. In contrast, too high a fluid flow rate may cause the adsorbed cells to detach more easily. In conclusion, an appropriately applied external fluid flow rate is required to ensure the immobilization process is efficient.

1.2.4 Design of immobilized cell reactor

A good bioreactor configuration and appropriate selection of the bioreactor system is important for a productive fermentation. The choice of bioreactor configuration is dependent on the type of immobilization and it is important to determine the mass and oxygen transfer requirements in the selected system. However, optimum conditions such as agitation rate, pH and temperature also need to be considered. Table 1.2 shows a variety of reactor types that are distinguished according to the location of the cell aggregates: suspended particles, fixed particles and moving surfaces.

Table 1.2: Type of immobilized cell bioreactors (adapted from (Margaritis and Kilonzo, 2005))

Bioreactor type	Advantages	Disadvantages
Suspended particles		
Stirred tank reactor	Flexible, variable mixing intensity, suitable for high viscosity	High power consumption, shear damage to particle, high costs
Air/gas-lift/bubble column	No moving parts, simple, high solid fraction, high mass transfer, good heat transfer	Low local mixing intensity, only for low viscosities
Fluidised bed	No moving parts, simple, low cost, very high solids contents, good heat transfer, variable mixing for solids and liquid	Difficult matching of feed & fluidisation rates, requirements on particle density (dense support), good local mixing intensity, only for low viscosities
Fixed particles		
Fixed bed/monolith	Simple, low cost, plug flow characteristics possible, large surface to volume ratio	Plugging by solids at low flow rates, high pressure drop, channelling problems (often for fixed bed)
Membranes	Very high cell densities, very high productivities, perfusion operation, possible, simultaneous product separation possible, separate feed of gas and liquid, low shear	Sterilization problems, microbial damage, membrane perforation, low capacities only, high cost
Moving surfaces		
Rotating surface (disc, cylinder or packing)	Low shear on biofilm, batch or continuous, excellent aeration, high productivity	Power consumption

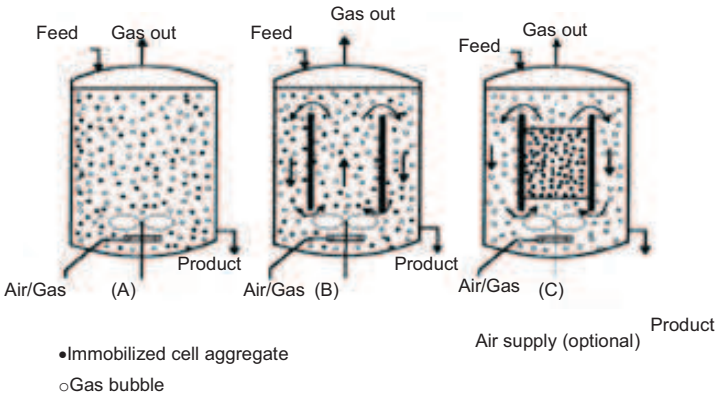

Figure 1.11: Stirred tank reactors: (A) simple tank reactor, (B) draf tube reactor, (C) packed draft tube tank reactor (Adapted from (Margaritis and Kilonzo, 2005))

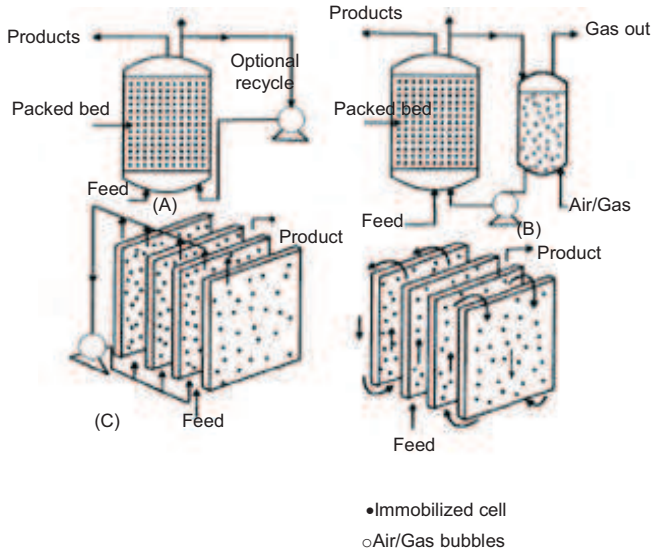

Figure 1.12: Packed and sheet reactors: (A) packed bed, (B) packed bed with external aeration, (C) sheet reactor with external circulation (Adapted from (Margaritis and Kilonzo, 2005))

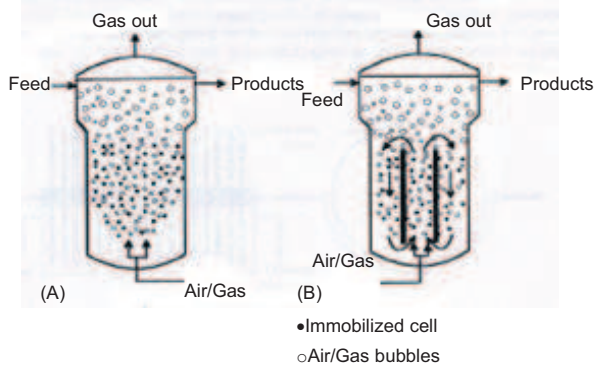

Figure 1.13: Bubble column and air/gas lift loop reactors: (A) bubble column, (B) air/gas lift loop reactor (Adapted from (Margaritis and Kilonzo, 2005))

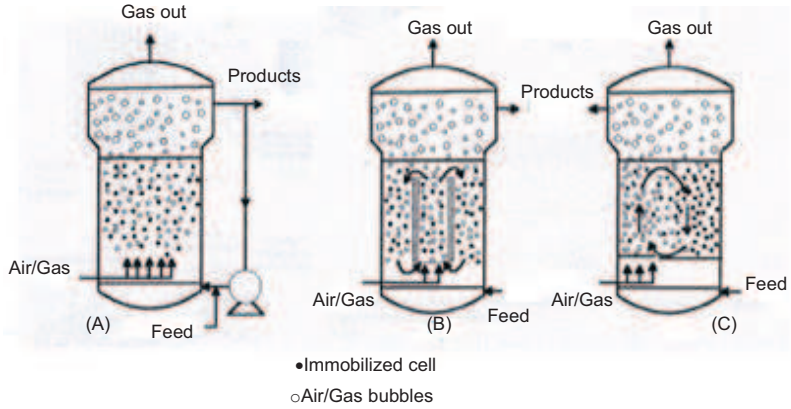

Figure 1.14: Fluidised bed reactors: (A) without draft tube, (B) with draft tube, (C) circulating bed (Adapted from (Margaritis and Kilonzo, 2005))

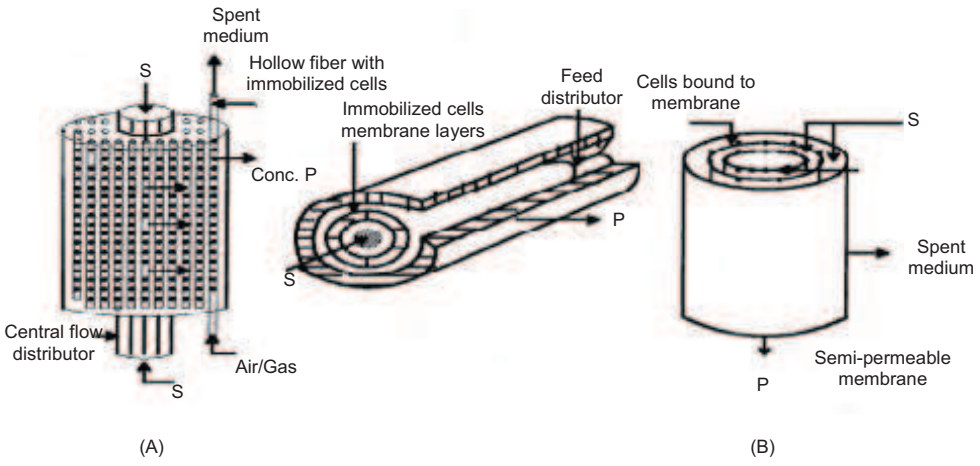

Figure 1.15: Membrane reactors: (A)hollow fibre reactor, (B) spiral-wound flat sheet reactor (Adapted from (Margaritis and Kilonzo, 2005))

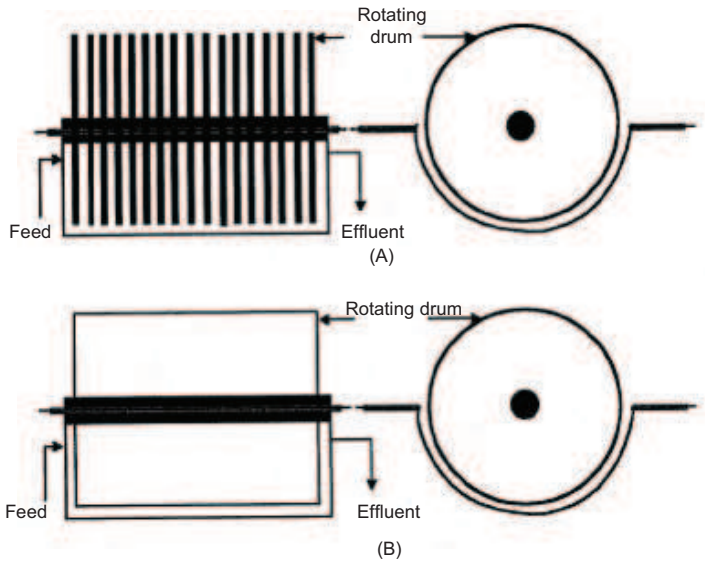

Figure 1.16: Rotating biological contactors:(A) disc reactor, (B) rotating cylinder reactor (Adapted from (Margaritis and Kilonzo, 2005))

In the study of immobilized *Bacillus subtilis* cells, the airlift bioreactor (Guo *et al*., 1990) and the fluidized-bed reactor (Ramakrishna *et al*., 1992) have been used to produce the α-amylase enzyme. In the latter fluidized-bed reactor study, varying the geometry of the gel from spherical to cylindrical improved oxygenation and thereby reactor performance.

Based on Table 1.2, the polyHIPE cell matrix can be used in a fixed bed/monolith type of bioreactor. This configuration had been used previously for the production of osteoblasts (Akay *et al*., 2004) and the phenol-degrading bacterium, *Pseudomonas syringae* (Akay *et al*., 2005d, Erhan *et al*., 2004).

1.2.5 Physiological changes of immobilized cells

Studies have shown that immobilization affects the physiology of cells. These changes include plasmid stability, diffusion, product production and morphology. These alterations are caused by changes in the microenviroment due to the diffusional restrictions. Increased plasmid stability was observed in a study of recombinant *Bacillus subtilis* cells in continuous immobilized cultures (Castet *et al*., 1994). This was due to the physical structure of the cavities within gel bead that allows only a limited number of cell divisions to occur in each microcolony before the cells escape from the gel beads. Immobilization acts as a protective microenvironment for cells exposed to toxic or inhibitory substrates. Additionally, the germination time of encapsulated *Bacillus subtilis* was significantly longer than free cells (Lamas *et al*., 2001), again due to the diffusional effects in the immobilization system. However, after a time lag due to encapsulation, the growth of the cells was uninhibited and no differences were observed between entrapped and free cells. Moreover, the production of enzymes such as α-amylase by immobilized cells was significantly higher than produced by free cells (Konsoula and Liakopoulou-Kyriakides, 2006). The morphology of immobilized *B. subtilis* cells tended to be longer and slimmer, compare to the short-rod shape found for freely suspended cells.

1.2.6 Metabolic changes of immobilized cells

Several hypotheses have been proposed for the changes in the metabolism of the cells in the immobilized state (Dervakos and Webb, 1991). These include disturbances to the growth pattern, cell-to cell communication, change in the cell morphology, media supplementation and diffusion limitations. The metabolic changes of immobilized cells included reduced specific growth rates and increased enzyme production rates. The growth pattern of cells attached to the surface material is likely to differ from freely suspended cells with respect to cell division, DNA replication and the synthesis of cell wall components, with consequential effects on their metabolic activity. Additionally, the high biomass concentration attained in immobilized cell systems compared to conventional free cell systems may signal the bacteria to enter the stationary phase earlier, leading to profound changes in the pattern of gene expression and, ultimately, cell survival. Bacteria such as *B. subtilis* often use cell-to-cell signalling (i.e. quorum sensing) to monitor their population density (Lazazzera, 2000). The composition of the media used for the growth of immobilized cell systems has a major influence on their performance. For example, the production of α-amylase by polyacrylamide immobilized cells varied according to the medium used (Kokubu *et al*., 1978). The highest α-amylase activity was obtained from medium containing meat extract and yeast extract. Media containing glucose, salts and yeast extract considerably improved the production of α-amylase activity from alginate immobilized cells compared to glucose alone (Ramakrishna *et al*., 1992), while κ-carrageenan immobilized cells were less susceptible to the catabolite repression of the α-amylase synthesis in the presence of high initial glucose concentrations (Duran-Paramo *et al*., 2000). On the other hand, more α-amylase enzyme was obtained when the bacterium was cultivated in a medium containing tryptone (Konsoula and Liakopoulou-Kyriakides, 2006).

Diffusional limitations lower the specific growth rate of immobilized cells compared to free cells (Shinmyo et al., 1982, Duran-Paramo *et al*., 2000). For example, the specific respiratory activity and the growth rate of entrapped cells were 10-50% of the activity of free cells (Shinmyo *et al*., 1982). They suggested

that these observations were due to resistance of the gel to nutrients and oxygen penetration to the cells.

1.3 *Bacillus subtilis* spores

1.3.0 Model Organism: *Bacillus subtilis*

1.3.1 Background

Bacillus subtilis is an aerobic, endospore-forming and rod-shaped Gram-positive bacterium which has been studied widely due to its lack of pathogenicity to humans, animals and plants. Additionally, it is recognized by regulatory bodies, including the Food and Drug Administration (USA), as having GRAS (generally regarded as safe) status. This organism has been widely used in the manufacture of industrial enzymes and, increasingly, heterologous proteins in large scale fermentation processes. This bacterium was chosen for this study. The heterologous proteins produce by this bacterium are usually secreted directly into the culture media. This confers, substantial benefits for the recovery and purification of these proteins. In addition, the extracellular overproduced proteins are usually correctly folded and better retain their biology activity.

The strain used in this study was *Bacillus subtilis* 168(pKTH10). This strain carries a recombinant plasmid (pKTH10) carrying the structural gene for α-amylase from *Bacillus amyloliquefaciens* in the high copy plasmid pUB110 (Palva, 1982). The construction of this plasmid is illustrated in the Figure 1.17. This transformed *B. subtilis* is able to synthesize α-amylase approximately 2500 times higher than that for the wild-type *B. subtilis* and approximately 5 times higher than the enzyme produced by the donor *B. amyloliquefaciens* strain (Palva, 1982).

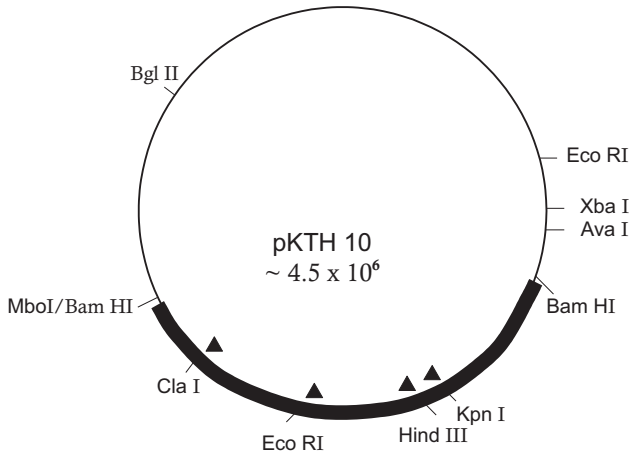

Figure 1.17: Plasmid pKTH10. The thin line represents pUB110 DNA and the heavy black line a 2.3-kb chromosomal DNA insert from *B. amyloliquefaciens*. Arrowheads indicate the restriction enzyme sites, in which foreign DNA was inserted to test the activation of the α-amylase gene (Palva, 1982).

1.3.2 *Bacillus subtilis* spores

The vegetative cells of *B. subtilis* are rod-shaped with a length of 1.2 - 2.4 µm and a diameter of 0.75 µm while its spores are oval-shaped with a dimensions of 0.6-0.9µm x 1.0-1.5µm. Table 1.3 summarizes the difference between the vegetative cell of *B. subtilis* and its spores.

Table 1.3: Differences between endospores and vegetative cells in *Bacillus* species

Property	Vegetative cells	Endospores
Surface coats	Typical Gram-positive PG cell wall polymer;	Thick spore coat, cortex, and unique peptidoglycan core wall;
Microscopic appearance	Nonrefractile	Refractile
Heat resistance	Low	High
Resistance to chemicals and acids	Low	High
Radiation resistance	Low	High
Sensitivity to lysozyme	Some sensitive; some resistant	Resistant

The spore's structure and chemical composition, which develops during sporulation, play major roles in spore resistance. The spore structure comprises several specific compartments as shown in Figure 1.18. The exosporium, made up of proteins including some glycoproteins, is a large-loose fitting structure, which is found on some species. *B. subtilis* either do not contain an exosporium or if they do it is greatly reduced in size (Setlow, 2006).

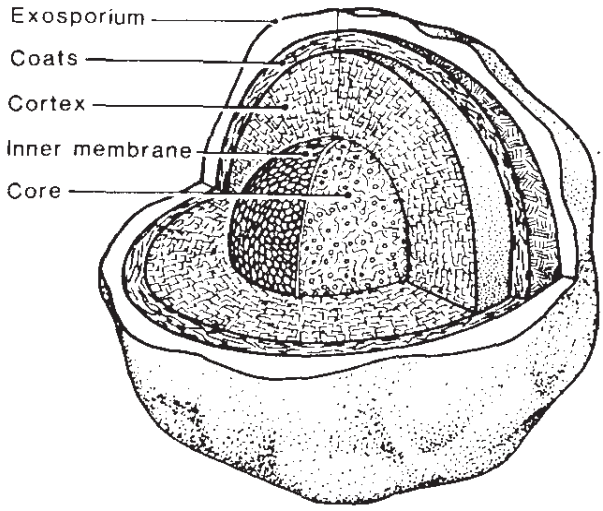

Figure 1.18: Generally, schematic diagram of structure of bacterial endospores (Foster and Johnstone, 1990).

The *B. subtilis* spore coat is a complex structure composed of several layers and containing ≥ 50 proteins, most of which are spore-specific gene products (Driks, 2002b, Driks, 1999). It has been reported that this coat is essential in spore resistance to various chemicals, to exogenous lytic enzymes that can degrade the spore cortex and to predation by protozoa. However, it has no role in spore resistance to heat, radiation and certain other chemicals (Driks, 1999, Setlow, 2002a, Setlow, 2006, Paidhungat and Setlow, 2002). The outer membrane, which underlies the spore coats is an essential structure in the formation of the spore (Piggot and Hilbert, 2004). Nonetheless, the role of this structure is not clear. It has been claimed that the integrity of this structure may not be retained in the dormant spores and thus its role as a permeability barrier is likely insignificant (Setlow, 2006).

The next layer, the spore cortex, is important for the development of a dormant spore and for the reduction of the water content of the spore core (Setlow, 2006). Its structure is similar to that of vegetative peptidoglycan, but with several spore-specific modifications (Popham, 2002, Setlow, 2006). This structure is degraded during spore germination to facilitate the expansion of the spore core and subsequent outgrowth (Setlow, 2003).

The spore structure which plays a major role in the spore's resistance to many chemicals, particularly those that damage the spore DNA, due to its strong permeability barrier is the inner spore membrane (Setlow et al., 2000, Cortezzo and Setlow, 2005).

The spore core, the final layer of spore structure, includes three types of small molecule which are essential in spore resistance including spore-specific enzymes as well as DNA, ribosomes and tRNAs (Setlow, 2006). The extremely low water content of the core is a major factor in the spore's enzymatic dormancy, and is an important factor determining the spore's resistance to wet heat (Setlow, 2006). Pyridine-2,6 dicarboxylic acid (dipicolinic acid, DPA) represents 5-15% of the dry weight of the spore. It is extensively chelated with divalent cations, mainly $Ca^{2+.}$ The accumulation of DPA in the spore core is likely to be responsible for the reduction in the core's water content (Setlow, 2006). Acid-soluble spore proteins (SASP) of the α/β-type are 60-75 residues in length and are extremely abundant. The structure and properties of spore DNA is altered dramatically due to the binding of these proteins. Furthermore, these proteins play a major role in the resistance of spores to heat and many chemicals and UV radiation (Setlow, 2006) that damage DNA. Prior to spore outgrowth, these proteins must be degraded otherwise they would inhibit outgrowth, presumably by blocking DNA transcription (Hayes and Setlow, 2001).

1.3.2.1 Sporulation, Germination and Outgrowth

Spores of *Bacillus* species are produced during sporulation, a process that is triggered in response to nutrient exhaustion. Sporulation is initiated at the end of exponential growth and involves a sequence of phases which are recognised according to morphological features (Figure 1.19). The seven stages of sporulation take approximately 8h at 37^0C under laboratory conditions and are illustrated in Figure 1.19 (Nicholson and Setlow, 1990b). The resulting spores are resistant to heat, chemicals, solvents, pH extremes, radiation and desiccation. When conditions are favourable for growth, dormant spores germinate and subsequently outgrow, eventually being converted back into a growing cell (Paidhungat and Setlow, 2002).

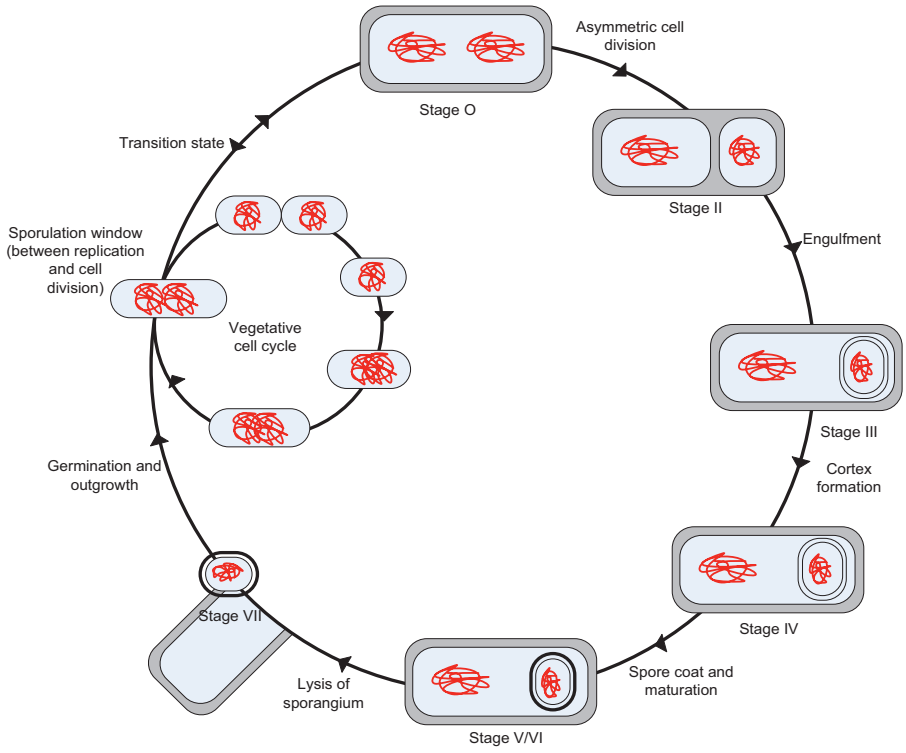

Figure 1.19: The sporulation pathway in *B. subtilis* and its relationship to the vegetative cell cycle (Nicholson and Setlow, 1990b).

Spore germination involves a series of rapid chemical and physiological changes involving the degradation of the spore cortex, disruption of the spore coat, rehydration and swelling. It is accompanied by a loss of resistance properties (Nicholson and Setlow, 1990b). The germination of *B. subtilis* spores is activated

by L-alanine or a mixture of asparaginase, glucose, fructose and KCl. The germination process is divided into two stages (Figure 1.20). The first stage comprises three steps: (1) release of cations probably from the spore core and their excretion, (2) release of the spore core's large deposit (~ 10% of spore dry wt) of pyridine-2, 6-dicarboxylic acid (dipicolinic acid [DPA] and its associated divalent cations, predominantly Ca^{2+}, (3) partial core hydration. At this stage the spore loses some of its resistance properties. The second stage involves hydrolysis of the spore's peptidoglycan spore cortex, swelling of the spore core through further water uptake and expansion of the germ cell wall. At this stage, the spores have lost more of their resistance and their dormancy (Setlow, 2003). Spore outgrowth follows germination, which subsequently leads to the production of a new vegetative cell.

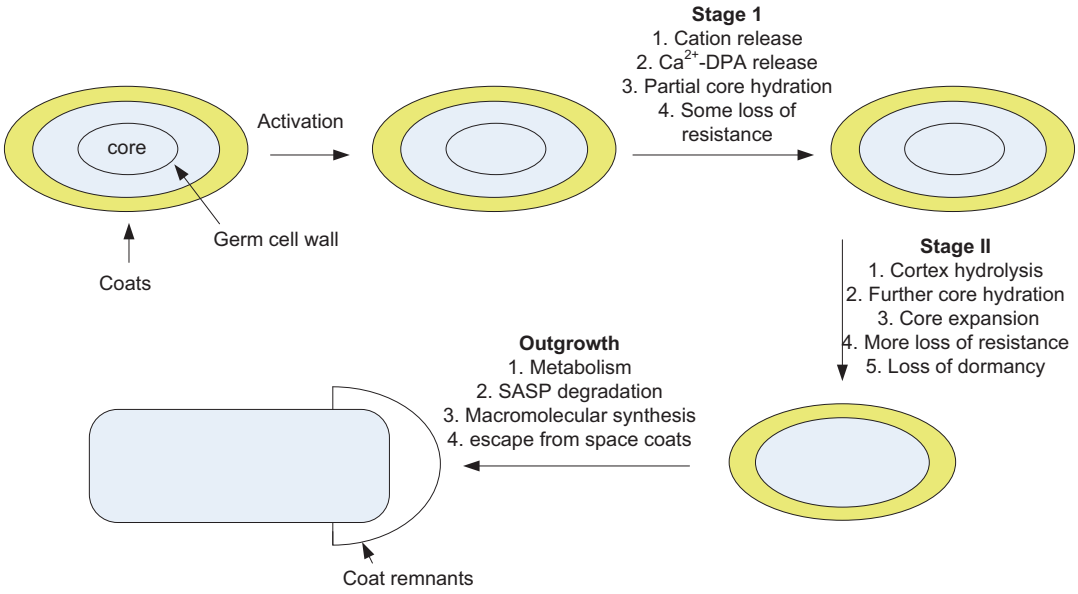

Figure 1.20: Spores germination and outgrowth (Adapted from (Setlow, 2003)).

Germination and outgrowth overlap to a significant degree. The outgrowth follows germination and is continuous until the cell is converted back to a vegetative cell. This requires both metabolism and macromolecular synthesis (Paidhungat and Setlow, 2002). However, it is possible that outgrowth events such as initiation of metabolism, can begin prior to completion of germination-specific events such as hydrolysis of spore cortex (Paidhungat and Setlow, 2002).

Early in this process is the synthesis and assembly of both membrane and cell wall components.

1.3.3 Surface properties of *Bacillus subtilis*

Bacillus subtilis cells are enveloped with a single (cytoplasmic) membrane surrounded by a thick cell wall which is composed of a heteropolymeric matrix of peptidoglycan and covalently attached anionic polymers such as teichoic and teichuronic acids (Figure 1.21). The thickness of this Gram-positive cell wall ranges from 20 to 50nm, which is approximately 10 times the thickness of the peptidoglycan layer of a typical Gram-negative bacterium such as *E. coli.* The anionic polymers confer on the wall a high degree of negative charge. *B. subtilis* also synthesises a membrane-anchored lipoteichoic acid which contains polyanionic hydrophilic chains. The unsubstituted carboxyl groups of muramyl peptide contribute other negative charges. The negative surface-charge property of *B. subtilis* results in significant binding and concentration of metal cations such as Ca^{2+} and Fe^{3+} at the membrane/wall interface. The culture conditions may change the composition and structure of the wall and lead to the changes in its porosity and ion exchange capacity.

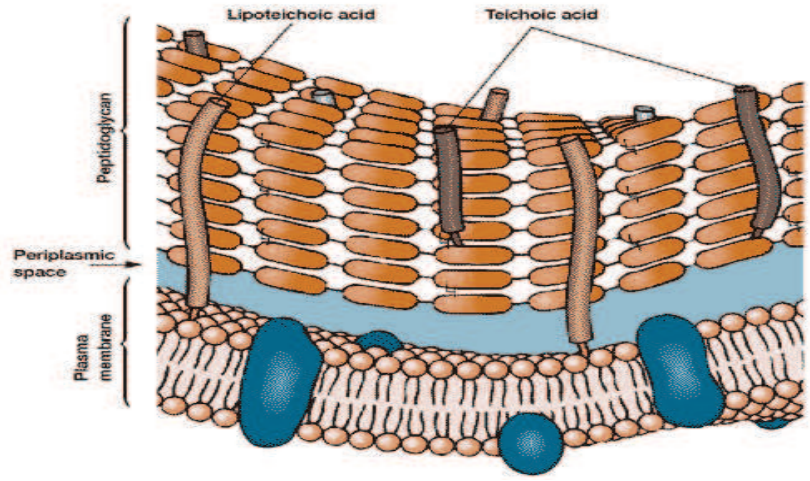

Figure 1.21: The Gram-positive cell wall (Source: (Prescott et al., 2004))

Previous studies have demonstrated that *Bacillus* spores that are enveloped with an exosporium were more hydrophobic than those lacking an exosporium (Koshikawa *et al*., 1989). Their findings show that the exosporium is more hydrophobic than the spore coat and these physico-chemical properties contributed to the surface hydrophobicity of spores. They suggested that it might be because of the protein and lipid components of the exosporium. *B. subtilis* spores are less hydrophobic than other spore-forming bacilli such as *B. brevis*, *B. cereus* and *B. thuringiensis* which possess strong hydrophobic properties. The vegetative cells of *B. subtilis* also exhibited very low levels of surface hydrophobicity compared to the vegetative cells of other *Bacillus* species such as *B. thuringiensis* (Thwaite *et al*., 2009).

1.3.4 Growth Condition

The majority of *Bacillus* species grow at mesophilic temperatures in a simple salts media comprising ammonium or amino acids as nitrogen sources and glucose or other simple sugars as carbon sources. However, since ammonium is a poor nitrogen source, it is often replaced by glutamine as a nitrogen source. Other sources of amino acids can also be utilized, for example arginine, glutamine, glutamate, asparagine and aspartate (Harwood, 1990).

Many species of *Bacillus* such as *B. alvei*, *B. circulans*, *B. coagulans*, *B. licheniformis* and *B. macerans* are able to grow fermentatively under anaerobic conditions. However, *B. subtilis* only grows weakly in the absence of oxygen and must be aerated during growth. It can be grown in a batch or continuous culture. During the growth cycle in batch culture, the physiology, metabolism and morphology undergoes changes, the most significant of which take place during transition to and throughout stationary phase. It also includes the formation of spores (Harwood and Archibald, 1990). Therefore, continuous culture is preferred as this operation mode provides steady state conditions. Thus, any physiological changes in cultures can be easily studied.

1.3.5 α-amylase enzyme

α–Amylase is one of the main products secreted by most *Bacillus* species. This enzyme is also produced by a wide variety of plants and animals. There are several *Bacillus* species that can produce this enzyme such as *B. subtilis*, *B. brevis*, *B. licheniformis* and *B. stearothermophilus*. α–Amylase is an endoamylase catalyzing randomly the hydrolysis of internal α-1,4-glycosidic linkages of long-chain starch to give low molecular weight products. *Bacillus licheniformis* produces an extremely thermostable α–amylase (temperature optimum 92°C). α–Amylase is one of the oldest industrial enzymes. This enzyme is in high demand due to its application in many major industries such as the food, paper and textile industries. Therefore, it is of value to improve the performance of its production system in order to meet a growing industrial demand for this enzyme. Production of this enzyme through microbial production is preferred due to its economical bulk production as well as the ease of microbial manipulation to obtain enzymes with the desired characteristics.

1.3.5.1 Factor influence the production of microbial enzyme

There are various factors that influenced the productivity of microbial enzymes. They include the composition of the growth medium, pH, temperature, aeration, inoculum age, carbon source and nitrogen source. In developing an industrial fermentation product, the composition of the nutrient medium is the most important factor as it significantly affects the product concentration, yield and productivity. Previous studies identified that different carbon sources used in *Bacillus* cultures showed considerably variation with respect to α-amylase production. The rate of α-amylase produced was higher when starch used as a carbon source and the opposite for glucose and maltose (Coleman and Elliott, 1962, Coleman and Grant, 1966, Saito and Yamamoto, 1975, Santos and Martins, 2003, Ryan *et al*., 2006, El-Banna *et al*., 2007, Dharani Aiyer, 2004). Various forms of starch can be used which include corn, wheat malt and potato since, unlike glucose, they are non-catabolite repressing (Yoo *et al*., 1988). Other studies have shown the effect of yeast extract and peptone on optimal α-amylase

production and cell growth (Alam *et al*., 1989, Santos and Martins, 2003, El-Banna *et al*., 2007, Dharani Aiyer, 2004). The highest levels of protein secretion are usually observed when *B. subtilis* is grown in rich medium such as complex medium containing yeast extract, tryptone and sodium chloride (Antelmann *et al*., 2001). In this type of medium, protein secretion is highest during stationary phase and the main production of α-amylase is during this phase. The use of recombinant strains genetically modified to enhance α-amylase production also contributes to production levels that can exceed 20g/l.

1.3.6 Immobilization of *B. subtilis*

Various types of support matrices have been used in studies on the immobilization of *Bacillus* strains. They include κ-carrageenan gel beads, polyacrylamide gel, activated acrylonitrile/acrylamide, polysulphone membrane and calcium alginate gel capsules. These studies have shown that the immobilization of whole cells confers several advantages compared with conventional fermentation using free or planktonic cells. The production and activity of α-amylase produced by immobilized whole cells was significantly greater than that produced by free cell systems (Kokubu *et al*., 1978, Tonkova *et al*., 1994, Dobreva *et al*., 1998, Konsoula and Liakopoulou-Kyriakides, 2006). This is probably due to the microenvironmental changes in the immobilization system which alters aspects of the metabolism, physiology and morphology of the cells.

A summary of immobilized *Bacillus* species producing α-amylase is shown in Table 1.4.

Table 1.4: Several studies on immobilization of *Bacillus* cells producing α-amylase enzyme

Type of support	Micro-organism	Type of bioreactor	Results/observations	Ref.
Polyacrylamide gel	Whole cell *Bacillus subtilis*	500ml Takaguchi flask with 30ml media at 30^0C for 5h	▪ The growth of immobilised bacteria reached a stationary phase after 15h cultivation ▪ achieved the maximum rate α–amylase production, 3000Units/ml/h ▪ After 12h incubation, the growth cells were leaked from the gel	(Kokubu *et al*., 1978)
κ- carrageenan gel beads	*Bacillus subtilis*	Erlenmeyer flask with 50ml of Schaeffer's media at 37^0C	▪ The entrapped cells reached the steady state - 1.2 x 10^9 cells/ml of support in gel beads. ▪ the same timing of the sporulation process in cultures of immobilized and of free cells ▪ Immobilization influenced the growth of *B.subtilis* cells but did not affect their sporulation.	(Baudet *et al*., 1983)
agar beads and on formaldehyde activated acrylonitrile/acrylamide membranes	*Bacillus licheniformis*	Conical flasks with 50ml of nutrient media at 40^0C (for 168h)	▪ the α-amylase production by immobilised cells was significantly greater than that by the control especially late in the fermentation ▪ the operational stability of the biocatalyst investigated was retained at a high level for a long time	(Tonkova *et al*., 1994)
(i) polysulphone membrane (PS) with 260-290 μm thickness and Ø = 0.43μm and 0.16μm (ii) polyacrylonitrile membrane (PN) with 250 μm thickness and 20kDa cut-off.	*Bacillus licheniformis*	Conical flasks with 50ml of nutrient media at 40^0C (for 120h)	▪ produced higher amounts of thermostable α - amylase than the free cells (37-62% higher yields after 120h cultivation). They retained up to about 90-97% of their initial activity after 480h at repeated batch fermentation ▪ The aeration and stirring conditions in the bioreactor are important parameters for cell growth and bioproduction. ▪ Pre-treatment and activation were required for these membranes but they can be reused by washing with sterile water.	(Dobreva *et al*., 1998)

κ- carrageenan gel beads	*Bacillus subtilis*	1L lab. fermentor with 0.3L of LB-media	▪ They found that the biomass immobilized and that released were 2.5x higher than that obtained in the free-cell system. ▪ After prolonged incubation, the gel matrix lost much of its mechanical rigidity, and consequently, the cavities near the support surface exploded, releasing cells to the solution. ▪ Immobilised cells presented a lower maximal specific growth rate compared with that of free cells; 0.18/h and 0.27/h respectively	(Duran-Paramo *et al*., 2000)
Calcium alginate gel capsules	*Bacillus subtilis*	250ml of Conical flasks with 50ml of nutrient media at 40^0C (for 48h)	▪ the productivity of α -amylase by the immobilised cells - significantly greater than that of the freely suspended cells – approximately 2.5-fold increase in the alpha-amylase yield ▪ a high specific activity of α-amylase produced from the immobilised system was obtained compared to free cells ▪ Modifying the capsules' characteristics – resulted to prolong the capsules operational stability and efficiency ▪ Repeated use of the biocatalysts in 15 successive and efficient fermentation operations	(Konsoula and Liakopoulou-Kyriakides, 2006)

1.4 Objectives

In this thesis, the main objective is to develop a novel production system that enhances the production of an extracellular enzyme, namely α-amylase from *Bacillus subtilis,* by immobilizing onto polymeric material known as polyHIPE.

Specific aims:

1. To produce matrix, polyHIPE polymers (PHPs) with a range of controlled pore and interconnect sizes.

2. To develop a system for growing immobilised *B. subtilis* on a foam matrix, polyHIPE support

3. To study the growth, viability and proliferation of *Bacillus subtilis* immobilised onto polyHIPE support

4. To investigate the effect of the pore size and chemical modification of the support on growth and enzyme productivity

5. To investigate the effect of medium composition and cell loading on growth and enzyme productivity

6. To compare the productivity of the developed immobilized system for the production of the enzyme α-amylase with that of a batch culture of the same medium

2 Materials and methods

2.1 Preparation of PolyHIPE (PHP) support

2.1.1 Materials

Styrene, Span 80 or sorbitan monooleate, divinyl benzene (DVB), potassium persulfate, vinylpyridine, hydroxyapatite, phosphoric acid, sodium hydroxide and isopropanol were purchased from Aldrich Chemicals, UK.

2.1.2 Poly(styrene-divinylbenzene) polyHIPE

The composition of oil and aqueous phase were as follows:

Aqueous phase consists of:

Distilled water with 1% potassium persulphate as an initiator

Oil phase consists of:

78% styrene
8% divinylbenzene
14% Sorbitan Mono (Span 80)

PolyHIPE polymers were prepared by polymerization of a high internal phase emulsion, as described in Section 1.1.2. The procedures and experimental set up are illustrated in Figure 1.5. The dispersed (aqueous) phase (consisting of distilled water with initiator) was continuously dosed into the continuous phase (containing monomer, crosslinker and surfactant). The dispersed phase was delivered by peristaltic pump at a constant rate during the dosing period. The resulting emulsion was stirred with flat impellers arranged at 90^0 to each other. Mixing was continued during the addition of the aqueous phase to reduce the large droplet size. The emulsification was carried out at 25^0C, with an initial aqueous phase volume of 85%. The prepared emulsion was collected into plastic containers with an internal diameter of 2.8 cm, then polymerized at 60^0C for at

least 8 hours. After polymerization, the formed polymers were cut into discs with a thickness of 5 mm. The resulting discs were washed extensively using a Soxhlet system to eliminate all the residual monomer/crosslinker and initiator (Figure 2.1). For the first 4 hours, the discs were washed with a mixture of distilled water/isopropanol, followed overnight by distilled water. Finally, the washed PHP discs were dried under vacuum in an oven at 60^0C and stored at room temperature until needed.

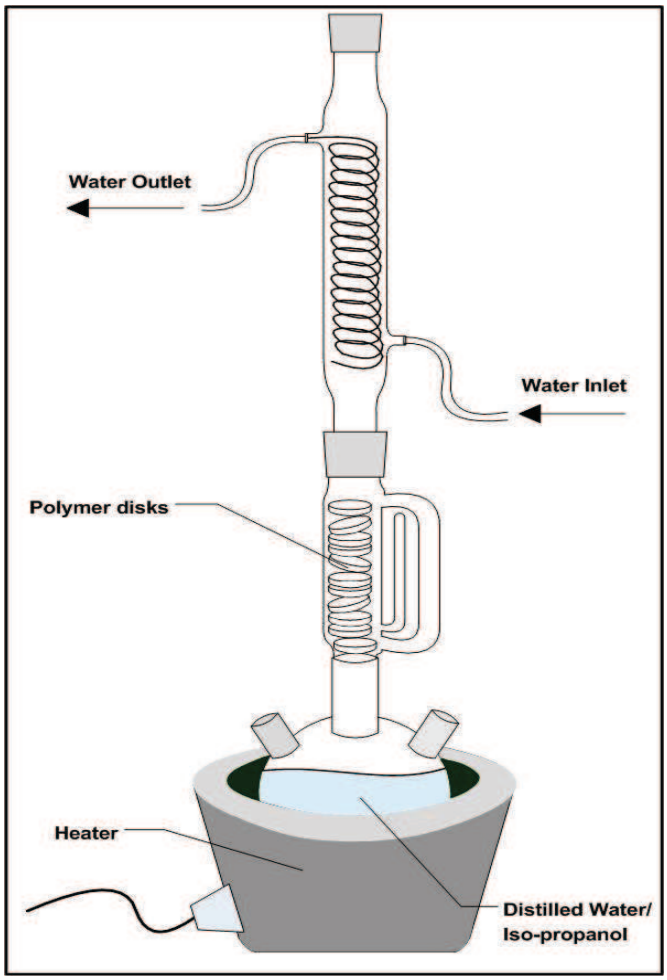

Figure 2.1: Schematic diagram of the Soxhlet system used in the washing step of PHP production.

2.1.3 Inclusion of vinyl pyridine into poly(styrene-divinylbenzene) polyHIPE

The composition of oil and aqueous phases were as follows:

Aqueous phase:

1% potassium persulphate as an initiator

Oil phase:

73.0% styrene

5.0% vinyl pyridine

8.0% divinylbenzene (DVB)

14.0% sorbitan monoleate (Span 80)

The procedures were similar to those used for poly(styrene-divinylbenzene) polyHIPE (Section 2.1.2) except that the prepared emulsion was left to polymerize at 40°C for the first 6 hours and then prolonged for an additional 6 hours at 60°C.

2.1.4 Sulphonation treatment to Poly(styrene-divinylbenzene) polyHIPE

The composition of oil and aqueous phases were as follows:

***Aqueous phas*e**:

1% of potassium persulphate as an initiator and 5% of sulphuric acid

Oil phase:

76.0% styrene

10.0% divinylbenzene (DVB)

14.0% sorbitan monoleate (Span 80)

The procedures for making sulphonated polyHIPE were similar to those described in Section 2.1.2 with a few additional steps before washing and drying the polyHIPE polymer. After cutting the prepared polyHIPE polymer into discs of 5 mm of thickness, they were dried in an oven at 60°C overnight. The discs were then soaked in concentrated sulphuric acid for 3 hours, subsequently microwaved in a conventional 1 kW domestic microwave oven 5 times for 30 seconds in a fume cupboard. During this step, the door of microwave was opened between each session to allow fumes to escape and to cool the oven. At the same time the discs were flipped over to ensure even sulphonation.

After completion of sulphonation, the discs were washed with deionised water and a mixture of 50% deionised water and 50% ammonium hydroxide. Each washing was carried out twice for 30 minutes. The later washing was performed to neutralise any remaining acid, adjusting the pH to 5.5 if necessary with ammonium hydroxide. Finally, the discs were dried overnight in a fume cupboard and washed using the Soxhlet system.

2.2 Determination of the process conditions for the production of PHP of specific pore sizes

Initially, the dosing time was varied from 5 to 10 minutes while maintaining a mixing time of 20 minutes. Then, the mixing time was varied from 20 to 100 minutes while keeping the dosing time constant at 10 minutes (Table 2.1). All experiments were repeated three times.

Table 2.1: The experimental set-up to obtain pores of a specific size in the PHP.

PHP Code No.	Dosing time (t_D, min.)	Mixing time (t_M, min.)
T3	5	20
T5	10	20
T7	10	30
T9	10	60

2.3 Characterization of the polyHIPEs polymer (PHP)

2.3.1 Determination of pore and interconnect size by scanning electron microscopy (SEM)

Pore and interconnect sizes of each type of the PHPs were analyzed using scanning electron microscopy (SEM, Cambridge s240). Each sample was fractured in order to obtain a fresh internal surface and was then mounted onto aluminium stubs at room temperature using conductive carbon cement (LEIT carbon or glued-sticker). The samples were then left overnight. For high magnification analysis, the samples were sputter coated with gold at 20nm, using a Polaron e5100 sputter coater, and stored in silica gel until analysed. The analysed micrograph images of each polymer were used to determine the diameter of 50 pores and interconnects. The physical characteristics of the PHP were determined using Image J software (NIH image). The pores and interconnect sizes of PHP were calculated by averaging the raw data. Measurements were carried out on three independently prepared PHP samples in order to obtain a more accurate distribution of pore and interconnect sizes.

2.3.2 Estimation of the surface area of polyHIPE by surface area analysis

Surface area of the PHP matrix was measured using the Coulter SA 3100 surface area and pore size analyzer (Beckman Coulter company). Initially, the samples were pre-heated in the oven at 60^0C for a few hours and then weighted (the minimum ideal weight is 1.00g per analysis). They were subsequently placed in the sample tube with volume of 9 cm^3. Next, the samples were degassed for at least 6 hours at constant temperature, for the polyHIPE polymer this was usually 50^0C. The tube containing the degassed polymer was connected to the analytical port of the SA 3100 and immersed in liquid nitrogen while the instrument calculated the Brunaeur, Emmet and Teller (BET) surface area. A typical analysis takes between 30 min and two hours.

2.3.3 Uptake of water of polyHIPE

For the determination of water uptake, the sulphonated polyHIPE samples were completely immersed in water for 24h or 48h. The weights of the PHP samples before and after immersion were measured and the percentage of water uptake was calculated using the following formula:

$$\frac{\left(W_f - W_i\right)}{W_i}\left(100\right) \qquad \text{Equation 2.1}$$

W_f = final weight of PHPs

W_i = initial weight of PHPs

Three measurements were carried out from independent samples of the same batch of PHP.

2.4 Preparation of PolyHIPE using a glass vessel

A schematic diagram of the experimental setup designed to produce polyHIPE using a glass vessel is shown in Figure 2.2. The polyHIPE produced using this rig was analysed using SEM in order to ensure the characteristics (pore and interconnect sizes) were the same as that prepared using a stainless steel vessel. This apparatus was used to synthesize polyHIPE with an *in situ B. subtilis* spore suspension.

Figure 2.2: The glass vessel apparatus for preparation of polyHIPE

2.5 Preparation of stock *B. subtilis* spores

2.5.1 Preparation of liquid media/agar and buffer solution

Two media were used for the growth of *B. subtilis*; Schaeffer's sporulation medium and a general-purpose medium known as Luria-Bertani medium (LB). 1.5% (w/v) agar was added to the prepared media for the preparation of agar plates.

2.5.1.1 Schaeffer's sporulation medium/agar

This medium was also known as Difco sporulation medium (DSM). The following were added for 1 litre of medium:

Bacto-nutrient broth	8g
10% (w/v) KCl	10ml
1.2% (w/v) $MgSO_4.7H_2O$	10ml
1M NaOH	0.5 ml

The prepared medium was autoclaved at 15psi for 30 min. The following sterile solutions were added after the autoclaved medium had cooled to 50^0C.

1 M $Ca(NO_3)_4$	1.0ml
0.01 M $MnCl_2$	1.0ml
1mM $FeSO_4$	1.0ml

The $FeSO_4$ solution tends to precipitate after autoclaving, and was resuspended before use.

2.5.1.2 LB (Luria-Bertani) medium/agar

1 litre of LB medium contained:

Bacto-tryptone	10g
Bacto-yeast extract	5g
NaCl	10g
1M NaOH	1.0 ml

The medium was then autoclaved at 15psi for 30 min.

2.5.1.3 Potassium phosphate buffer

100ml of potassium phosphate buffer contained:

1M K_2HPO_4	0.802 ml
1M KH_2PO_4	0.198 ml
5M KCl	1.0 ml
0.1M $MgSO_4$	1.0 ml
Distilled water	97.0 ml

The prepared buffer was autoclaved at 15psi for 30 min.

2.5.2 Induction of sporulation by nutrient exhaustion

A fresh colony of *B. subtilis* 168(pKTH10) was emulsified by vortexing in 5ml of Schaeffer's medium. Then, 0.1ml of emulsified cells was used to inoculate four Schaeffer's agar plates and incubated overnight at 30^0C. On the following day, each of the plates was flooded with 4 ml of Schaeffer's medium and the cells were carefully resuspended using a sterilized glass spreader. The resuspended cells were used to inoculate two Erlenmeyer flasks, each containing 750 ml of pre-warmed Schaeffer's medium containing 10µg/ml kanamycin. The flasks were incubated overnight at 37^0C with vigorous aeration.

2.5.3 Preparation of the spore suspension

After overnight incubation, the cell cultures were centrifuged at 10,000*g* for 10 minutes. The pelleted cells were washed five times with sterilised distilled water to remove all cell debris. The supernatant was discarded and the spores resuspended in sterilised distilled water and stored at -20^{0}C.

2.5.4 Determination of spore resistance properties

As discussed in Section 1.3.2, bacterial spores are metabolically inactive and much more resistant than vegetative cells to a variety of environmental stresses such as treatment with heat, organic solvents, lysozyme and ultraviolet radiation (Nicholson and Setlow, 1990a). The resistance of the spore suspensions prepared in Section 2.5.3 to heat, organic solvents, lysozyme was determined to ensure that they were fully matured.

2.5.4.1 Assay for lysozyme and heat resistance

A suspension of spores (1 ml) of *B. subtilis* strain 168 (pKTH10) was added to an equal volume of phosphate buffer (1mM) and the mixture incubated with lysozyme (250µg/ml) for 1 hour at 37^{0}C. The lysozyme-treated sample was washed five times with sterilized distilled water by microcentrifuging (13,000rpm, 4min.) to remove traces of lysozyme. Dilutions of the treated spore suspension were plated onto LB agar (Figure 2.3) and incubated overnight at 37˚C. The spore suspension was prepared without lysozyme and evaluated under the same condition as the control. The number of colonies from the treated sample was compared with that of an untreated sample.

Similarly, the spore suspension was also subject to heat treatment. A sample of spore suspension was heat-treated at 80^{0}C for 10 min. Dilutions of the treated spore suspension were plated onto LB agar (Figure 2.3) and incubated overnight at 37˚C. The number of colonies was compared with that of an untreated sample.

(A) NO TREATMENT

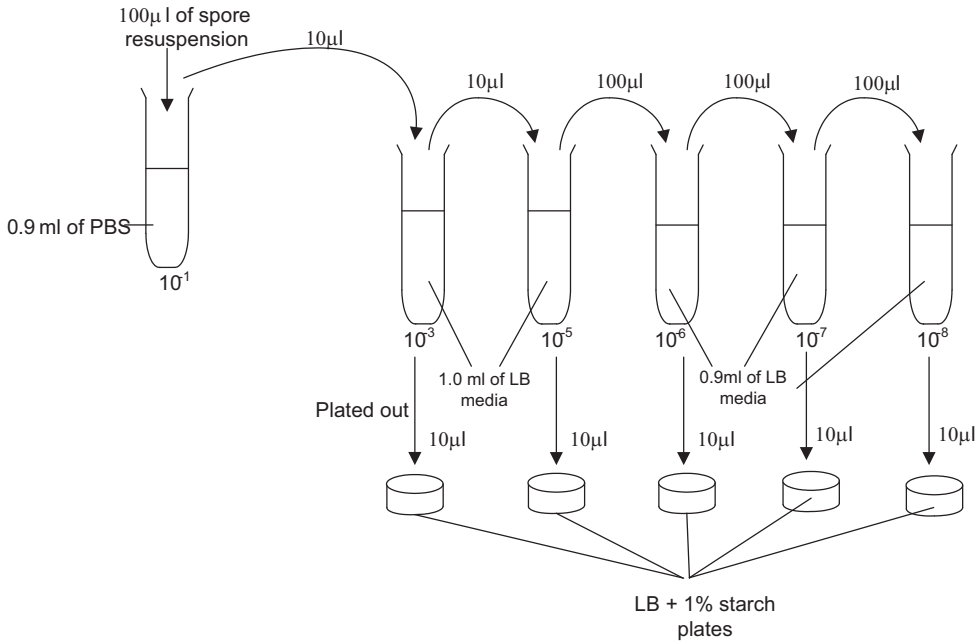

(B) HEAT/LYSOZYME TREATMENT

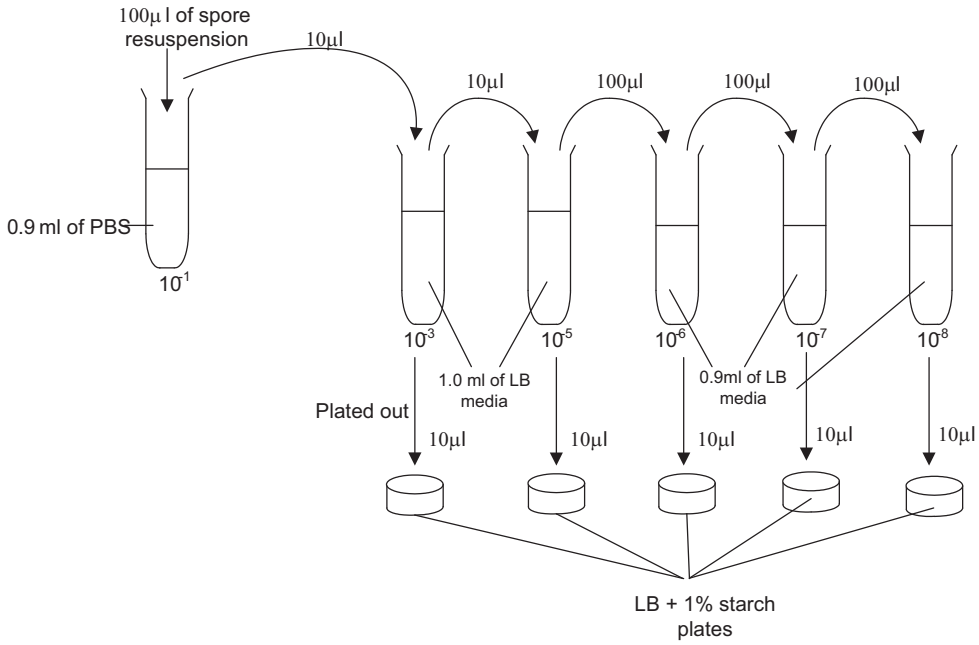

Figure 2.3: Schematic diagram showing the dilution procedures for vegetative cell and spores; (a) without treatment (b) With heat/lysozyme treatment

2.5.4.2 Assay for organic-solvent resistance

Treatment with water-immiscible organic solvents

Oil phase of polyHIPE was prepared as described in Section 2.1.2 and Section 2.1.3. 50µl of this oil phase was added to 0.45 ml of the spore suspension in a microfuge tube and mixed vigorously with a vortex mixer. Dilutions of the treated spore suspension were plated onto LB agar (Figure 2.4) and incubated overnight at 37˚C. The number of colonies was compared with that of an untreated sample.

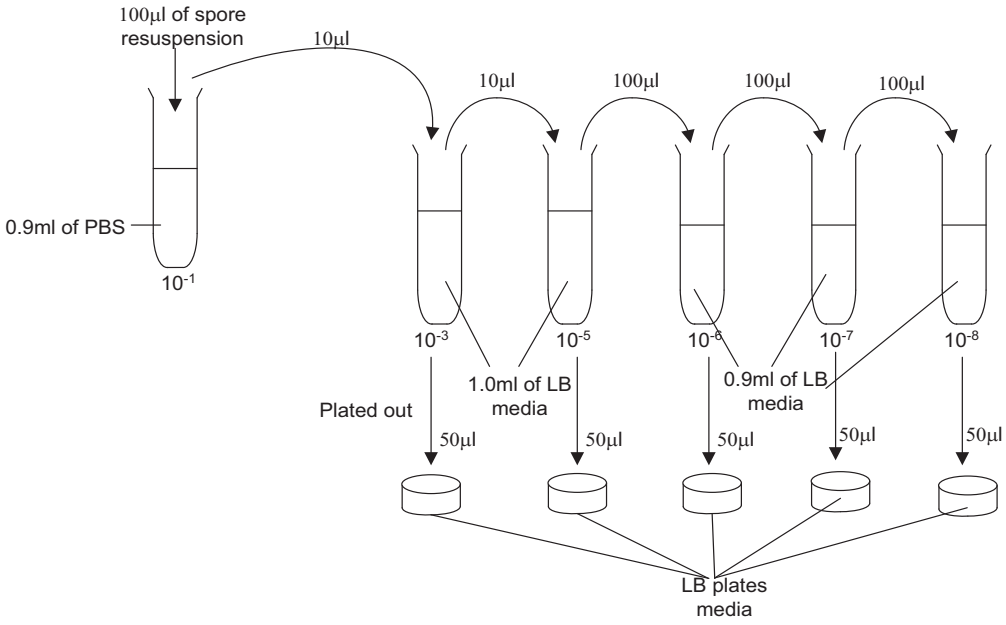

Figure 2.4: Schematic diagram represents the dilution procedures

2.5.5 Preparation of *B. subtilis* cells for scanning electron microscopy

Samples of lysozyme-treated spores (Section 2.5.4.1) were fixed in 2% gluteraldehyde/phosphate buffered saline (PBS) and stored at 4^0C until required. A sample of fixed spores was dropped on the surface of a cleaned cover slip and left to dry for 30 min. Prior to SEM analysis, the sample was dehydrated in an ethanol series, as shown in Table 2.2. Once in 100% ethanol, the cover slip was subject to a critical-point drying procedure with liquid CO_2. The sample was

mounted on aluminium stubs with sliver cement and coated with gold, using a Polaron e1500 Sputter Coater. Finally, the sample was examined under SEM (Cambridge s240).

Table 2.2: Ethanol series used for the dehydration samples for SEM analysis

Concentration of ethanol (%)	Duration (min)
25	10
50	10
75	10
100	15
100	15

2.5.6 Testing for plasmid stability

The strain of *B. subtilis* used throughout these studies contained a plasmid (pKTH10) that encoded an amylase gene from *B. amyloliquefaciens* (AmyQ) and a kanamycin resistance gene. To ensure that the plasmid was partitioned to the spore during sporulation, the presence of the plasmid in germinated vegetative cell was determined by comparing the number of cell on LB plates with and without the selective antibiotic. The samples were heat-treated at 80^0C for 10 min. Dilutions of the treated spore suspension were plated onto LB agar plates containing 1% of starch in the presence or absence of 10μg/ml of kanamycin and incubated overnight at 37˚C. Then, the number of colonies from these plates were counted and compared; all colonies which appeared on the plate in the presence of 10μg/ml of kanamycin showed the presence of plasmid.

2.6 Bacterial Cell Adhesion

The "bacterial cell adhesion to hydrocarbon" (BATH) assay was performed (Rosenberg, 1984) to determine the hydrophobicity of *B. subtilis* cells. Cultures of *B. subtilis* 168 (pKTH10) grown for 5, 10 and 16 hours at 37˚C in LB broth were harvested, washed twice with sodium phosphate (pH 6.8) and resuspended to an OD_{440nm} of 1.0. N-hexadecane (1 ml) was added to 3ml of the bacterial suspension, the mixture agitated vigorously for 1 min and the phases allowed to separate at room temperature for 15 min. The aqueous phase was carefully removed and its optical density determined at 440nm. The partitioning in the hydrocarbon phase was calculated as follows:

$$\frac{\left(D_i - D_f\right)}{D_i}\left(100\right) \qquad \text{Equation 2.2}$$

D_f = OD_{440nm} of aqueous phase

D_i = OD_{440nm} of initial bacterial suspension

The assay was carried out in duplicate and the average from three independent experiments was taken.

2.7 Batch culture

Batch cultures of *B. subtilis* strain 168(pKTH10) were grown in LB media for the determination of growth rate, optical density, viable cell counts, cell dry weight and α-amylase activity. All media and apparatus used were autoclaved at 121^0C for 30 min. LB medium, 100 ml in a 500 ml flask, was inoculated from an overnight culture in the same media and incubated at 37^0C for 24h in a rotary shaker. 3 ml of samples was collected every hour for α-amylase activity, OD, CFU and cell dry eight (CDW). Three independent experiments were carried out and the data averaged.

2.8 Immobilization of *B. subtilis* spore suspensions

2.8.1 *In-situ* synthesis of vinylpyridine polyHIPE containing *B. subtilis* spores

The synthesis of vinylpyridine polyHIPE was identical to that described in Section 2.1.3 excepting the aqueous phase contained of 1ml of *B. subtilis* spore suspension (~2 x 10^8). After polymerization, the polymers containing *B. subtilis* spores were cut into discs with a thickness of 5 mm. The resulting discs were washed using a Soxhlet system to eliminate all the residual monomer/crosslinker and initiator (Figure 2.1). For the first 2 hours, the discs were washed with a mixture of distilled water/isopropanol, followed overnight by distilled water. Finally, the washed PHP discs were stored at 4^0C until needed. In order to reduce contamination from environmental microorganisms, the apparatus was autoclaved before used and all steps were carried out under aseptic conditions.

2.8.1.1 Activation of *B. subtilis* spores inoculated in-situ synthesized vinylpyridine polyHIPE

The *B. subtilis* spores that had been incorporated into the polymerized micro-porous vinylpyridine polyHIPE were activated by continuously pumping LB broth through the matrix at a flow rate of 1.0 ml/min for 24h (Figure 2.5). This matrix was placed in a well of sterilised block-shaped microchamber as shown in Figure 2.5. The supplied LB broth was continuously aerated and the experiment was carried in a constant temperature room at 37^0C. Samples were collected at various time intervals to determine the numbers of cells released from the PHP matrix and for α-amylase activity. At the end of experiment, sterile 0.1M phosphate buffered saline was pumped through the matrix at the same flow rate to remove the remaining medium. As a control the same amount of medium was also added into the PHPs discs, without spores and then incubated overnight at 37^0C.

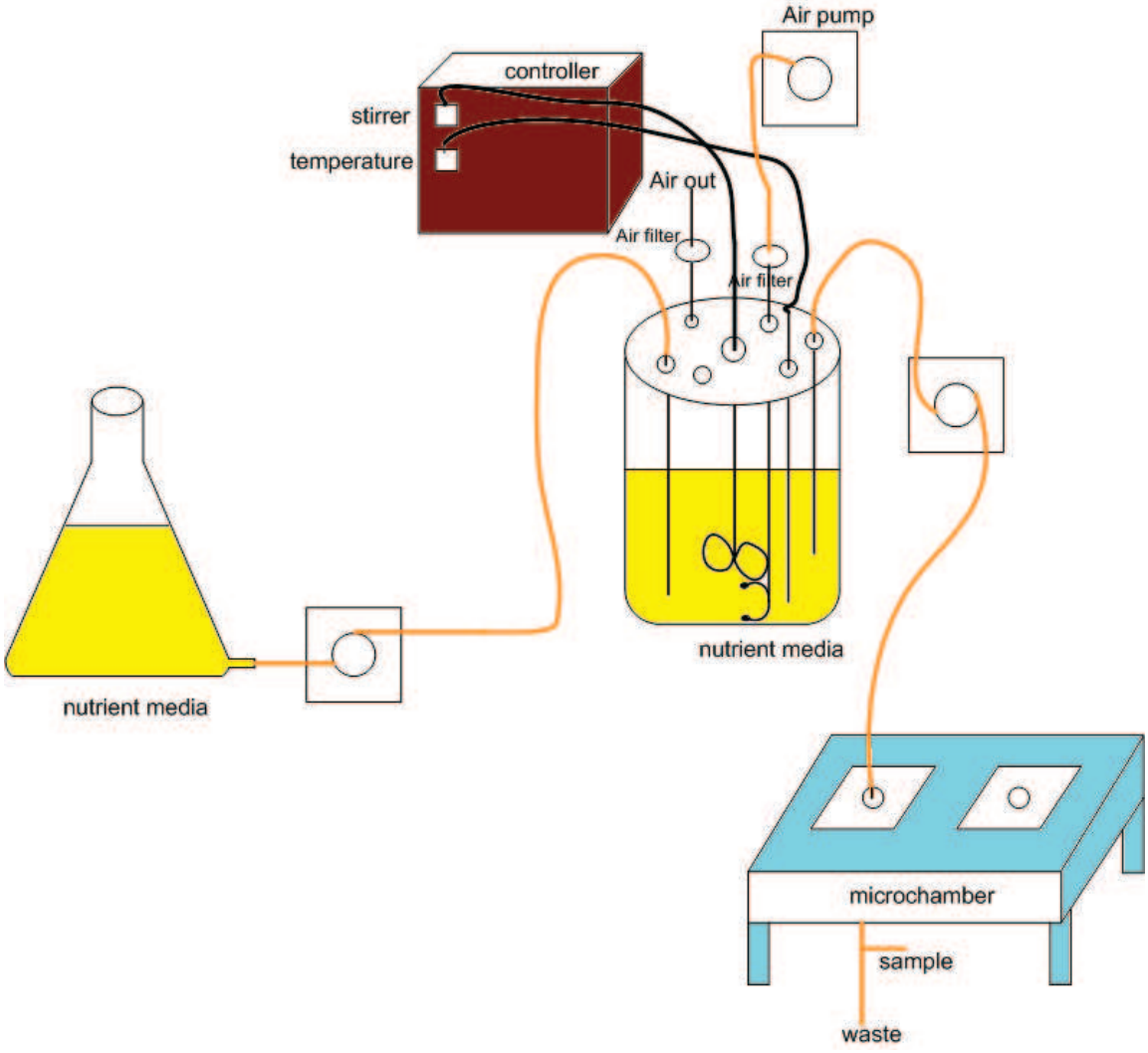

Figure 2.5: Flow diagram of immobilized cell growth system using polyHIPE polymeric matrices

2.8.2 Immobilization of *B. subtilis* spores into generic polyHIPE polymeric matrices (vinylpyridine polyHIPE or sulphonated polyHIPE)

The PolyHIPE (PHP) discs were mounted into a sealed PTFE block (Figure 2.5) and sterilised in an autoclave at 121^0C for 15 min. Then, this PHP disc was initially wetted with distilled water overnight and then with LB media for an hour before use. Spores of *B. subtilis* strain 168 (pKTH10) (~2x 10^8) were suspended in 2ml of LB broth and pre-germinated by incubating for 90 min at 37^0C. The pre-germinated spores were force-seeded into the PHP by passing the suspension through the matrix at a flow rate of 0.55ml/min using a syringe pump. The seeded PHP was left for an hour to allow the pre-germinated spore to attach to the surface of the PHP, and then culture medium (LB broth) was pumped continuously through the matrix at a flow rate of 1.0ml/min (Figure 2.5). This experimental setup was placed in a 37^0C constant temperature room. Samples were collected at various time intervals to determine the numbers of cells released from the PHP matrix and for α-amylase activity. At the end of experiment, sterile 0.1M phosphate buffered saline was pumped through the matrix at the same flow rate to remove the remaining medium. As a control the same amount of medium was also added into the PHPs discs, without inoculated spores and then incubated overnight at 37^0C.

2.8.3 Immobilization of *B. subtilis* spores into generic porous sulphonated polyHIPE

In the case of sulphonated polyHIPEs, the procedures in section 2.8.2 were used excepting that the pre-wetting of the PHPs matrix with distilled water and LB medium was carried out for just an hour each. The cell growth phase was carried out using different concentrations of LB medium (0.5 dilution, 0.75 dilution, 1x and 2x) and different concentrations of cell loading (2 x 10^8/ml, 2 x 10^7/ml and 2 x 10^6/ml) to establish the relationships between yield, cell numbers and media concentration.

2.8.4 Quantification of released cell numbers

The numbers of cells released from the PHP matrix were determined by plating serial dilutions (Figure 2.4) of the out flowing medium onto LB agar plates containing 1% starch. The plates were incubated overnight at 37^0C and the number of colonies determined. Exposing the surfaces of these plates to iodine vapour revealed clear zones around the colonies able to hydrolyse starch.

2.8.5 α-amylase assay

Phadebas®Amylase tablets, a water-insoluble starch substrate was used to determine α-amylase activity. The Phadebas substrate is formed by cross-linking a starch polymer to a blue azo dye that, when hydrolysed by the activity of amylase, forms a water-soluble fragment. The activity of amylase in the sample is determined from the absorbance of the blue dye that is released into solution. The samples for α-amylase activity analysis were centrifuged to remove the cells. One tablet of Phadebas was resuspended in 5ml of sterile distilled water. 40µl of sample was added to 0.8ml of Phadebas suspension and the mixture incubated with frequent mixing at 37^0C in a water bath for 15 minutes. The reaction was stopped by the addition of 200 µl of 0.5M NaOH and vortexed immediately. The mixture was centrifuged at 10,000*g* for 5 minutes and the supernatant transferred into a cuvette. The absorbance of the supernatant was measured at 620nm against a LB broth blank subjected to the same assay conditions. Samples with very high α-amylase activity were diluted up to 5-fold using distilled water. Each sample was duplicated and the average was taken. One unit (U) of α-amylase activity is defined as the amount of enzyme catalyzing the hydrolysis of 1µmol glucosidic linkage per minute at 37^0C.

2.8.6 Quantification of protein

1ml of protein assay reagent (Coomassie Plus (Bradford) Assay reagent, Thermo Scientific) was added to 1 ml of sample and mixed by vortexing. The mixture was incubated for 10 minutes at room temperature then the absorbance determined at 595nm against a distilled water blank. Each sample was treated in duplicate and the average value determined. The protein concentration of each sample was determined from the standard curve using known concentrations of bovine serum albumin (BSA).

2.8.7 Quantification of cell dry weight (CDW)

Cells were recovered from batch culture samples (with volume of 1ml) by centrifugation (3000*g,* 10 min, 4^0C) and washed twice with 0.9% NaCl. The resulting pellet was dried at 105^0C for 24h to constant weight. In the case of cells in the polyHIPE matrix, they were washed by passing distilled water through the matrix to remove culture medium, and the matrix dried to constant weight (by weighing several times) and then weighed. The cell dry weight was determined by subtracting the weight of the polyHIPE at the start and end of the experiment. Weight of blank polyHIPE disc (without cells) was also determined as a control.

2.8.8 Preparation of matrix samples for SEM analysis

The matrix samples were fixed in 2% gluteraldehyde/phosphate buffered saline (PBS) and stored at 4^0C until required. Prior to SEM analysis, the samples were dehydrated in an ethanol series; 30%, 50%, 70%, 80%, 90%, 100% (each step for 15 minutes excepting 100% ethanol treatment was for 1 hour). The dehydrated sample in 100% ethanol was critical-point dried with liquid CO_2. The sample was mounted on aluminium stubs and coated with gold using a Polaron e1500 Sputter Coater. Finally, the sample was examined under SEM (Cambridge s240). SEM analysis for samples without cells was also undertaken. In this case, the samples were directly coated with gold without dehydration and critical-drying.

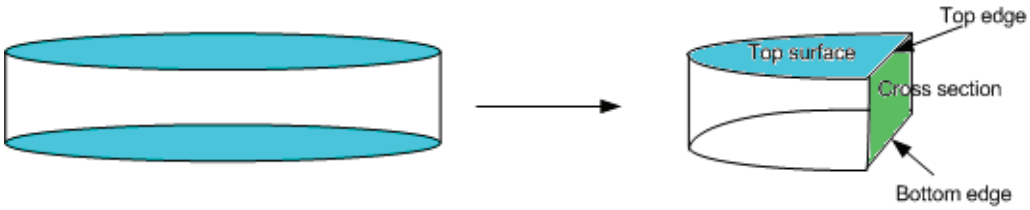

Figure 2.6: Diagram showing the regions of the polyHIPE matrix that were examined under SEM: top surface, top edge, cross-section, bottom edge

3 Germination and growth characteristics of *Bacillus subtilis* strain 168 (pKTH10)

3.1.0 Spore of *Bacillus subtilis* strain 168 (pKTH10)

3.1.1 Introduction

The transition of vegetative *Bacillus subtilis* cells to dormant spores occurs when this bacterium undergoes deprivation of nutrients, in a process known as sporulation. The development of spores involves a number of stages that are categorized on the basis of the resulting changes in morphology. The unique structure and composition of the spores serve major roles in their resistance to extreme environments such as high temperature, toxic chemicals, solvents, radiation and mechanical shock. Sporulation can be induced in several ways, such as allowing cells to grow in limited or poor nutrient conditions using specially formulated media such as Schaeffer's medium or 2x SG medium (Setlow, 2002b). These media can be prepared either as liquid or agar media. In this study, the former medium was used to induce the sporulation through the nutrient exhaustion method.

This study attempts to exploit the resistance properties of spores by their entrapment into the matrix of polyHIPE during its synthesis. If this study is successful, it will facilitate the production of pre-inoculated matrices that can be stored indefinitely at room temperature but activated within a few minutes by the addition of culture medium.

Therefore, the objectives of this section are to:

- Quantify the number of *Bacillus subtilis* spores produced from Schaeffer's medium using the nutrient exhaustion method
- Determine the stability of plasmid pKTH10 carrying the α-amylase gene in *B. subtilis* strain 168

3.1.1 Quantification of *Bacillus subtilis* spore numbers

The determination of spore numbers was carried by counting colony numbers obtained on nutrient agar plates following exposure to either lysozyme or heat (80^0C, 10 min), both treatments known to kill vegetative cells. The treated samples were plated out on the LB plates containing 1% of starch (Figure 3.1).

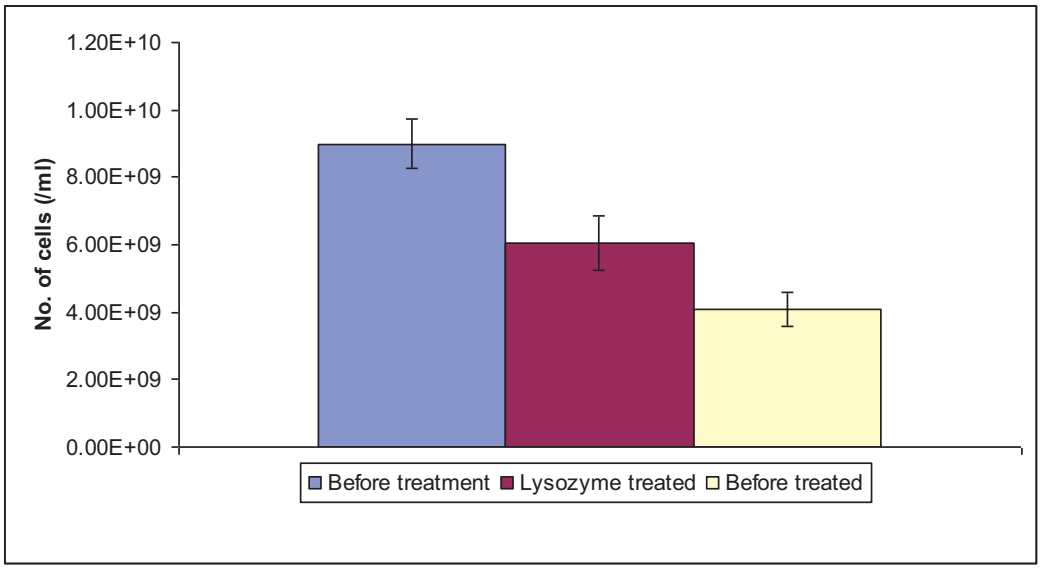

Figure 3.1: Average number of spores for *B. subtilis* strain 168 (pKTH10)

3.1.2 Stability of *Bacillus subtilis* plasmid

An experiment was carried out to determine whether the colonies of the surviving cells had developed from spores encoding plasmid pKTH10 that encodes the α-amylase gene, AmyQ. The treated samples were plated on LB plates containing 1% of starch, the substrate for α-amylase. Exposing the surface of the agar plate to iodine vapour stains starch purple. Therefore α-amylase-producing colonies that degrade starch showed an unstained zone hydrolysis immediately around the colonies (Figure 3.2). The results showed that the great majority of the spores that the colonies had developed from had retained a copy of pKTH10 throughout the sporulation process. Although the number of colonies that had lost the plasmid were not quantified directly, no colonies of *B. subtilis* were observed without zones of amylase hydrolysis.

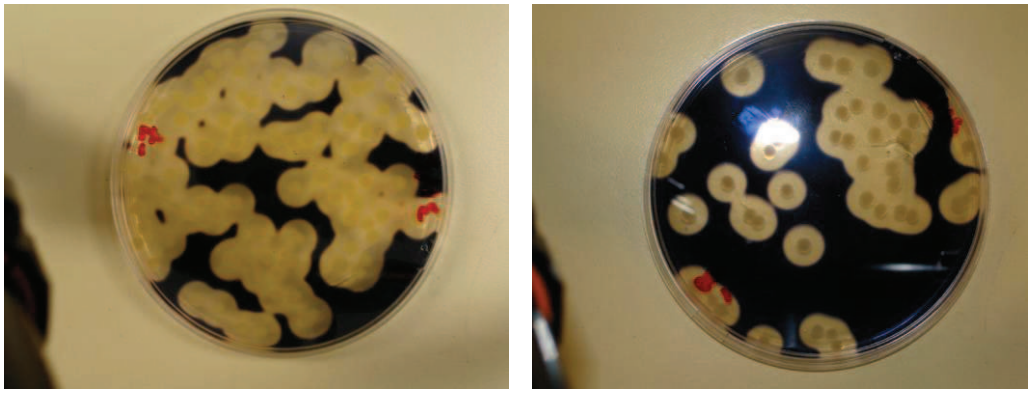

Figure 3.2: The appearance of clear zones surrounding colonies of *B. subtilis* strain 168 (pKTH10) on LB agar containing 1% of starch, after exposure to iodine vapour.

3.1.3 Scanning electron microscopy of *Bacillus subtilis* spores

Samples of the prepared *B. subtilis* spores were visualised using scanning electron microscopy and the micrograph images are shown in the Figure 3.3. The micrographs confirm that the suspension is very homologous with few, if any, signs of vegetative cells.

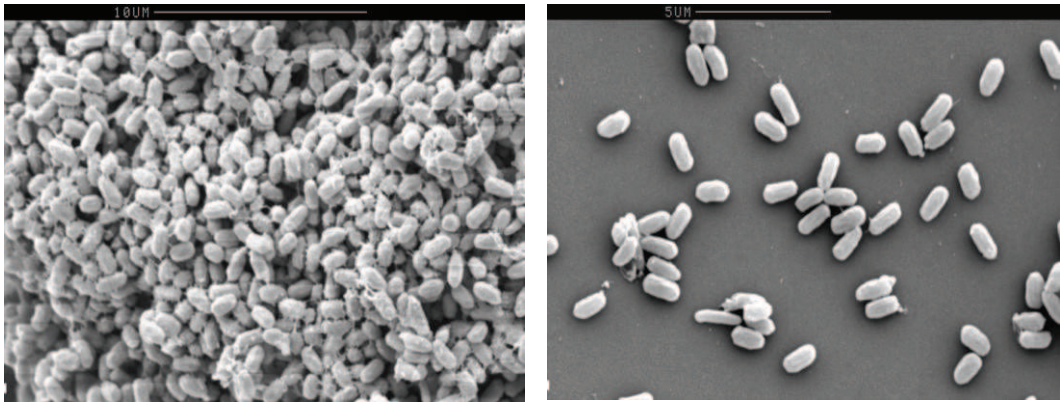

Figure 3.3: Scanning electron microscopy images of the prepared *B. subtilis* spore suspension.

3.1.4 Discussion

In this study, *B. subtilis* spores were produced by the nutrient exhaustion method. The number of spores was determined from the number of colonies that developed on nutrient medium following treatments known to kill vegetative cells, namely exposure to lysozyme or heat treatment (80^0C, 10 min.). During the routine preparation of spores, the cells were treated with lysozyme to remove vegetative cells. Once a spore preparation was prepared, heat treatment was used to determine the proportion of heat-resistant spores in the final spore suspension. In the case of *B. subtilis* strain 168 (pKTH10), the number of fully heat-resistant spores was found to be about 40% (from 9.2 x 10^9cells/ml to 3.6 x 10^9cells/ml). As can be seen also there was a reduction of cells number from 6.2 x 10^9cells/ml to 3.6 x 10^9cells/ml after lysozyme treatment. This result showed that more vegetative cells can be removed by treating with heat rather than lysozyme as some vegetative cells were not lysed by lysozyme. They also confirm that the spores were resistant to heat. As can be seen in Figure 3.3, the shape of the spores was elliptical and not spherical like some other members of the genus *Bacillus* (*e.g. B. megaterium*). The size of spores was estimated to be approximately 0.6 x 1.1μm, which is consistent with the size of *B. subtilis* spore quoted in the literature of 0.6-0.9 x 1.0-1.5μm (Burdon, 1955).

In order to determine whether the α-amylase encoding plasmid had been maintained in the cells during sporulation, the heat-treated spores were plated on LB agar containing 1% of starch and 10μg/ml of kanamycin. The appearance of zones of clearing around the colonies after exposure to iodine vapour indicated that the spores contained the plasmid carrying the α-amylase and kanamycin resistance genes (Figure 3.2). α-amylase (α-1,4-glucan 4- glucanohydrolase) is an enzyme that degrades starch (Figure 3.4), initially to oligosaccharides and subsequently to maltose and glucose, by hydrolyzing α-1,4-glucan bonds (Figure 3.5). The absence of purple coloration indicated that the starch immediately around the colonies has been hydrolyzed by the α-amylase.

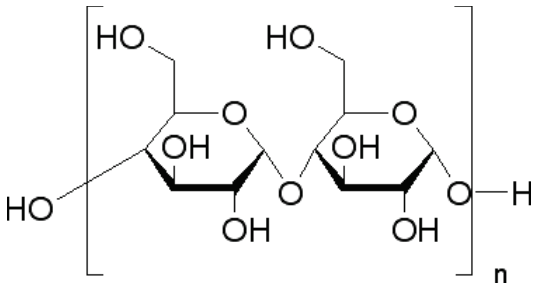

Figure 3.4: Chemical structure of starch, $(C_6H_{10}O_5)_n$

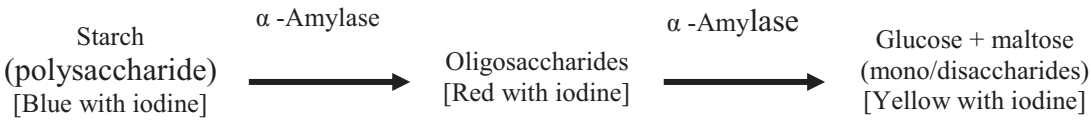

Figure 3.5: Degradation of starch to glucose and maltose by α-amylase

3.2.0 Batch Culture *Bacillus subtilis* strain 168 (pKTH10)

3.2.1 Introduction

Bacillus subtilis and other members of the genus *Bacillus* are aerobic and tend to grow weakly in the absence of oxygen, although species such as *Bacillus licheniformis* are an exception. *B. subtilis* is able to grow in simple salts media containing ammonium or amino acids as nitrogen sources and glucose or other simple sugars as carbon sources. *Bacillus* species are mesophilic and grow adequately and produce good-sized colonies within 24h if grown at 37^0C (Harwood and Archibald, 1990). In this study, a complex media containing yeast extract and acid-hydrolyzed casein, was used as the main source of nutrients in the culture medium

Microorganisms, rather than plants and animals, are the preferred source for the large-scale production of α-amylase. This is because of the economical advantages of bulk production capacity and recombinant cell technology that has allowed microorganisms to be engineered as efficient α-amylase producers. *B. subtilis* and its close relatives are the main commercial producers of α-amylase. In this study, a strain of *Bacillus subtilis* 168 encoding pKTH10 was used for the high level production of α-amylase. Recombinant plasmid pKTH10, based on the high copy number plasmid pUB110, encodes the structural gene for the *Bacillus amyloliquefaciens* α-amylase AmyQ (Palva, 1982). Like most α-amylases, AmyQ is catabolite repressed and therefore synthesized during stationary phase following the exhaustion of simple carbon sources from the culture medium. The use of LB medium, which is complex medium both lengthens productive stationary phase and delays the onset of sporulation.

Therefore, the objectives of this section are to:

- Determine the growth kinetics and α-amylase production by *B. subtilis* 168 (pKTH10) in batch culture.
- Evaluate the effect of media of different compositions on α-amylase productivity by varying the concentrations of casein hydrolysate, yeast extract and sodium chloride.

The kinetic data were used to for comparative purposes with respect to the process intensified immobilized system developed in this study.

3.2.2 Growth curve and enzyme production

B. subtilis 168(pKTH10) was grown in LB medium with shaking at 37˚C and samples taken at various points during growth for the determination of growth and α-amylase production (Figure 3.6).

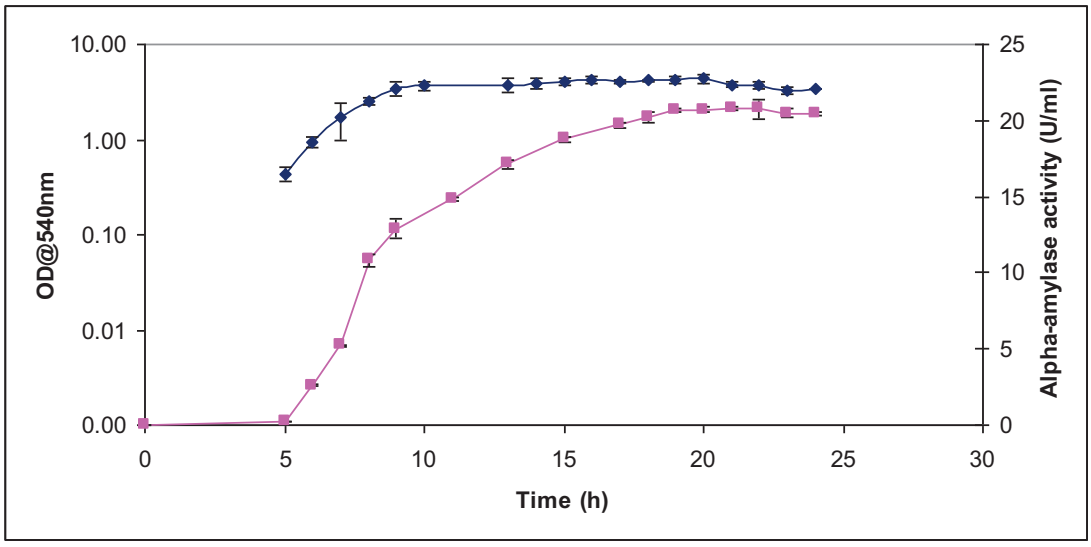

Figure 3.6: Growth curve and kinetic of extracellular α-amylase production by a batch culture of *B. subtilis* 168 (pKTH10). ◆, Optical density; ■, amylase production.

As can be seen from Figure 3.6, the cells grow rapidly for the first 8 hours, while in exponential phase. Cell mass then reached a plateau for the next 12h, before slightly declining for the last 4h. The specific growth rate, μ (h^{-1}) and doubling time, td (h^{-1}) of the batch culture were determined from the growth curve; the values are 0.41h^{-1} and 35 minutes respectively. The concentration of α-amylase in the culture medium continued to increase from the exponential phase until the first 5h of stationary phase. Although the rate of production dropped during stationary phase, α-amylase continued to accumulate in the culture medium for at least another 12 hour before finally levelling off. The α-amylase production rate was calculated and plotted against time (Figure 3.7). The resulting curve showed that the production of α-amylase peaked during late exponential phase but gradually declined throughout stationary phase. The cell dry weight of culture medium obtained was approximately 1.3 mg/ml. Based on the above data, the total α-amylase produced, the volumetric and specific production rates and yield of α-amylase per ml of medium were determined and shown in Table 3.1

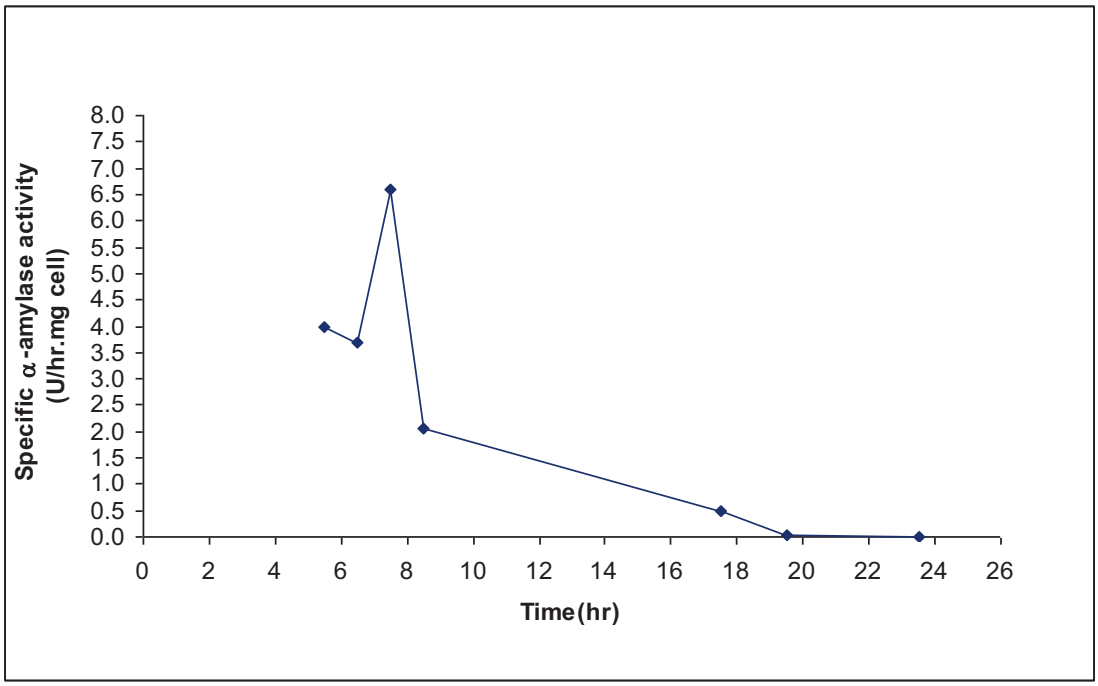

Figure 3.7: Specific production rate of α-amylase of *B. subtilis* 168 (pKTH10) grown in LB medium with shaking at 37˚C for 24 h.

Table 3.1: Summary of the data for α-amylase production of *B. subtilis* 168 (pKTH10) grown in LB medium with shaking at 37˚C for 24h. The data was obtained from three independent experiments

Total α-amylase produced (U)	Volumetric productivity (U/mL/h)	Yield of α-amylase per ml of medium used (U/mL)	specific α-amylase production rate (U/h/mg cell)	specific α-amylase (U/mg protein of culture)
2167 ± 2	0.90 ± 0.001	21.67 ± 0.02	0.69	1083.5 ± 1.2

3.2.3 Effect of nutrient media composition

3.2.3.1 Effect of diluted of LB media to the production of α-amylase

In order to examine the efficiency of α-amylase production in batch culture, five different concentrations of nutrient media were used and designated D1, D2, D3, D4 and D5 (Table 3.2). The concentrations of nutrient media used in this experiment were determined on the basis of the concentrations of each component of the LB media. For instance concentrations of each component of D1 medium were a quarter of concentrations of each component in LB medium (D3). In the case of D2, D4 and D5 media, the concentrations of each component were 50%, 200% and 250% of concentrations of each component in LB medium (D3). The influence of using different concentrations of LB media to increase and/or maintain the α-amylase production during 24h batch cultivation was examined. The results obtained are shown in Figure 3.8 and Figure 3.9 and summarized in Table 3.3.

Table 3.2: Variations to the components of LB medium (D3)

Different conc. media	Media composition (g/L)		
	Tryptone	NaCl	Yeast extract
D1	5	5	2.5
D2	7.5	7.5	3.75
D3 (LB)	10	10	5
D4	20	20	10
D5	25	25	12.5

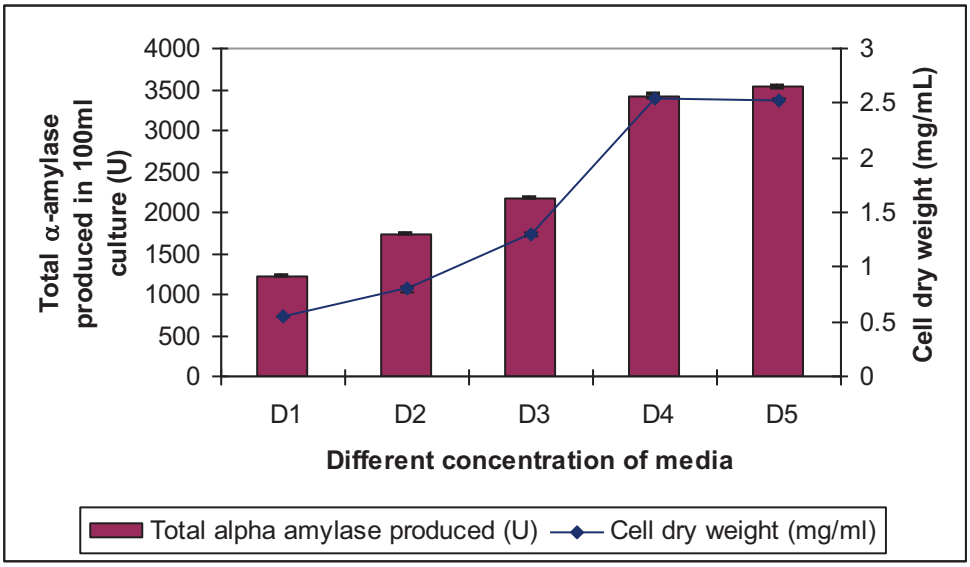

Figure 3.8: Effect on α-amylase production and cell dry weight (mg/mL) of varying the composition of LB medium (Table 3.2). Cells were grown in 100ml medium at 37˚C with shaking. α-Amylase production and cell dry weight (CDW) were determined after 24h. Statistical significance was determined with one-way ANOVA where total α-Amylase production, $p<0.05$ while p-value for CDW is not significant ($p = 0.341$).

The α-amylase production from 100 ml LB medium (D3) was 2167U. When the concentration of the components was reduced (D1 and D2), the level of α-amylase production decreased approximately proportionately. However, when the nutrient components were doubled (D4), the yield increased significantly, but not in proportion to the increase in the components (3527U). Increasing the components still further failed to increase either the α-amylase production. The same pattern was observed for the obtained cell dry weight for the five different concentrations of LB media components. The cell dry weight of medium D1 (0.55mg/mL) was less than 50% that of LB medium (D3; 1.3mg/mL). However, the same cell dry weight was obtained for media D4 and D5 (2.54mg/mL).

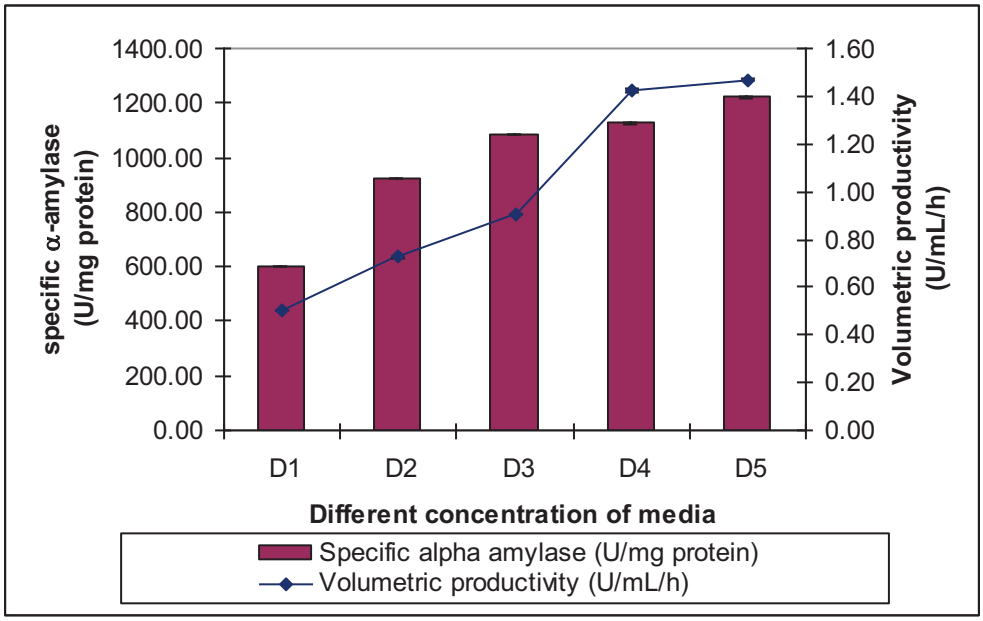

Figure 3.9: Effect of specific α-amylase (U/mg protein) and volumetric productivity (U/mL/h) of varying the composition of LB medium (Table 3.2). Cells were grown in 100ml medium at 37˚C with shaking. Statistical significance was determined with one-way ANOVA where $p<0.05$.

As shown in Figure 3.9, the specific α-amylase activity (per mg protein of the culture) for D3, D4 and D5 is greater than 1000U/mg while for D1 and D2 it is less than 1000U/mg. The volumetric productivity for α-amylase was increased 1.6-fold when D5 medium was used in place of LB medium (D3). There was a 44% reduction in volumetric productivity of α-amylase in D1 medium (0.5U/mL/h) as compared with LB medium (D3; 0.9U/mL/h).

Table 3.3: Yield and specific α-amylase production rate (U/h/mg cell) of *B. subtilis* 168 (pKTH10) grown in LB medium with shaking at 37˚C.

Different conc. media	Yield of α-amylase per ml of medium used (U/mL)	specific α-amylase production rate (U/h/mg cell)
D1	12.11 ±0.02	0.92 ± 0.0021
D2	17.41 ±0.01	0.91 ± 0.0010
D3 (LB)	21.67 ±0.02	0.69 ± 0.0008
D4	34.14 ±0.14	0.56 ± 0.0032
D5	35.27 ±0.10	0.58 ± 0.0024

As can be seen from Table 3.3, the highest yield of α-amylase per ml was obtained from cells cultured in D5 medium, followed by D4, D3, D2 and D1. These calculations of yield were based on the assumption that all of the nutrients had been consumed. D3, D4 and D5 media appeared to yield almost the same specific α-amylase production rate. The specific rates of these media were slightly lower (0.7-fold decreased) compared to D1 and D2 mediums.

3.2.3.2 Effects on the kinetics of α-amylase production of increasing individual components of LB medium

Previous results (Section 3.2.3.1) have shown that the volumetric productivity of α-amylase increased 1.6-fold when the composition of LB medium (D3) was changed to D4 or D5. Further studies were carried out to determine the relative contributions of the individual components of LB medium (NaCl, tryptone, yeast extract) were responsible for the increase in α-amylase production. Since the volumetric productivity of α-amylase for D4 (1.42U/mL/h) and D5 (1.47U/mL/h) is almost identical, further investigations were carried out to investigate which element in D4 medium is responsible for the increased α-amylase production, by increasing the concentrations of NaCl, tryptone or yeast extract individually (designated as D6, D7 and D8, Table 3.5).

Table 3.4: Variations to the components of LB medium (D3)

	Media composition (g/L)		
	Tryptone	NaCl	Yeast extract
*D3 (LB)	10	10	5
D4	20	20	10
D6	10	20	5
D7	10	10	10
D8	20	10	5

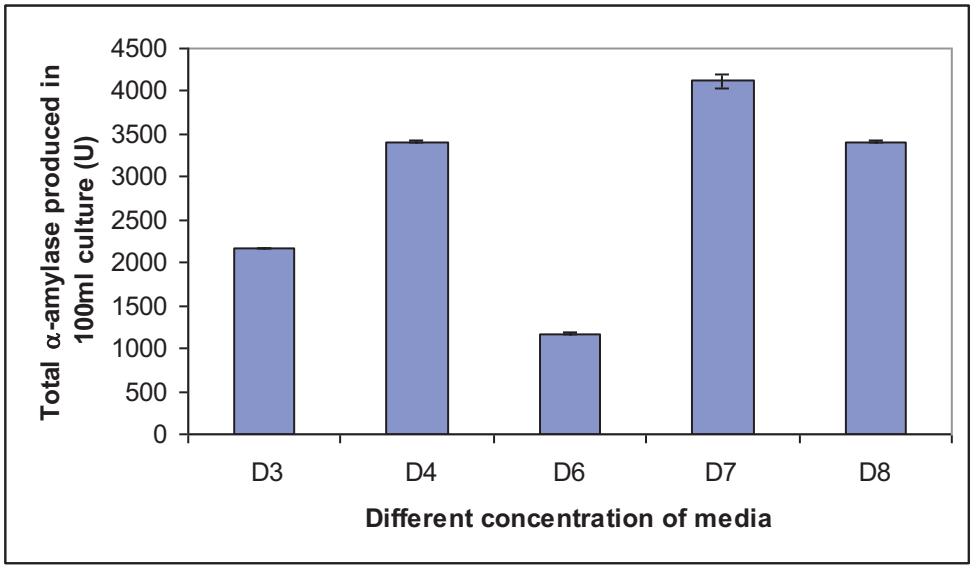

Figure 3.10: Effect on total α-amylase produced (U) of varying the composition of LB medium (Table 3.4). Cells were grown in 100ml medium at 37˚C with shaking. Statistical significance was determined with one-way ANOVA where $p<0.05$.

As can be seen in Figure 3.10, doubling the amount of yeast extract (D7 medium) improved the yield of α-amylase (4116U) considerably, almost doubling the yield obtained from LB medium (2167U). In contrast, doubling the concentration of acid-hydrolysed casein (D8 medium) only led to a 50% increase in the yield of α-amylase (3414U). Doubling the concentration of sodium chloride (D6 medium) actually lowered the amount of α-amylase produced (1173U), to about half that of LB medium (D3). As a result, the highest and lowest volumetric productivities were obtained in D7 and D6 media, respectively (Table 3.5).

Table 3.5: The kinetic data of α-amylase production for different media composition used in the batch culture of *B. subtilis* 168(pKTH10). Cells were grown in 100ml medium at 37˚C with shaking. *Statistical significance was determined with one-way ANOVA where $p<0.05$ while ** indicates that p-value = 0.488 (not significant).

Different conc. media	*Volumetric productivity (U/mL/h)	Yield of α-amylase per ml of medium used (U/mL)	**CDW (mg/ml)	*Specific activity (U/mg protein of culture)	specific α-amylase production rate (U/h/mg cell)
*D3 (LB)	0.90 ± 0.0012	21.67 ±0.02	1.30 ±0.0001	1083.5 ±1.2	0.69 ± 0.0008
D4	1.42 ± 0.0082	34.14 ±0.14	2.54 ± 0.002	1126.8 ±6.5	0.56 ± 0.0032
D6	0.49 ±0.0064	11.73 ±0.11	1.07	586.5 ±7.7	0.46 ±0.0060
D7	1.72 ±0.0436	41.16 ±0.74	2.57± 0.007	1030.0 ±26.1	0.67 ±0.0169
D8	1.42 ±0.0041	34.14 ±0.07	1.96	1138.0 ±3.3	0.73 ±0.0021

The highest cell dry weight (CDW) was obtained in D7 medium and was almost identical to the CDW in D4 medium. D6 medium produced the lowest CDW and specific α-amylase production rate, indicating that *B. subtilis* was sensitive to salt concentrations above 0.34M. On the other hand, the specific α-amylase production rates for D3, D7 and D8 media were similar, with D8 yielding the highest rate. The specific activity (per mg protein of culture) for all mediums except for D6 medium were found to be quite similar and a slightly more than 1000 U/mg protein.

3.2.3.3 Scanning electron microscopy of *Bacillus subtilis* cultures

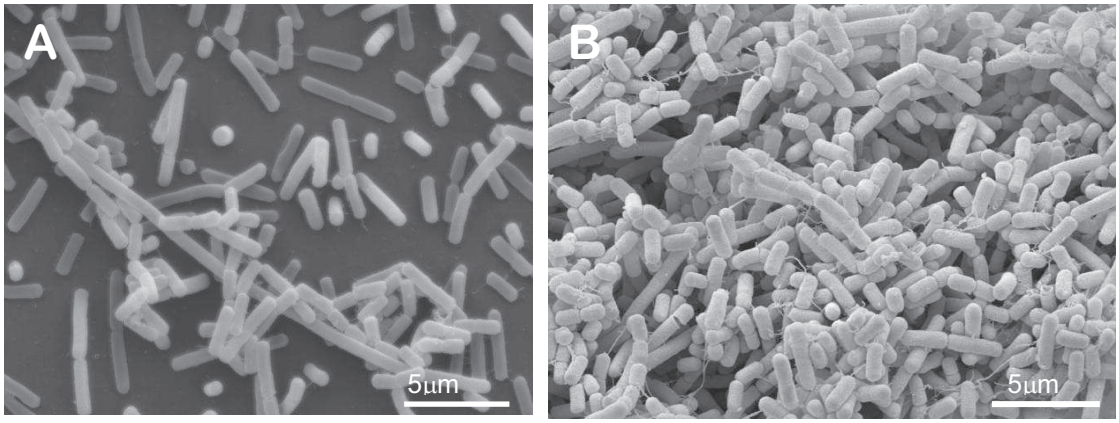

Figure 3.11: Scanning electron micrograph of batch culture (A), after 10h and (B), after 24h incubation (magnification x 5000). Cells were grown in 100ml medium at 37˚C with shaking.

LB medium was inoculated with spores of *B. subtilis* 168(pKTH10) (1 x10^6 cells) and the culture incubated with shaking at 37˚C. Samples were taken at 10h (exponential phase) and 24h (stationary phase) and prepared for scanning electron microscopy (SEM). Samples taken at 10h were heterologous in length and many were in the process of dividing (Figure 3.11). The sample also showed evidence of ungerminated spores. At 24h the cells were similarly heterogeneous in length, although generally shorter. After 10h incubation, the average cell length was 2.3 μm of length, while that at 24h was 1.5 μm of length, consistent with their being in stationary rather than exponential growth phase.

3.2.3.4 Discussion

Batch culture is a closed system or environment for growing cells, usually in a conical flask or fermenter, and operated under optimal conditions of temperature and pH. The growth cycle and kinetics of a closed system is determined by a combination of the inherent properties of the organism, the culture medium and the physical parameters (Scragg, 1991). This is in contrast to a continuous culture system, in which the growth rate can be controlled and maintained. The growth cycle of a closed system can be determined by plotting a growth curve to show the four phases of growth (lag, exponential, stationary and

death phases). Therefore, as an initial study, a batch culture of *Bacillus subtilis* 168 (pKTH10) was performed. Moreover, conventionally, this system is used for α-amylase production due to the main production phase being during stationary phase (Harwood, 1990).

Bacteria reach stationary phase due to the limitation of one or more nutrients, the accumulation of a growth inhibitory compound or a change in the physiological conditions (e.g. pH, cell density). Based on the growth curve, stationary phase was initiated after 8h incubation (Figure 3.6). The transition phase of bacteria from exponential to stationary results in a dramatic shift in the pattern of gene expression that allows the cell to survive in the changed environment.

In this study, LB (Luria-Bertani) medium, consisting of casein hydrolysate, yeast extract and sodium chloride, was used as a nutrient medium to study the productivity of α-amylase. Casein hydrolysate contains free amino acid and is expected to be an important nutrient for protein production (Pedersen and Nielsen, 2000), while yeast extract provides a source of various amino acids, simple sugars, vitamins, minerals and other growth factors to sustain a good growth of the microorganisms (Alam *et al*., 1989). The composition of this well-established medium was manipulated and to study its influence to the production of α-amylase in batch culture.

Based on the results in Figure 3.8, reducing the concentrations of the individual components (media D1 and D2), reduced the yield of α-amylase, while conversely increasing their concentration (D4 and D5) increased α-amylase production. However, there was very little difference between the amounts of α-amylase produced when media D4 and D5 were used. This might be due to a component of the D5 medium being too concentrated. The same pattern was observed for cell dry weight where the stronger concentration of media, the higher cell dry weight produced. This result indicated, as expected, that the available nutrients affect the amount of cell produced. The highest specific α-amylase production rates were obtained using the D1 and D2 media. However, since these cultures produced low amounts of α-amylase and CDW, from a total yield point of view, cells grown in the D3, D4 and D5 media were more productive (Table 3.3).

A significant increase of α-amylase production and CDW (2.57mg/mL) was observed in D7 medium (containing additional yeast extract). This indicated that α-amylase production was related to cell growth and that LB might be limiting for sources of simple sugars. The CDW obtained from this medium was similar to D4 medium. However, more α-amylase was produced in the former medium (4116U) compared to D4 medium (3414U). This showed that the supplied substrate was utilised and converted to form product rather than formation of cell mass. This was confirmed by the improved specific α-amylase production rate from 0.56U/h/mg cell to 0.67U/h/mg cell. The productivity of D8 medium was similar to that of D7 medium, but the slightly lower cell yield was reflected in a lower yield of α-amylase (Table 3.5). Finally, the higher sodium chloride content of the D6 medium reduced both CDW and the yield of α-amylase, suggesting that *B. subtilis* is sensitive to high salinity. Previous studies have reported that at high salt concentrations, *B. subtilis* secretes proline and synthesizes osmoprotectants such as glutamate and glycine-betaine (Kempf and Bremer, 1998, Wood, 1999). The decreased specific α-amylase production rates associated with D4 and D6 media was therefore most possibly due to the osmotic sensitivity of *B. subtilis* to the high content of sodium chloride in both these media.

In conclusion, production of α-amylase enzyme could be improved by manipulation the composition of the growth medium. In this study, doubling the concentration of yeast extract improved cell growth and resulted in the production of more α-amylase. On the other hand, doubling the concentration of sodium chloride had precisely the opposite effect. These results were useful for comparative studies with the immobilized cell cultures developed later in this study.

4 Viability and adhesion of *Bacillus subtilis* spore suspension

4.1.0 Introduction

The immobilization of bacterial cells onto a support matrix is affected by many factors including the physico-chemical properties of both the cells and the support matrix. As a result it is necessary to understand the cell-surface interaction and to determine how this interaction affects viability, proliferation and the migration of cells throughout the matrix.

Therefore, initial experiments were carried out to:

- Determine the physico-chemical properties of *B. subtilis* spores
- Determine whether spores can remain viable if incorporated into a polyHIPE matrix during polymerisation
- Determine whether *B. subtilis* spores germinated *in situ* on polyHIPE matrix
- Investigate whether *B. subtilis* can be cultured *in situ* on the polyHIPE matrix

4.1.1 Adhesion of *Bacillus subtilis* in relation to hydrophobicity

A simple experiment, known as bacterial adherence to hydrocarbon (BATH) assay, was carried out to determine the hydrophobicity at the surface of *B. subtilis* spores and vegetative cells. The determination of this characteristic of the bacterium was essential for understanding their likely interaction with the material surface of the various support matrices used in the experimental systems. The interaction between the bacteria and the matrix polymer is likely to influence their proliferation, viability and penetration through the support matrix.

A number of methods can be used to determine the surface hydrophobicity of bacterial cells, such as bacterial adherence to hydrocarbon (BATH) (Rosenberg, 1984, Rosenberg *et al*., 1980), hydrophobic interaction

chromatography (Ronner *et al*., 1990, Ahimou *et al*., 2001), water contact angle measurement (Ahimou *et al*., 2001) and atomic force microscopy (AFM) (Bowen *et al*., 2002). However, the former method was chosen for its simplicity and speed compared to the other methods.

BATH is based on the degree of adherence of cells to a liquid hydrocarbon following the mixing of a bacterial cell suspension with a known volume of hydrocarbon in an appropriate buffer. The results are shown in Figure 4.1.

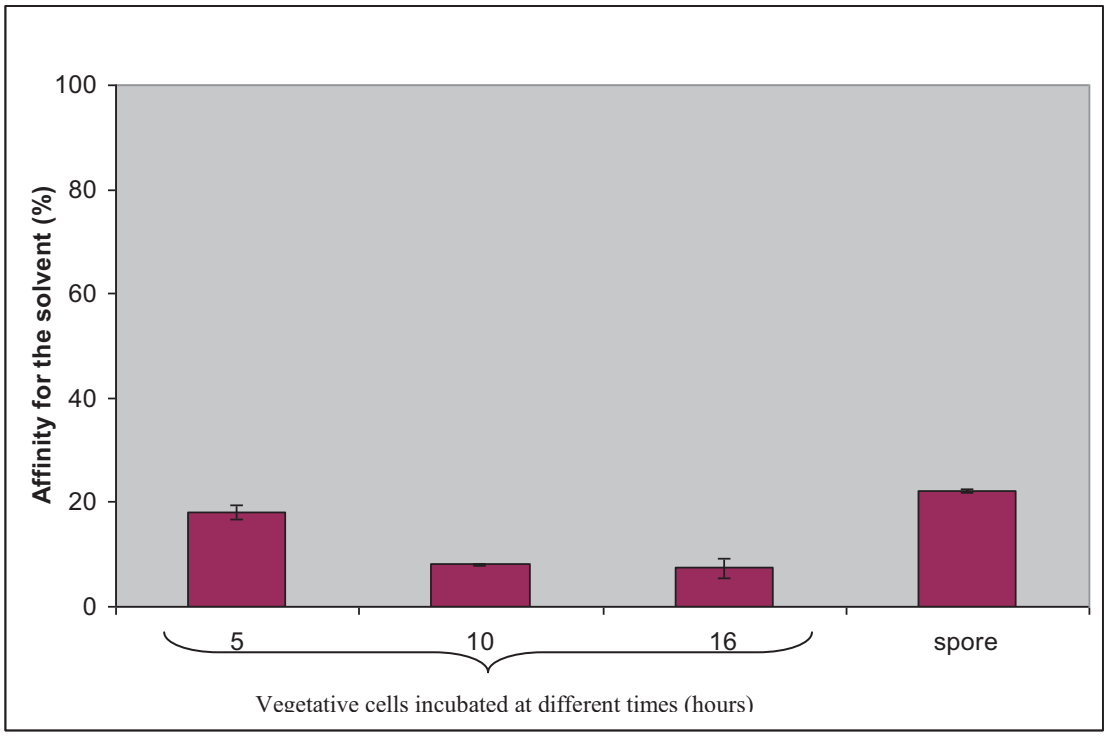

Figure 4.1: The hydrophobicity of *B. subtilis* 168 strain (pKTH10) measured using the bacterial adherence to hydrocarbon method (BATH). Two separated phases were formed after the cell suspensions were vigorously mixed with hexadecane solvent and reduction of initial absorbance of cell suspensions showed that some cells were bound to hexadecane droplets.

As shown in Figure 4.1, both the vegetative cells and spores of *B. subtilis* strain 168 (pKTH10) had a low affinity towards the hydrocarbon hexadecane. This finding was similar to previous studies that reported that vegetative cells of *Bacillus* species exhibit very low levels of surface hydrophobicity (Thwaite *et al*., 2009). Spores are generally more hydrophobic than vegetative cells, however, the observation that they had the same level of hydrophobicity as the vegetative cells might be due to a lack an exosporium in this strain (Ronner *et al*., 1990,

Koshikawa *et al*., 1989, Thwaite *et al*., 2009). In contrast, other members of the genus (e.g. *B .cereus*), which have an exosporium, show a high level of surface hydrophobicity (Ronner *et al*., 1990, Koshikawa *et al*., 1989). The exosporium consists mainly of proteins (52%), lipids (13%) and phospholipids (6%) which contribute to the hydrophobic properties of this strain (Warth, 1978).

4.1.2 Viability and resistance of a *Bacillus subtilis* spore suspension to the oil phase of PolyHIPE

One aspect of the current study was to establish whether spores could be incorporated into the polyHIPE matrix during the polymerisation reaction. This would require *B. subtilis* spores to be resistant to the chemical environment generated during polyHIPE synthesis. In other words, *in situ* inoculation of a spore suspension into the synthesized porous polyHIPE matrix. This would have the advantage of using the matrix for the storage of the *Bacillus subtilis* spores, avoiding the need to inoculate the matrix prior to use. Instead the spores can be activated as required by the addition of the growth medium. Currently, purified *Bacillus subtilis* spores are stored for long periods either lyophilised or in deionized water at 4˚C (Harwood and Cutting, 1990). Consequently, experiments were performed to study the viability of *Bacillus subtilis* spores following treatment in the oil phase of polyHIPE, which consists of styrene, divinylbenzene, vinyl pyridine and span 80.

4.1.2.1 Treatment of spore suspensions with the oil phase of polyHIPE

An experiment was carried out by adding 50µl of oil phase of polyHIPE to 0.45 ml of the spores suspension or vegetative cells in a microfuge tube and mixed vigorously with a vortex mixer. The samples were incubated at room temperature for 10 min and then, dilution plated onto LB agar plates containing 1% of starch in the presence of 10µg/ml of kanamycin. The resistance of *B. subtilis* spores to the oil phase of polyHIPE was determined by determining the numbers of colonies on LB agar plates before and after treatment with oil phase

of polyHIPE. The number of untreated and treated spores was similar, at approximately 10^8 spores per ml. The results indicated that the spores were unaffected by the treatment and that they also retained copies of the plasmids pKTH10, since all of the colonies were able to hydrolyse the starch in the medium (Figure 4.2).

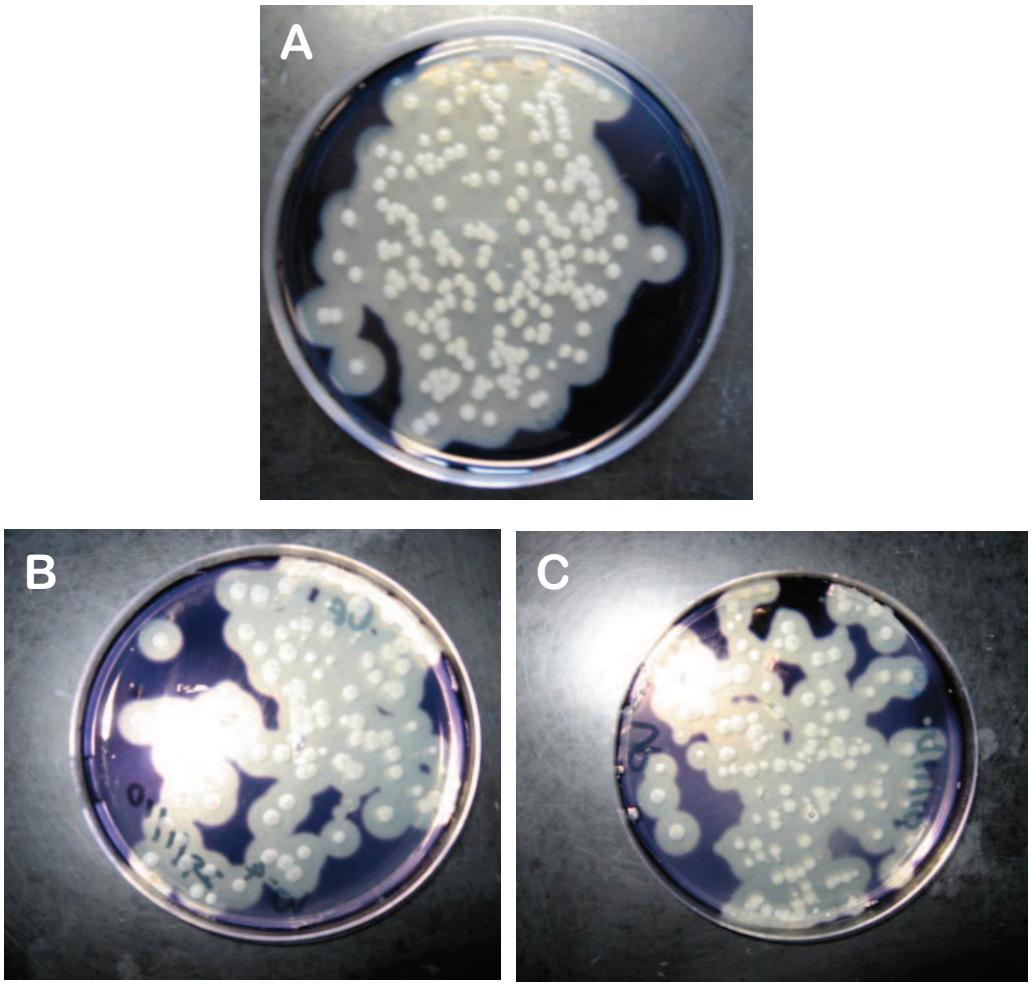

Figure 4.2: The appearance of colonies of *B. subtilis* strain 168 (pKTH10) (A) untreated and (B)&(C) treated with oil phase of polyHIPE on plates containing 1% of starch followed by exposure to iodine vapour. (B) oil phase consists of styrene, DVB and Span 80; (C) same as (B) includes vinyl pyridine.

4.1.2.2 Initial results of incorporation of *B. subtilis* spores into the synthesized porous matrix, polyHIPE

The initial results of experiments in which *B. subtilis* spores were inoculated in situ into synthesized polystyrene- divinylbenzene polyHIPE (designated as polystyrene-DVB PHPs) matrix, are illustrated in Figure 4.3. The SEM micrograph illustrates the images of polystyrene-DVB PHP inoculated with a spore suspension. There was some debris found within the matrix structure and the details of this are shown in Figure 4.3(B).

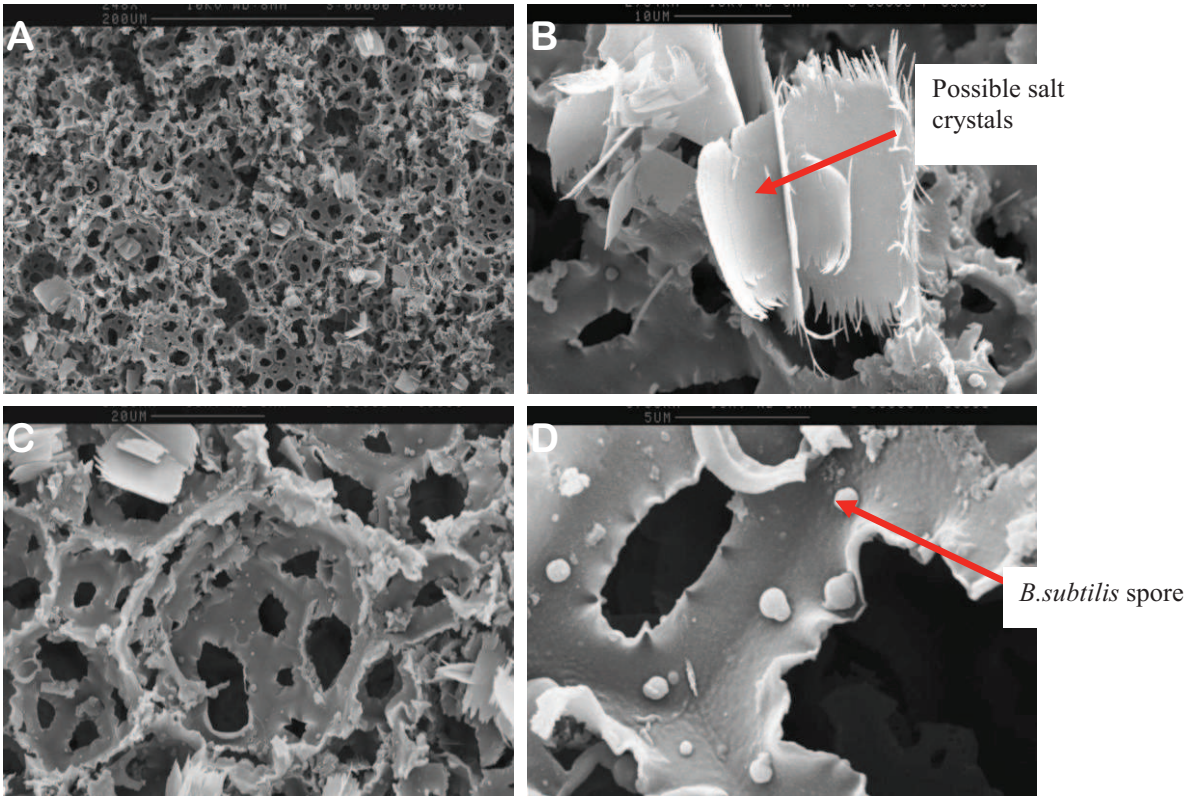

Figure 4.3: Appearance of the top surface of polystyrene-DVB PHPs matrix at various magnifications. (A) Low magification (x 250) (B) High megnification (x 2500) showing surface debris (C) a PHP matrix pore (x 1200) (D) *B. subtilis* spores attached to the surface of a pore (x 6000).

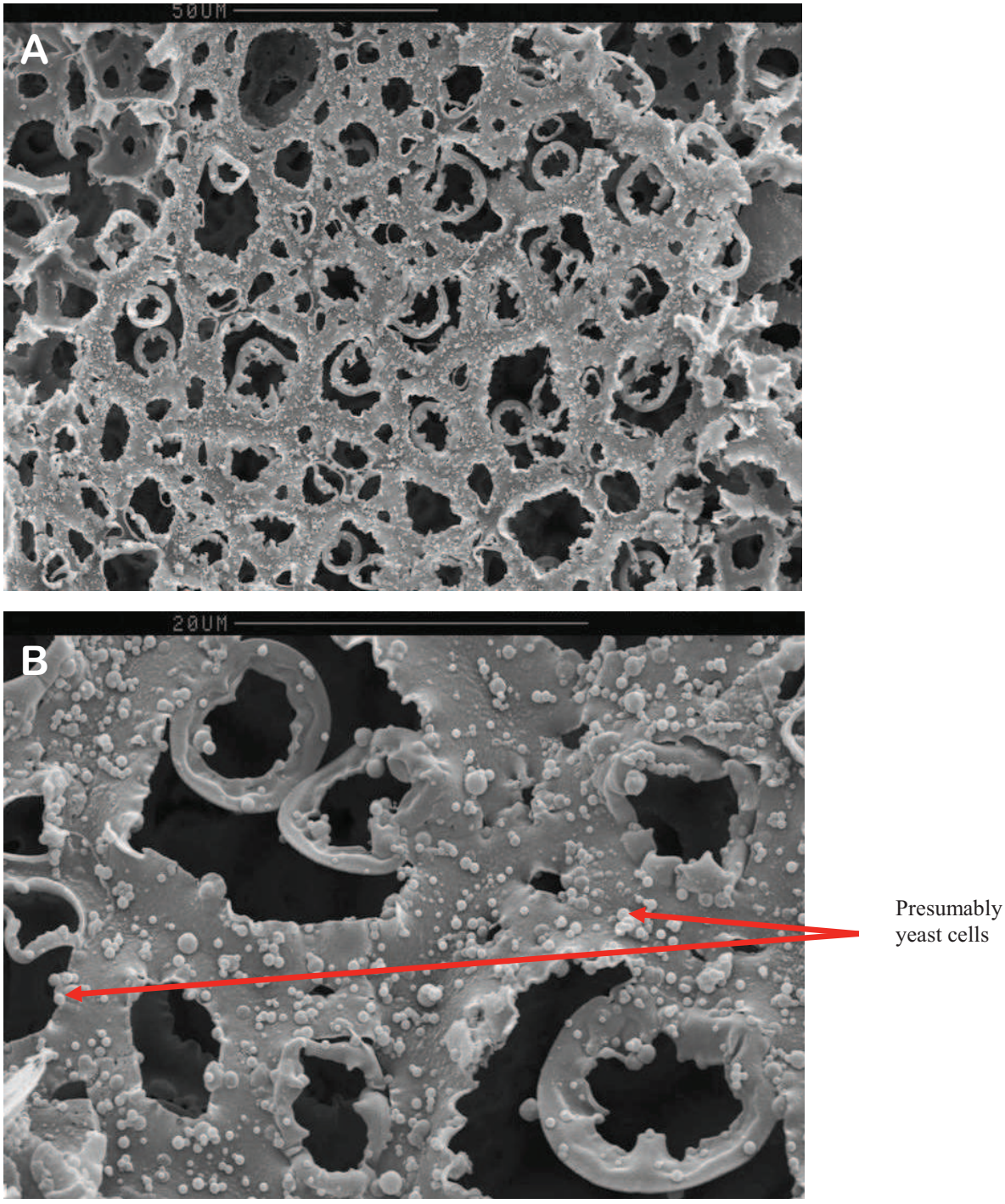

Figure 4.4: Cross-sectional appearance of the polystyrene-DVB PHP structure: (A) General area (at magnification of x 600) (B) at high magnification (x 2500)

The spores were relatively evenly distributed throughout the polystyrene-DVB PHPs matrix structure (Figure 4.4). However, in contrast to the starting suspension (Figure 3.3), the spore-like cells were heterologous in size. Although this was not confirmed, the smaller number of larger cells were thought likely to be yeast cells that were contaminating one of the solutions used to make the support matrix. After incubating overnight with a nutrient medium, the spores were activated to form vegetative cells (Figure 4.5A). During the growth of vegetative cells, an extensive extracellular matrix was observed (Figure 4.5B). It was also observed that the cells tended to attach to each other to form of a microcolony (Figure 4.5C). When viewed at a distance of 200µm from the surface, it was found that some cells were still spherical (Figure 4.5D) and these were presumably ungerminated spores.

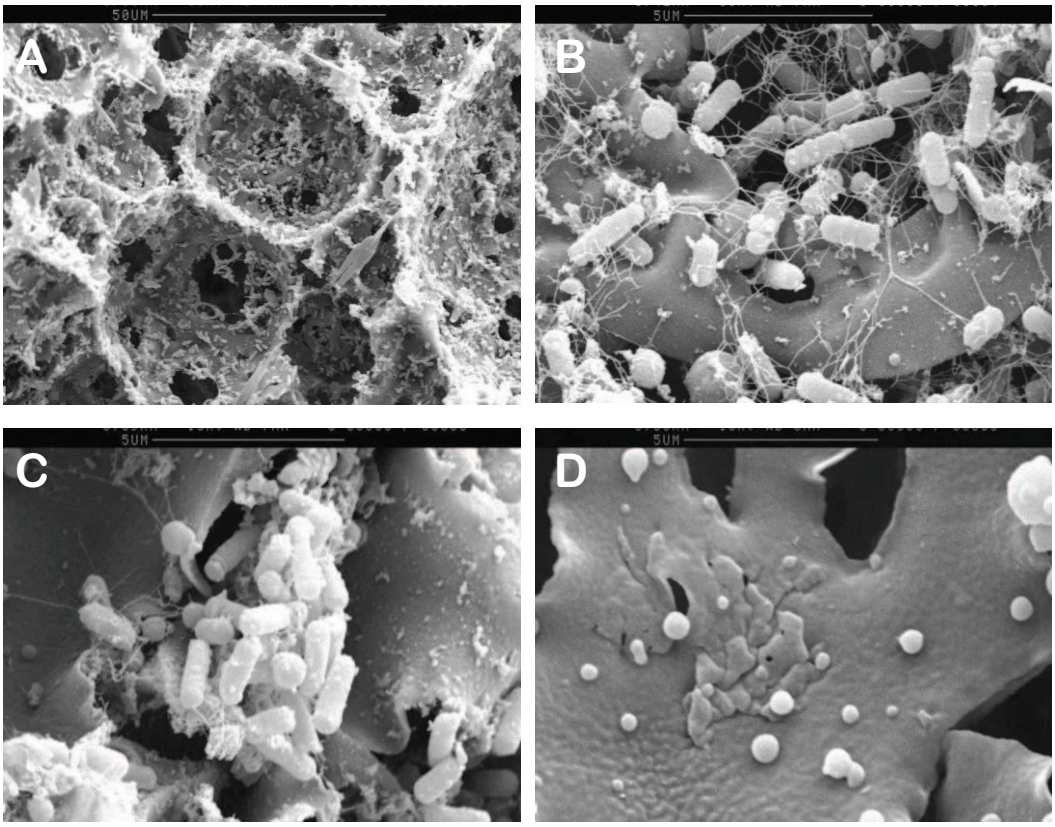

Figure 4.5: SEM of cells of *B. subtilis* 168 in the polystyrene-DVB PHPs matrix following incubating overnight in nutrient medium. The images, A-D show the same part of the matrix at different spots. The images magnification are as follows: (A) x1000, (B) x8500, (C) & (D) x8600

4.1.2.3 Discussion

The structure of *Bacillus* endospores includes, from the outside to inside, an exosporium, a spore coats, outer membrane, cortex, germ cell wall, inner membrane and central core. These multi-layered structures are responsible for the spore's resistance to a number of chemicals such as acids, bases, oxidizing agents, alkylating agents, aldehydes and organic solvents. However, certain chemicals, such as as formaldehyde, are effective in killing *B. subtilis* spores (Setlow, 2006). Many strains of *B. subtilis* are not surrounded by an exosporium or, if they are, it is greatly reduced in size, and this is likely to increase the susceptibility to inactivation by various chemicals. The result obtained in Section 4.1.2 showed that spores of *B. subtilis* were resistant to the chemicals in the oil phase of polyHIPE which contains potentially toxic chemicals such as styrene. Previous studies have reported that there are several factors that are responsible for the chemical resistance spores (Setlow, 2006). They include: i) the spore coat which provides a barrier against toxic chemicals, detoxifying these chemicals before they further diffuse deeper into more sensitive components within the spore; ii) the low permeability of spore's inner membrane which impedes the access of toxic chemicals into the core; iii) the protection of spore DNA due to the abundance of its α/β-type small acid soluble proteins (SASP) of between 60 and 70 amino acids in length; iv) DNA repair by DNA damaging chemicals.

The results of initial experiments in which spores of *B. subtilis* were inoculated in-situ into the synthesized polyHIPE matrix, showed that the spores survived this treatment and were able to germinate into vegetative cells after incubation with nutrient medium (Figure 4.5A). However, as can be seen in Figure 4.5D, some spores were found not to germinate. This might be due to their inaccessibility to the nutrient medium and/or and oxygen, and this was the subject of later studies (Chapter 6). The appearance of some contaminants or debris on the surface of the matrix was possibly because these initial experiments were not carried out under aseptic conditions. However, these experiments did show that the spores were extremely resistance to the harsh environment generated during the polymerisation reaction, and that the resulting matrix could be inoculated in-

situ with viable spores. The next chapter will discuss further study about this work.

5 Establishment of PolyHIPE polymer (PHPs)

5.1.0 Introduction

The highly porous polyHIPE polymers have made significant contributions to many technological areas, such as the separation of biological and synthetic compounds (Bhumgara, 1995a, Bhumgara, 1995b, Noor, 2006), enzyme and cell immobilisation (Erhan *et al*., 2004, Bokhari *et al*., 2003, Griffiths and Bosley, 1993, Akay *et al*., 2004, Akay *et al*., 2005a, Akay *et al*., 2005d, Bokhari *et al*., 2005, Christenson *et al*., 2007, Bokhari *et al*., 2007b) and supports for heterogeneous catalysis (Dizge *et al*., 2009a, Dizge *et al*., 2009b). These materials are synthesized by polymerising the continuous phase of a high internal phase emulsion (HIPE) in which their physical and chemical characteristics can be modified and optimized as required. This ability to modify and control their physical and chemical characteristics is the main reason for their use in a wide range of applications. Additionally, the morphology of porous polymeric materials prepared through the high internal phase emulsion process produces a well-defined structural morphology, which is more easily controlled that other methods of synthesis such as gas blowing. The physico-chemical properties of porous polymeric polyHIPE can be tailored in two approaches: the manipulation in the polyHIPE composition and modification of the operational parameters used in the preparation of the polyHIPE. The first approach can be carry out by changing the concentration of surfactant, co-monomers and cross-linking agent, and inclusion of inert diluent or non-polymerizable solvent (porogen). The latter approach involves changing operational parameters such as the dosing and mixing time, multiple feed points and the temperature of the emulsion. PolyHIPE polymers can be characterised by their architectural, chemical and mechanical properties. In this study, only the first two properties were characterised in relation to changes in the operational conditions used for the synthesis of the polyHIPE polymers.

The synthesis of porous polymeric materials can be carried out through water-in-oil (W/O) and oil-in-water (O/W) HIPEs. Materials used to produce

W/O polyHIPE polymers are based on compounds such as styrene/divinylbenzene, 4-vinylbenzyl chloride, aryl acrylates and glycidyl methacrylate. W/O polyHIPE polymers exhibit high porosities and interconnectivities and hydrophobic properties. In this study, styrene/DVB PHPs was used to synthesize polyHIPE polymers (designated as polystyrene-DVB PHPs), and these were then subject to chemical modification to modify their characteristics.

PolyHIPE matrix pore sizes can be classified into four types: basic pores, coalescence pores, microcapillary pores and nanopores. The pore sizes of basic pores are smaller and their structure is more stabilize than coalescence pores. Larger sized coalescence pores are formed from unstable HIPE during polymerization where the film ruptures and turn affects the dispersion of the water droplets in the emulsion (Akay *et al*., 2005b) (where two droplets combine to form a large droplet). A special fabricated mould with inserted-rods is used to synthesize the microcapillary pores and which have minimum diameters as low as 10 microns.

Previous studies have shown that the penetration, differentiation and viability of biological cells are effected by the architecture of the matrix. The affected parameters include pore and interconnects sizes and chemical structure (Akay *et al*., 2002a, Akay *et al*., 2004, Erhan *et al*., 2004). The sizes of pores and interconnects are of the utmost importance in the design of carriers because they influence the efficiency of cell immobilization and the efficiency of the bidirectional transport of substrates and waste through the carrier. Moreover, this physical architecture is also essential for the migration of cells through the carrier/matrices. If optimal pore and interconnect sizes can be identified, the leakage of cells from the bottom of the matrix or their accumulation at the top can be minimized. Additionally, the homogeneous distribution of internal structure of the carriers is also important to ensure that the same or similar physiological condition exist throughout the matrix, resulting in the consistent growth and behaviour of individual cells throughout the entire population (Bokhari *et al*., 2007b).

According to previous studies, the optimal pore size for bacterial or yeast cells was between one and four times of the largest dimension of the cells (Karel *et al*., 1985b). Therefore, the target pore and interconnect sizes in this study were

20μm, and 5μm, respectively, based on the size of *B. subtilis* spores and vegetative cells. As discussed in Section 1.1.2.1, the microstructure of PHP can be controlled by changing the dosing and mixing times, and the emulsification temperature. In this study, the target pore and interconnect sizes were determined by changing the first two parameters since the latter parameter would yield PHP with a larger pore size. Similar processing conditions were subsequently used to produce the chemically modified polyHIPE through inclusion of vinyl pyridine into the oil phase.

Therefore, the objectives of the work in this chapter were to:

- investigate the effect of polyHIPE pores and interconnects size and their distribution by changing dosing and mixing time parameters,
- produce polyHIPE with the targeted pore and interconnects size,
- investigate the effect of chemically modifying polyHIPE with respect to its physical architecture (pores and interconnects size).

5.1.1 Results

5.1.1.1 Determination of operating conditions for preparation of PolyHIPE polymers

In this study, the target pore and interconnect sizes were 20μm and 5μm, respectively. Two parameters were controlled to achieve these micro-architectural properties, namely the dosing and mixing times. The dosing time, t_D, is defined as the time taken for the aqueous phase to be transferred to the mixing vessel which contained the oil phase initially. The mixing time, $t_{M,}$ is denoted as the time the aqueous and oil phases are mixed by the impellers to create an emulsion. The phase volume used in this study was 85% which has been demonstrated from pervious work (Akay *et al*., 2005d) to produce small pore and interconnect sizes and a more closed structure, the latter due to the smaller number of interconnecting holes per pore. The phase volume is equivalent to the total porosity of the polymeric material which is the associated of the void spaces provided by the sum of all the pores and interconnects contained within the

structure. The reduced volume of the aqueous phase at the emulsion stage provides a sufficient surface area for the bacteria to attach to.

The operating conditions used in these experiments are shown in Table 5.1. A general view of micro-structure of polystyrene-DVB PHPs is shown in Figure 5.1 and the details of its microstructure are shown in Figure 5.2. All experiments were carried out three times.

Table 5.1: Experimental conditions used for making polystyrene-DVB PHPs

PHP Code No.	Dosing time (t_D, min.)	Mixing time (t_M, min.)
T3	5	20
T5	10	20
T7	10	30
T9	10	60

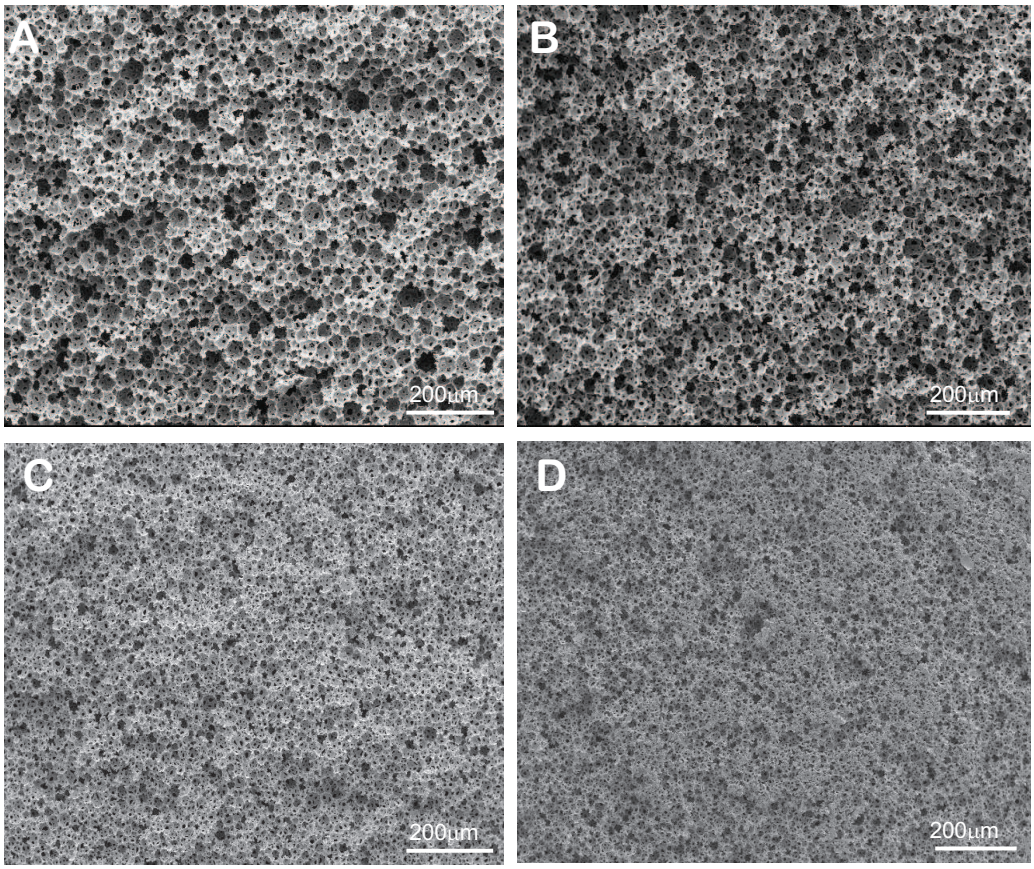

Figure 5.1: Micrographs showing the effects of dosing and mixing times on the micro-physical architecture of polystyrene-DVB PHPs (A) T3 (t_D5/t_M20) (B) T5 (t_D10/t_M20), (C) T7 (t_D10/t_M30) and (D) T9 (t_D10/t_M60). Magnification bar for all micrograph images is 100x.

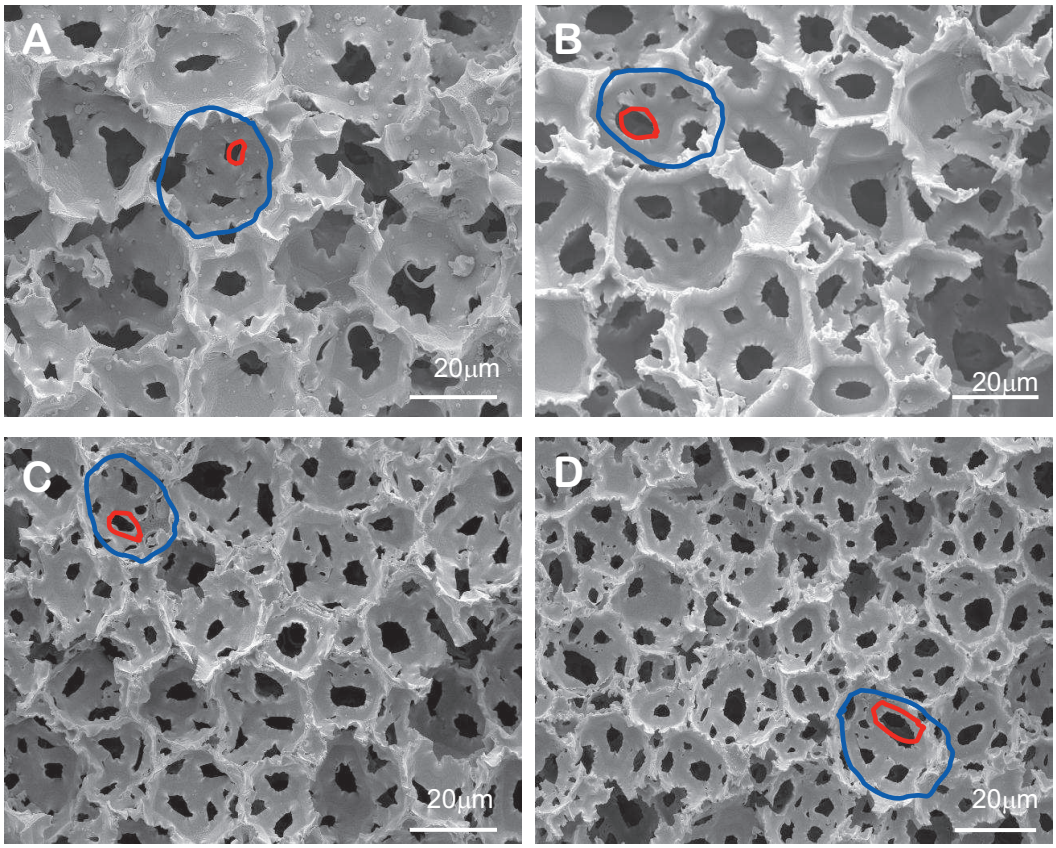

Figure 5.2: High resolution micrograph images illustrating the effects of dosing and mixing rates to the micro physical architecture of polystyrene-DVB PHPs. (A) T3 (t_D5/t_M20) (B) T5 (t_D10/t_M20), (C) T7 (t_D10/t_M30) and (D) T9 (t_D10/t_M60). Magnification bar for all micrograph images is 1000x. (The red and blue circles represent the interconnect and pore sizes, respectively).

As can be seen in Figure 5.2(A) & (B), and Table 5.2 the pores size of sample T3 (43.0μm ± 0.60) is slightly bigger than sample T5 (36.0μm ± 0.04), even though the mixing time was similar. However, even though the interconnect sizes of the T3 and T5 samples are similar, the variance of the T3 interconnects sizes is slightly lower than that of the T5 sample. It appears that the additional 5 minutes of dosing time of the T5 sample results in the more uniform formation of interconnects throughout the structure. When the mixing time was increased from 20 to 30 minutes (samples T5 and T7, repectively), the average pore size decreased from 36.0μm to 24.0μm and the interconnect size from 9.0 μm to 7.0 μm. Extending the mixing time still further to 60 min (sample T9) have very little effect on the pores and interconnects (compare T7 and T9). It was found that the additional 30 minutes of mixing time from 30 to 60 minutes resulted only 10% different of pore size as shown in Figure 5.2. The summary of all experimental conditions and evaluation of pore and interconnect sizes of PHPs is shown in Table 5.2.

Table 5.2: Average of pore and interconnect sizes determined from four independent samples prepared under different experimental conditions to establish the optimal mixing and dosing time for preparation of PHPs. The composition of the standard aqueous and rigid oil phases are given in Section 2.1.2.

PHP Code No.	Dosing time (t_D, min.)	Mixing time (t_M, min.)	Pore size (μm)	Interconnect size (μm)
T3	5	20	43.0 ± 0.60	9.0 ± 0.13
T5	10	20	36.0 ± 0.04	9.0 ± 0.17
T7	10	30	24.0 ± 0.98	7.0 ± 0.01
T9	10	60	20.0 ± 0.43	6.0 ± 0.21

The data from the mixing/dosing experiments established that the parameters required to obtain an average pore size of approximately 20μm and consistent interconnect sizes are a dosing time of 10 minutes and a mixing time of 30 minutes, giving at total preparation time of 40 minutes. Doubling the mixing time only had a small affect on the pore size, reducing it from 24μm to 20μm.

Similar observation was also found to interconnect size (from 7.0μm to 6.0μm, not very much different with target size of interconnect 5.0μm).

5.1.1.2 Distribution of pores and interconnects size of PolyHIPE polymers

A key property of any porous materials used as cell carriers/matrices is to ensure that it has a homogeneous morphology. This is because the matrix structure will affect the growth pattern of the immobilized cells and, as reported in previous studies (Akay *et al*., 2004, Akay, 2005, Bokhari *et al*., 2007b) will influence to their metabolic activity. Therefore, in this study, the distribution of pores and interconnects size of polyHIPE polymers was evaluated (Section 2.3.1) by plotting the diameter of the determined physical structures against frequency, using the statistical software Minitab v. 15.0. Based on this analysis, the ratio of average diameter interconnects (d) and pores (D) was calculated to provide an indication of the degree of interconnected pore network of the generic porous material. The higher the value of d/D, the greater the interconnection of the porous material (Bokhari et al., 2007b). Matrices with higher d/D values allow true three-dimensional cell growth because they allow the cells to permeate through the entire void volume enclosed within the carrier (Barbetta *et al*., 2005b).

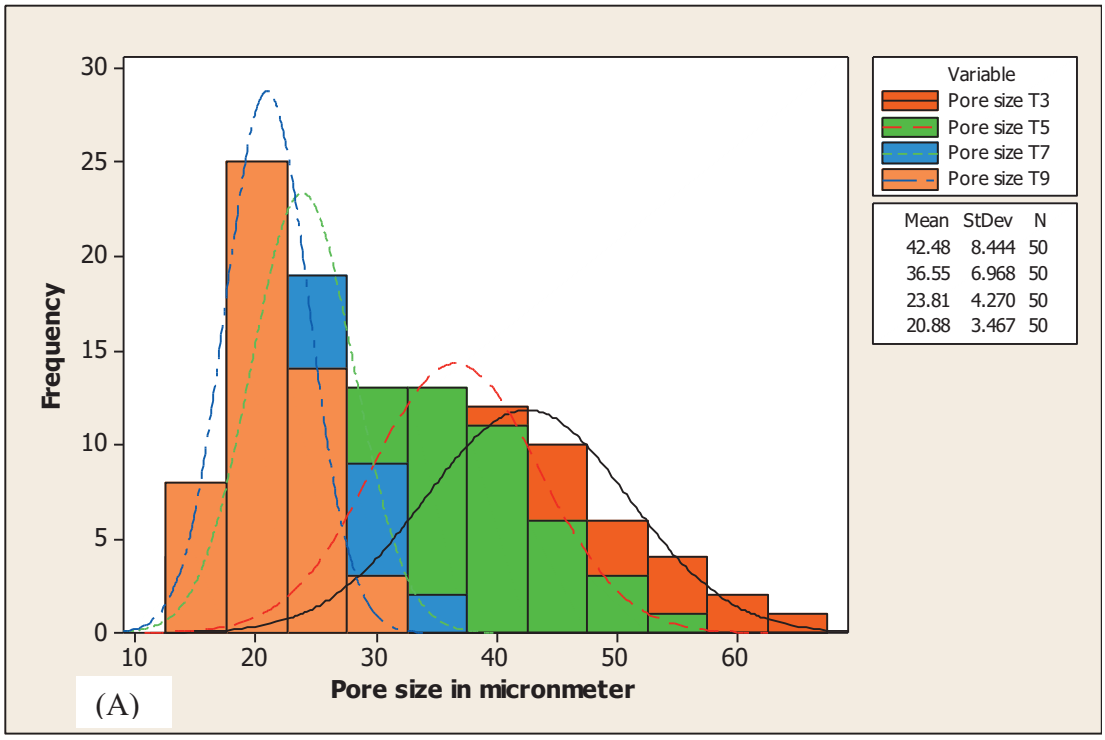

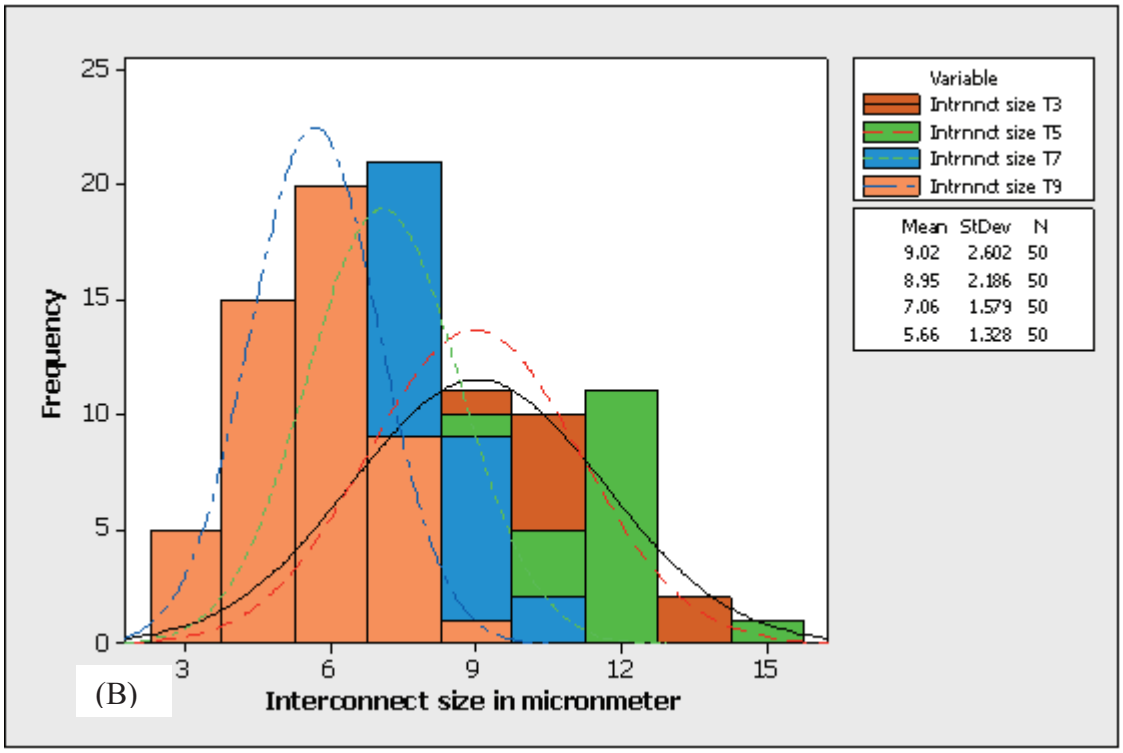

Figure 5.3: Distribution of the diameter of (A) pores and (B) interconnects, as determined from SEM images for polystyrene-DVB PHPs samples T3, T5, T7 and T9 using software Minitab 15.0.

Generally, the distribution of pore sizes for samples T3 and T5 are wider than those of samples T7 and T9, as can be seen in Figure 5.3A. The relatively narrow pore size distribution of samples T7 and T9 peaked at between 20 and 25μm. The same trend was observed for the distribution of interconnects sizes. The distribution of interconnect sizes was narrower for samples T7 and T9 than for samples T3 and T5 and the distribution of samples T7 and T9 peaked at between 5 and 7μm (Figure 5.3B). It appears that the extended mixing time in samples T7 and T9 allows the emulsion droplets to be broken up into more uniform sizes , which in turn provides an matrix with a more uniform structure. This is confirmed by the d/D value of samples T7 and T9, which is 45% higher than for sample T3. The summary the evaluation of pore and interconnect sizes of PHPs is shown in Table 5.3.

Table 5.3: Pore and interconnect diameter sizes of four independently prepared polystyrene-DVB PHPs samples used to calculate the d/D parameter.

PHP Code No.	Pore size (D,μm)	Interconnect size (d,μm)	d/D
T3	43.0 ± 0.60	9.0 ± 0.13	0.21
T5	36.0 ± 0.04	9.0 ± 0.17	0.25
T7	24.0 ± 0.98	7.0 ± 0.01	0.30
T9	20.0 ± 0.43	6.0 ± 0.21	0.30

5.1.1.3 Effect of chemical modified PHPs to the pores and interconnects size

There are a number of methods that can be used to modify the physico-chemical properties of polyHIPE polymers (PHPs) to suit various applications. They are including the manipulation of the composition oil and aqueous phases used to prepare polyHIPE polymers. For examples, there are reports outlining the influence of changing the surfactant concentration (Sorbitan monooleate, Span 80) in the oil phase (Williams *et al*., 1990), the additional of electrolytes ($K_2S_2O_8$) in the aqueous phase (Williams *et al*., 1990), the additional of 2-ethylhexyl acrylate (2-EHA), 4-vinylbenzyl chloride (4-VBC) (Jeřábek *et al*., 2008) in the oil phase and others. In this study, the polyHIPE polymer matrices were chemically modified through an additional of the co-monomer, 2-vinyl pyridine (2-VP; Figure 5.4a) into the oil phase used in preparing PHP to enhance the hydrophilicity of PHP. The presence of pyridinic nitrogen atoms in 2-VP may facilitate interactions such as hydrogen bonds with the styrene groups of polyHIPE polymers. The 2-VP monomer also had been used in several studies for the synthesis miscible polymer blends, including poly(hydroxyether terephthalate ester with poly(4-vinylpyridine) (Liu *et al*., 2005), poly(vinyl phenyl ketone hydrogenated) and poly(styrene-co-4-vinylpyridine) (Maldonado-Santoyo *et al*., 2004) and many others. This chemically modified polymeric matrice is then called vinylpyridine polyHIPE polymers (TVP-PHPs).

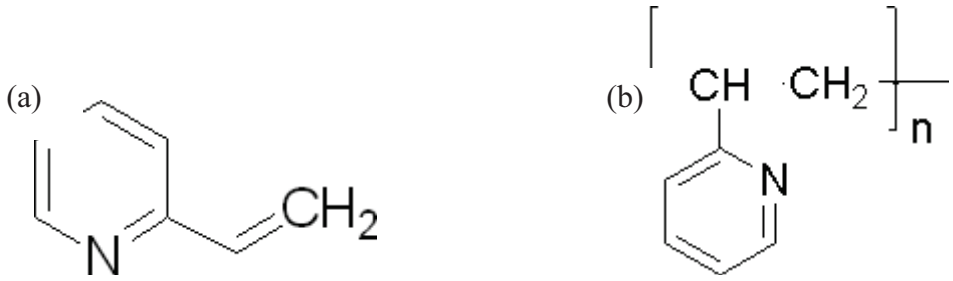

Figure 5.4: Chemical structure of (a) 2-vinylpyridine and (b) poly(2-vinylpyridine

Table 5.4 shows the operating conditions used to prepare chemically modified polymeric matrix called vinylpyridine polyHIPE polymers (TVP-PHPs) and the

details of the microstructure of these modified polyHIPE polymers are shown in Figure 5.5.

Table 5.4: Experimental conditions used for making vinylpyridine polyHIPE polymers (TVP-PHPs)

PHP Code No.	Dosing time (t_D, min.)	Mixing time (t_H, min.)
TVP-3	5	15
TVP-4	10	10
TVP-5	10	30

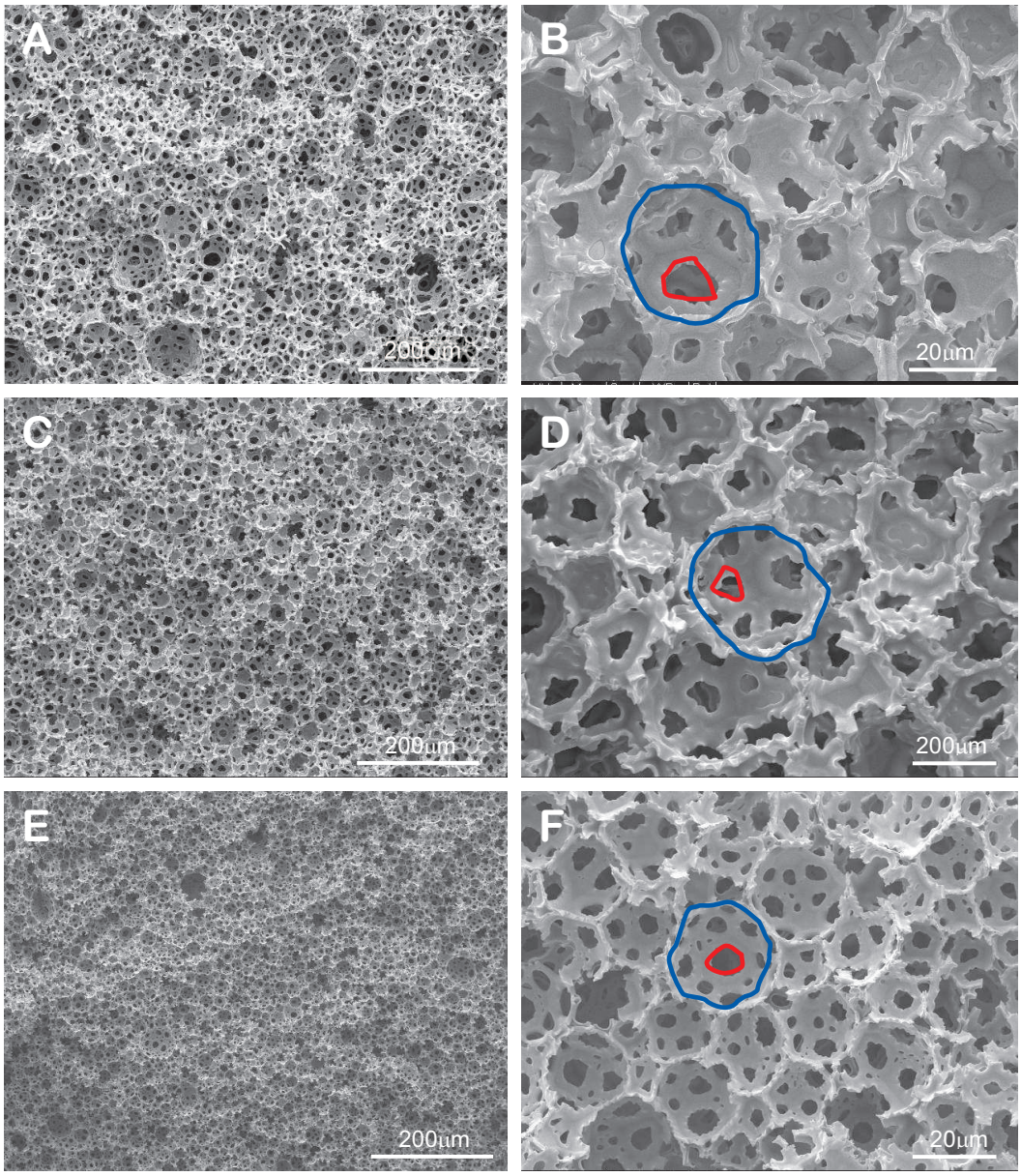

Figure 5.5: Scanning electron microscopy images showing the micro physical architecture of (A&B) TVP-3, (C&D) TVP-4 and (E&F) TVP-5. (The red and blue circles identify, respectively, typical interconnects and pores).

The same trend of microstructures of modified polyHIPEs were obtained when different dosing time and mixing time were used; the longer the mixing time, the smaller and more uniform were the pores sizes obtained. As can be seen in Figure 5.5(A) & (B), and Table 5.5 the pore size of sample TVP-3 (34.0µm ± 0.22) was 13% higher than TVP-4 (30.0µm ± 0.42), even though the total preparation time was similar (20 min.). However, the interconnects sizes of the TVP-3 was 30% higher than TVP-4 sample. As explained before, the additional of 5 minutes of dosing time of the TVP-4 sample resulted more uniform

formation of interconnects throughout the structure. When the same condition of dosing and mixing time used to prepare the T7 sample was applied for preparation of TVP-5, and the pore and interconnect sizes were similar. However the variance of interconnect size of TVP-5 was higher than the interconnect size of T7.

The summary of the evaluation of pore and interconnect sizes of PHPs as well as its d/D values are shown in Table 5.5.

Table 5.5: Evaluation of diameter of pore and interconnect of three different vinylpyridine polyHIPE polymers (TVP-PHPs) samples to determine the d/D parameter compared to polystyrene-DVB polyHIPE polymers, T7 sample.

PHP Code No.	Pore size (D,μm)	Interconnect size (d,μm)	d/D
T7	24.0 ± 0.98	7.0 ± 0.01	0.30
TVP-3	34.0 ± 0.22	13.0 ± 0.37	0.38
TVP-4	30.0 ± 0.42	10.0 ± 0.20	0.33
TVP-5	24.0 ± 1.05	6.5 ± 1.16	0.27

The distribution of pore size and interconnect size of all vinylpyridine polyHIPEs samples is shown in Figure 5.6.

The distribution of pore sizes for samples T7 and TVP-5 was narrower than that of samples TVP-3 and TVP-4, as can be seen in Figure 5.6A. The pore size distribution of samples T7 and TVP-5 peaked at between 20 and 25μm. The same trend was observed for the distribution of interconnect sizes. The distribution of interconnect sizes was wider for samples TVP-3 and TVP-4 than for samples TVP-5 and T7 and the distribution of the latter two samples peaked at between 6 and 8μm (Figure 5.6B). The pore and interconnect size of TVP-5 were similar with T7 (Table 5.5) as the same operating condition was used. It appears that the additional of 5% of vinyl pyridine into the oil phase did not change very much the microstructure of polyHIPEs samples.

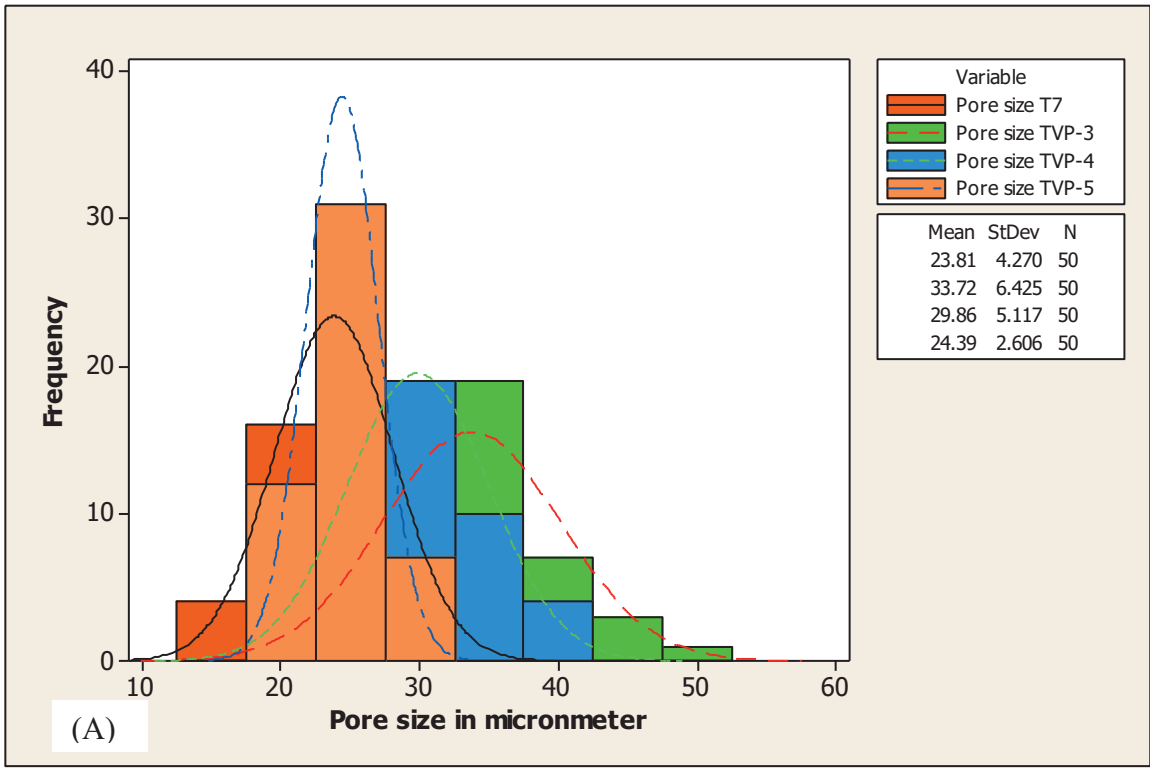

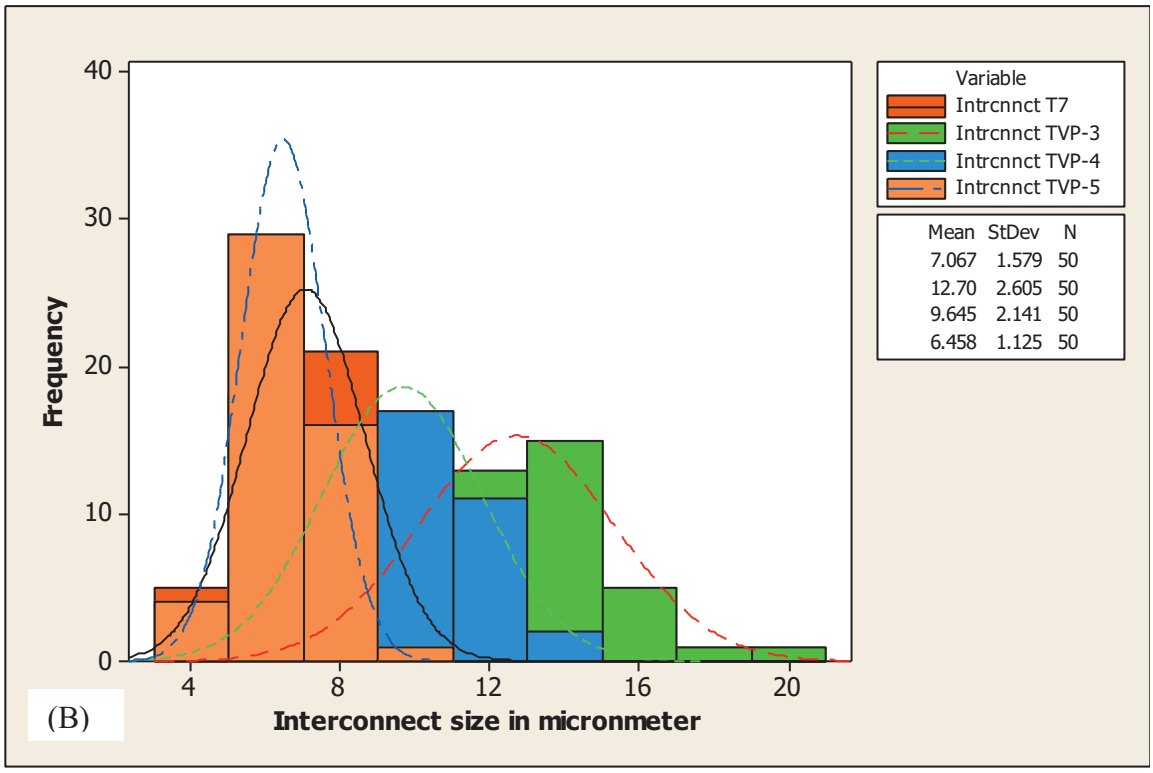

Figure 5.6: Distribution of diameter of (A) pores and (B) interconnects from SEM images for vinylpyridine polyHIPEs samples TVP-3 TVP-4, TVP-5 and compare with T7 using software Minitab 15.0.

5.1.1.4 Characterisation of vinyl pyridine modified PHPs by Fourier Transform Infrared Spectroscopy (FT IR)

Fourier transform-infrared spectroscopy (Varian 800 FT-IR fitted with a Pike ATR unit, Varian Inc.) was used to examine the chemical composition of TVP-PHP. This technique gives useful structural information about the presence of both authentic compounds and of any unexpected compounds in the matrix, based on the obtained FTIR spectra. The FTIR spectrum is generating from the molecular absorption and the conversion of the frequencies of the infrared radiation into molecular vibration energy, which is then represented as series of bands. The FTIR spectra of the unmodified PHP, polystyrene-DVB PHP (T7) and vinylpyridine PHP (TVP-5) are shown in Figure 5.7A and Figure 5.7B, respectively.

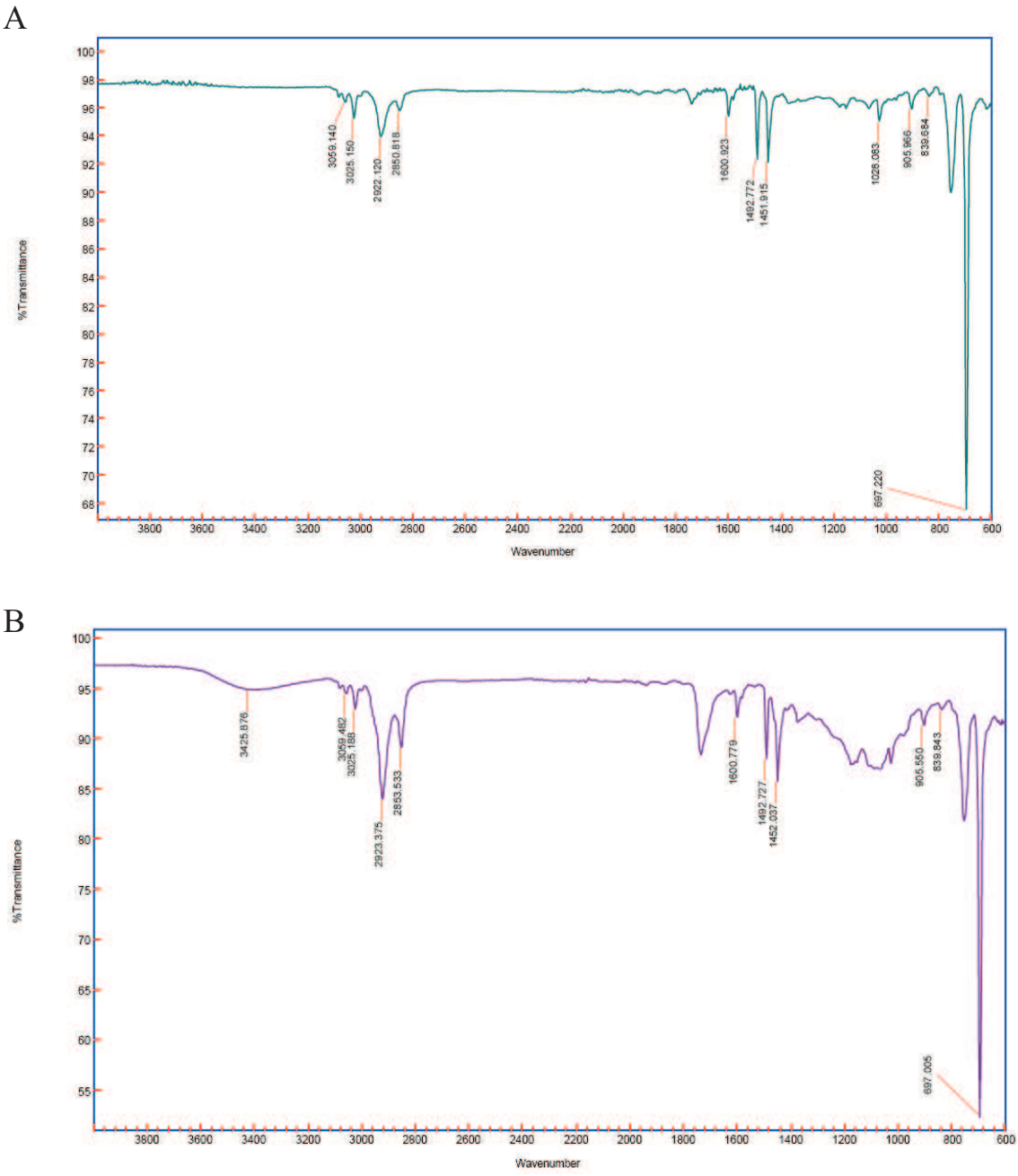

Figure 5.7: Infrared spectra of (A) polystyrene-DVB PHP, sample T7 and (B) vinylpyridine-PHP, sample TVP-5.

As can be seen from the FTIR spectrum (Figure 5.7A), the characteristic absorption bands of sample T7 (polystyrene divinylbenzene polyHIPE) are assigned as follows: (1) 697.2 cm^{-1} : out of phase ring deformation; (2) 839.7 cm^{-1}: represents a doublet band of polystyrene; (3) 905.9cm^{-1}: monosubstituted phenyl ring; (4) 1451.9 cm^{-1}: C-H bending; (5) 1492.7 cm^{-1} represents C-C bonds of polystyrene; (6) 1600 cm^{-1}: aromatic C=C stretching; (7) 2922.1 cm^{-1} : asymmetric CH_2 stretching (8) 3025.2 cm^{-1} and 3059.1 cm^{-1} :

aromatic C-H stretching. The same peaks were observed for TVP-5 sample excepting for the broad absorption band caused by the hydrophilic 2-vinyl pyridine at 3100 – 3650 cm^{-1}, as shown in Figure 5.7B.

5.1.1.5 Surface area measurement

The measurement of surface area of all PHPs samples were performed using the Coulter SA3100^{TM} Series Surface Area and Pore Size Analyzer. The gas sorption method is used by this analyser where nitrogen and helium are used as gas adsorbates. This method can be simplified as the physical characterisation of material structures using a process where gas molecules of known sizes are condensed (or adsorbed) on unknown sample surfaces. The quantified amount of condensed gas and the recorded resultant sample pressure at constant temperature are then used for subsequent calculation. These data are required for construction of isotherm which is subjected to a variety of calculation models to obtain surface area results. The BET (Brunauer, Emmett and Teller) is the most commonly model used calculation method for the sample specific surface area determinations. The results of all PHPs samples determined by the BET calculations are shown in Table 5.6. The surface area of the chemically modified TVP-PHP was slightly lower than the unmodified PHP, T7.

Table 5.6: The BET surface area of chemically modified vinylpyridine-PHP compared to polystyrene-DVB PHPs

PHP code	BET surface area (m^2/g)
T5	4.68 ±0.34
T7	5.10 ± 0.10
TVP-5	4.15 ± 0.41

5.1.1.6 Capacity water uptake by polystyrene-divinylbenzene polyHIPE and vinylpyridine polyHIPE

The water uptake capacities of the polystyrene-DVB PHP and vinylpyridine PHP were calculated on basis of the mass increase (with respect to the original dry mass) obtained after being held under water of water surface for 24h. The result is shown in Figure 5.8.

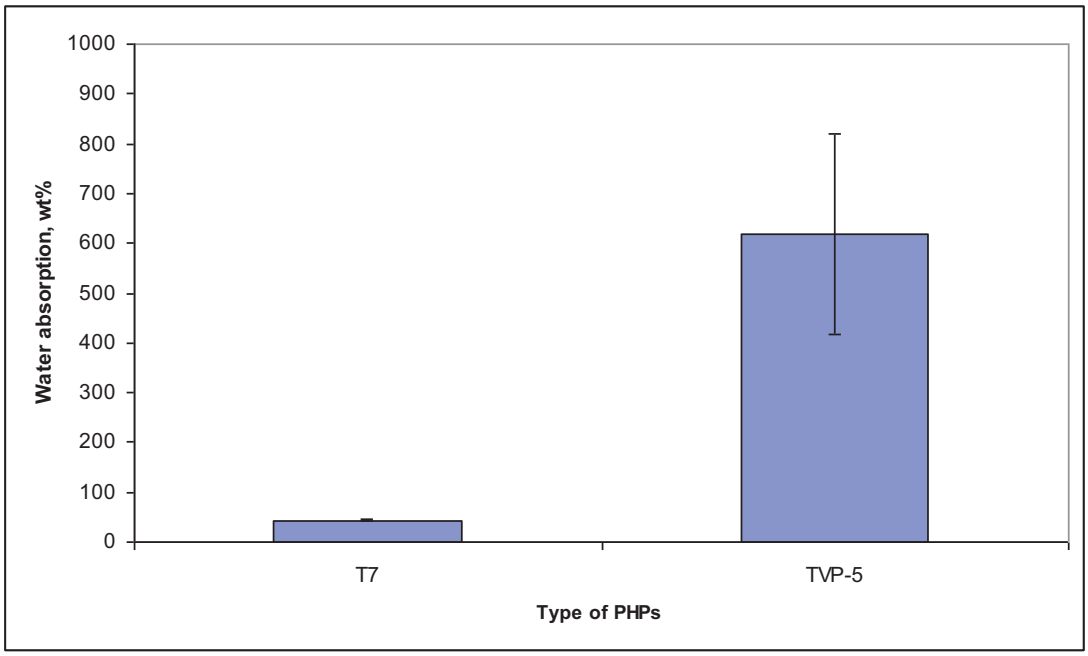

Figure 5.8: Comparison of the water absorption characteristics of polystyrene-DVB PHP, T7 and vinylpyridine PHP, TVP-5.

These data showed that the water uptake by sample T5 of the polystyrene-DVB PHP matrix was very much lower (less than 100 wt%) than that of vinylpyridine PHP, TVP-7 (more than 600 wt%).

5.1.2 Discussion

In this chapter, polyHIPE polymers (PHPs) were prepared at different dosing time and mixing time and the effect of these parameters on the microstructures of PHPs were investigated before these PHPs are used as a matrix for immobilization cell. A key parameter for the production of PHP matrices is to identify mixing and dosing parameters that were able to produce reletively homogeneous polymers with a pore size of between 20 and 25μm and consistent interconnect sizes. Short dosing times yielded irregular pore and interconnect structures as can be seen in Figure 5.2(A). As shown in Figure 5.1 and Table 5.2 increasing the mixing time upto about 30 min led to a clear reduction in the pore size. This is because increasing the mixing time provides a longer period to supply energy to the droplets in the emulsion: the higher energy state results in a smaller droplet size. However, there is a limit to the amount of energy supplied to the emulsion and further increases in the mixing time only had a small influence on reducing pore size. A higher mixing rate leads to an increase in the viscosity of the polyHIPE formed. Since the composition and volume of the oil and water phases were kept constant, the changes in viscosity were likely to be the result of an increased in droplet-droplet interactions. Additional of 5% of 2-vinyl pyridine into oil phase of polyHIPE polymers did not affect very much the pore and interconnect sizes of polyHIPE polymers (Table 5.5 and Figure 5.6).

Samples T7 and T9 yielded the highest d/D values. These two samples were prepared using the longer of mixing times that stabilizes the formation of emulsion. As a result, they developed a more highly interconnected pore structure of polyHIPE than samples T3 and T5, with shorter mixing times.

The water absorbing capacity of polystyrene-DVB PHP matrices were limited by their hydrophobicity. Therefore experiments were carried to determine whether the water absorbing capacity of the matrices could be increased by changing the chemical composition of the PHP by adding 2-vinylpyridine to the oil phase. The vinylpyridine PHP matrix had almost similar pore and interconnect size as the polystyrene-DVB PHP but about 6 times the water uptake capacity. The higher water uptake capacity of vinylpyridine PHP was likely to be due to the

polar nature of the pyridine groups in this type of PHP as compared with the nonpolar nature of the styrene groups in polystyrene-DVB PHP.

The surface area of TVP was slightly smaller than that of unmodified samples T5 and T7. Previous studies reported that polyHIPE based on water-in-oil (W/O) HIPE polymers exhibit low surface areas (around $5m^2/g$).

In conclusion, the current studies have shown that the conditions used for the preparation of HIPE emulsions influences the cellular morphology of the final polyHIPE matrices. Specific chemically modifications can be targeted to produce PHPs with appropriately changed physical properties. In this study, the produced modified polyHIPE with vinyl pyridine which prepared with the same operating condition (TVP-5 compared to T7) has the same pore (24μm) and interconnect size (7μm) and its surface area ($4.15\ m^2/g$) is almost similar with the polystyrene-DVB polyHIPE ($5.10m^2/g$). However, the modification of the polymer by the introduction of pyridine groups increased the hydrophilicity (approximately increased by 14%) of the polymer and a concomitant increase in its capacity to take up water.

6 Incorporation of a *Bacillus subtilis* spore suspension into a PolyHIPE matrix during synthesis

6.1.0 Introduction

Living microbial cells can be immobilized by entrapment into preformed porous matrices or *in situ* during the synthesis of the matrix. The selection of the materials used to entrap the microbes is important since they must be biocompatible and not have negative affects on cell viability or on any products they produce (e.g. extracellular enzymes). Moreover, the matrix should be sufficiently permeable to facilitate the diffusion of nutrients, oxygen and waste products (Margaritis and Kilonzo, 2005).

Immobilization technology had been applied by a number of researchers to a variety of microbial cells or their spores. For example spores of the fungus *Curvularia* have been entrapment in polyacrylamide granules, calcium alginate beads (Ohlson *et al*., 1980) and photo-cross-linked resin gels (Sonomoto *et al*., 1983, Sonomoto *et al*., 1981). Subsequent germination of the spores, initiated by supplying appropriate nutrients, resulted in the homogeneous distribution of mycelia throughout the beads after 48h. Polyvinyl alcohol PVA-cryogel beads have been used to entrap *B. subtilis* (Szczesna-Antczak *et al*., 2004, Szczesna-Antczak *et al*., 2001) and the entrapped cells were able to secrete both neutral and alkaline proteases. Currently, there are few studies reporting the use of polyHIPE materials as a matrix for the immobilization of microbial cells. These studies describe the use of polyHIPE to immobilize ethanol-producing cells of the yeast *S. cerevisiae* (Karagöz *et al*., 2009) and *Pseudomonas syringae,* phenol degrading bacteria (Akay *et al*., 2005d). The current study reports attempts to use polyHIPE matrices to entrap spores of a starch-degrading strain of *B. subtilis*.

The *B. subtilis* spores used in this work exhibit high-level resistance to heat, toxic chemicals and radiation. However, they can be killed by treatment with chemical such as formaladehyde and strong acids (Setlow, 2006) or by agents that disrupt the spore's permeability barrier (Setlow *et al*., 2002). During their

development, spores retained a minimal amount of water which, when removed, results in the loss of their viability (Ishihara *et al*., 1994). Additionally, spores can also be inactivated in extreme dry conditions due to damage to hydrophobic structures (e.g. membranes and some proteins) and DNA (Dose and Gill, 1995). *B. subtilis* spores can survive for decades or even longer, while maintaining their viability. However, when exposed to an appropriate germinant, they can be "triggered" within a few minutes to germinate and form vegetative cells. One of the best studied germinant is L-alanine. This germinant interacts with a specific receptor on the spore which, in turn, triggers the release of cations and pyridine-2,6-dicarboxylic acid (dipicolinic acid or DPA) and its associated divalent cations, predominantly Ca^{2+}, from the spore core (Paidhungat *et al*., 2002, Setlow, 2003). The release of Ca^{2+}-DPA triggers the hydrolysis of the spore cortex and subsequently allows the spore core to swell and fully hydrate. Once the core is fully hydrated existing spore enzymes complete the process of germination. This is followed by the production of new enzymes that are required for the transformation of the spore into an actively growing vegetative cell (Paidhungat *et al*., 2002). Just as certain compounds trigger germination, others can inhibit germination. Known inhibitors of germination include inert gases, aliphatic alcohols, fatty acids, phenols, and sulphydryl agents (Trujillo and Laible, 1970, Yasuda-Yasaki *et al*., 1978, Parker, 1969, Cortezzo *et al*., 2004). These compounds inhibit the action of, or response to, one or several of the nutrient receptor proteins that are activated by germinants. In *B. subtilis* these receptors are encoded by homologous tricistronic operons, namely *gerA* (sufficient to trigger spore germination with L-alanine), *gerB* and *gerK* (Moir *et al*., 2002). The proteins encoded by these operons are located in the inner membrane of spore (Paidhungat and Setlow, 2001). For example, alcohols are good inhibitors of L-alanine-induced germination, with the degree of inhibition increasing with chain length (Trujillo and Laible, 1970). Consequently, when considering the chemistry involved in the in situ encapsulation of *B. subtilis* spores, consideration need to be give to compounds that may inhibit sporulation or even inactivate the spore itself.

Spores of *B. subtilis* are able to survive for very long periods of time if stored appropriately under conditions that do not trigger germination. One advantage of encapsulating spores *in situ* during polyHIPE matrix formation is that the matrix itself could serve as a carrier for spores that can be easily for stored and transported. These spores can then be activated when and where required.

The objectives of this chapter are to:

- Inoculate *Bacillus subtilis* spores into polystyrene-divinylbenzene (polystyrene-DVB) and vinyl pyridine PolyHIPE (TVP-PHP) matrices during synthesis
- Activate the inoculated spores by supplying a germinant in the form of a nutrient medium
- Determine the productivity of the germinated cells with respect to the production of α-amylase produced and released cells from the matrix

6.1.1 Morphology of spore suspension in aqueous phase used in preparation of polystyrene-divinylbenzene polyHIPE

An experiment was carried out to determine the effect of incubating a suspension of *B. subtilis* 168(pKTH10) spores in the aqueous phase of polystyrene-divinylbenzene polyHIPE, which consists of 1% (w/v) of potassium persulphate, in an oven at 60^0C for 8h (the duration for polyHIPE polymerization). This experiment was designed in establish if any changes occurred in the morphology of the spores under these conditions. Any changes in spore morphology might result in the spores losing their resistance to the chemicals used to synthesis polyHIPE. The treated sample was prepared for scanning electron microscopy as described in Section 2.5.2.3. As can be seen in Figure 6.1, the size of spores was slightly longer compared to the starting spore's size. It changed from approximately 1.2μm to 1.6μm.

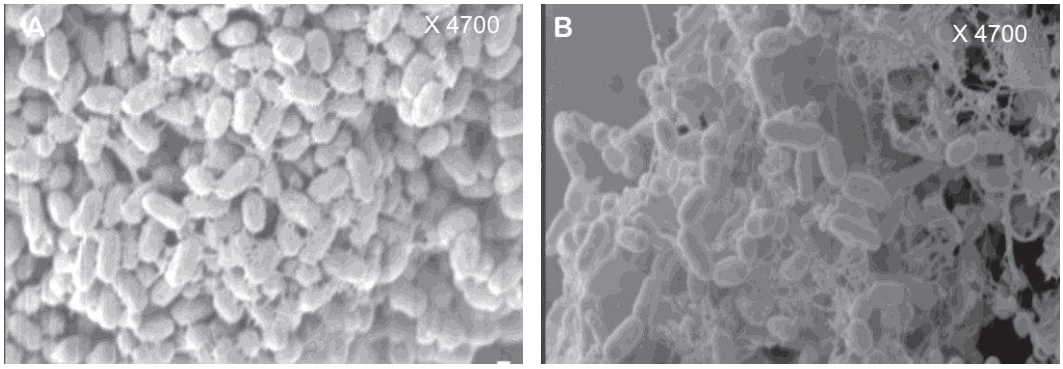

Figure 6.1: Scanning electron micrograph showing the appearance of *B. subtilis* strain 168 (pKTH10) spores (A) before treatment and (B) after incubating in aqueous phase of polystyrene-divinylbenzene polyHIPE (containing 1% of potassium persulphate) in the oven for 8h at 60^0C.

6.1.2 Electron Microscopy of the in-situ *Bacillus subtilis* spores

Several batches of matrix were prepared in the presence of spores of *B. subtilis* 168 (pKTH10) with the same chemical composition and phase proportion of polyHIPE (Table 6.1). The glass vessel use to prepare polyHIPE (Figure 2.2) for this experiment was sterilised in an autoclave at 121^0C for 15 min prior use. All procedures were carried out under aseptic conditions. After the spore-incorporated polyHIPE emulsion was polymerized, the resulting cylindrical matrix was cut into discs of 0.5cm thickness. Before, the matrix discs were transferred into one of two wells in the sterilised PTFE microchamber (Figure 6.13A), they were washed with a mixture of water/isopropanol to remove residual monomer, crosslinker and initiator, which might be toxic to vegetative cells. Nutrient medium was fed through the matrices and samples before and after the activation of spores were prepared for scanning electron microscopy (SEM) analysis (Section 2.8.8). The production of α-amylase and numbers of cells released from matrices were also estimated.

Table 6.1: The batches of polyHIPE synthesized with incorporated *B. subtilis* spores

In-situ incorporation of *B. subtilis* spore suspension during polyHIPE synthesis	
Batch (Polystyrene-DVB polyHIPE)	Observation
1	failed to polymerise
2	failed to polymerise
3	failed to polymerise
4	failed to polymerise
5	Polymerised, but inoculated spores failed to germinate following addition of nutrient medium
Batch Vinylpyridine- PolyHIPE	
1	failed to polymerise
2	failed to polymerise
3	Polymerised, and inoculated spores germinated after addition of nutrient medium

In the case of batches of matrix made with polystyrene-DVB polyHIPE, only one was successfully polymerised. SEM was used to observe the appearance of spores on the surface and the cross-section of polystyrene-DVB polyHIPE (Figure 6.2 and Figure 6.3 respectively) prior to the addition of nutrient medium The spores incorporated polyHIPE were activated by continuously pumping nutrient media through the matrix at a flow rate of 1.0 ml/min for 24h. This supplied nutrient media was continuously aerated at 37^0C. The appearance was unaltered at 8h and 24h following the addition of nutrient medium, indicating that the spores had not germinated (Figure 6.4). This was confirmed by the failure to detect any α-amylase activity or viable cells in the nutrient medium flow through. The size of spores before and after cultivation was approximately 0.6-0.8μm in diameter and they were heterogeneous (Figure 6.4C).

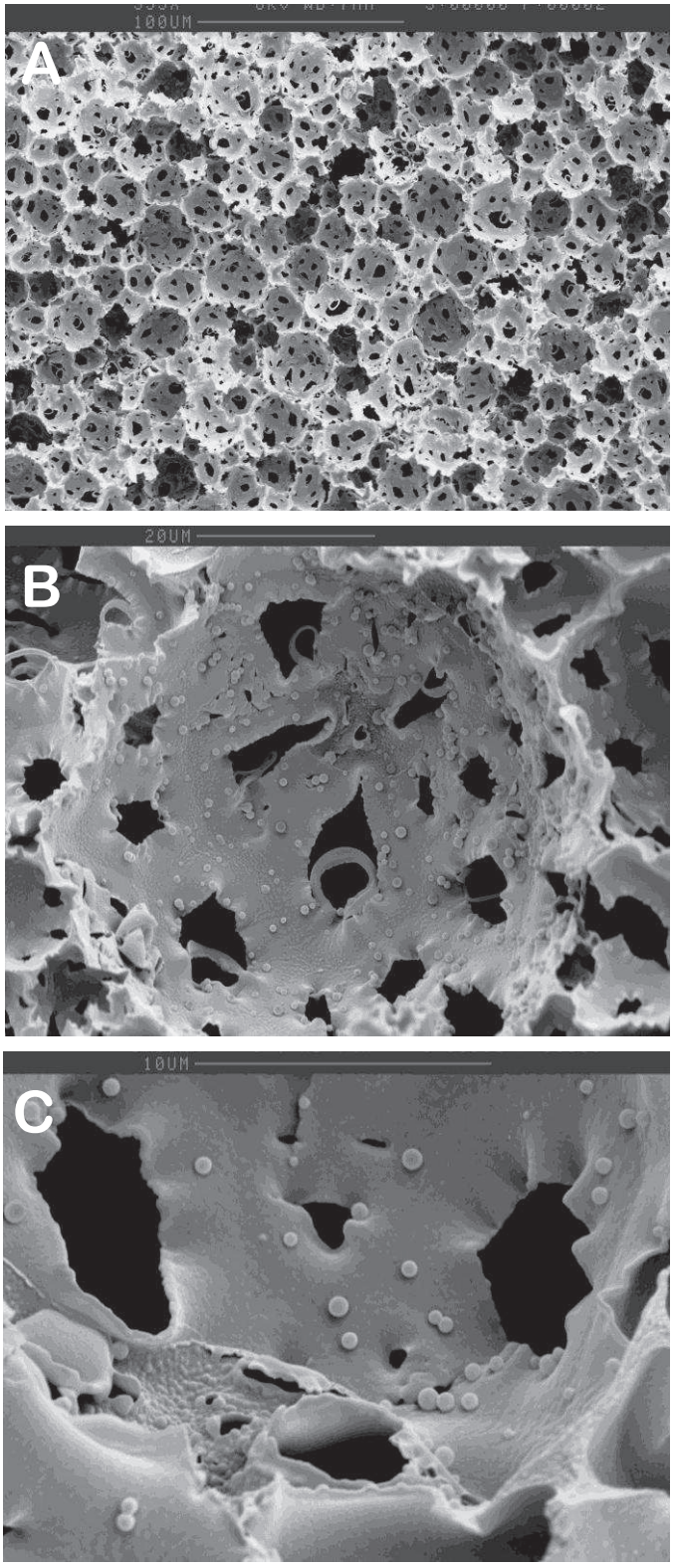

Figure 6.2: Scanning electron micrograph of spore-incorporated polystyrene-DVB polyHIPE before cultivation on the top surface (A) General view (x 350), (B) showing the distribution of spores in pore (x1500) (C) high magnification view (x5000)

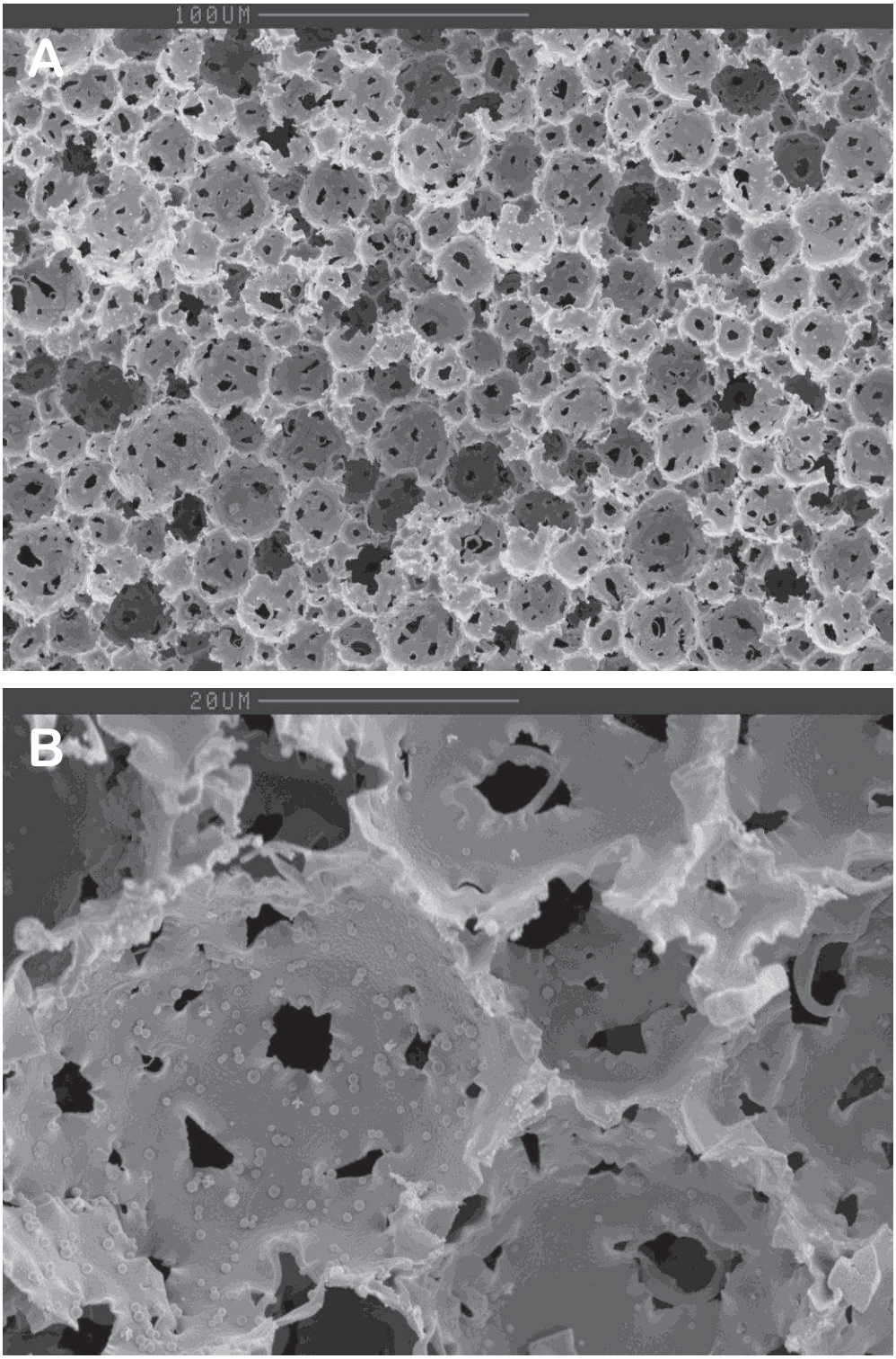

Figure 6.3: Scanning electron micrograph showing the appearance of spore-incorporated polystyrene-DVB polyHIPE before cultivation in the cross-section of matrix: (A) General view (x 350), (B) higher magnification showing the distribution of spores in the matrix pores (x1600)

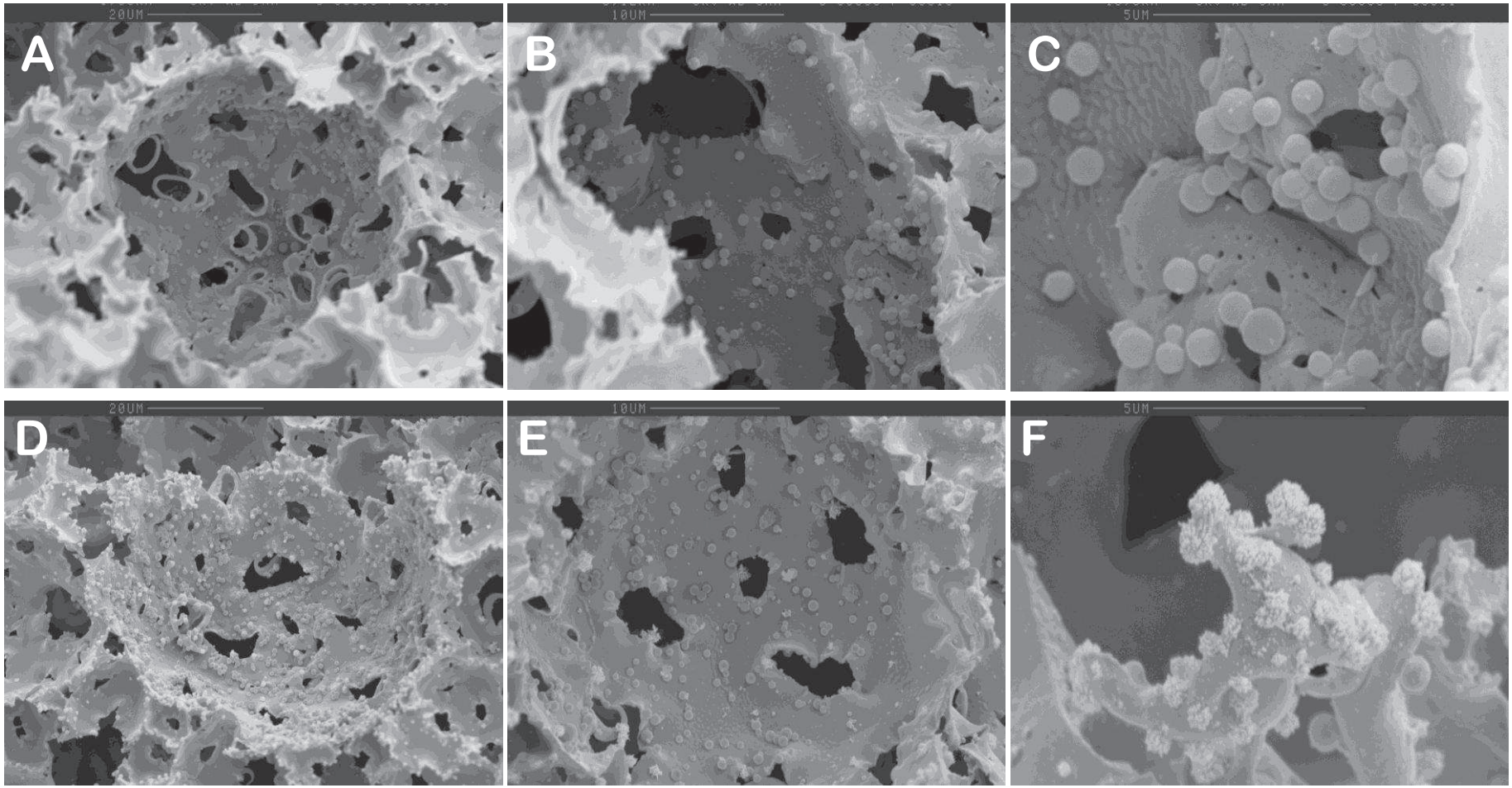

Figure 6.4: Scanning electron micrograph showing the appearance of spores incorporated into polystyrene-DVB polyHIPE after 8h incubation: (A) the distribution of spores in matrix pores (x1300), (B) slightly higher magnification (x 3000) and (C) ungerminated spores with heterogeneous-sized (x10,000) and 24h incubation time: (D) showing the distribution of spores in matrix pores (x1300), (E) ungerminated spores (x 3000) and (F) closer view of probably damaged spores (x10,000)

Since the incorporation of spore suspension onto the polystyrene –DVB polyHIPE matrix during synthesis was unsuccessful due to its failure to polymerise the composition of the matrix was change to one based on vinyl pyridine polyHIPE. As shown in the same

Table 6.1, one of the prepared batches was successfully polymerised in the presence of spores and a SEM analysis is shown in Figure 6.5. The appearance of the *in-situ* inoculated spores was different from those associated with the polystyrene-DVB polyHIPE matrix, and indeed appears to be partially embedded in the structure of the matrix. The matrix was treated with nutrient medium and after 24h incubation, there was clear evidence that a significant proportion of the cells near the surface of the matrix had germinated and developed into vegetative cells (Figure 6.6). In contrast, when a cross-section of the treated matrix was similarly analysed very few spores within the body of the matrix had germinated (Figure 6.7). The appearance of the outlow sample of the matrix after 24h activation of *in-situ* inoculated spores with nutrient medium was also shown on LB plates containing 1% of starch, the substrate for α-amylase (Figure 6.11B). It found that the colonies on this plate were slightly bigger compared to the initial inoculated spores (Figure 6.11A).

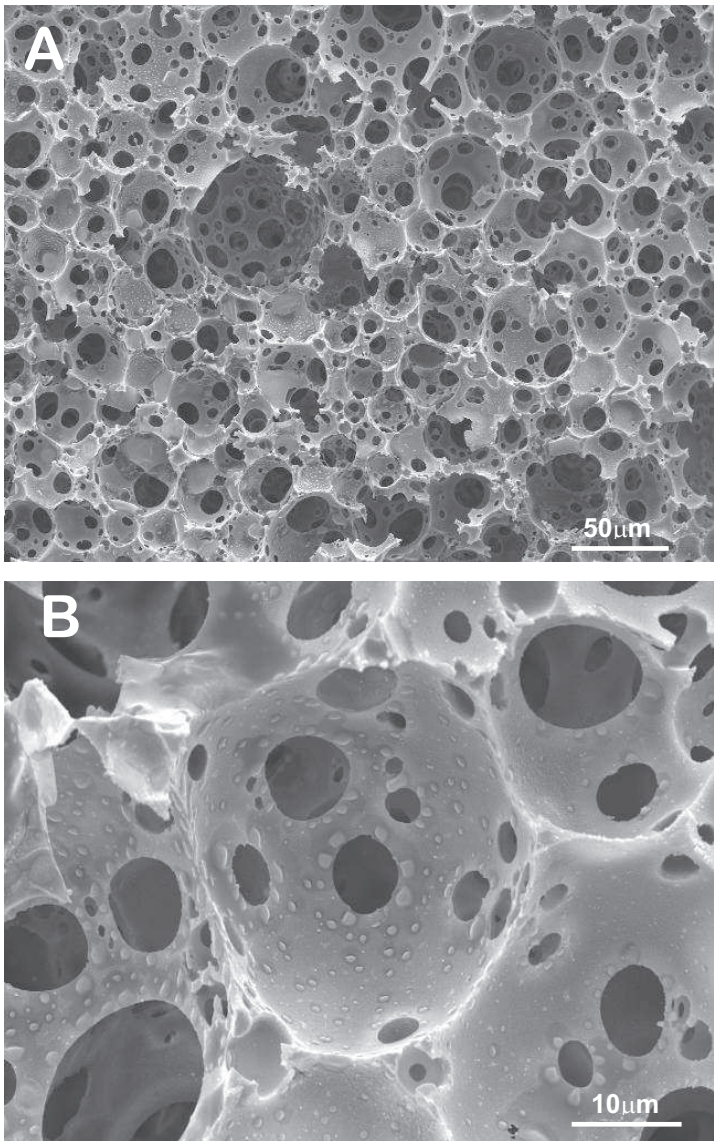

Figure 6.5: Scanning electron micrographs of spore-incorporated vinyl pyridine polyHIPE before cultivation. The top surface of matrix was shown (A) General view (x 350), (B) showing the distribution of spores in pore (x2000).

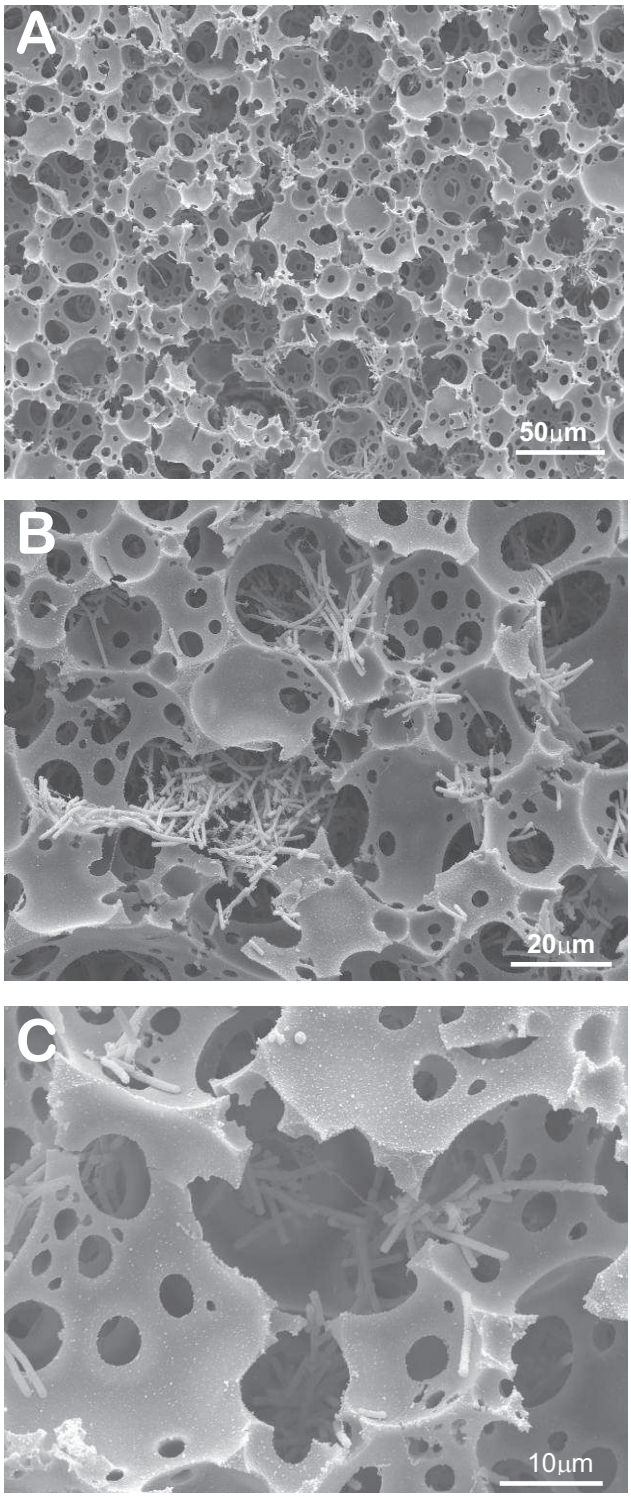

Figure 6.6: Scanning electron micrographs showing the appearance of germinated spores after 24h cultivation on the top surface of vinyl pyridine polyHIPE matrix: (A) General view (x 350), (B) showing some germinated spores located at the edge of matrix (x1000) (C) view at high magnification (x2000).

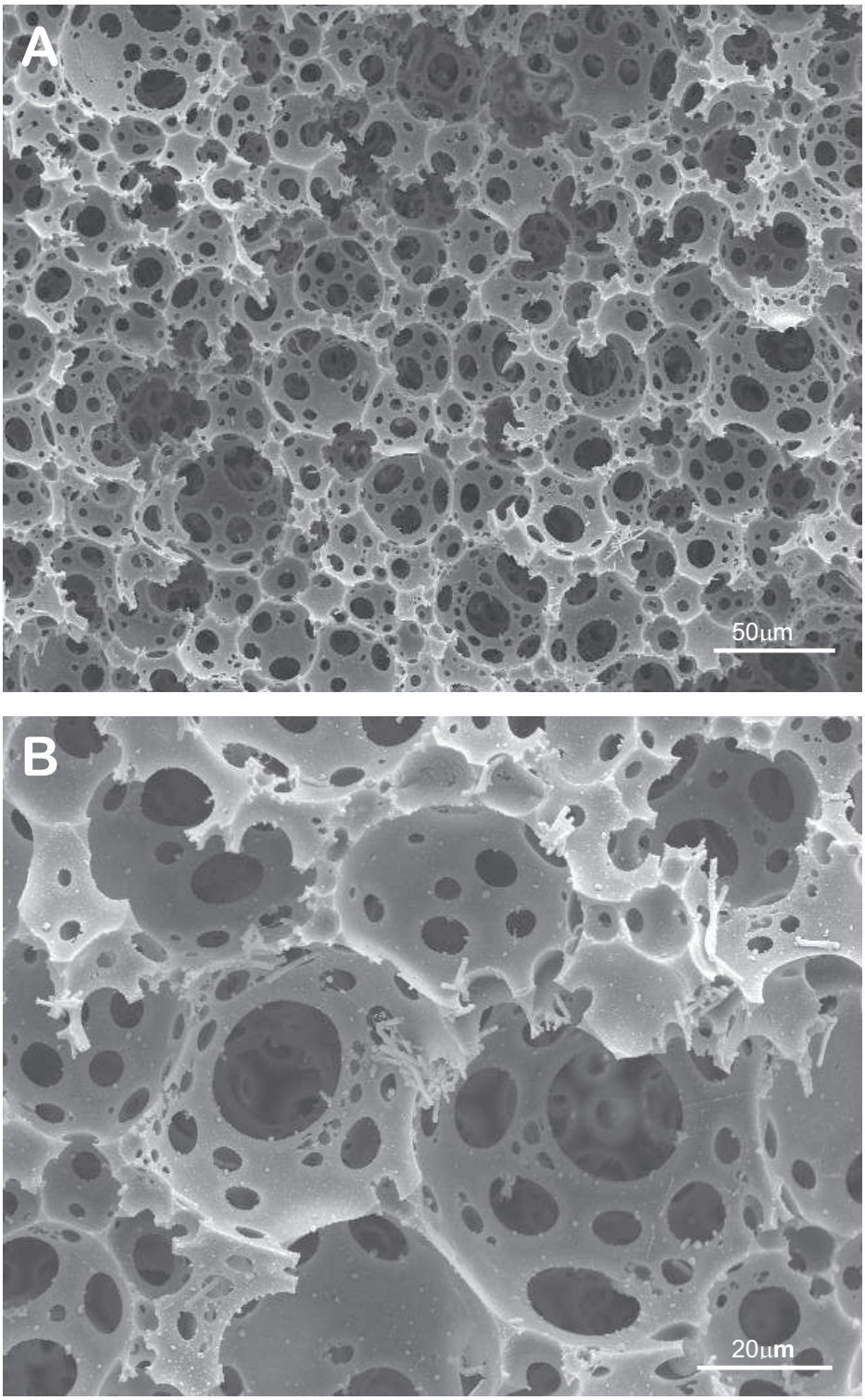

Figure 6.7: Scanning electron micrograph of spore-incorporated vinyl pyridine polyHIPE after 24h cultivation. Cross section of matrix: (A) General view (x 350), (B) a few germinated cells were found at the edge of pores (x1000).

SEM analysis of the spore-incorporated vinyl pyridine polyHIPE, showed that many vegetative cells were found at the bottom surface of the matrix (Figure 6.8), often associated with ungerminated spores (Figure 6.8B). Ungerminated spores were observed on both the top and bottom surfaces of this sample (Figure 6.9 and Figure 6.10).

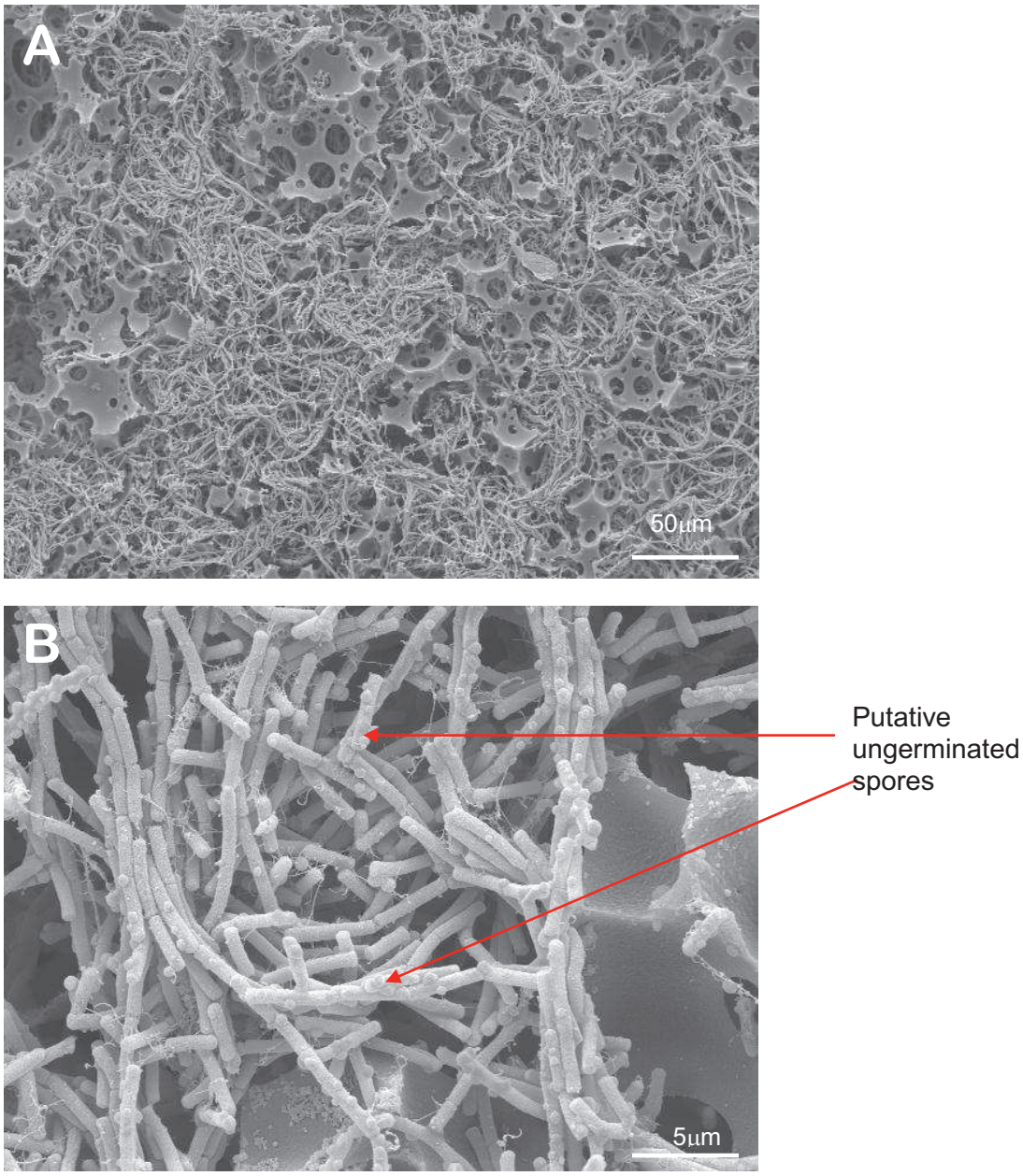

Figure 6.8: Scanning electron micrograph of spore-incorporated vinyl pyridine polyHIPE after cultivation. Analysis at the bottom surface of matrix: (A) General view of accumulated cells (x 350), (B) germinated cells with attached putative ungerminated spores (x3500).

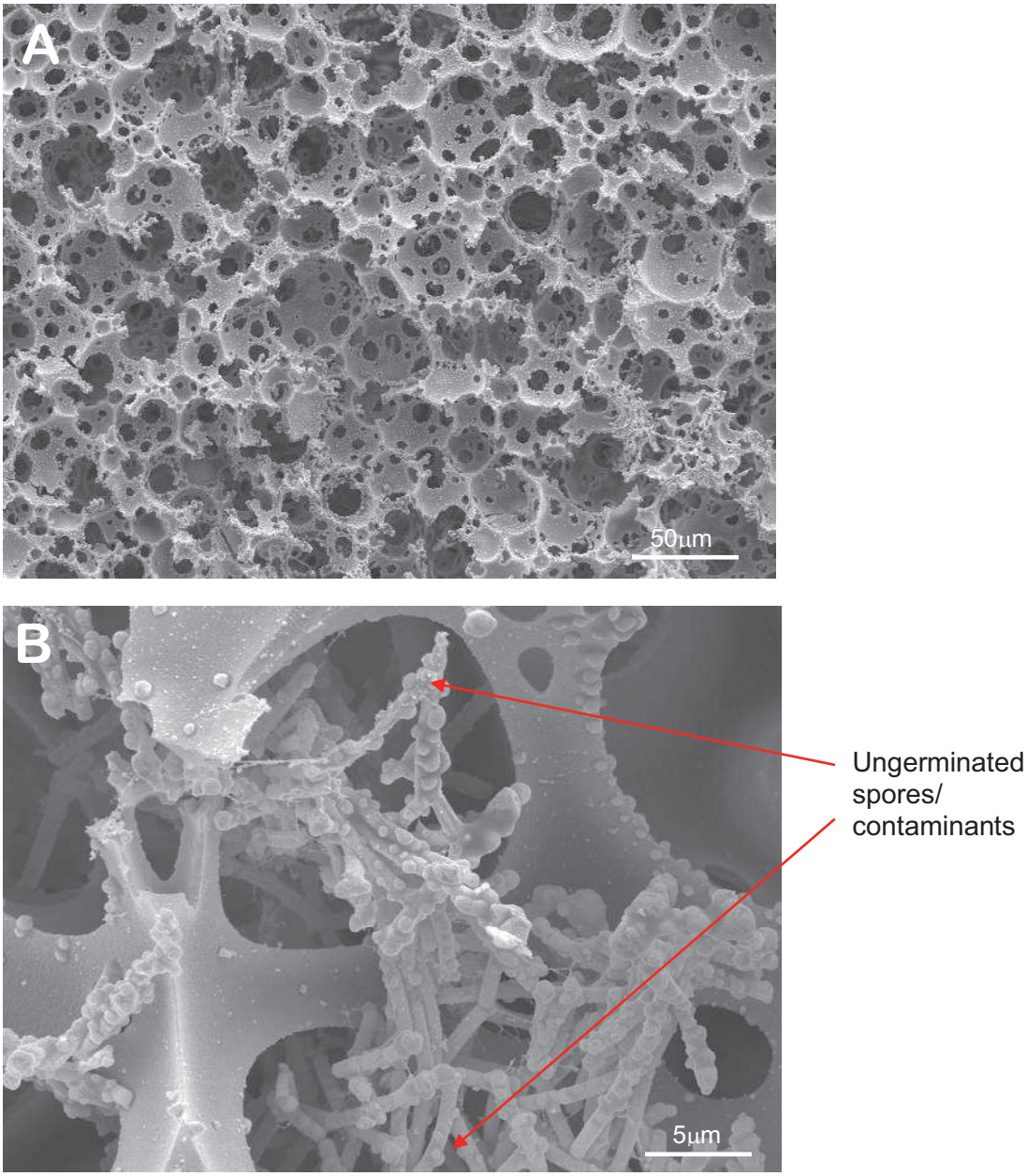

Figure 6.9: Scanning electron micrograph showing the appearance of germinated cells with attached ungerminated spores after cultivation. Top surface of vinyl pyridine polyHIPE matrix: (A) general view (x 350), (B) view at high magnification (x3500).

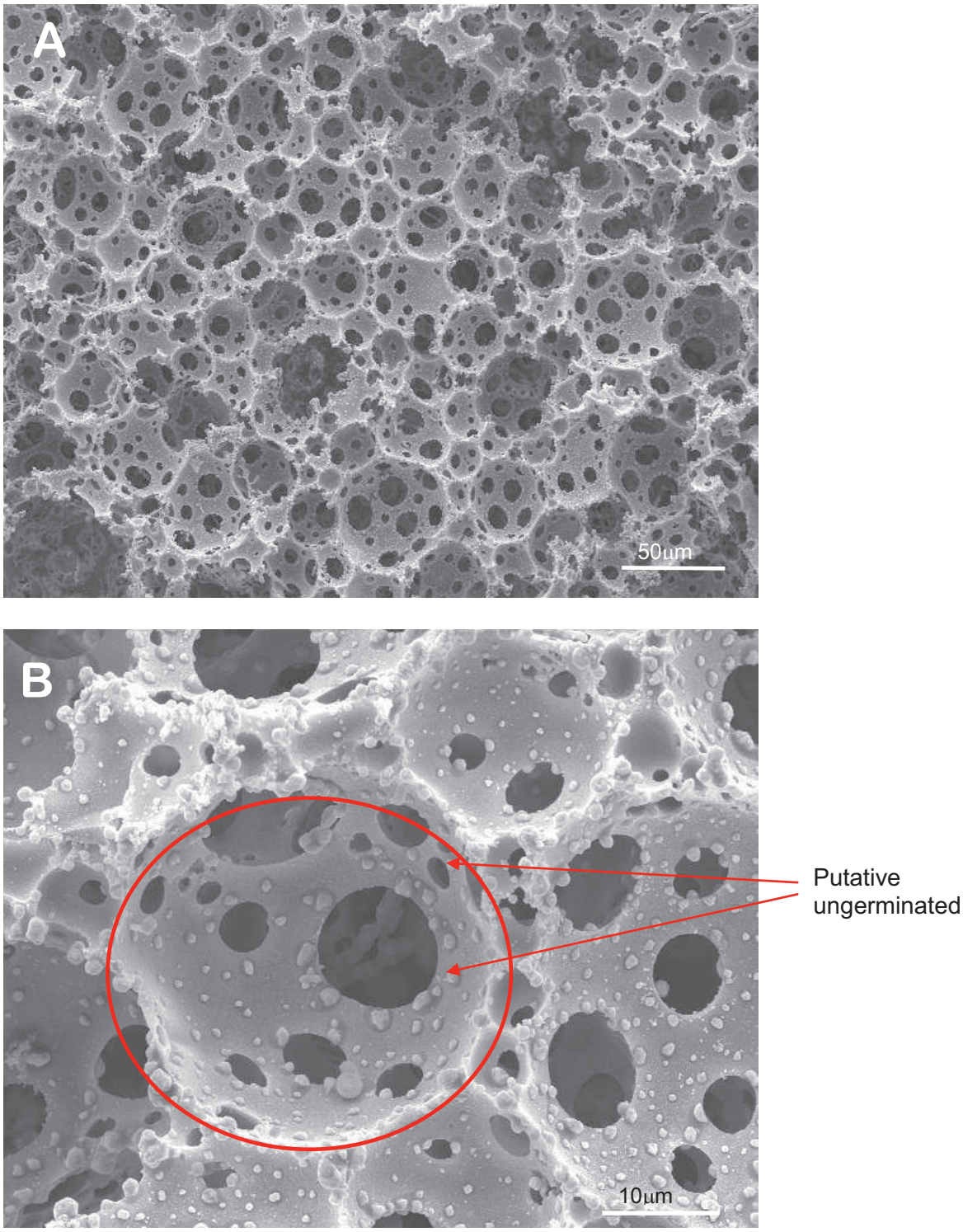

Figure 6.10: Scanning electron micrograph showing the appearance of ungerminated spores after cultivation. Bottom surface of vinyl pyridine polyHIPE matrix: (A) general view (x 350), (B) view at high magnification (x2000)

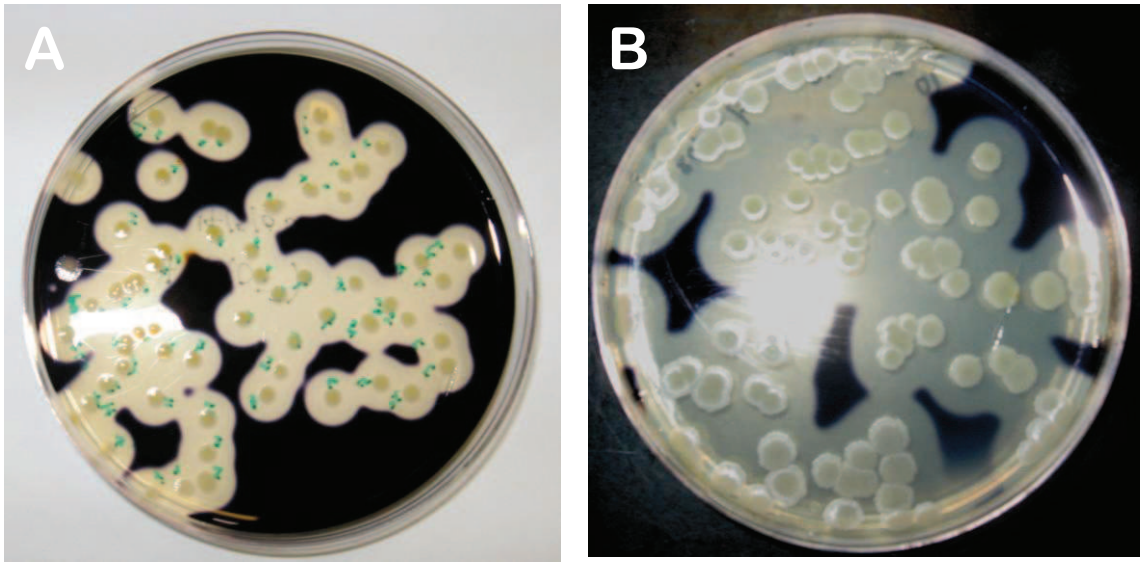

Figure 6.11: The appearance of colonies of *B. subtilis* strain 168 (pKTH10), on plates containing 1% of starch after exposure to iodine vapour: (A) sample of the spore suspension used to inoculate the matrices, (B) cells recovered for the outflow of the matrix after activation of spores incorporated into the polyHIPE matrix during synthesis.

6.1.3 Enzyme production from germinated *B. subtilis* spores incorporated into the polyHIPE matrix during synthesis

The production of α-amylase and the release of cells from the matrix were determined during the perfusion with nutrient medium (Figure 6.12). The production of α-amylase increased continuously throughout the experiment. In contrast, the number of released cells tended to fluctuate and then settle down at ~10^5 cells per ml.

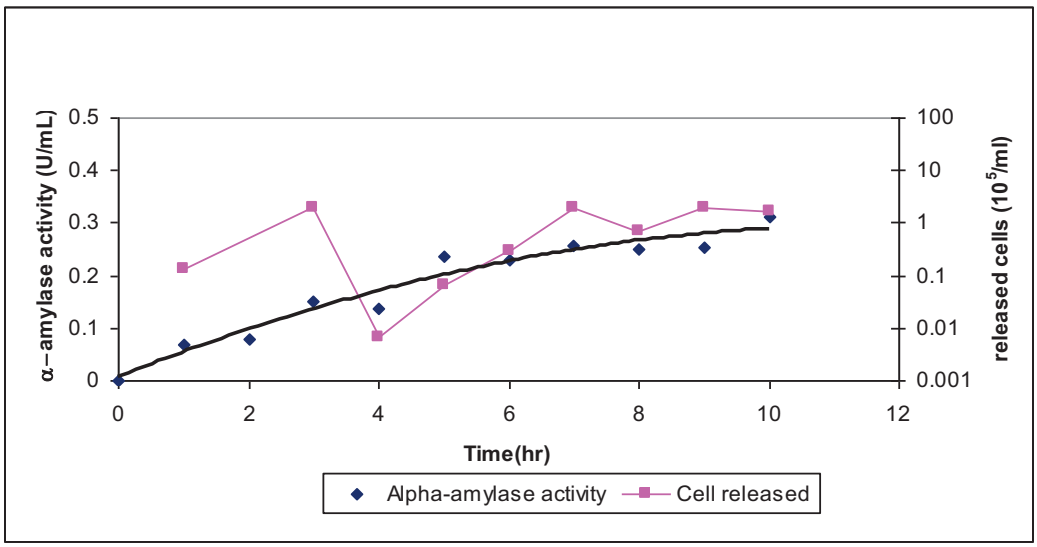

Figure 6.12: Graph showing the production of α-amylase and numbers of cells released from a vinyl pyridine polyHIPE matrix with *in situ* incorporated spores. The matrix was continuously supplied with fresh aerated nutrient medium for 12h at 37^0C.

6.1.4 Discussion

Cell immobilization has been shown to provide several advantages over planktonic cultures with respect to increased volumetric productivity, product concentration and, ultimately, decreased substrate utilisation (Karel *et al*., 1985b). Additionally, immobilization can serve to separated biomass from the product due to the confinement of producer cells within the matrix, facilitating the use of a continuous reactor without significant cell washout (Karel *et al*., 1985b). Consequently, the cost of downstream processing can be reduced as compared with conventional, free-cell culture systems. The synthesis of the porous matrix around spores of the cells to be immobilized should ensure their even distribution throughout the matrix. However, the adequate diffusivity of nutrients and oxygen throughout the matrix is also important and if diffusivity is inadequate this is likely to have a severe affect on the performance of the immobilization system. The diffusivity of nutrients and oxygen is depends on the biocompatibility of materials used to synthesise the immobilized matrix. These materials will determine whether the immobilized matrix is hydrophobic or hydrophilic, with the latter affecting the capability of fluids to permeate throughout the matrix. Therefore, the selection of materials used for this purpose is of utmost importance.

This chapter addressed attempts to incorporate *Bacillus subtilis* spores into polystyrene-divinylbenzene (polystyrene-DVB) and vinylpyridine polyHIPE matrices during synthesis and the subsequent activation of the spores by exposure to nutrient medium. Subsequently, productivity of the germinated cells for the production of α-amylase was determined. However, a number of problems were encountered, including the failure of the polyHIPE emulsion to polymerize and difficulties removing residual unreacted chemicals and excess of isopropanol from the polyHIPE discs.

The use of isopropanol to remove all of the residual monomer, crosslinker and initiator could potentially result in the inactivation of the incorporated spores due to interactions between the hydrophobic regions of the spore and the hydrophobic chain of alcohols (Trujillo and Laible, 1970, Yasuda-Yasaki *et al*.,

1978). This inhibition was shown to be reversible, and germination was restored when the alcohol was removed from the environment of the spore, but only if the percentage of isopropanol was less than 1%. In this study, the concentration isopropanol was 50% and this could explain why the spores incorporated into the polyHIPE matrix failed to germinate. As can be seen in Figure 6.2 (C), Figure 6.3 (B) and Figure 6.4 (C), the spores-incorporated into the polyHIPE matrices were heterologous in size compared to those of the initial spore suspension (Figure 3.1, Section 3.1.2). The change in spore size might be due to the presence of potassium persulphate, which was used as an initiator in the polymerization reaction. Potassium persulphate is an oxidizing agent, which may alter the structure of the spore coat that provides the barrier against toxic chemicals. As shown in Figure 6.4(C), there was a slight change of spore size after 8h incubating in the aqueous polymerization solution that contains potassium persulphate, although we can not rule out influence of other components in this mixture.

As shown in Figure 6.5, the inoculated spores were partially embedded in the structure of the matrix. This result indicates that the spores were entrapped in the polyHIPE matrix. After 24h incubation, germinated cells were found on the top surface (Figure 6.6), in the cross section (Figure 6.7) and at the bottom surface (Figure 6.8) of the matrix. More cells were observed at the bottom surface of matrix, possibly due to the accumulation of nutrient media in this area.

The polystyrene-DVB polyHIPE is hydrophobic and consequently has low diffusivity and permeability to aqueous fluids. Due to its low wetability, the flow of fluid in this matrix is restricted and relies on capillarity. This is likely to be the main reasons for the failure of the majority of the spores to germinate. In the case of the vinyl-pyridine polyHIPE matrix, a higher proportion of the spores germinated (Figure 6.5, Figure 6.6 and Figure 6.9). This is likely to be due to the fact that this matrix material is more hydrophilic than polystyrene-DVB polyHIPE, allowing better access to the inflowing nutrient medium. However, the larger pore and interconnect sizes of this matrix meant that the vegetative cells were able to migrate through the matrix and accumulate at the bottom surface. α-amylase production from the vinyl-pyridine polyHIPE matrix increased throughout the incubation time (Figure 6.12), implying either that the cells

continued to proliferate, or that there was a switch between substrate utilisation for increasing cell mass to product formation. One problem that was encountered was a limitation in the design of the micro-chamber into which the polyHIPE discs were inserted. It was difficult to seal the disc which meant that there were spaces at the sides and the bottom in which nutrient medium and vegetative cells could accumulate (Figure 6.13(A) & (B)). A modification of this micro-chamber (Figure 6.13(C)) was needed to avoid this problem.

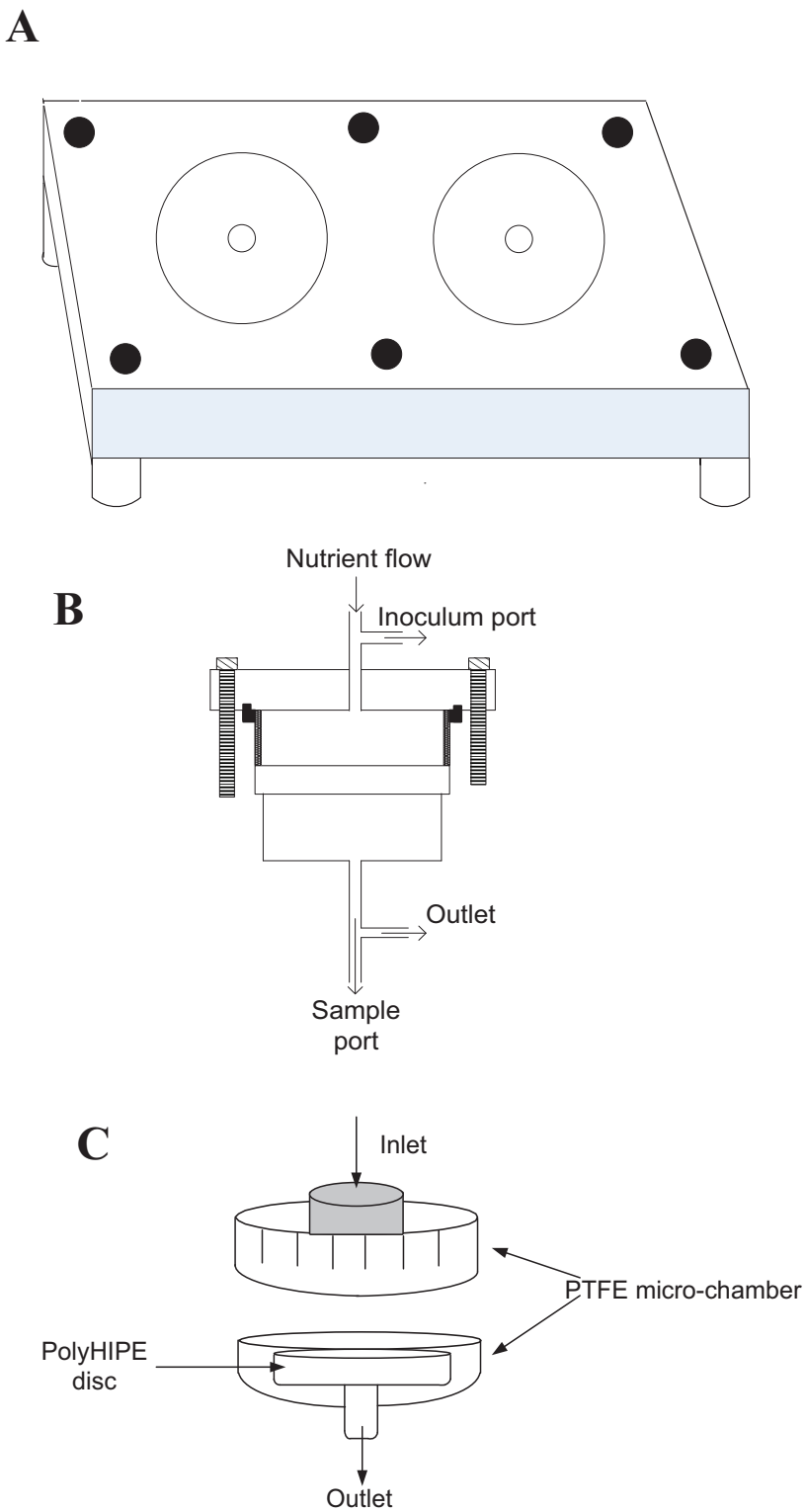

Figure 6.13: PTFE micro-chamber: (A) the apparatus used in the initial experiments, a PTFE block with two wells, (B) detail of the PTFE block well and, (C) new screw-shaped PTFE micro-chamber

7 Immobilization of *Bacillus subtilis* spores onto the matrix of polymeric polyHIPE matrix

7.1.1 Introduction

Conventional microbial cell cultivation can be carried out by using simple glassware such as test tubes or conical shake flasks as well process controlled bench-scale bioreactors equipped to control pH, temperature and dissolved oxygen (DO). The former systems can be operated in a static or shaking incubator while the latter systems can be operated in batch or continuous mode according to the bioreactor type, which might be a stirred-vessel or airlift reactors. In all of the above systems, the fermentation process requires hydrodynamic conditions that facilitate the effective agitation of the culture to ensure the uniform distribution of substrates/nutrients and microorganisms. The same principle also applies to immobilized cell systems where the hydrodynamic conditions are of the utmost importance to ensure efficient and rapid entrapment and penetration of the cells into the porous matrix and the adequate transport of substrates and waste products to and from the immobilized cells. These parameters are dependent on the porosity of the matrix used, in particular its pore and interconnect sizes and its physico-chemical characteristics. Others considerations in the design are a high surface area for the attachment of cells, mechanically robust properties for long-term operation and a suitable cell/matrix interaction via hydrophobicity, hydrophilicity or charge. These factors are important in designing the immobilized cells system and also in circumventing problems, such as the uneven distribution of cell or their failure to migrate within the matrix, that areoften associated with such systems.

Previous studies have show that α-amylase productivity by *B. subtilis* and related strains can be enhanced by using a cell immobilization system. A number of matrices have been used as immobilisation supports including κ-carrageenan gel beads (Baudet *et al*., 1983, Duran-Paramo *et al*., 2000), agar beads, formaldehyde-activated acrylonitrile/acrylamide membranes (Tonkova *et al*., 1994), polysulphone/ polyacrylonitrile membranes (Dobreva *et al*., 1998), and

calcium alginate gel capsules (Konsoula and Liakopoulou-Kyriakides, 2006). Immobilized cells matrices such as alginate or κ-carrageenan are often used in the form of small beads which are placed in a conical shake flask containing growth medium. The microbial cells that need to be immobilized are either inoculated into this growth medium or mixed first with the immobilized matrices before being transferred into the growth flask. In the current study, the poly(styrene-divinylbenzene) polyHIPE was in the form of a disc with a diameter of 24mm and a thickness of 5mm. This required the construction of an appropriate chamber to ensure that the flow of culture medium is sufficient to allow its permeation throughout the polyHIPE matrix. One of the problems with such a system is to ensure that the inoculated cells are able to migrate across the matrix and do not simply remain on the top surface. This requires an appropriate technique to inoculate microbial cells into this matrix in such a way as to ensure strong initial entrapment within the matrix. The method that was used is "forced flow seeding", a technique that was developed previously to ensure osteoblast-like cells penetrated deeply and uniformly into the scaffold of a mineralized matrix (Bokhari *et al*., 2003). Moreover, forced flow seeding was also used to ensure that the proliferation and adhesion of immobilized *Pseudomonas syringae,* a phenol-degrading bacterium, to the pore walls of a polyHIPE matrix (Akay *et al*., 2005a).

In this study a modified polymeric polyHIPE matrix known as vinylpyridine polyHIPE (TVP-PHP) was used as a support carrier for the immobilisation of a starch-degrading bacterium, *B. subtilis.* Thus, the aims of this chapter were:

- To perform preliminary experimental work on the effect of different seeding technique onto the polyHIPE immobilized system
- To perform preliminary experimental work on the effect of pretreatment of polyHIPE matrix prior its use as an immobilized cell
- To evaluate the growth and penetration of the immobilized cells, to measure their productivity with respect to α-amylase production and to determine the stability of the system by determining the rate at which cells were released in the outflowing medium.

7.1.2 Static inoculation with a *B. subtilis* spore suspension

A preliminary experiment was carried out to investigate the effects of inoculating pre-germinated spores (2 ml of nutrient medium with 50µl of spore suspension with density of 2 x 10^8cells) directly onto the surface of a sterilized vinyl-pyridine polyHIPE (TVP-PHP) disc placed in Petri dish containing 5 ml of LB medium (Figure 7.1). After manual inoculation the Petri dish with the TVP-PHP matrix was incubated in a gently shaking incubator shaker at 37^0C for 24h. The samples were then prepared for scanning electron microscopy (SEM) analysis (Section 2.8.8) to determine cell morphology. Cell-free samples were also prepared under the same conditions as a control. The results are shown in Figure 7.2.

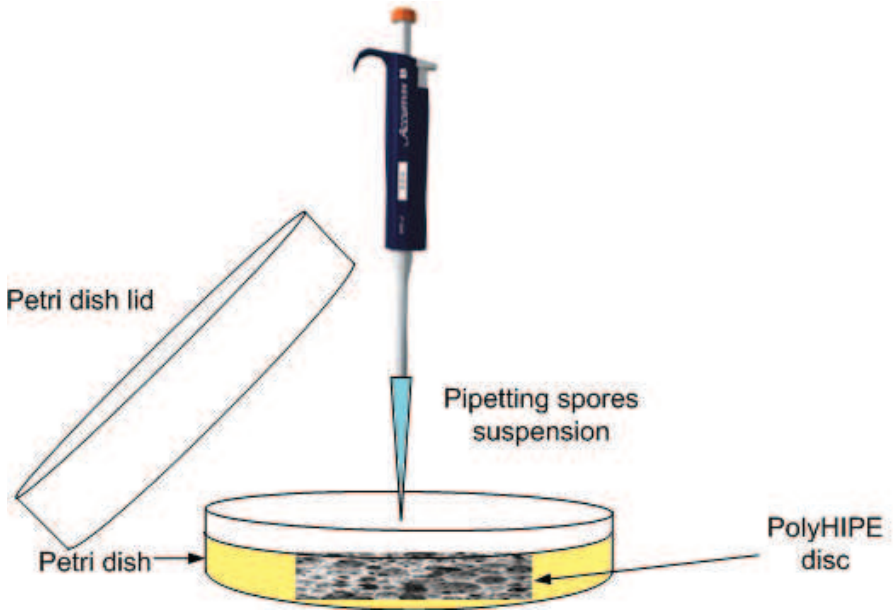

Figure 7.1: Static inoculation of spore suspension onto the surface of a polyHIPE disc placed in petri dish containing LB medium

As can be seen in Figure 7.2, the majority of cells that were observed on vinylpyridine polyHIPE (TVP-PHP) matrices were either germinating or vegetative cells with some ungerminated spores. Also seen in the micrographs are evidence of either cell debris and/or extracellular matrix (Figure 7.3a). The same observations were also seen in micrographs of the bottom surface of the matrices (Figure 7.3b).

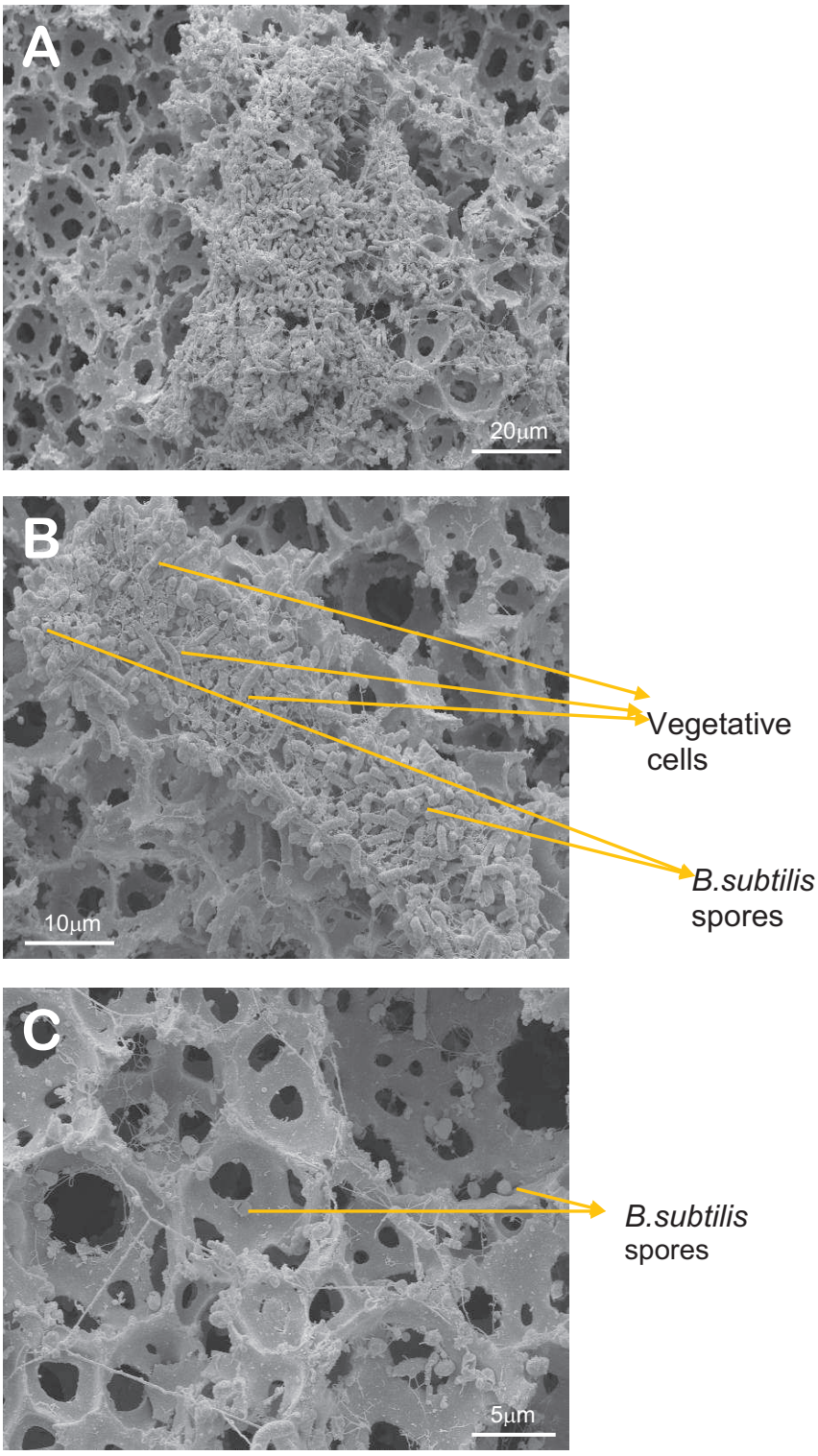

Figure 7.2: SEM results for statically seeding technique. Scanning electron micrograph of the top surface of a vinyl pyridine polyHIPE (TVP-PHP) matrix after 24h incubation at 37°C: (A) General view (x 1000) and other spot areas at high magnification (B) (x2000) & (C) (x 3500).

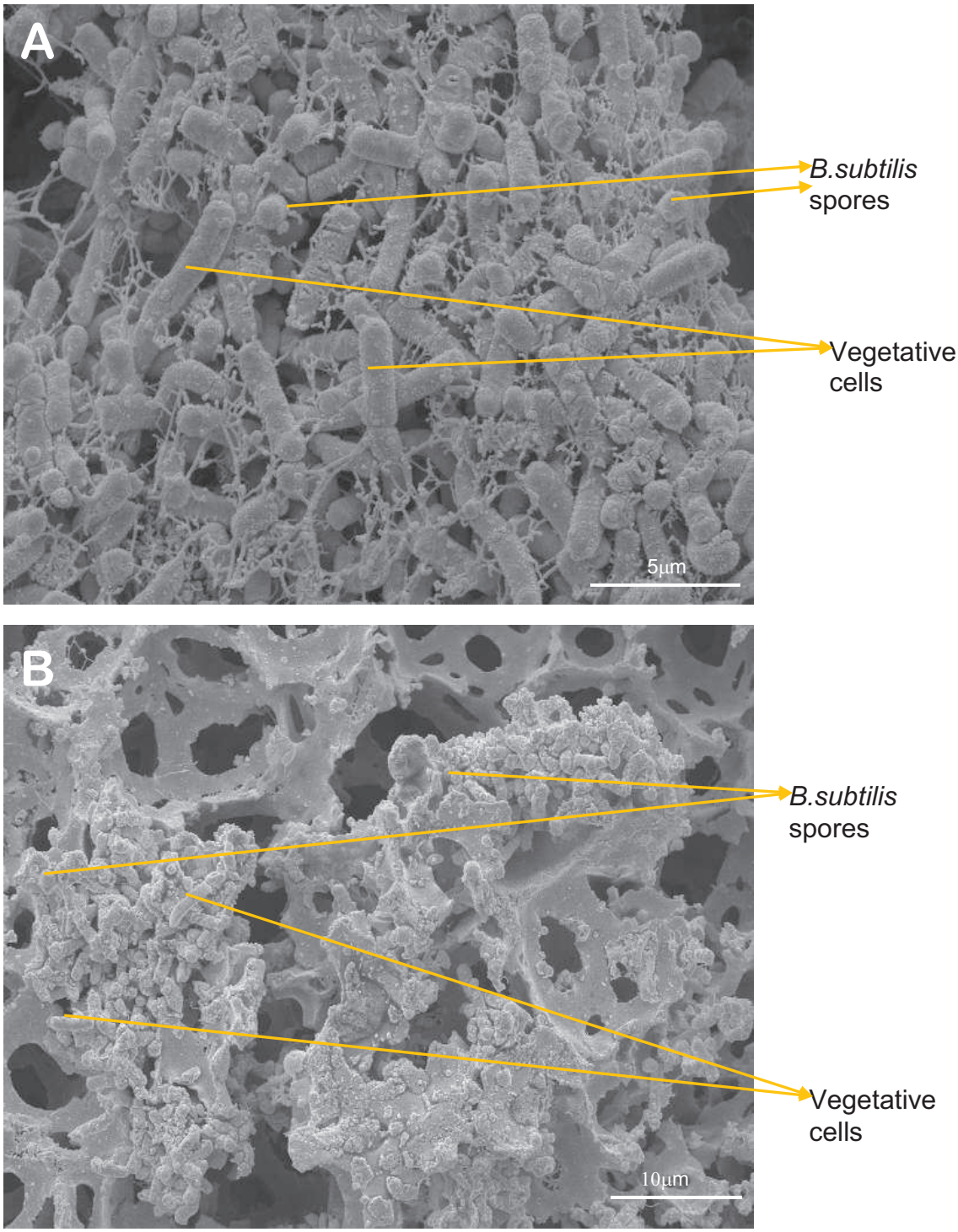

Figure 7.3: Appearance of germinated cells with some ungerminated spores and cells debris on the (A) top surface (x 5000) and (B) bottom surface of vinyl pyridine polyHIPE (TVP-PHP) at high magnification (x2000) after 24h incubation.

7.2.1 Immobilization of *B. subtilis* spores onto vinylpyridine polyHIPE matrix

Initial experiments were designed to evaluate the distribution of germinated cells on untreated and treated vinylpyridine-polyHIPE (TVP-PHP) matrices. Prior to use, these matrices were treated by pre-wetting them with sterilised distilled water and LB medium. The TVP-PHP matrices were autoclaved prior to use and then placed into one of the two wells in a block-shaped PTFE microchamber. The dimension of the inner well chamber was 28mm and the outer diameter was 38mm (manufactured in the Chemical Engineering Department, Newcastle University). The microchamber was similar to that used previously (Fig. 6.13 A-B). 50µl of spores of *B. subtilis* strain 168 (pKTH10) (~2x 10^8 /mL) were suspended in 2ml of LB broth and pre-germinated by incubating for 90 min at 37^0C. The TVP-PHP disc was inoculated with these pre-germinated spores by forced flow seeding using the syringe pump set at a flow rate of 0.55ml/min (Figure 7.4A). The seeded TVP-PHP was left for an hour to allow the pre-germinated spores to attach to the surface of the PHP, and then culture medium (LB broth) was pumped continuously through the matrix at a flow rate of 1.0ml/min using a peristaltic pump (Figure 7.5). Samples were collected at various interval times for the determination of the number of cells released from the TVP-PHP matrix and for α-amylase activity. The above procedures were repeated for the TVP-PHP disc that was wetted prior to use by continuously pumping sterilized distilled water at a flow rate of 1.0ml/min for 8h followed by LB media for 2h the next day. Pre-wetting the matrix with sterilised distilled water and LB media was designed to acclimatize its microenvironment with the growth nutrients that are essential for the seeded bacteria. The well of the block-shaped PTFE microchamber was also sealed with silicone sealant to prevent any leakage of nutrient medium and cells to the edge of the well. At the end of experiment, sterile 0.1M phosphate-buffered saline was pumped through the matrix at the same flow rate to remove the remaining medium.

B. subtilis is an obligate aerobe, and it was therefore important that the growth medium pumped through the microchamber was well aerated. Therefore air was continuously pumped into the nutrient medium reservoir to ensure the LB medium was well oxygenated.

One problem that arose with the block-shaped PTFE microchamber was that it was difficult to seal the polyHIPE disc in the well. This led to the accumulation of nutrient medium and vegetative cells at its sides and the bottom spaces, rather than throughout the entire matrix. This limitation was likely to affect the performance of this immobilized culture system. After the above preliminary experiments, the same procedures were repeated, but with the TVP-PHP disc being located in a filter-shaped PTFE microchamber (Figure 7.4B and Figure 7.5). This microchamber had the advantage of securely holding the polymer disc in place and ensuring that the only flow path was through the polyHIPE disc.

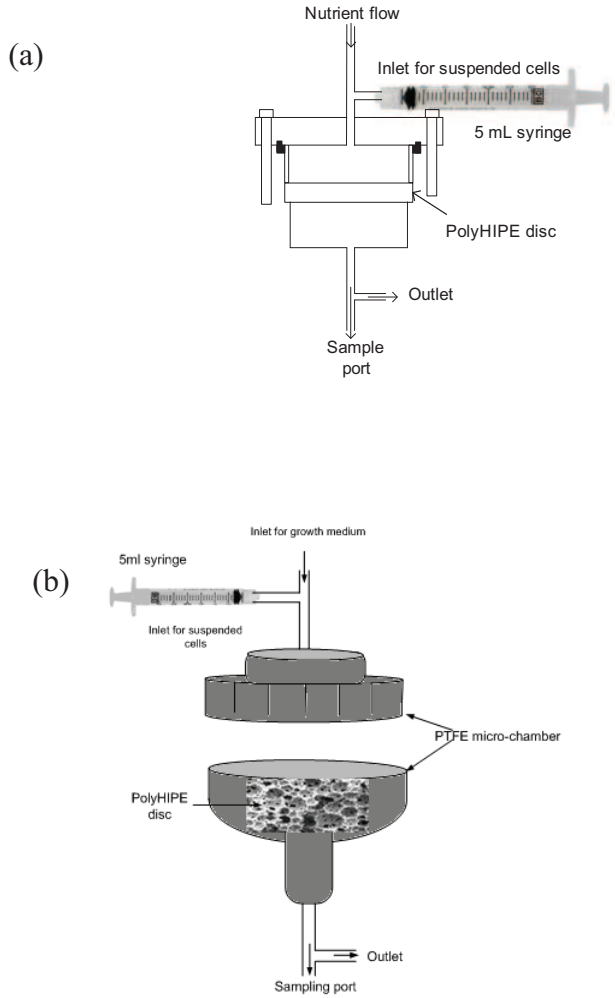

Figure 7.4: PTFE microchamber used in the study: (a) block-shaped and (b) filter-shaped. The syringe, attached to a syringe pump, was used to inoculate the disc with spore suspensions - a technique known as forced-flow seeding.

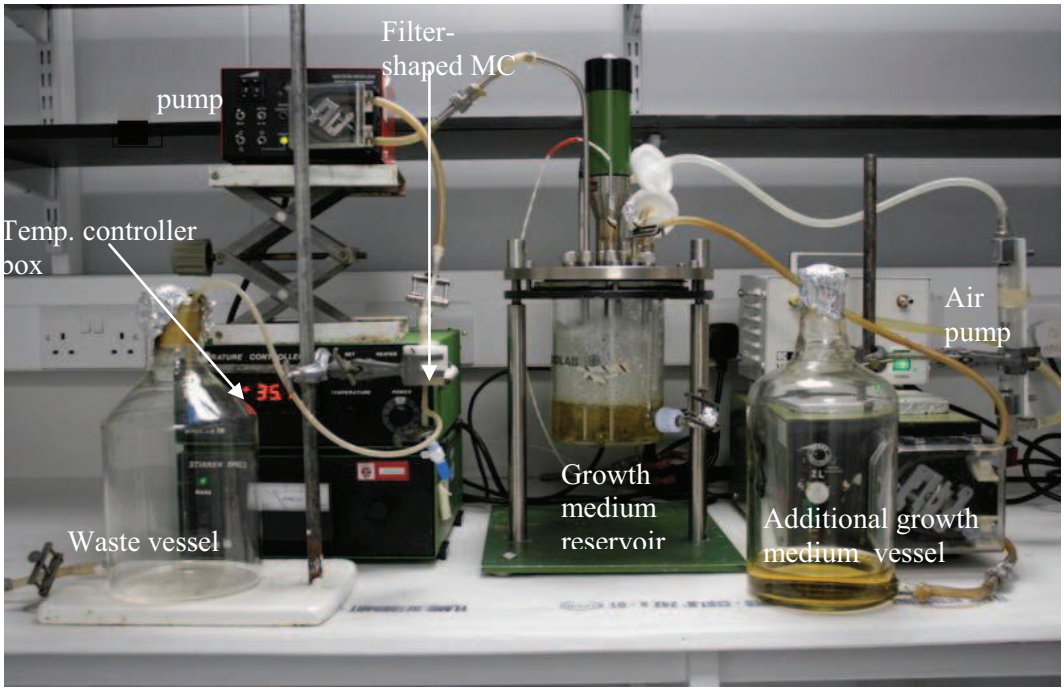

Figure 7.5: Experimental set up for the growth of *B. subtilis* immobilized on polyHIPE matrix in a filter-shaped PTFE microchamber. The equipment was located in a constant temperature room at 37^0C.

7.2.2 Results

The performance of an untreated TVP-PHP matrix located in a block-shaped microchamber was evaluated and compared to the treated vinylpyridine polyHIPE polymers, placed either in block-shaped or filter-shaped microchamber. In both cases the matrices were sealed in place with silicone sealant. The performance was determined by monitoring the outflow for α-amylase activity and the number of released cells. The morphology and proliferation of the immobilized cells in the TVP-PHP matrix were observed by scanning electron microscopy (SEM). The α-amylase activity and viable count of the cells released from matrices were calculated from samples collected throughout the 24h duration of the experiment.

The data shows that the production of α-amylase from the sealed block-shaped microchamber was first detected after 7h of inoculation and reached a steady state level (~0.5U/mL) after 12h (Figure 7.6). In contrast, the production of α-amylase by the immobilized *B. subtilis* cells on untreated TVP-PHP matrix (placed in an unsealed block-shaped microchamber) increased continuously to a peak of ~1U/mL at 16h, but then fluctuated for the remaining 8h to ~0.7U/mL at the end of incubation time. The production of α-amylase from the filter-shaped PTFE microchamber after an initial rise during the first 5h was constant throughout the experiment at ~ 0.25 U/mL.

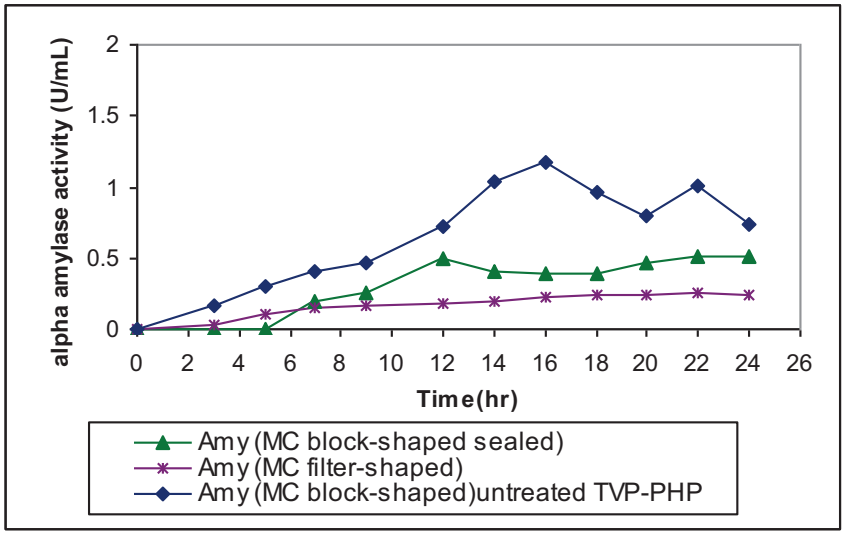

Figure 7.6: Time-course of the production of α-amylase by immobilized cells on untreated and treated TVP-PHP matrices placed in block-shaped PTFE microchambers compared with treated TVP-PHP matrix placed in filter-shaped PTFE microchamber (for 24h incubation with 1ml/min of nutrient medium flow rate).

The data showed that the release of *B. subtilis* cells from the untreated TVP-PHP placed in unsealed block-shaped PTFE microchamber was 10-fold higher than the TVP-PHP matrix placed in the same microchamber but sealed with silicone sealant (Figure 7.7). The large amount of cells released from this microchamber is likely to be due to the empty spaces at the edges and bottom of well that accumulate the nutrient medium. This result was confirmed by the SEM images that showed a large number of cells had accumulated at the bottom surface of this matrix (Figure 7.10A). This probably also accounted for the high level of

α-amylase produced from these matrices (Figure 7.6). On the other hand, the numbers of cells released from the sealed block-shaped PTFE microchamber were less than ~5 x 10^6 cells/mL, although the pattern of release fluctuated throughout growth compared to that from the filter-shaped PTFE microchamber. The cells released from the filter-shaped PTFE microchamber almost plateaued at ~5 x 10^6 cells/mL before slightly dropping towards the end of incubation time (Figure 7.7). Sealing the matrices into their respective microchambers led to a significant reduction in the numbers of cells released, as confirmed by SEM (Figure 7.10C-F). Even though, the numbers of cells released by the sealed block-shaped and filter-shaped PTFE microchambers were similar, the amount of α-amylase produced in the latter microchamber was more consistent. This is likely to be due to the design of the filter-shaped microchamber which only allows the passage of fluid through the matrix, in contrast to the block-shaped microchamber which, despite being sealed, allowed leaks of some culture at its edge.

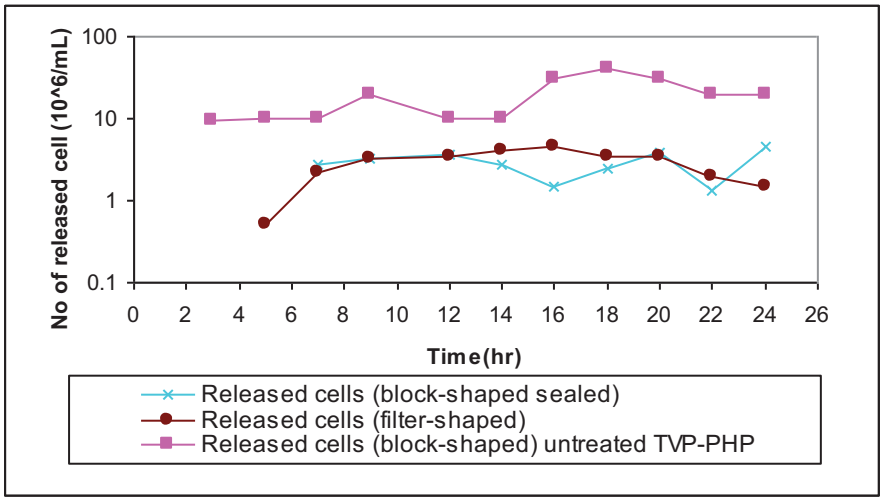

Figure 7.7: *B .subtilis* cells released from untreated and treated vinylpyridine polyHIPE matrices placed in a block-shaped PTFE microchamber compared with treated TVP-PHP matrix placed in filter-shaped PTFE microchamber, after 24h incubation at 37°C with a media flow rate of 1ml/min.

SEM was used to analyse the morphology and distribution of cells at various points within the structure of the vinylpyridine polyHIPE (TVP-PHP) matrices. The untreated TVP-PHP placed in the well of block-shaped microchamber was compared with treated TVP-PHP matrices placed in the sealed well of block-shaped microchamber and filter-shaped of PTFE microchambers. As can be seen in Figure 7.8C&E, the germinated cells were more evenly distributed on the pre-treated matrix (wetted with distilled water and LB medium prior to inoculation) compared to untreated matrix (Figure 7.8A&B), and therefore these conditions were used in later experiments.

Well rod-shaped vegetative cells were observed in all TVP-matrices placed in all PTFE microchamber systems (block-shaped and filter-shaped microchamber; Figure 7.9A&B). In the case of the cells immobilized on the untreated TVP-PHP matrix (unsealed PTFE block-shaped microchamber), elongated vegetative cells were observed without any apparent cell (Figure 7.9A). However, only a few cells were observed in the cross section of the polyHIPE matrix and some cell debris was seen in this area of all microchamber systems (Figure 7.9.

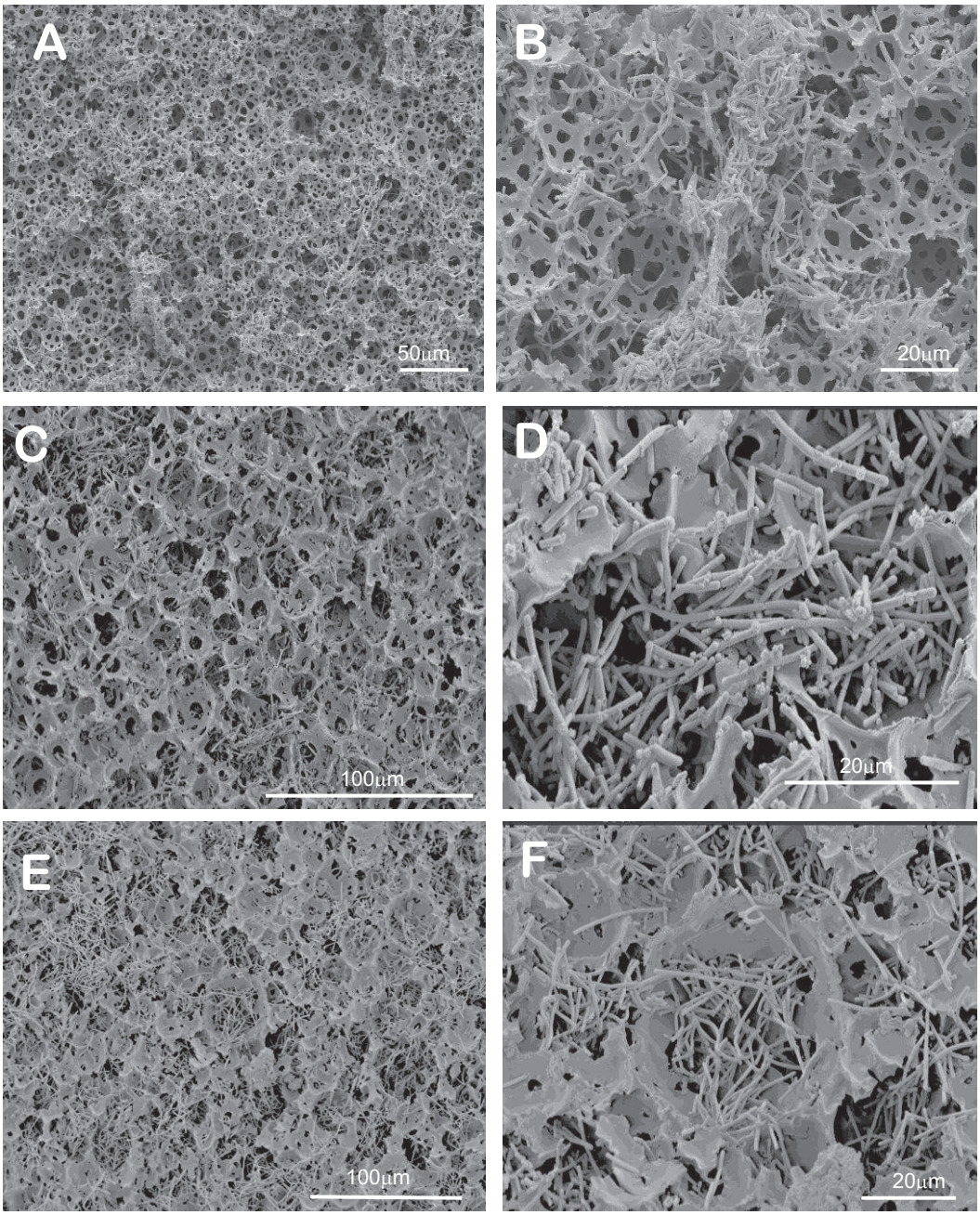

Figure 7.8: Appearance of vegetative cell of *B. subtilis* on the top surface of TVP-PHP matrices after 24 h incubation: untreated matrix (A) general view (x350), (B) view at high magnification (x1000); treated matrices (C) general view (x350), (D) view at high magnification (x1000), (E) general view (x350), (F) view at high magnification (x1000)

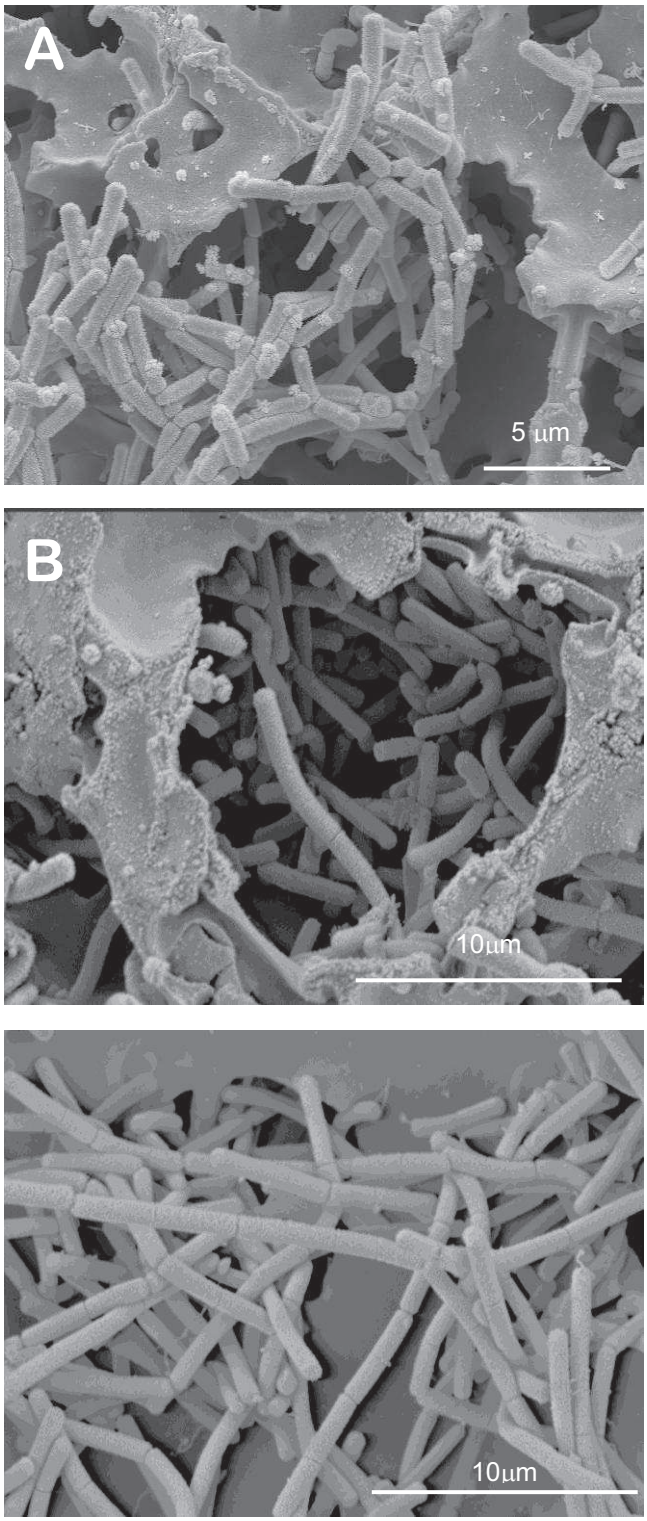

Figure 7.9: Appearance of vegetative cell of *B. subtilis* on the top surface of TVP-PHP matrices after 24 h incubation at high magnification: (A) untreated matrix placed in block-shaped microreactor (B) treated matrix placed in sealed block-shaped microreactor (C) treated matrix placed in sealed filter-shaped microreactor.

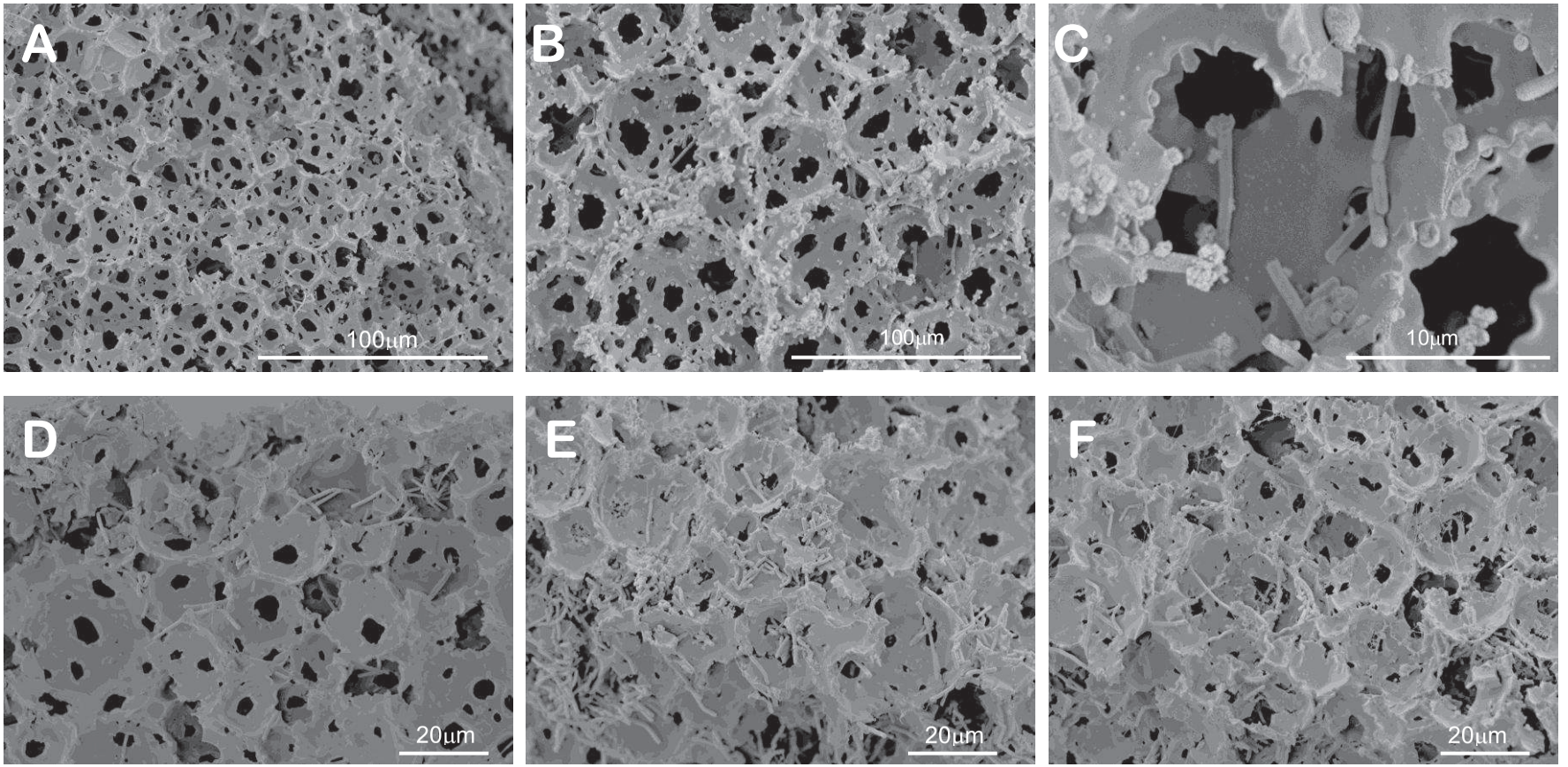

Figure 7.10: Appearance of vegetative cells of *B. subtilis* immobilized on TVP-PHP after 24 hours incubation, placed in sealed block-shaped microchamber: (A) general view (x500), (B) on other spot areas (x1000), (C) high magnification (x4500) and sealed filter-shaped microreactor: (D) general view from the top edge (x1000), (E) a slightly further from the top edge (x1000) and (F) on other spot areas

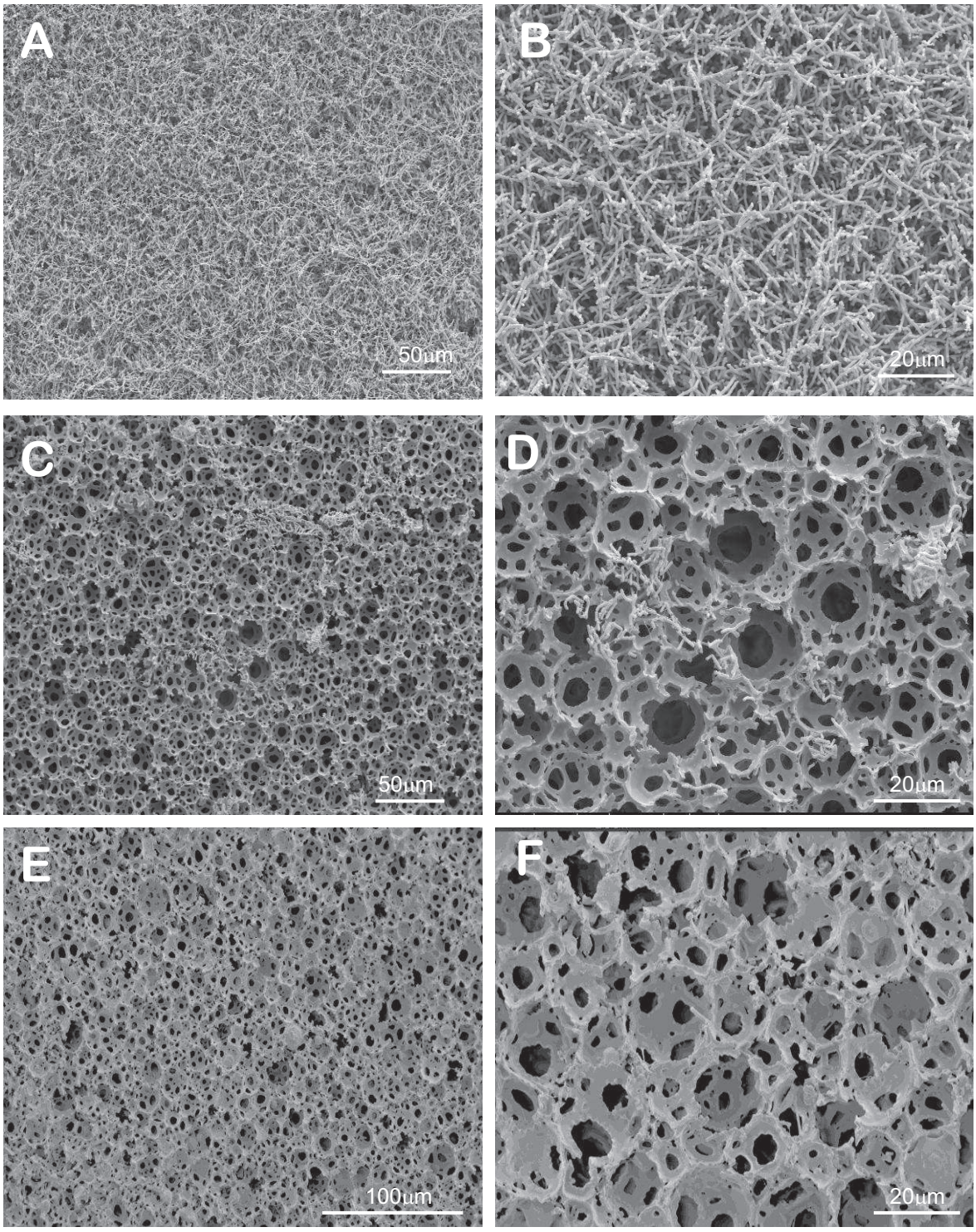

Figure 7.10: Appearance of vegetative cells *B. subtilis* immobilized on TVP-PHP after 24 hours incubation on the bottom surface of vinyl pyridine polyHIPE placed in: unsealed block-shaped microreactor (A) general view (x350), (B) a higher magnification (x1000), sealed block-shaped microreactor (C) general view (x350), (D) a higher magnification (x1000) and sealed filter-shaped microreactor (E) general view (x350), (F) a higher magnification (x1000)

7.2.3 Discussion

The aim of this chapter was to establish a combination of matrix and microchamber that optimised the production of α-amylase. This involved three stages: the development of an efficient means of inoculating the matrices; the design and operation of various matrix/microchamber formats; and the monitoring of α-amylase production. A better result was obtained when the forced-flow seeding technique was used to innoculate cells onto the TVP-PHP matrix and placing the matrix in a block-shaped PTFE microchamber. It showed that the inoculated spores germinated and grew without the appearance of cell debris (Figure 7.8B). When spores were manually loaded onto the matrix a clump of aggregated cells was observed on the top and bottom surfaces of matrix (Figure 7.2A & Figure 7.3) with significant cells debris. There was also evidence of many ungerminated spores. The forced-flow technique appears to provide the hydrodynamic force required to ensure that the spores penetrated the matrix, avoiding the accumulation of cells at the matrix surface.

The flow-through of nutrient medium to the matrix was improved by placing the TVP-PHP matrix into a block-shaped PTFE microchamber. The resulting dynamic flow resulted in the disappearance of cell debris. However, the distribution of cells on the surface was still not even (Figure 7.8A&B) and some small bead-like cells, presumably ungerminated spores, were also observed. Significant numbers of cells were also found at the bottom surface of this matrix due to the leakage of nutrient medium to the edge wall and the bottom flat-designed of this microchamber (Figure 7.10 A&B). Therefore, the edge of this microchamber was sealed with silicone sealant before placing the TVP-PHP matrix and this matrix was wetted with sterilized distilled water and LB medium prior to use. As a result, a homogeneous distribution of vegetative cells on the TVP-PHP matrix surface (Figure 7.8 C&D) and a huge reduction of cells number on the bottom surface of matrix were observed Figure 7.10 C&D). The pre-wetting of this matrix appears to change the surface characteristics of the matrix which promotes the proliferation and more even distribution of cells. Moreover, the implementation of forced seeding technique to inoculate spores using a syringe pump also contributed to this improved cell distribution.

However, few vegetative cells were found in the cross-section of the matrix of this system. On the other hand, when the design of the PTFE microchamber was modified to one with a filter-shape, the vegetative cells were clearly seen to have migrated throughout the cross section of the matrix D-F). This might be due to the placement of the polyHIPE matrix in the filter-shaped microchamber enhancing nutrient transport into the pores of the polyHIPE.

The α-amylase production rate of immobilized *B. subtilis* cells from the filter-shaped PTFE microchamber was low compared to the other systems. The production rate only reached ~0.25 U/ml by the end of the incubation time (Figure 7.6). The α-amylase production rate stabilized early (after ~ 5h) and the proliferation and growth of the vegetative cells were much better than the other two systems. A high α-amylase production rate of the other two systems is likely to be due to cell leakage at the edge of the block-shaped microchamber (Figure 7.6). In both systems, the growth and proliferation of cells was mainly limited at the upper areas and edges of the matrices and the cells failed to penetrate deep in the matrix. This results in a severe limitation in the internal mass transfer of nutrients and oxygen within the polyHIPE matrix. This limitation is likely to be related to the physico-chemical properties and microarchitecture of vinyl pyridine polyHIPE matrices which are slightly hydrophilic compared to poly(styrene-divinylbenzene) polyHIPE matrices. The flow of fluid in this type of matrix might be only through the capillary action and therefore to have low fluid diffusivity and permeability. Moreover, the pore (25.0 μm) and interconnect (7.0 μm) sizes are probably not large enough to allow the cells to penetrate across the matrix and hindered removal of wastes products or cells debris.

Although, the germinated cells failed to penetrate deep into this type of polyHIPE, the developed system has shown that the inoculated spores were able to germinate in a permissive environment. Many germinated cells were observed on the top surface of this matrix where nutrient availability was high (Figure 7.8 E & F). However, further investigations are required to improve the performance of the system. For example, modifications to the physico-chemical properties of the vinylpyridine polyHIPE matrix to make it more hydrophilic might improve its biocompatible and permeability to fluids. Additionally, the optimal pore and interconnect sizes need to be optimised to improve substrate transport and cell

penetration. However, no further studies were carried out for this type of polyHIPE, but instead poly(styrene-divinylbenzene) polyHIPE was modified to improve its hydrophilicity via sulphonation treatment.

8 Sulphonated PolyHIPE as a support matrix

8.1 Characterisation of sulphonated-PolyHIPE

8.1.0 Introduction

Functionalisation of polyHIPE polymers (PHPs) can be carried out through manipulation of their components and/or variations in operating conditions for their synthesis. The former approach includes the used of 2-hydroxyethyl acrylate, 2-hydroxyethyl methaclarylate (Kulygin and Silverstein, 2007), acrylamide (Gitli and Silverstein, 2008) as monomer and/or macromonomers in the internal aqueous-phase in synthesizing polyHIPE. These generic polyHIPEs are examples of hydrophilic polymeric substrates that exhibit good biocompatibility, based on oil-in-water (o/w HIPE). However, these types of polyHIPEs have low porosities and poor interconnectivities due to the instability of o/w HIPEs that limit the internal phase content. In the case of polyHIPEs based on water-in-oil (w/o-HIPE), high porosities and interconnectivities can be obtained due to their high stability. However, most of these polymeric substrates are hydrophobic, and result in diffusion-related problems that greatly restrict their application to water-based systems. Consequently, the establishment of a uniform chemical modification of these polymeric materials was considered to be essential to improve their porosity. Several methods can be employed to chemically modify these materials, one of which is the electrophilic aromatic substitution of the styrene residues. The reactions include sulphonation, nitration and bromination. Previous studies have demonstrated that synthesizing uniformly functionalized monolithic porous poly(styrene/divinybenzene) polyHIPE can be achieved under mild conditions, using hydrophobic reagents and homogeneous reaction conditions (Cameron *et al*., 1996).

In this study, PHPs were synthesized through the water-in-oil HIPE route in order to obtain a polyHIPE with good structural stability. The resulting PHPs have high porosities and interconnectivities. In order to enhance its hydrophilicity and diffusivity, the resulting w/o HIPE was subjected to sulphonation using sulphuric acid. The treated porous, hydrophilic polymeric support, called

sulphonated PHP (SPHP), was washed to remove traces of sulphuric acid and then used to immobilise the industrial starch-degrading bacterium, *Bacillus subtilis*.

The physical and chemical characteristics of materials used as immobilized cell matrices are important factors for the initial physical interaction between the bacterial cells and the carrier matrix. The physico-chemistry of the matrices includes pore size, distribution, surface area, porosity, mechanical strength and smoothness and surface chemistry (hydrophobicity/charge, ligand-complexes). Thus, the first three properties of SPHP matrices and its capacity to take up water were also determined.

Based on previous results (Chapter 5, section 5.1.1.1), the use of poly(styrene-DVB) polyHIPE with pore and interconnect sizes between 5μm and 20μm hindered the penetration of cells through the cross-section of polyHIPE. This might have been because the pore sizes and interconnects were too small for the transportation of substrates and waste products into and out of the matrices and to and from the cells. Therefore, the appropriate pore and interconnect size of sulphonated-polyHIPE matrices are determined by manipulating the dosing time, t_D and mixing time, t_M.

The objectives of this chapter are to:

- investigate the effect of chemically modified polyHIPE on its morphology and physical architecture (pores and interconnects size)
- investigate the effect of sulphonated polyHIPE pores, interconnect size and their distribution by changing dosing and mixing time parameters
- determine the surface area of the sulphonated polyHIPE
- study the capacity for water uptake of sulphonated polyHIPE

8.1.1 Results

8.1.1.1 Morphology of sulphonated polyHIPE

The initial protocol for the production of polyHIPE matrices involved maintaining a dosing time of 5 minutes while changing the mixing time from 1 to 5 minutes. Micrographs of the resulting matrices (Figure 8.1) show that at the shorter mixing times (labelled SPHP-1) the pore sizes were highly variable and the interconnect sizes much larger and these were obtained with longer mixing times (SPHP-2). The shorter mixing time appears to affect the appearance of interconnects within the structure, presumably because there was less time to establish a stable emulsion.

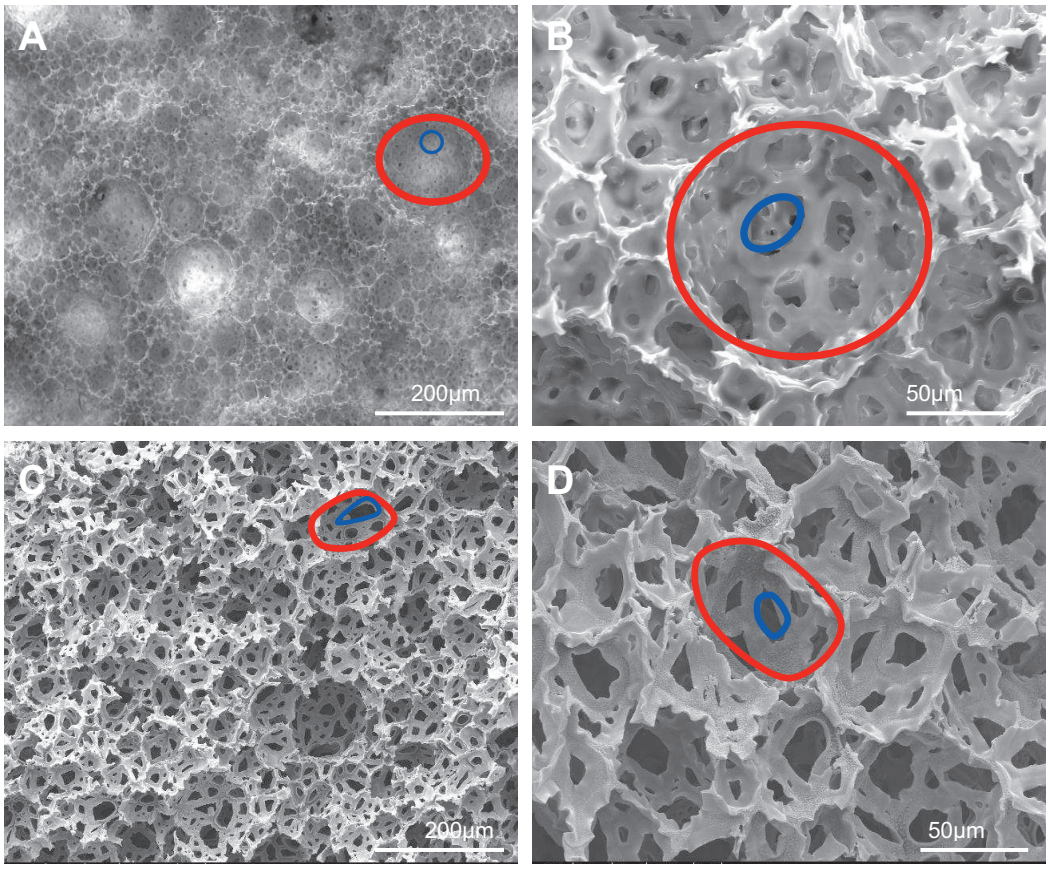

Figure 8.1: Micrographs illustrating the effects on the physical architecture of sulphonated polyHIPEs of varying mixing time: (A & B) SPHP-1 and (C & D) SPHP-2. The red circles outline typical pores while the blue circles outline typical interconnects.

The initial experiments were followed by experiments in which dosing time (t_D) was increased to 10 min, while the mixing times (t_M) were increased to either 10 min or 20 min. The resulting matrices were labelled SPHP-4 (t_D = 10 min and t_M = 10 min) and SPHP-6 (t_D = 10 min and t_M = 20 min). The micro-structure of both polyHIPEs were examined by scanning electron microscopy and representative images, including those from sample SPHP-2 (t_D = 5 min and t_M = 5 min) are shown in Figure 8.2.

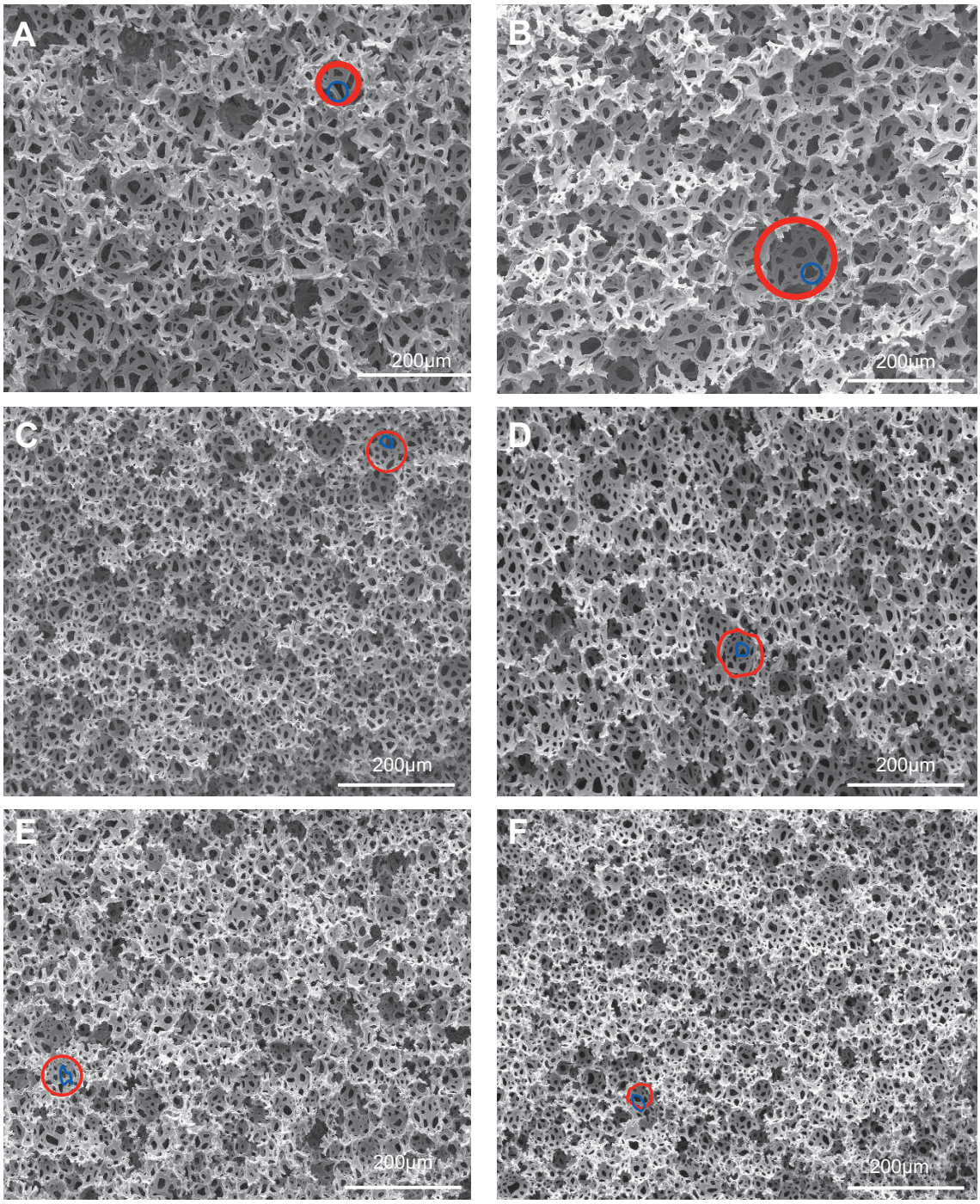

Figure 8.2: Micrograph images illustrating the effects of dosing and mixing rate on the micro physical architecture of sulphonated polyHIPEs. SPHP-2 (A) before and(B) after sulphonation; SPHP-4 (C) before and(D) after sulphonation; SPHP-6 (E) before and (F) after sulphonation. The red circle outline pores, the blue circle interconnects.

As can be seen in Figure 8.2A & B, the pore sizes in sample SPHP-2 (t_D5/t_M5) are significantly larger than those for samples SPHP-4 and SPHP-6. The pores and interconnects size of samples SPHP-4 and SPHP-6 are well distributed and

uniform, and this may be due to the additional 5 minutes dosing time, allowing for the uniform formation of interconnects throughout the structure. The increase in mixing time resulted in the emulsion reaching higher energy state, with a resultant decrease in droplet size (refer to section 1.2.2.1.2). However, since the pores and interconnect sizes of SPHP-6 were only marginally smaller than those of SPHP-4, it appears that the additional 10 minutes of mixing time had little or no affect on the final structure of the PHP. This is likely to be due to the emulsion having reached a highly viscous and stabile state such that the further break-up of the droplets was not possible without increasing the vigour of the stirring.

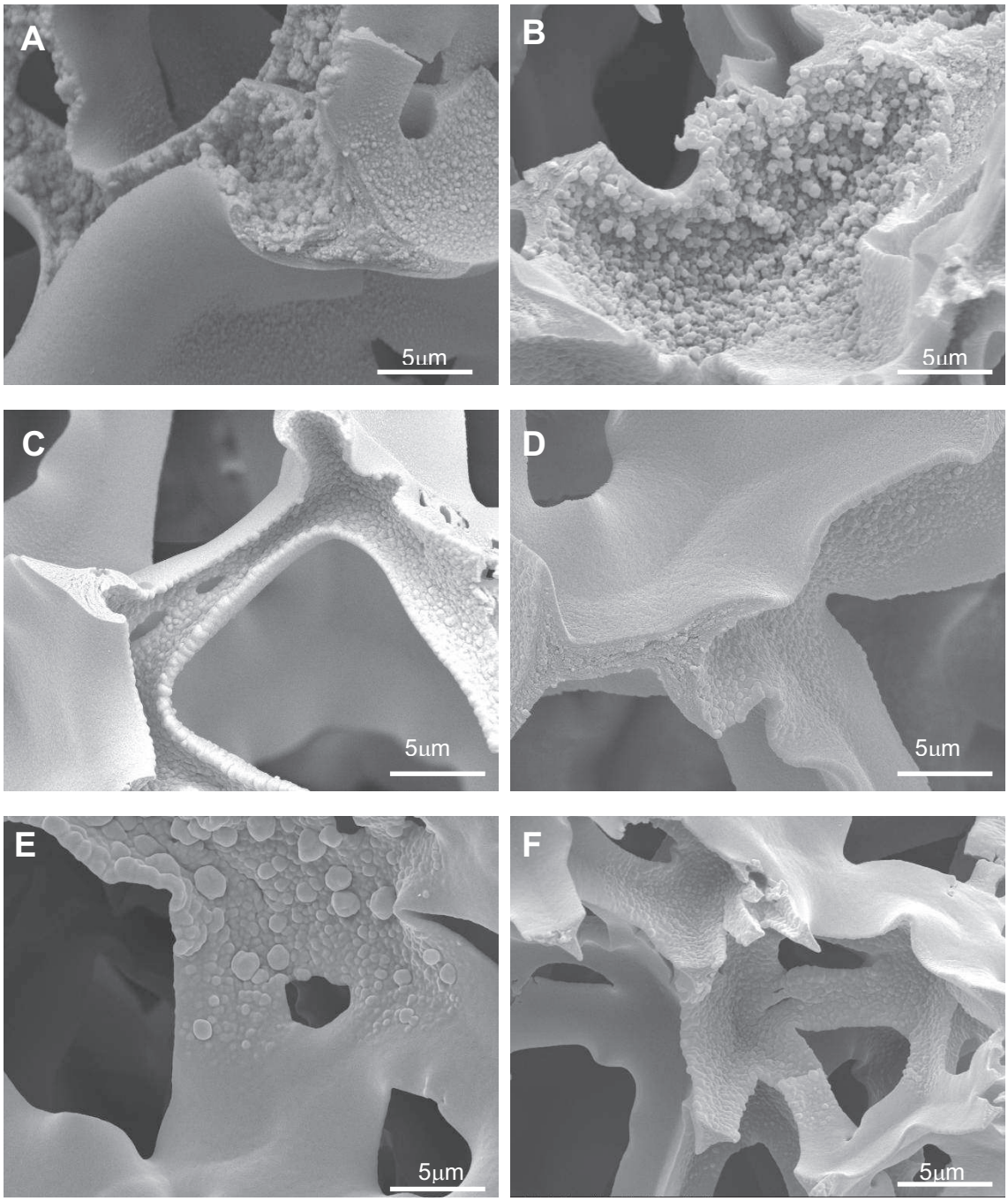

Figure 8.3: SEM images of micro-architecture of sulphonated polyHIPEs at high magnification (x5000): SPHP-2 (A) before and (B) after sulphonation; SPHP-4 (C) before and(D) aftersulphonation; SPHP-6 (E) before and(F) after sulphonation.

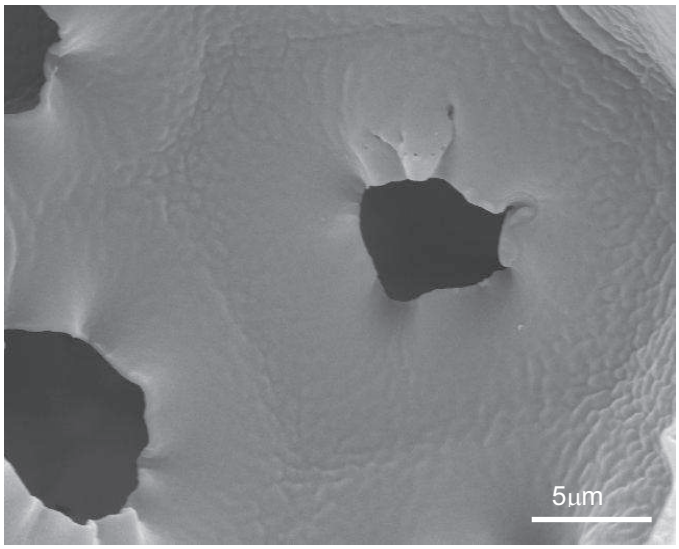

Figure 8.4: SEM images of micro physical architecture of poly(styrene-DVB) polyHIPE, T5 at high magnification (x5000)

The inclusion of 10% of sulphuric acid into the aqueous phase resulted in the formation of blisters in the samples SPHP-2, SPHP-4 and SPHP-6 as can be seen in Figure 8.3A, C and E. This is likely to be due to the adsorption of sulphuric acid to some pores. Blisters did not appear in sample T5, which is a poly(styrene-DVB) polyHIPE (Figure 8.4) .

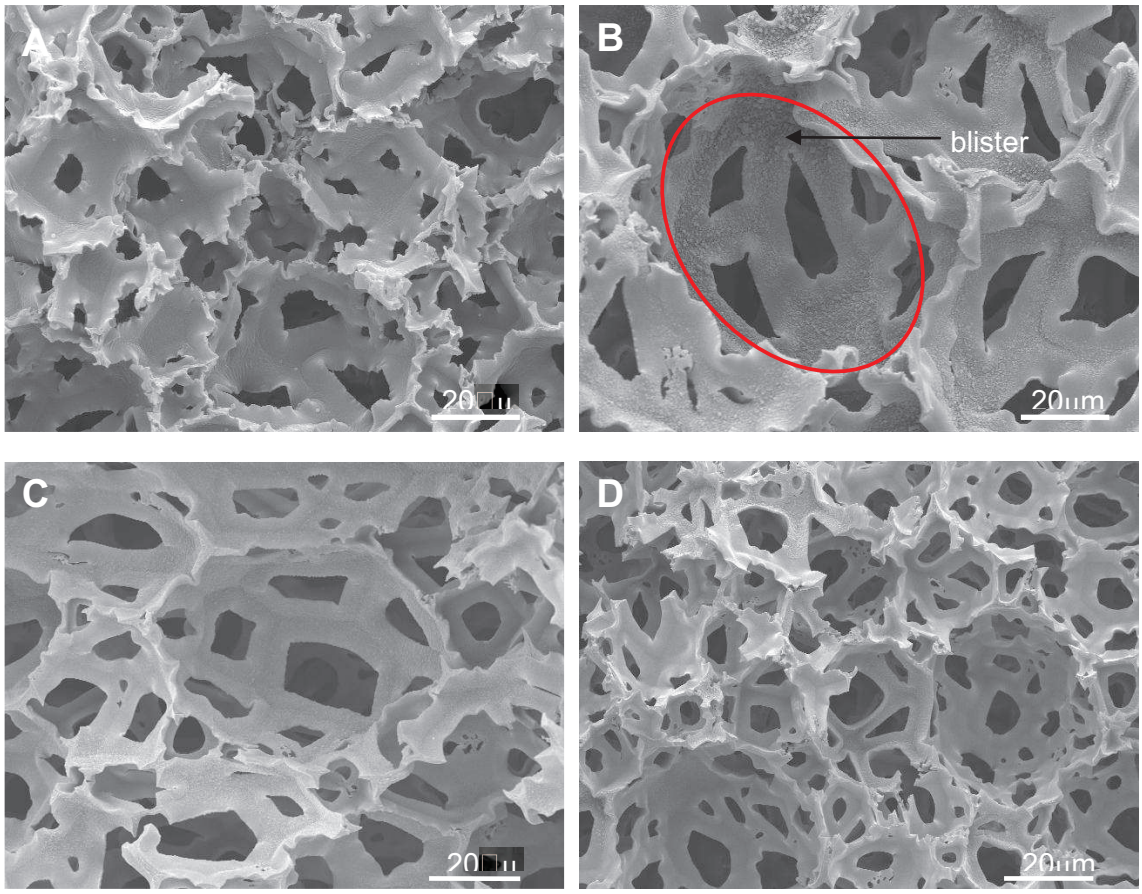

Figure 8.5: Micrographs showing the pore structures of (A) poly(styrene-DVB) polyHIPE T5 and sulphonated polyHIPEs (B) SPHP-2, (C) SPHP-4 and (D) SPHP-6

The structure of polyHIPE is slightly different before and after sulphonation treatment as shown in Figure 8.3. One consequence of sulphonation was the appearance of "blisters" on the surface of the matrix (Figure 8.3). These were more obvious for SPHP-2 (Figure 8.5B) than SPHP-4 and SPHP-6 (Figure 8.5C & D). Blistering might be a consequence of the difference pore and interconnect sizes among the samples since this would allow for the more even distribution of sulphuric acid into the sample with the largest pores, namely SPHP-2. If blistering is a reflection of the degree of sulphonation, the samples with small pores (SPHP-4 and SPHP-6) would need to be treated for longer to ensure the homogeneous permeation of sulphuric acid.

8.1.2 Evaluation of pore and interconnect size of sulphonated PolyHIPE

A summary of the operating conditions and the calculated pore and interconnect sizes are shown in Table 8.1. SPHP-1 and T5 (poly(styrene-DVB) polyHIPE) are included for comparative purposes. The experiments were repeated three times and the average values were calculated from fifty measurements. The compositions of the oil and aqueous phases of rigid polyHIPE were used for these experiments (Refer to Chapter 2 for the compositions), carried out at 25^0C. The aqueous phase used contains 10% of sulphuric acid.

Table 8.1: Experimental conditions used for making sulphonated polyHIPEs and the evaluation of average of their pore and interconnect sizes compared with poly(styrene-DVB) polyHIPE, T5.

			Pore size (D) (μm)		Interconnect size (d) (μm)	
PHP Code No.	Dosing time (t_D, min.)	Mixing time (t_H, min.)	*before	*after	*before	*after
SPHP-1	5	1		62.0±2.16		20.0±0.58
SPHP-2	5	5	46.0±0.62	42.0±0.61	20.0±1.56	22.0±0.10
SPHP-4	10	10	31.0.±3.61	36.0±0.50	14.0±0.95	16.0±0.89
SPHP-6	10	20	30.0±2.09	30.0±0.64	13.0±1.32	11.0±0.76
T5	10	20	36.0 ± 0.04		9.0 ± 0.17	

* before and after sulphonation reaction

As can be seen, after sulphonation, the sample with the shortest mixing time (SPHP-1 t_H = 1 min) yielded the largest pore size. There was a significantly different pore size between SPHP-1 (t_H = 1 min) and SPHP-2 (t_H = 5 min), although their interconnect sizes were similar. The similarity of their interconnect sizes may be due to their having the same dosing time. The pore and interconnect sizes of samples SPHP-4 and SPHP-6 were only slightly different indicating that a physical limit had been reached and that increasing the mixing times beyond 10 minutes has little or no influence on these parameters. The physical appearances of most samples were affected by sulphonation, although there was a lack of consistency in these changes.

8.1.3 Distribution of pores and interconnects size of PolyHIPE polymers

The distribution of pore and interconnect sizes of the polyHIPE polymers were evaluated by plotting frequency against the diameter of their physical structures using the Minitab ver 15.0 statistical software (Figure 8.6 and Figure 8.7). The ratio of the average interconnects and pore (D) diameters (d) were also calculated to provide an indication of the interconnected pore network of the porous material (Table 8.2).

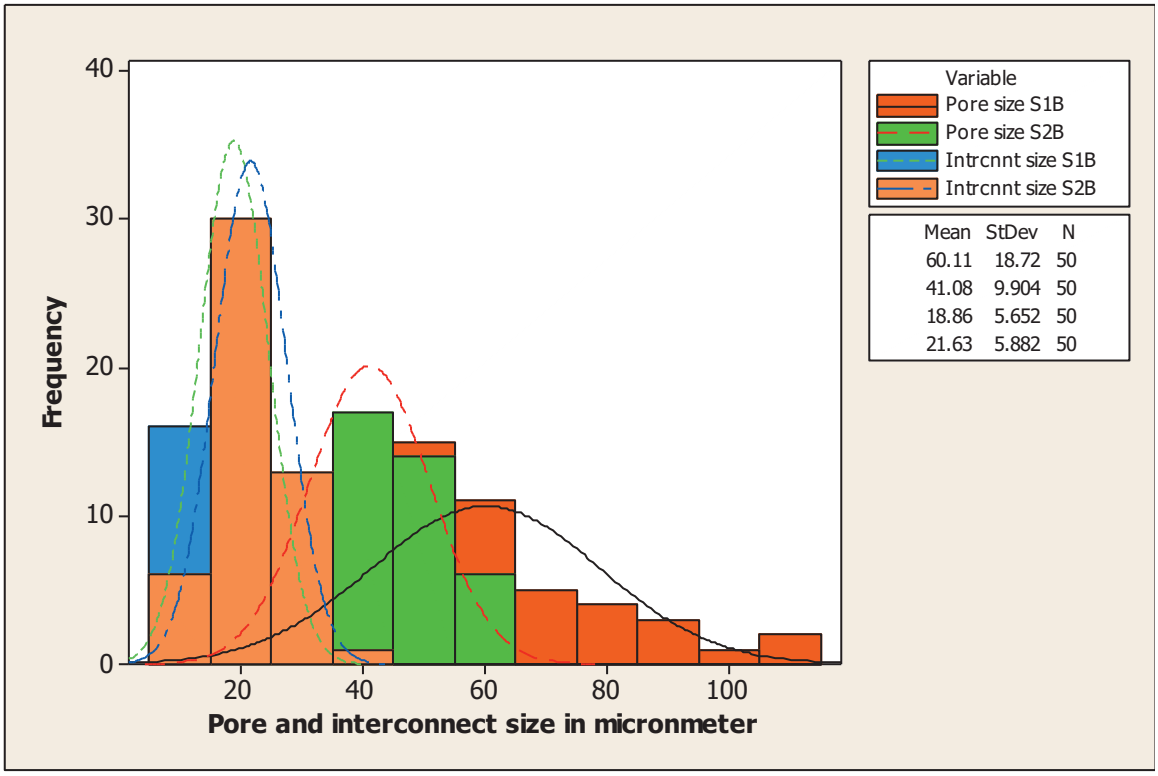

Figure 8.6: Comparison of diameter of pores and interconnects between samples SPHP-1 and SPHP-2. SPHP-1 and SPHP-2 denoted as S1 and S2 respectively after sulphonation treatment (B).

Generally, the pore size distribution of SPHP-1 was wider than that of SPHP-2 (Figure 8.6). The pore size distribution of the former sample was more than 100μm with peak maximum approximately 60μm. In the case of SPHP-2, the average pore size was approximately 40μm with a relatively narrow distribution. This is likely to be the result of the extended mixing time breaking-up droplets in the emulsion. On the other hand, the interconnect pore of the SPHP-1 and SPHP-2 samples had very similar average interconnect pore sizes of approximately 20μm and a relatively narrow size distribution. The value d/D of SPHP-1 (0.32) was slightly lower than that of SPHP-2 (0.52). This result indicates the interconnection pores of SPHP-2 are better connected than in sample SPHP-1. The summary of the calculated ratio of average diameter interconnects (d) and pores (D) is shown in Table 8.2.

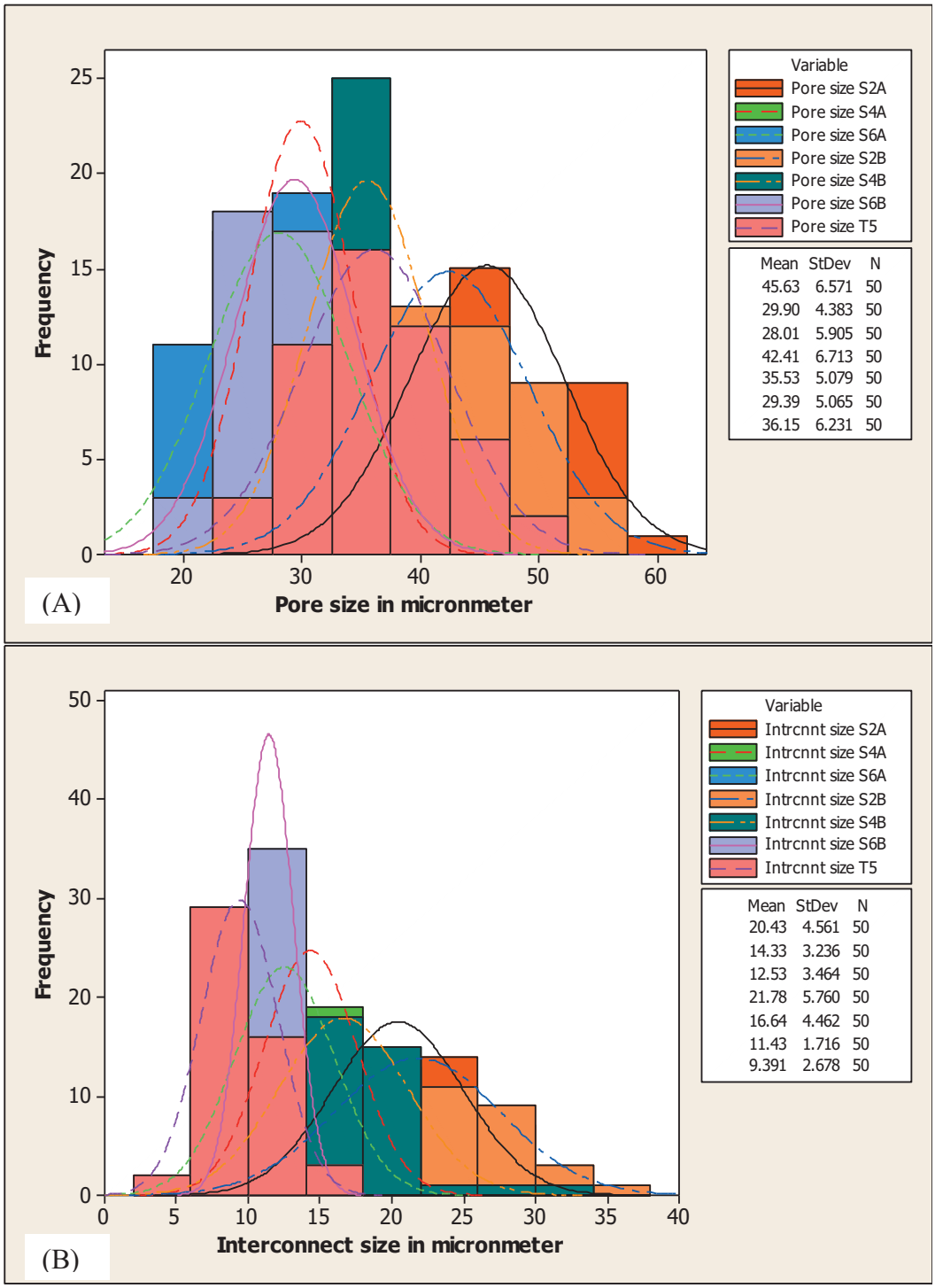

Figure 8.7: Evaluation of diameter of (A) pores and (B) interconnects from SEM images for samples SPHP-2, SPHP-4, SPHP-6 (S2, S4 and S6, respectively), compared with T5 (Minitab 15.0). A and B refer to measurements before and after sulphonation, respectively.

Generally, SPHP-2 has a wider pore size distribution in comparison to other samples (Figure 8.7A). The pore size distributions of polyHIPE matrices after sulphonation reaction were slightly changed. There was a slight shift in the pore size distribution of SPHP-2, from the mean of 46μm to 42μm. On the other hand, the mean pore size of SPHP-4 was slightly increased, from 30μm to 36μm. The pore size of SPHP-6 was not significantly changed in response to sulphonation, unlike the T5 sample, being produced using the same operating condition. The same trend was observed for the distribution of interconnect sizes (Figure 8.7B).

There was a significant shift in the interconnect and pore size distribution of sulphonated polyHIPE samples in comparison to T5, non-suphonated polyHIPE sample (Figure 8.7B). The interconnect pore size distributions of SPHP-2 was wider than other samples. There was a significantly increased frequency of interconnect pores, within range 10 – 15μm, before and after sulphonation treatment of SPHP6; from less than 30x up to more than 40x. The summary of the calculated ratios of average diameter interconnects (d) and pores (D) is shown in Table 8.2.

Table 8.2: Evaluation of diameter of pore and interconnect of polyHIPE samples to determine the d/D parameter.

	d/D (μm)	
PHP Code No.	*before	*after
SPHP-1		0.32
SPHP-2	0.43	0.52
SPHP-4	0.45	0.44
SPHP-6	0.43	0.37
T5	0.25	

8.1.4 Characterisation of vinyl pyridine-modified PHPs by Fourier Transform Infrared Spectroscopy (FTIR)

Sulphonated polyHIPEs were analyzed by Fourier Transform Infrared Spectroscopy (FTIR) to determine changes in their chemical composition following sulphonation (Figure 8.8A-C).

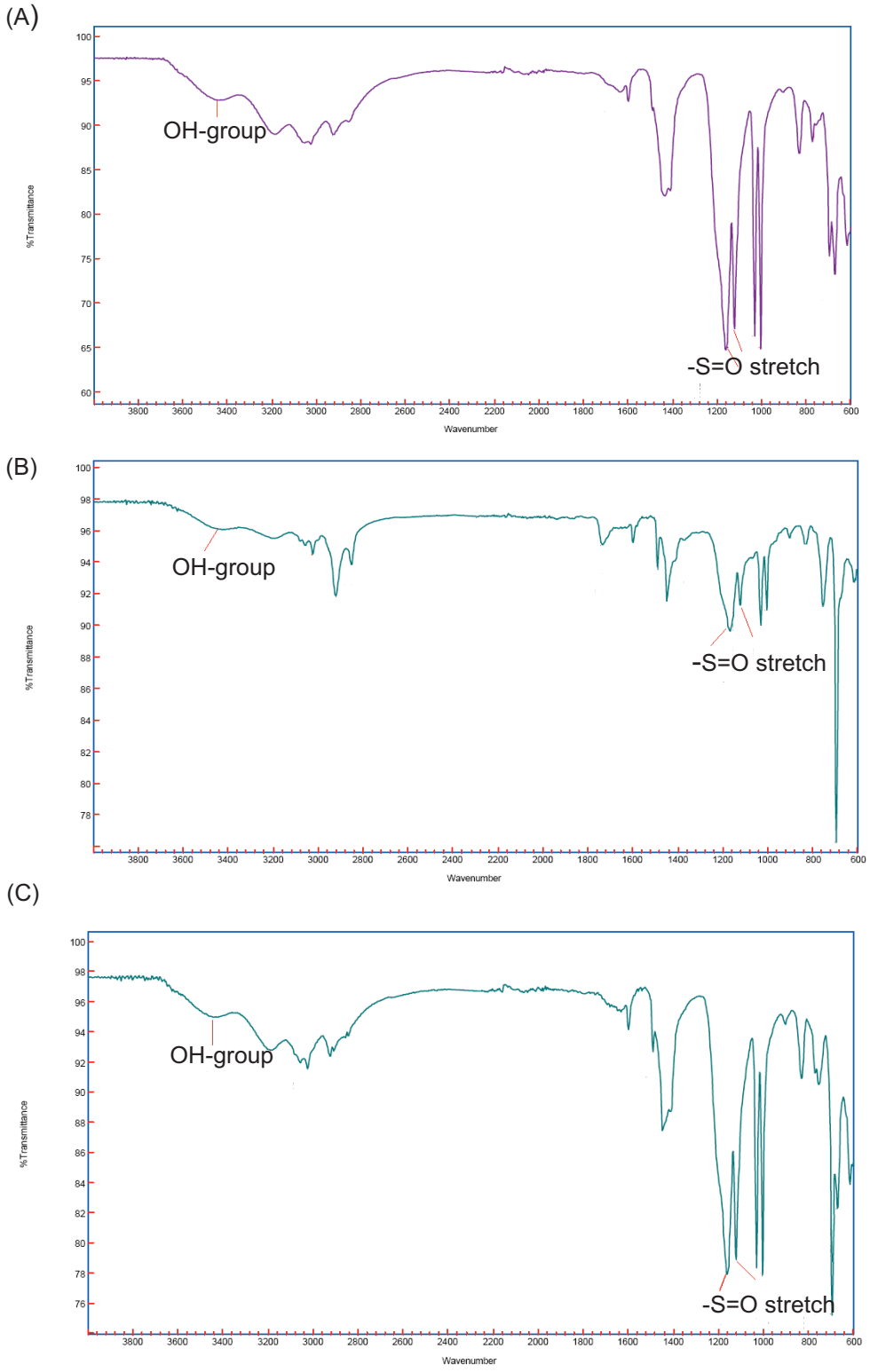

Figure 8.8: Infrared spectra of sulphonated polyHIPEs (A) SPHP-2, (B) SPHP-4 and SPHP-6. The hydroxyl groups and the –S=O bonds are indicated in the spectra

As can be seen from the FTIR spectrum (Figure 8.8A-C), the presence of aromatic acid groups in all samples were confirmed by a –OH stretch peak at 3434-3440 cm^{-1} and a –S=O stretch at peak between 1195 – 1168 cm^{-1}.

Table 8.3 shows the absorption peaks and the designation for three different sulphonated polyHIPE with sulfonic acid groups.

Table 8.3: Characteristic infrared absorption spectroscopy data for SPHPs samples.

Peak cm^{-1}	Assignment
3440	Stretching mode of the hydroxyl group
1163	Symmetric SO_2 stretching
1125	Hydrogen bonds of the sulfonic acids group
620	C-S linkage

8.1.5 Surface area of sulphonated polyHIPE

The surface area of the sulphonated polyHIPE materials was determined with a Coulter SA 3100 analyser (Beckman-Coulter, California, US) using the gas sorption technique (Brunauer-Emme-Teller (BET) model). The results obtained are shown in Table 8.4.

Table 8.4: Results of BET Surface Area of polyHIPE materials

PHP Code No.	Surface area (m^2/g)
SPHP-2	0.84
SPHP-4	1.42
SPHP-6	1.83
T5	4.68

8.1.6 The water uptake capacities of sulphonated and unsulphonated polyHIPE

The water uptake capacities of the sulphonated and unsulphonated polyHIPE samples were calculated on the basis of their mass increases (with respect to the original dry mass) obtained after being held under water for 24h and up to 48h. The results are shown in Figure 8.9 and Figure 8.10 and compared with other type polyHIPEs (Figure 8.11).

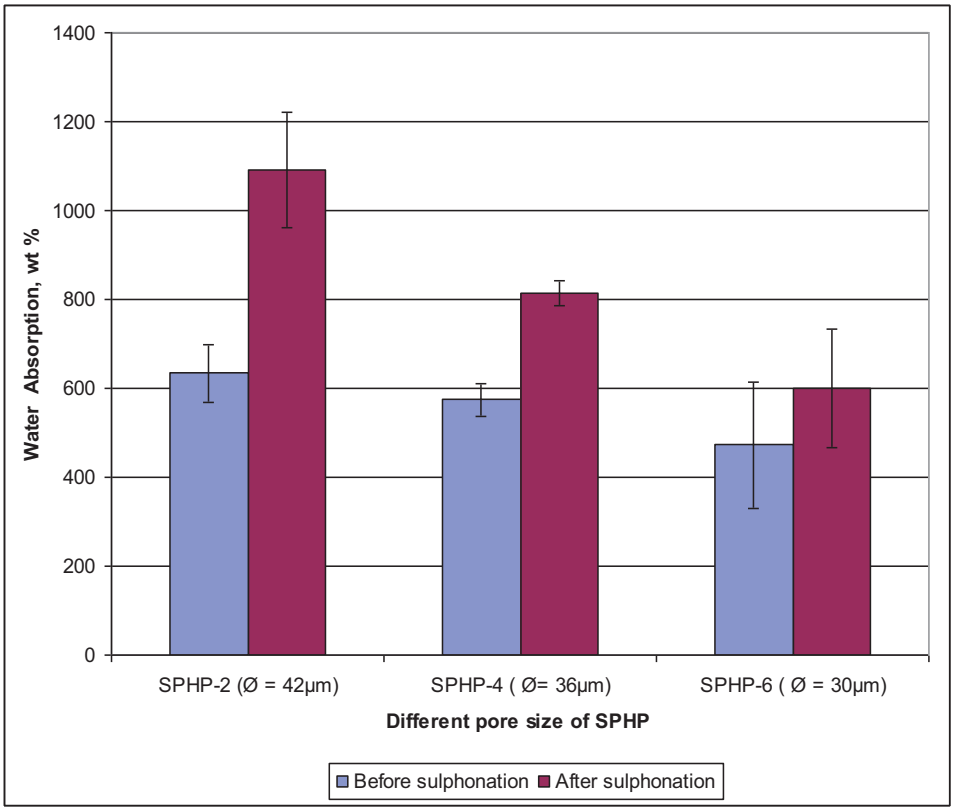

Figure 8.9: Water absorption of polyHIPE samples before and after sulphonation

As can be seen in Figure 8.9, there was a significant increased of water absorption associated with sulphonation. The water absorption of SPHP-2, SPHP-4 and SPHP-6 were approximately 630 wt%, 580 wt% and 470 wt% respectively, before sulphonation treatment (Figure 8.9). After sulphonation treatment, water absorption increased to approximately 72%, 42% and 27%, respectively, for SPHP-2, SPHP-4 and SPHP-6. It was found that the matrix with the largest pores, SPHP-2 obtained the highest water uptake capacities compared to others

SPHPs. Its physical microstructure was probably more permeable compared to other SPHPs. There was some incremental increase of absoprtion after 48h which was approximately 24wt%, 16wt% and 30wt%, respectively for SPHP-2, SPHP-4 and SPHP-6 as shown in Figure 8.10

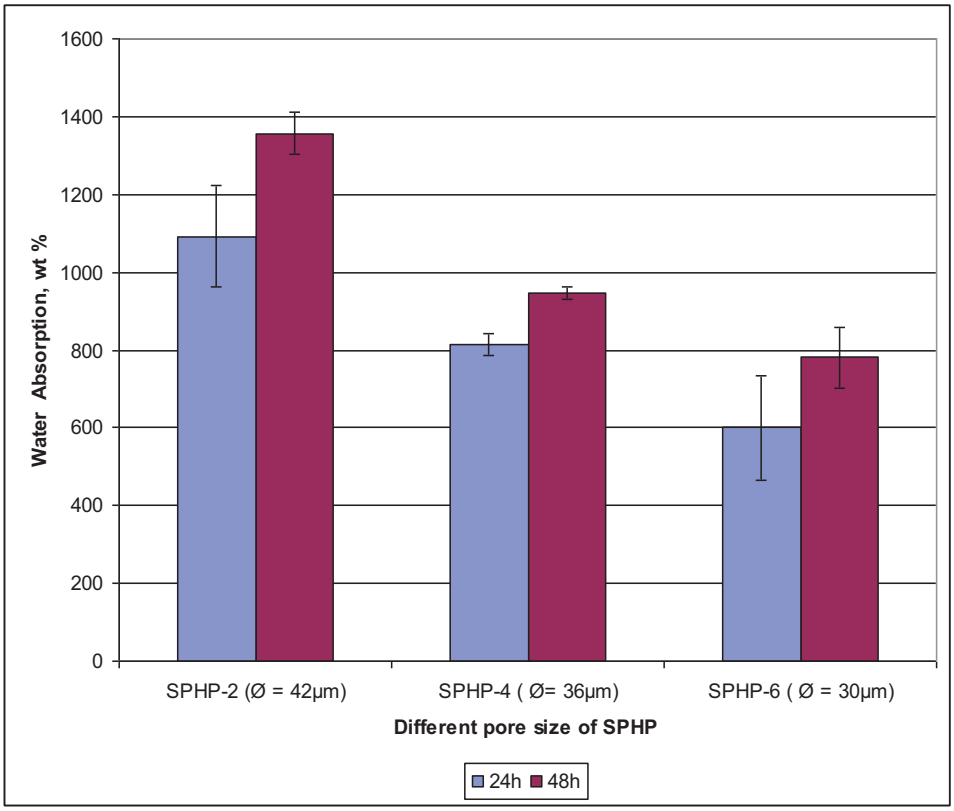

Figure 8.10: Water uptake of sulphonated polyHIPE for 24h and 48h

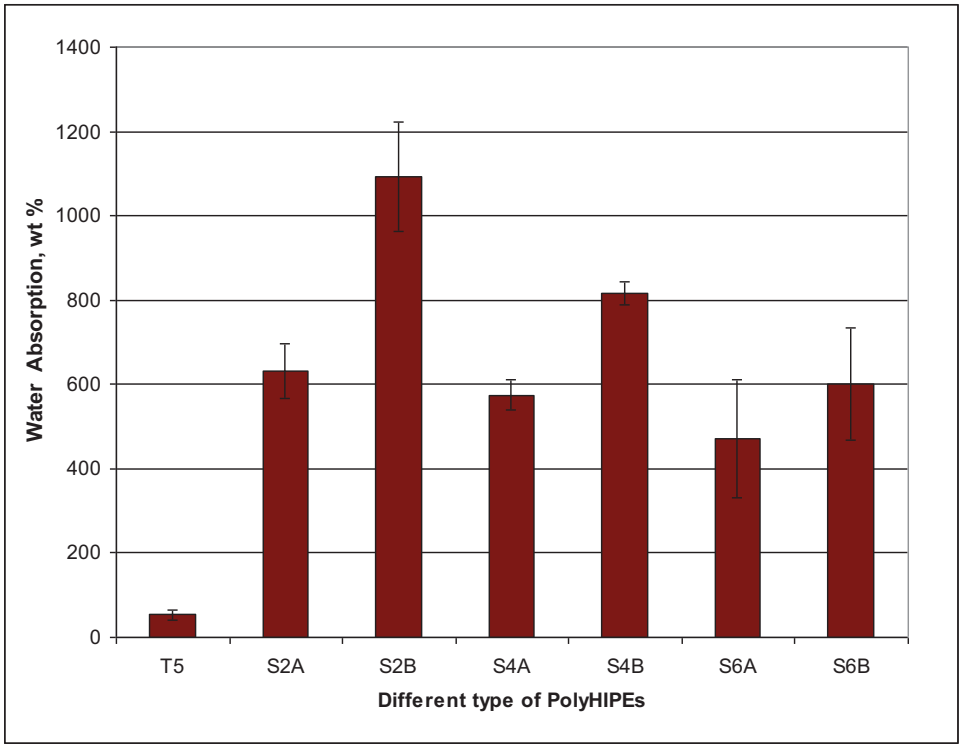

Figure 8.11: Comparison of water uptake by sulphonated polyHIPE and poly(styrene-DVB) polyHIPE, T5. SPHP-2, SPHP-4 and SPHP-6 (S2, S4 and S6, respectively). (A) before and (B) after sulphonation.

As expected the poly(styrene-DVB) polyHIPE (T5), which is the most hydrophobic, absorbed very little water. The uptake of water by the sulphonated polyHIPEs SPHP-2 and SPHP-4 was 12-fold and 9.2-fold higher than that of T5. These results demonstrated that a hydrophilic, water absorbing polyHIPE can be synthesized by chemically modifying hydrophobic porous polyHIPE materials.

8.1.7 Discussion

As shown in previous studies, the sulphonation of poly(styrene-DVB) polyHIPE enhances its porosity for aqueous liquids (Millar *et al*., 1963). This approach has been used for the synthesis of polystyrene catalysts with controlled crosslinking and superabsorbent properties for use in biodiesel production (Vieira Grossi *et al*., 2010). A modified sulphonation process (see Section 2.1.4) has been used in this study to enhance the hydrophilicity properties of otherwise hydrophobic poly(styrene-DVB) polyHIPE materials to improve their fluid

diffusivity. Sulphonation generates acidic SO_3H groups, which are easily neutralised by conversion into to salts (e.g. $SO^{3-}NH_4^+$).

SPHP-4 and SPHP-6 matrices have slower dosing rates than SPHP-1 and SPHP-2, and consequently yielded much smaller pore diameters (Figure 8.1). Increasing the mixing time would allow substantially longer time for emulsion to form droplets with smaller diameter.

As shown in Figure 8.1, SPHP-1 had the largest pore size of all the SPHPs matrices. SPHP-1 also yielded a broader pore size distribution (Figure 8.6) with a peak of ~60μm. This is likely to be due to a short mixing time (1 minute) used in the preparation of this emulsion leading to the formation of larger droplet sizes. Previous studies have shown that low emulsion viscosities cause the organic phase surrounding the water droplets (aqueous phase) to move easily from the films separating two pores to the shared edges (Lépine et al., 2008). However, this is unlikely to be the case for the SPHP-4 and SPHP-6 matrices in which the mixing time was extended. As a result a narrow pore distribution (Figure 8.7) was obtained. These results clearly show that extending the mixing time increases the number of droplets in the emulsion and consequently the number of pores. This finding confirms that of Lépine *et al*. (Lépine *et al*., 2008) who demonstrated that the pore size was decreased as the shear time increased.

Figure 8.12 shows a schematic diagram of the formation of droplets in water in oil (w/o) internal phase emulsion.

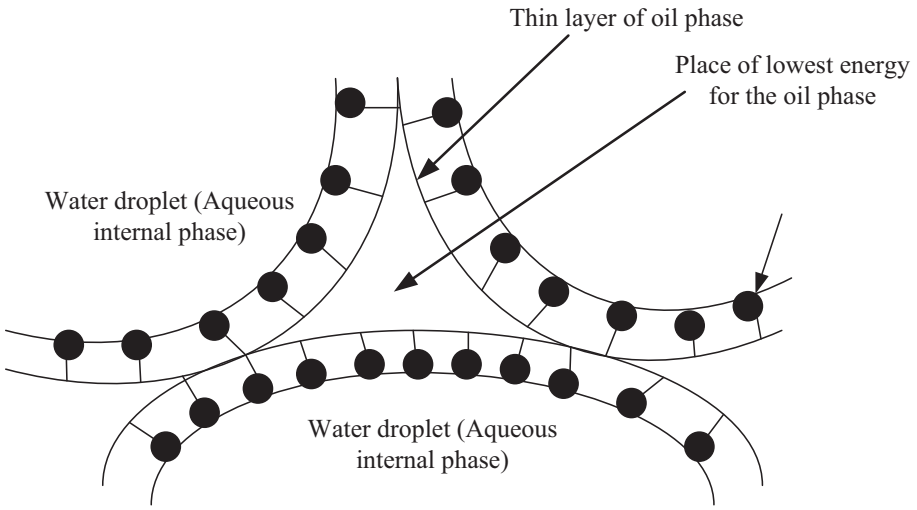

Figure 8.12: Diagram illustrated the droplets in a water in oil (w/o) internal phase emulsion

There was a small shift in the distribution of pore and interconnect sizes in matrices SPHP-2 and SPHP-4 after sulphonation, possibly due to the adsorption of sulphuric acid to their structure. However, the lack of change in the pore and interconnect diameters of SPHP-6 following treatment was most likely due to it having a highly stabilized emulsion that yielded smaller droplet sizes. This could have increased resistance to the migration of sulphuric acid throughout the matrix. Matrices with pore sizes in the range of 30 to 42μm exhibit a low surface area (Cameron and Barbetta, 2000). As shown in Table 8.1, the pore size of the sulphonated polyHIPE, SPHP-6 was 30μm and it was similar with pore size before sulphonation treatment. The pore size of this sulphonated polyHIPE was not very much different with non-sulphonated polyHIPE, T5 (36μm). Therefore, it was predicted that the surface area of both polyHIPEs not much different. However, as shown in Table 8.4, the surface area of SPHP-6 much lower (less than 2 m^2/g) than the non-sulphonated polyHIPE (T5; 4.68 m^2/g). It was unsure why there was a difference of this surface area. Nevertheless, polyHIPE matrices modified by sulphonation produce highly hydrophilic matrices, but not one with high surface area. Therefore, further studies are needed to increase the surface areas of sulphonated polyHIPE materials.

Poly(styrene-DVB) polyHIPE materials have superior water absorption capabilities compared with non-sulphonated polyHIPE (T5) (Figure 8.11). Previous studies have shown that reaction of polystyrene with sulfuric acid leads to an increase in its surface wetability and a change in its surface polarity (Berlinger *et al*., 2001). As predicted, sulphonated polyHIPE absorbed more water than untreated polyHIPE in which absorption is dependent on capillarity.

In conclusion, a highly hydrophilic polyHIPEs was generated following sulphonation. The resulting matrices had well-defined cellular morphologies with respect to their pore and interconnected network but had smaller surface areas. This confirms that water in oil (W/O) synthesis of polyHIPE has superior emulsion stability, a key factor for stable matrices. A slower dosing rate will produce smaller pore diameters. The length of the mixing time influenced the emulsion structure such that pore and interconnect sizes could be varied.

8.2 Immobilization and continuous culture of *B. subtilis* into sulphonated polyHIPE (SPHP)

8.2.0 Introduction

Polymeric polyHIPE matrices are highly interconnected porous structures that are mechanical durable under extreme conditions such as pH, temperature and the presence of toxic metabolites. Therefore, these porous materials can be sterilized and used for long-term operation without significant degradation. Some existing biomaterial matrices such as polyacrylamide gels and alginate beads, lack mechanical stability that results in them swelling and/or leaking cells into the surrounding medium. The architecture of polymeric materials allows for rapid absorption of large quantities of liquid through capillary action (Kulygin and Silverstein, 2007). These polymeric materials are sufficiently permeable to allow liquid flow-through and good accessibility of reactive sites. Moreover, polyHIPE materials provide a large surface area for cell attachment, allowing cells to proliferate and migrate through the structure of their matrix. In the case of matrices such as alginate gel, cell division and migration are limited to the peripheral surface because the matrix limits the diffusibility of nutrients and other materials to the centre. However, generic polyHIPE materials tend to be hydrophobic, and this can limit their suitability for biological applications.

Sulphonated polystyrene-divinylbenzene polyHIPE, which is a highly hydrophilic and permeable polymeric matrix, allows the free movement of aqueous fluids, which enhances the diffusion of nutrients and oxygen. This is of the utmost importance in allowing cells to grow homogeneously throughout the matrix and not only on the top surface of the support. Additionally, the high porosity of these matrices prevents clogging, which often occurs with other matrices.

The biological characteristics of living cells themselves, such as size, hydrophobicity or charge, also influence their interactions with the matrix. Additionally, other factors such as inoculum size, cell products and media components also impact cell immobilization. Furthermore, the hydrodynamic forces applied to the immobilization process will help to determine the

distribution and penetration of cells on the top and to the interior of the matrices. However, in this study, the latter was not studied due to limited pump capacity (this pump is only capable for flowrate more than 1 ml/min).

The objectives of this chapter were to:

- investigate the effect of polyHIPE pore and interconnect sizes on the growth, viability and penetration of immobilized *B. subtilis* cells
- investigate the effect of polyHIPE pore and interconnect sizes on the production of the starch-degrading enzyme, α-amylase by immobilized *B. subtilis* cells
- investigate the effect of the concentration of cell inoculum on the α-amylase production
- compare the enzyme production by immobilized *B. subtilis* cells with that of planktonic cell cultures

The final section of this chapter compares the growth, proliferation and penetration of the immobilized cells, *B. subtilis* between sulphonated polyHIPE (SPHP-4 & SPHP-6) and vinyl pyridine polyHIPE (TVP-5). The α-amylase production and released cells between these two types of polyHIPEs matrices were also evaluated and compared. This last section also shows that different pore and interconnect sizes, as well as chemically modified polyHIPE, affect the performance of polyHIPE as a matrix for immobilizing bacterial cells.

8.2.1 Immobilization of *B. subtilis* cells on sulphonated polyHIPE matrix (SPHPs)

Three ranges of pore and interconnect sizes of sulphonated polyHIPEs (SPHPs) were used and their characteristics are shown in Table 8.2.1.

Table 8.2.1: Characteristics of the sulphonated polyHIPE used in this study

PHP Code No.	Pore size (D) (μ m)	Interconnect size (d) (μ m)	BET surface area (m^2/g)
SPHP-2	42.0±0.61	22.0±0.10	0.844
SPHP-4	36.0±0.50	16.0±0.89	1.417
SPHP-6	30.0±0.64	11.0±0.76	1.832

Sulphonated polyHIPE (SPHP) discs were mounted into a sealed filter-shaped PTFE microchamber (Figure 7.4B) and the discs were initially wetted with distilled water and then LB media for an hour each before use. Spores of *B. subtilis* strain 168 (pKTH10) (~2x 10^8) were suspended in 2ml of LB broth and pre-germinated by incubating for 90 min at 37^0C. The pre-germinated spores were force-seeded into the SPHP by passing the suspension through the matrix at a flow rate of 0.55ml/min using a syringe pump. The seeded SPHP was left for an hour to allow the pre-germinated spores to attach to the surface of the SPHP, and then culture medium (LB broth) was pumped continuously through the matrix at a flow rate of 1.0ml/min (Figure 2.5). Samples were collected at various interval times for the determination of released cell numbers and α-amylase activity. At the end of the experiment, sterile 0.1M phosphate buffered saline was pumped through the matrix at the same flow rate onto to remove the remaining medium.

8.2.2 Effect of pore size to the α-amylase production and the release cells from the SPHPs matrices

The samples obtained from 24h cultivation of immobilized cells on three different pore sizes in sulphonated matrices were used to determine the production of α-amylase and cell release from the matrices. The α-amylase concentrations were determined using the Phadebas assay and the data shown in Figure 8.2.1**.** These α-amylase concentration data were then analysed to determine the total α-amylase enzyme production throughout growth which is shown in Figure 8.2.2.

The production of α-amylase by cells of *B. subtilis* immobilized in sulphonated-polyHIPE matrices with different pore sizes (42.0 ±0.61μm, 36.0 ±0.50μm and 30.0 ±0.64 μm) was determined at various times during cultivation (Figure 8.2.1**)**. The data show that SPHP with a pore size 36.0 ±0.50μm (SPHP-4) was the most productive - it reached an optimum production rate (~0.5 U/ml) after ~12 hours and maintained a similar rate throughout the experiment. This optimum enzyme production rate by SPHP-4 matrix was 20% more compared to SPHP-6 matrix (~0.4 U/ml). In the case of matrix with a pore sizes 42.0 ±0.61μm (SPHP-2), the production of α-amylase from *B. subtilis* immobilized on the SPHP-2 matrix reached a maximum production rate (~0.2 U/ml) after 15 hours and maintained at 0.25 U/ml towards the end of experiment. The total production of α-amylase in the three matrices can be seen from Figure 8.2.2.

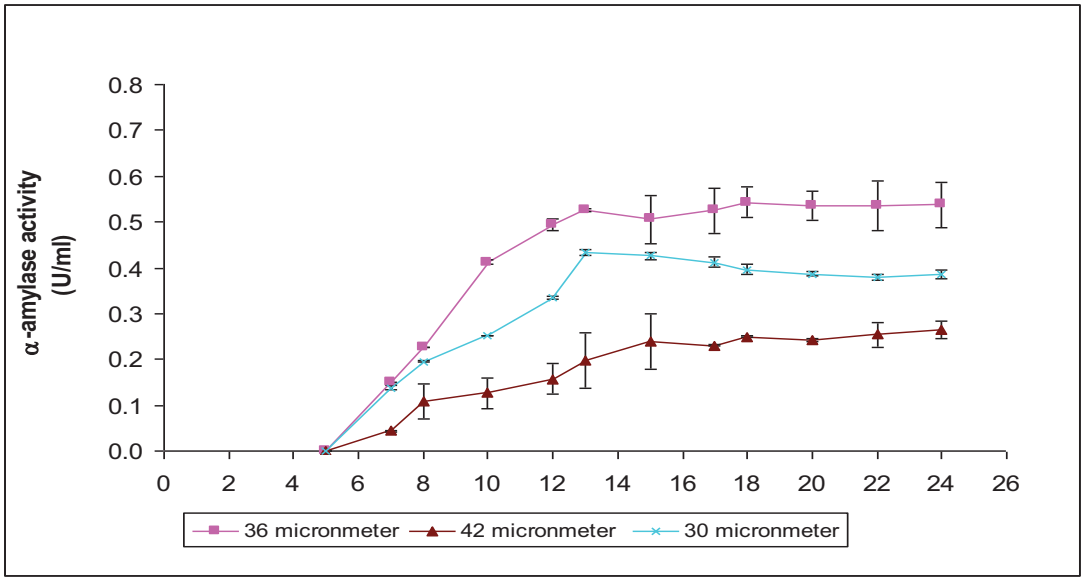

Figure 8.2.1: The time-course of the production of α-amylase by *B. subtilis* immobilized in sulphonated polyHIPE with pore sizes of 42.0, 36.0 and 30.0µm (for 24h incubation with 1ml/min of nutrient medium flow rate). The data is the result of independent triplicate experiments.

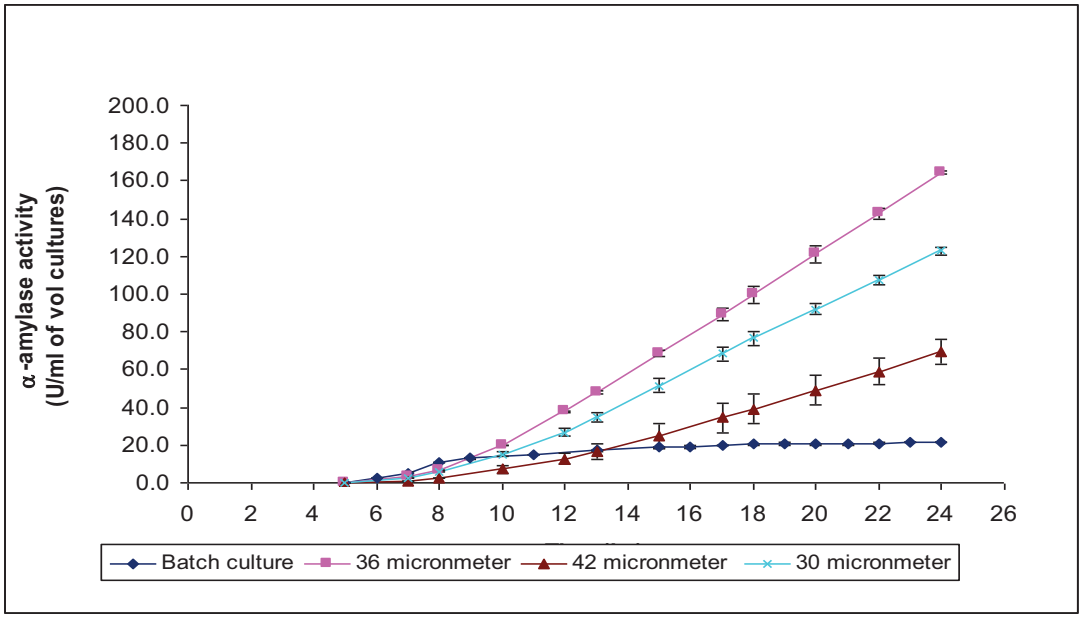

* α-amylase activity for immobilized cells was determined per volume of polyHIPE disc while planktonic batch cultures was determined per volume cultures

Figure 8.2.2: Cumulative α-amylase production by cells of *B. subtilis* immobilized on SPHP with pore size of 42.0 ±0.61µm, 36.0 ±0.50µm and 30.0 ±0.64 µm was compared with planktonic batch cultures. For the immobilized cells systems the total production of α-amylase was calculated on the basis of a flow rate of 1ml/min whereas the batch culture was based on 100ml of cultures for the same incubation time.

As shown in Figure 8.2.2, α-amylase production from the immobilized cells continuously increased and almost achieved 200U/ml towards the end of incubation period (24h). Conversely, α-amylase production by the batch culture increased rapidly during the first 8h but then stabilised at approximately 20U/ml. The α-amylase concentration was calculated per volume occupied by SPHPs, which is 3ml while for batch cultures were based on 100ml of culture. A detailed explanation about the comparison of the α-amylase production between free cell cultures and immobilized cells will be discussed in Chapter 9, Section 9.1.3.

The total α-amylase produced (U) for all SPHPs matrices were determined based on a flow rate of 1ml/min for 24 hours incubation. It was found that the highest total amount of α-amylase was obtained from the SPHPs with a pore size of 36 μm. The α-amylase produced by this matrix was 2.4-fold higher than that produced by the SPHPs with a pore size of 42 μm and 1.3-fold more than the SPHPs with a pore size of 30 μm (Table 8.2.2).

The volumetric productivities per total medium used for all SPHPs were also calculated and the values were relatively low (Table 8.2.2). These volumetric productivities were about 1000x lower than the volumetric productivity determined on the basis of volume occupied by polyHIPE matrix.

The performance of all SPHPs were also evaluated and compared by determining the yield of α-amylase per ml of medium used, dry weight of the cells per mass or volume of SPHPs, specific α-amylase production rates (per mg dry cell weight or protein of supernatant culture) and these analyses are shown in Table 8.2.2. Since, a complex medium was used in this study; the rate of removal of specific nutrients from the culture medium could not be estimated. However, if all nutrients in the medium were assumed be consumed, the yield of α-amylase per ml of medium used can be estimated and the data is shown in Table 8.2.2. It found that the yields for all SPHPs were also relatively low. The SPHP with a pore size of 36.0μm (SPHP-4) had the highest cell dry weight. However, the specific α-amylase production (per mg dry cell weight) for the SPHP-2 and SPHP-6 matrices appeared 7.6% and 11.1% higher than SPHP-4.

The release of bacterial cells from the SPHP matrices was determined from samples taken every 2 hours. The cells were enumerated by counting the number of colonies on nutrient agar plates after growth overnight at 37°C (Figure 8.2.3). The data show that the SPHP with the smallest pore size (30 um) released the fewest number of cells.

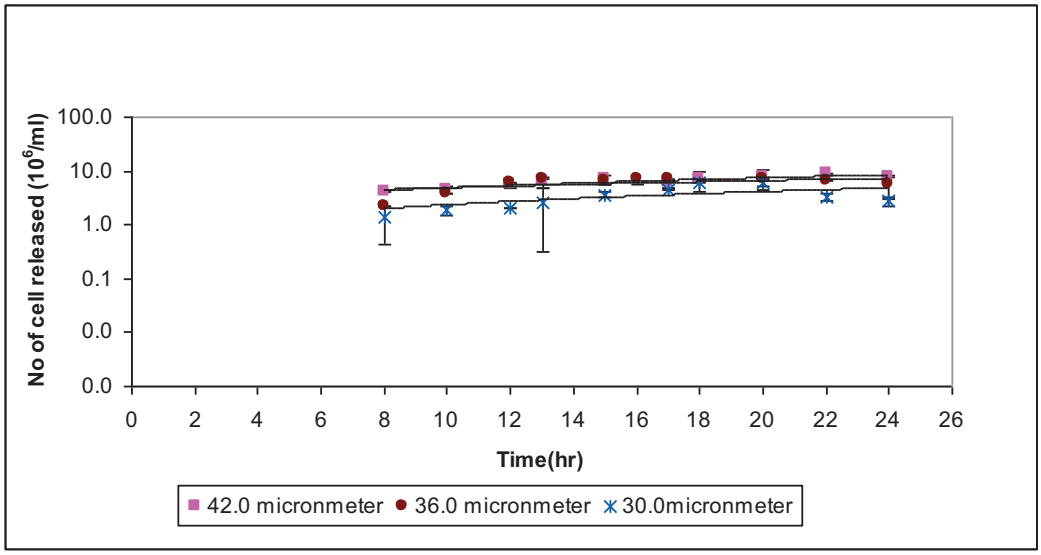

Figure 8.2.3: Released cells in10^6cells/ml from three different pore sizes of sulphonated polyHIPE matrices (for 24h incubation with 1ml/min of nutrient medium flow rate). The data is the result of independent triplicate experiments.

Table 8.2.2: Comparative analysis results of α-amylase produced by immobilized cells in sulphonated polyHIPE of three different pore sizes. Calculations were based on the volume of the polyHIPE discs, total medium used and the steady-state phase) *Statistical significance was determined with one-way ANOVA where $p<0.05$.

						Per volume of sulphonated polyHIPE disc (3ml)		
SPHPs Code No.	Pore size of SPHPs (μm)	Total α -amylase produced (U)	Yield of α-amylase per ml of medium used (U/ml)	*CDW (g/g SPHP)	CDW (mg/cm^3)	**Volumetric productivity (U/ml/h)	Specific α-amylase production rate (U/h/mg cell)	**Specific α-amylase (U/mg protein of supernatant culture)
SPHP-2	42.0±0.61	208.0 ±19.2	0.14 ± 0.013	0.18±0.05	16.33	2.90±0.27	0.18	3470 ±320
SPHP-4	36.0±0.50	492.8 ±2.35	0.34 ± 0.002	0.33±0.03	36.67	6.84±0.03	0.19	8210 ±39
SPHP-6	30.0±0.64	368.3 ±7.18	0.26 ± 0.005	0.23±0.04	28.00	5.12±0.1	0.18	6140 ±119

			Per ml of total medium used (1440ml)		
SPHPs Code No.	Pore size of SPHPs (μm)	Specific α-amylase (U/g biomass)	**Volumetric productivity (mU/ml/h)	Specific α-amylase production rate (mU/h/mg cell)	**Specific α-amylase (U/mg protein of supernatant culture)
SPHP-2	42.0±0.61	4245	6.02±0.0006	0.37	7.20 ±0.67
SPHP-4	36.0±0.50	3946	14.26±0.0001	0.40	17.14±0.08
SPHP-6	30.0±0.64	4384.5	10.66±0.0002	0.38	12.80 ±0.25

*Statistical significance was determined with one-way ANOVA where p-value = 0.080 (not significant).

**Statistical significance was determined with one-way ANOVA where $p<0.05$.

8.2.3 Morphology of immobilized *B. subtilis* cells

Following inoculation and incubation, a large number of vegetative cells were observed at the surface of all sulphonated polymeric matrices; SPHP-2, SPHP-4 and SPHP-6 after 24h incubation at 37^{o}C (Figure 8.2.4A-C). While the average dimensions of the inoculated *B. subtilis* spores were 0.6 x 1.1μm and the average dimensions of the vegetative cells in the immobilised microcolonies were 0.75μm x 2.4 μm. The sizes of the immobilized cells were both longer and more homogeneous in length compared to those cells grown planktonically in liquid culture (~1.5 μm of length (Chapter 3: Figure 3.10(b))). Additionally, the immobilised microcolonies were generally free of exopolysaccharide matrix or debris from dead cells. However, there was a small amount of cell debris on sulphonated polyHIPE matrix with pore size of 30μm. Appearance of *Bacillus circulans* microcolonies growth on calcium alginate matrix is also shown in Figure 8.2.4D (Kocher and Mishra, 2010).

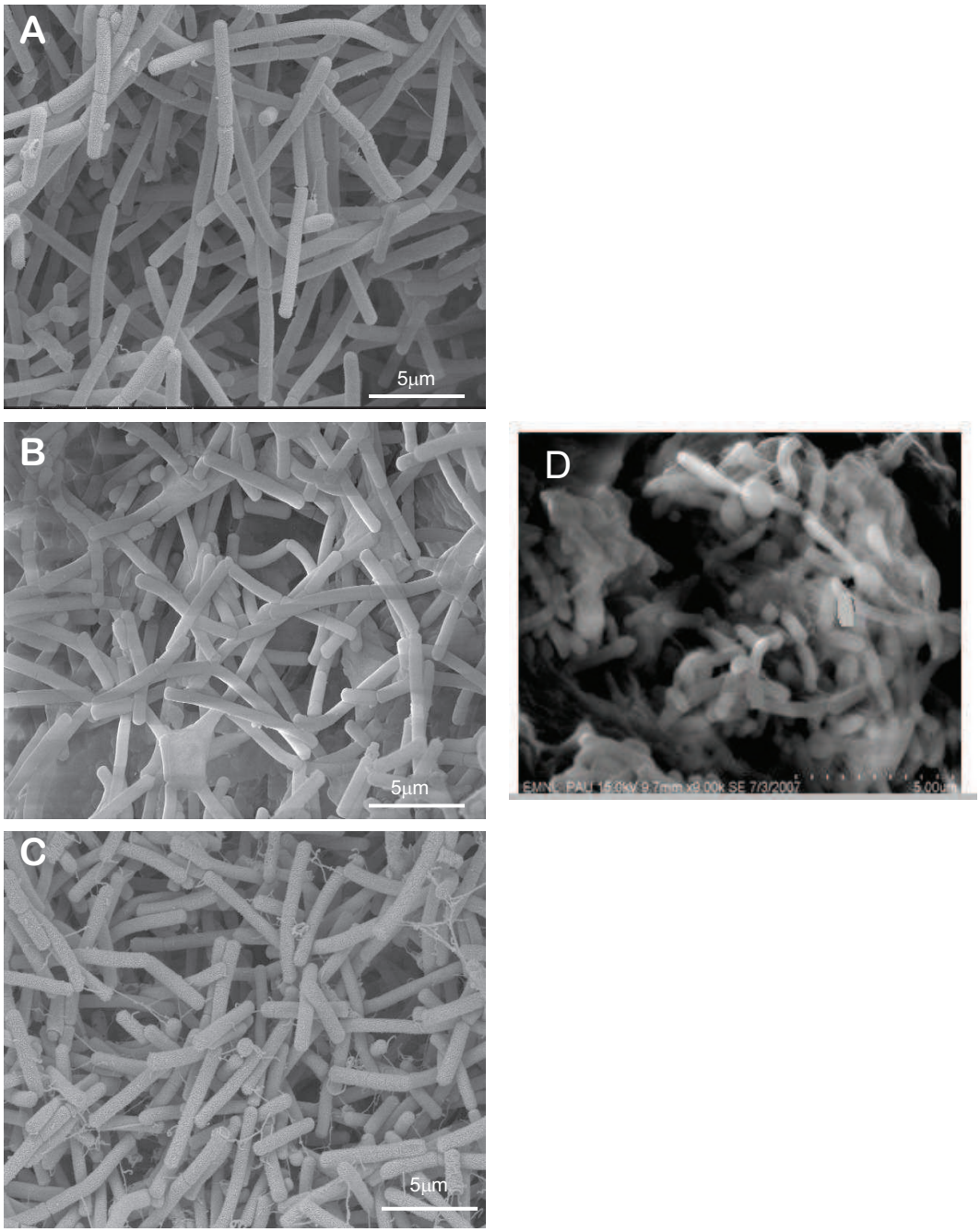

Figure 8.2.4: Scanning electron micrograph showing the morphology of vegetative cells of *B. subtilis* after 24h incubation. A surface of (A) SPHP-2 (ϕ = 42μm), (B) SPHP-4 (ϕ = 36μm), (C) SPHP-6 (ϕ = 30μm) and (D) *Bacillus circulans* entrapped in calcium alginate (Kocher and Mishra, 2010).

8.2.4 Effect of pore size to the cell growth and proliferation

After 24h cultivation at 37^0C with a continuously supplied well-aerated LB medium at a flow rate of 1ml/min, the surfaces of all three sulphonated polyHIPEs were covered by a dense homogeneous layer of vegetative *B. subtilis* cells that were free of an extensive extracellular matrix (Figure 8.2.5A-F). The germinated spores had successfully migrated throughout the matrix of the polyHIPE supports with pore sizes of 42μm (Figure 8.2.6) and 36μm (Figure 8.2.7). However, in the case of SPHP-6, a thick layer of cells had accumulated on the surface (Figure 8.2.8) only migrating up to approximately 3mm into the support. The pore walls had an almost continuous layer of bacterial cells on the top surfaces whereas smaller cells number were found further deep into the matrices.

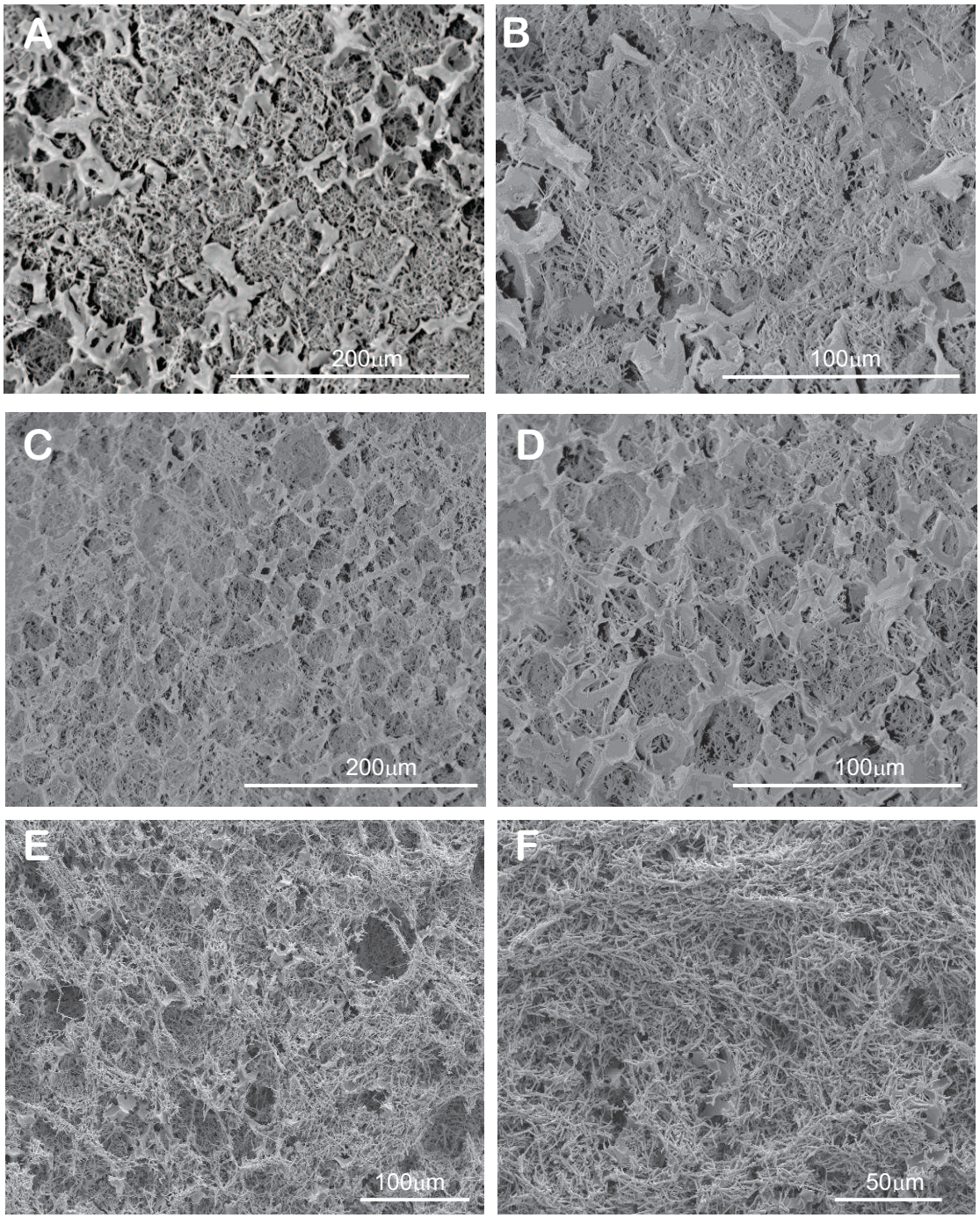

Figure 8.2.5: Scanning electron micrographs showing the growth and proliferation of vegetative cells of *B. subtilis* after 24h incubation. Surfaces of (A) & (B) SPHP-2 (ϕ = 42μm);(C) & (D) SPHP-4 (ϕ =36μm); (E) & (F) SPHP-6 (ϕ =30μm).

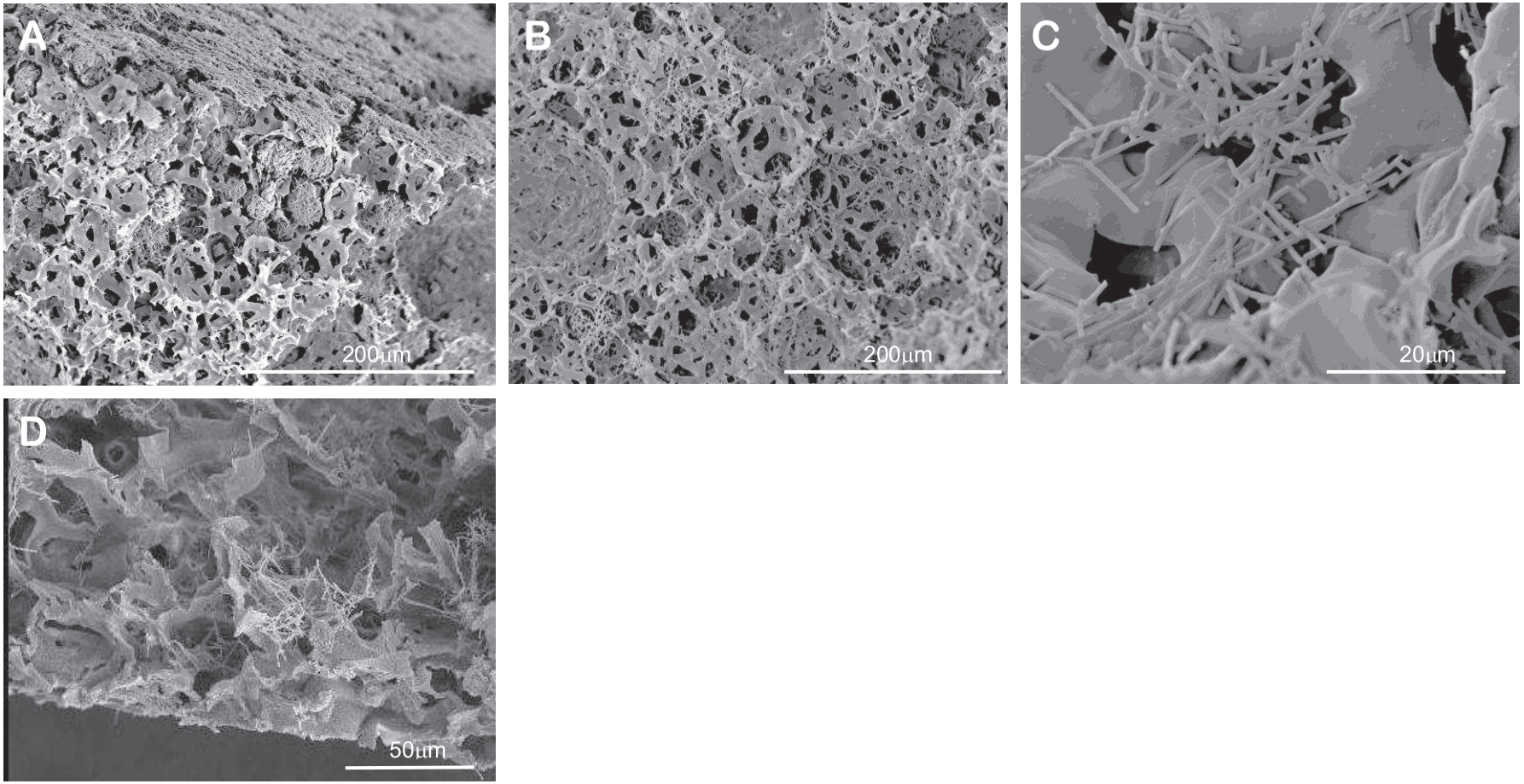

Figure 8.2.6: Electron micrographs of cross-section of the SPHP-2 (ϕ = 42μm) matrix, showing the appearance of vegetative cells of *B. subtilis* immobilized on after 24h cultivation. (A) top edge, (B) in the middle of cross section matrix (x250), (C) further deep (x2000) and (D) bottom edge. The terminology of the regions of the matrix is defined and illustrate in Fig. 2.6.

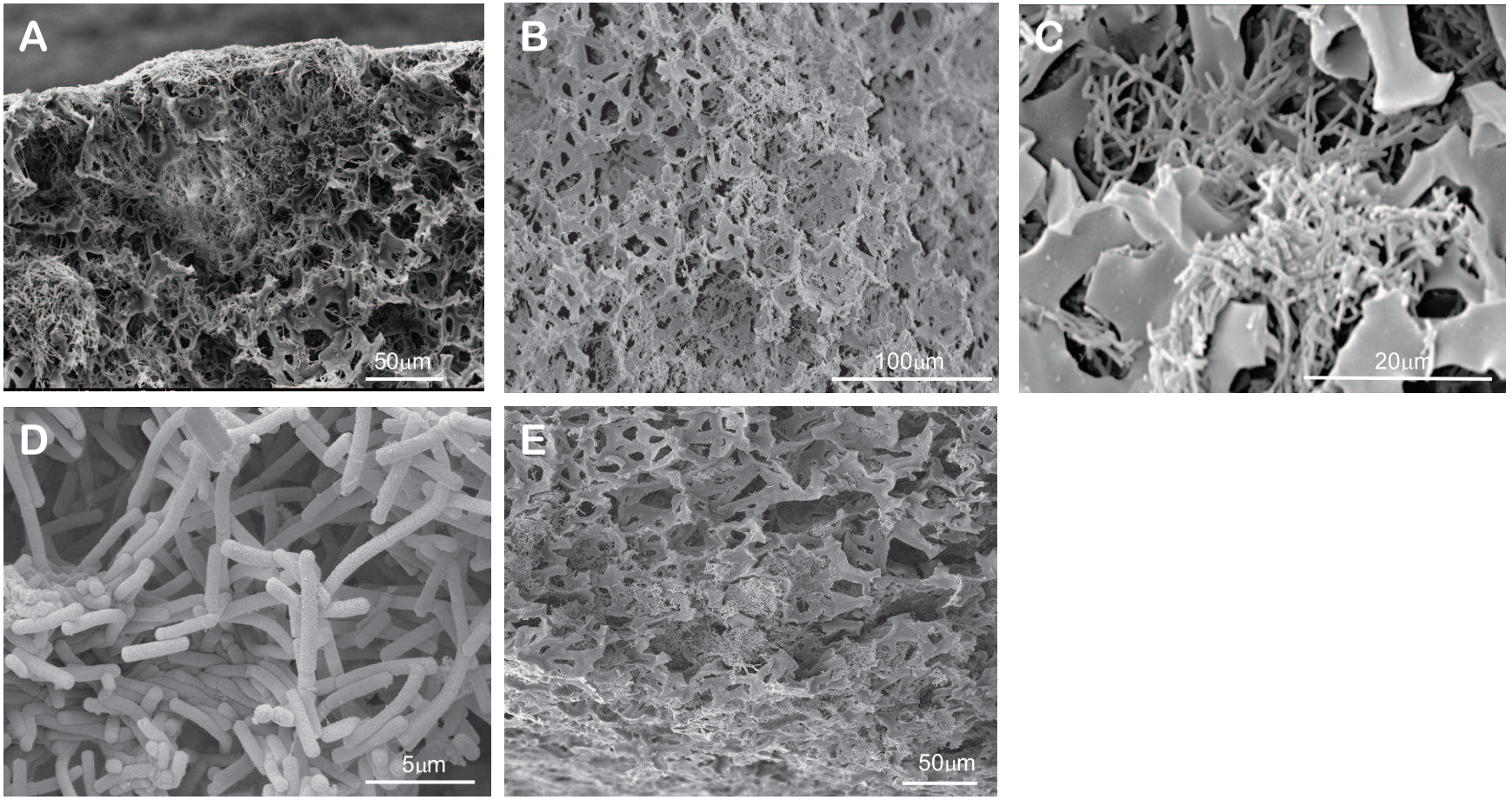

Figure 8.2.7: Electron micrograph of cross –section of the SPHP-4 (ϕ = 36μm) matrix, showing the appearance of vegetative cells of *B. subtilis* immobilized on after 24h cultivation. (A) top edge, (B) in the middle of cross section matrix (x350), in the middle of cross section matrix (C) x2000, (D) x5000 and (E) bottom edge. The terminology of the regions of the matrix is defined and illustrate in Fig. 2.6.

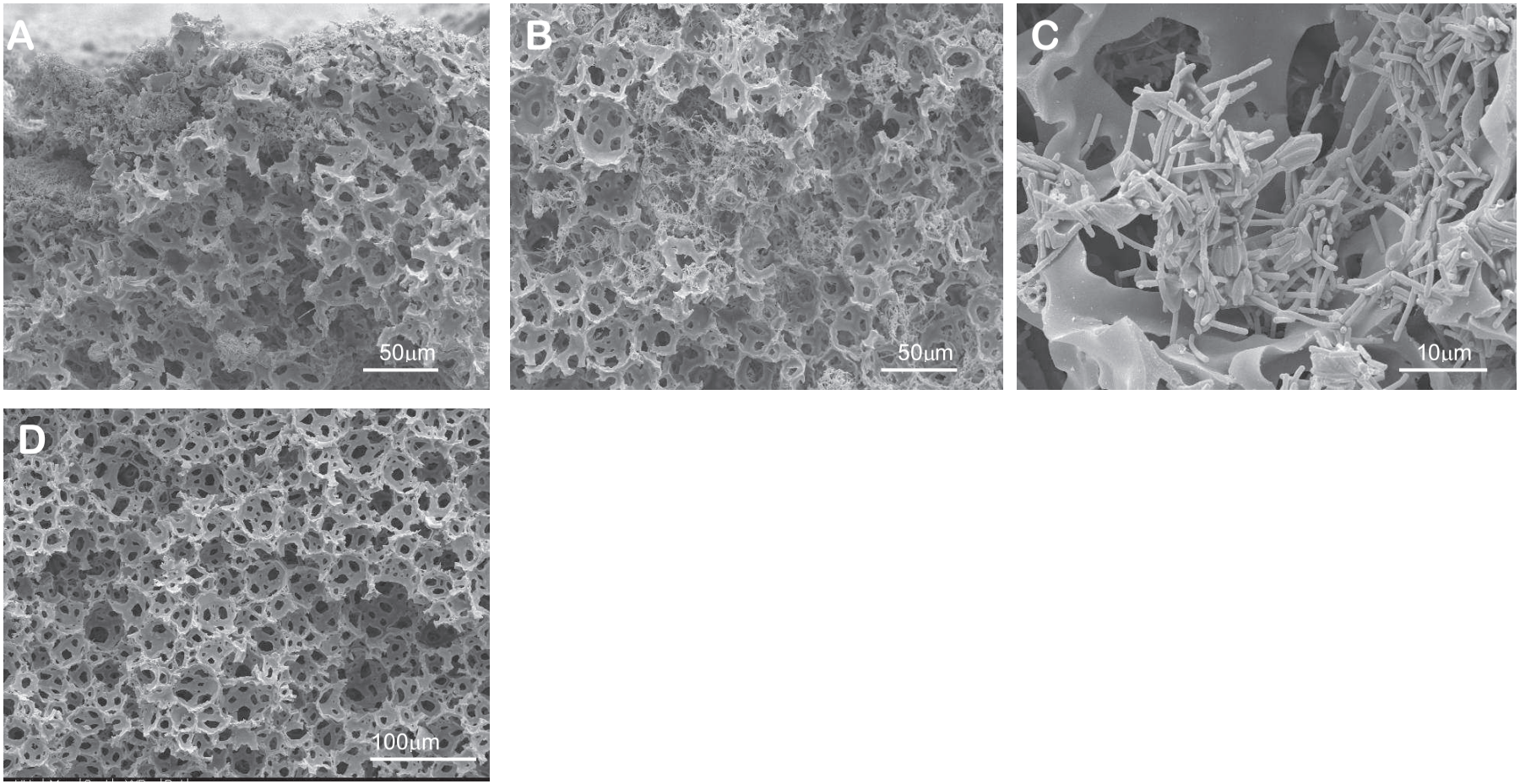

Figure 8.2.8: Electron micrograph of cross –section of the SPHP-6 (ϕ = 30μm) matrix, showing the appearance of vegetative cells of *B. subtilis* immobilized on after 24h cultivation. (A) top edge, (B) in the middle of cross section matrix (x350), (C) in the middle of cross section matrix (x2000) and (D) deep further. The terminology of the regions of the matrix is defined and illustrate in Fig. 2.6.

8.2.5 Effect of concentration of cell loading on enzyme production and the release cells from the SPHPs matrices

Based on previous results, sulphonated polyHIPE with a pore size of 36μm (SPHP-4) yielded much better results in comparison to the other types sulphonated polyHIPE (ϕ = 30μm and 42μm). Thus, this matrix was used to study the effect of the cell loading concentration on α-amylase production and the release of cells from the matrix. The polyHIPE matrix was pre-wetted with sterilized distilled water and nutrient medium for 60 minutes each and then sealed into the filter-shaped PTFE microchamber. Then, a pre-germinated spore suspension (~2 x 10^8, ~2 x 10^7 or ~2 x 10^6 cells/ml) in 2 ml of LB medium was forced-flow seeded into the matrix at a flow rate of 0.55ml/min, using a syringe pump. After an hour, well-aerated nutrient medium was pumped continuously into the seeded matrix for 24 hours. The experiments were conducted in a 37^0C room and samples collected for analysis of α-amylase production and cell loss at various times throughout growth.

Figure 8.2.9 shows the production of α-amylase for three cell loading concentrations. The concentration of α-amylase varied according to the concentration of cells loaded. The production of α-amylase by the matrix loaded with ~2x 10^6cells/ml was first detected 8 hours after seeding and reached an optimum ~0.1 U/ml 7 hours later. In the case of the matrix loaded with ~2 x 10^7 cells/ml, production also reached an optimum (~0.25U/ml) after 15 hours. However, when the matrix was loaded with ~2 x 10^8 cells/ml, the optimum α-amylase production of~0.5 U/ml was reached 3 hours earlier (i.e. 12 h) than the other two matrices. The total α-amylase produced by each of the three matrices was also estimated on the basis of a flow rate of 1ml/min for 24h, per volume of polyHIPE matrix (Figure 8.2.10).

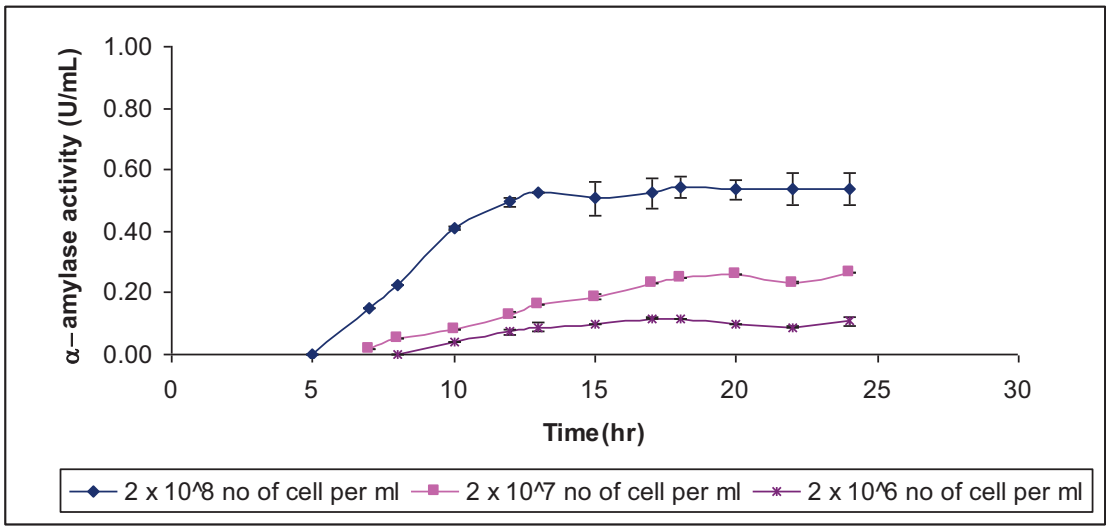

Figure 8.2.9: The time-course of production of α-amylase by *B. subtilis* immobilized in sulphonated polyHIPE (ϕ = 36μm) with three different starting concentrations of cells, incubated with nutrient medium for 24h at a flow rate of 1ml/min. The data is the result of independent triplicate experiments.

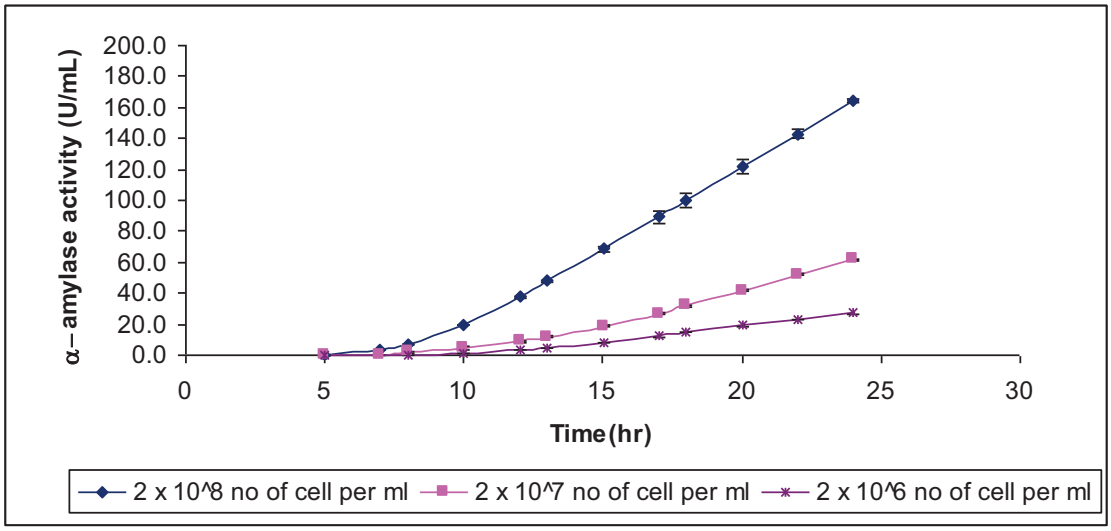

Figure 8.2.10: Comparative extracellular α-amylase production by immobilized cells in sulphonated polyHIPE (pore size of 36μm; SPHP-4) inoculated with different of concentration of cells. The calculated values were based on a flow rate of 1ml/min and adjusted for the volume of the polyHIPE matrix.

The data obtained from different cell loadings (Table 8.2.3) were analysed to determine the total production of α-amylase, the yield of α-amylase per ml of culture medium or volume of the matrix, cell dry weight per mass or volume of SPHPs and specific α-amylase production rates (mg dry cell weight of matrix or protein of supernatant culture).

Figure 8.2.11 shows that the amount of α-amylase produced and cell dry weight was dependent on the cell loading concentration. The total amount of α-amylase produced from the cells immobilized on the SPHP-4 matrix inoculated with ~2 x 10^8 cells/ml was ~500U. When the matrix was loaded with ~2 x 10^6 cells/ml, the amount of α-amylase produced was almost 5-fold lower.

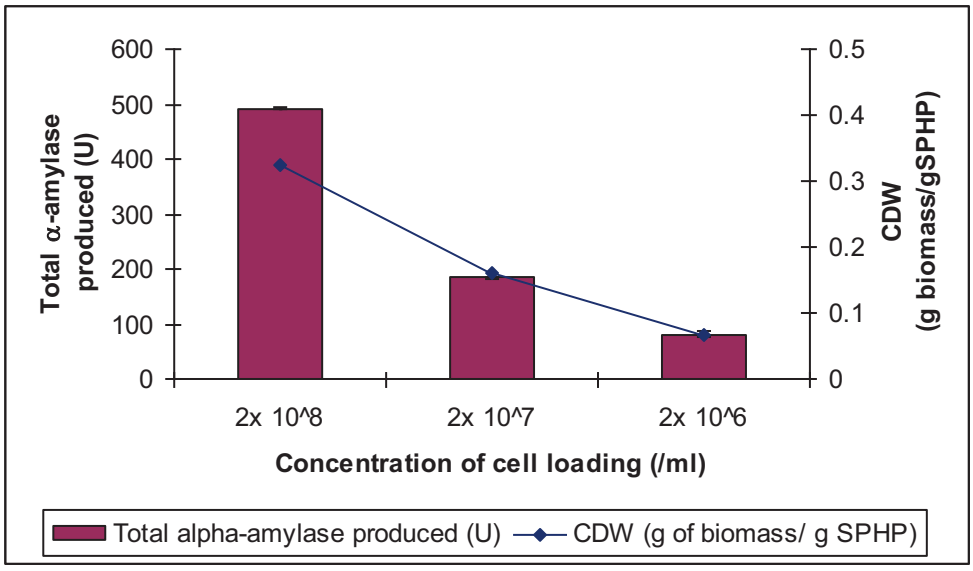

Figure 8.2.11: Effect of cell loading concentration on the total amount of α-amylase and cell dry weight (g biomass/g SPHP) produced by immobilized cells in sulphonated polyHIPE with pore size of 36μm, after incubation for 24h. Statistical significance for total α-amylase produced (U) was determined with one-way ANOVA where $p<0.05$.

The highest volumetric productivity (6.84 U/ml/h) was obtained when the cell loading concentration, of 2 x 10^8 cells/ml was used (Table 8.2.3). The estimated volumetric productivity were adjusted for the volume of the matrix. When the productivity calculation was based on the volume of nutrient medium used, the values correspondingly reduced (Table 8.2.3), The specific α-amylase production rates for each of the cell loadings (per mg dry cell weight) were similar, indicating that the different cell loadings had the same α-amylase production capacities.

Table 8.2.3: Analysis results of α-amylase produced by immobilized cells on sulphonated polyHIPE matrix with different cell concentration loadings.

*Statistical significance was determined with one-way ANOVA where $p<0.05$.

Conc. of cell loading (cells/ml)		Per volume of SPHPs discs		Per ml of total medium used		
	CDW (mg/cm^3)	*Volumetric productivity (U/ml/h)	Specific α -amylase production rate (U/h/mg cell)	*Volumetric productivity (mU/ml/h)	Yield (U/ml)	Specific α -amylase production rate (mU/h/mg cell)
2×10^8	36.67	6.84 ± 0.03	0.19	14.26±0.0001	0.34 ±0.002	0.40
2×10^7	16.67	2.57 ± 0.02	0.15	5.36±0.0000	0.13 ±0.001	0.32
2×10^6	7.6	1.27 ± 0.06	0.15	2.37±0.0001	0.06 ±0.003	0.31

The effect cell loading concentration on the release of cells from the SPHP matrices was also determined (Figure 8.2.12). The numbers of cells were determined by counting the number of colonies on nutrient agar plates after growth overnight at 37^0C. As can be seen in Figure 8.2.12 the highest concentration of cell loading of 2×10^8cells/ml yielded the highest number of released cells.

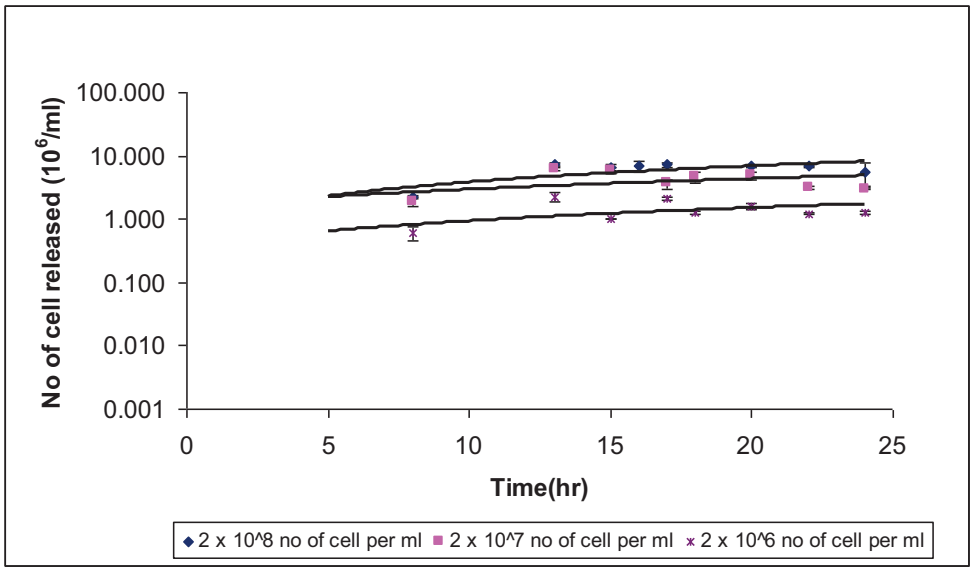

Figure 8.2.12: The release of cells from sulphonated polyHIPE matrices (pore size of 36μm) loaded at different cell concentrations. The data are the result of independent triplicate experiments.

8.2.6 Discussion

One of the design characteristics of matrices used for the immobilisation bacterial cells is the need to optimise pore and interconnect size to ensure good mass transport into and out of matrix. In this study, sulphonated-polyHIPE matrices with three different pore sizes were evaluated. The results indicated that pore size significantly affected the production of α–amylase by cells immobilised on sulphonated-polyHIPE matrices (Figure 8.2.1or Figure 8.2.2). SPHP matrices with a pore size of 36μm (SPHP-4) yielded the highest total α-amylase enzyme and cell dry weight. The volumetric productivity obtained by SPHP-4 was 2.4-fold and 1.3-fold higher than obtained by the SPHPs with pore sizes of 42 μm and 30 μm, respectively. As expected, there was a direct relationship between dry cell mass and α–amylase production and entrapping a high proportion of cell in the matrix a high priority. The low level of α–amylase production and low cell mass in the matrix with the smallest pore sizes (30μm) is likely to be due to diffusional limitations that restrict the access of nutrients and oxygen to the cells and the release of the secreted enzyme to the medium. It might be also due to limited loading of cells onto this matrix.

Steady-state α–amylase production was achieved after 13 hours, indicating that the matrix had reached the limit of its capacity to sustain further increases in biomass. Such a steady-state represents the most efficient state for the production of α–amylase since net cell growth and nucleic acid syntheses are repressed while protein synthesis is still active (Kinoshita *et al*., 1968). This represents a shift from biomass increase to cell maintenance and product formation. Moreover, in *B. subtilis*, the secretion of macromolecular hydrolases like α–amylase is higher during stationary phase than exponential phase (Antelmann *et al*., 2001).

Bacterial cells were released from all of the SPHP matrices (Figure 8.2.3) although the SPHP matrix with the smallest pore size (30μm) released the fewest numbers. The release of cells from the SPHP matrices with pore sizes of 36μm and 42μm was similar.

Previous studies have shown that polyHIPE provides a suitable matrix for the immobilisation of both bacterial (Akay *et al*., 2005; Erhan *et al*., 2004) and

eukaryotic (Akay *et al*., 2004, Bokhari *et al*., 2005) cells. These studies have shown that *B. subtilis* can migrate up to 3mm into such matrices over 30 days cultivation. Multicellular layers of osteoblast were seen on the top surface of polyHIPE, migrating to a maximum depth of 1.4mm within the matrix. Previous studies used styrene-divinylbenzene polyHIPEs, which are hydrophobic and therefore exhibit reduced permeability to aqueous fluids. In the current study, we used sulphonated polyHIPEs, which are hydrophilic and show increased permeability to aqueous fluids. Sulphonated polyHIPEs (SPHPs) were used to immobilize *B. subtilis* spores, which were then germinated and cultured in-situ. After 24h continuous culture, a dense layer of *B. subtilis* cells was seen on the top surface of all the SPHPs matrices, irrespective of pore size. SEM analysis showed that the cells were elongated rods with little evidence of an extracellular matrix or cell lysis. This result indicates that the *B. subtilis* spores can be efficiently germinated and cultured throughout hydrophilic polymeric supports that provide a permissive microenvironment.

A thick homogeneous layer of cells on the top surface of the polymeric supports is likely to be due to the presence of high nutrient and oxygen concentrations in this location. The reduction in cell concentration within the matrix probably reflects that fact that nutrient and oxygen concentrations are likely to decrease as the culture medium passes through the matrix.

The production and excretion of extracellular substances, such as polysaccharides, is another parameter that affects the diffusive resistance in a cell mass (Karel et al., 1985a). However, in this study, virtually no exopolysaccharide matrix was formed and there was little or no evidence of cells debris resulting from cell lysis. This indicates that the microporous architecture of the polymeric matrix provided efficient dynamic flow conditions and presumably the continuous removal of dead and degraded cells and toxic materials. The only minor exception was the sulphonated polyHIPE, with pore size of 30μm (SPHP-6), which was found to contain small amounts of cell debris.

As can be seen in Figure 8.2.9 and Figure 8.2.10, a high initial cell loading of spores (2×10^8 spores/ml) resulted in a high total α-amylase yield and volumetric productivity. There was a linear correlation between α-amylase and cell loading, indicating that cell concentration was a limiting factor of this

bioreactor. The same observation has been reported for the production of butanediol by *Bacillus licheniformis* (Perego *et al*., 2003). Consequently, there is a trade off between high initial loading, α-amylase production and the rate of cell release from the matrix.

The results obtained in this chapter have shown that the microarchitecture of the matrices is important for the growth, viability and penetration of cells, and was dependent on the pore size and the physico-chemical properties of the matrix. The concentration of cell loading used also affected the performance of the immobilized system. A comparison of performance of sulphonated polyHIPE matrices with matrices of different compositions is shown in Table 8.2.4. The productivity of the SPHP with pore size of 36μm is 0.73-fold lower that that obtained with calcium alginate gel capsules and 1.4-fold higher than with a κ-carrageenan gel.

Table 8.2.4: Comparison of sulphonated PolyHIPE (SPHPs) with other immobilized cell supports performance

	Strain	Incubation time (h)	Volumetric productivity (U/ml/hr)	Specific activity of α-amylase (U/mg protein)
[a]Immobilised cells in κ-carrageenan gel	*B. subtilis* BF7658	24	4.875	N/A
[b]Immobilised cells in calcium alginate gel capsules	*B. subtilis*	48	9.34	9800
[c] Shake flask			3.7	4080
[d] Immobilised cells in - κ-carrageenan & Ca-alginate - κ-carrageenan & Ca-alginate mixed with polyethylene oxide agar	*B. licheniformis* 44MB82-G	120	 0.875 1.5	N/A
[e] Microreactor with polyHIPE matrices	*B. subtilis* 168 (pKTH10)	24		
SPHP-2 (ϕ = 42μm)			2.89	3470
SPHP-4 (ϕ = 36μm)			6.84	8210
SPHP-6 (ϕ = 30μm)			5.12	6140
[f] Shake flask			0.90	1083

[a] 120g Immobilised cell gel beads were added to 400ml airlift bioreactor containing 300ml medium (Guo *et al*., 1990)

[b] Immobilised cells (12.5ml gel capsules) were added to 250ml flasks containing 50ml medium (Konsoula and Liakopoulou-Kyriakides, 2006)

[c] Shake flask with 50ml medium (Konsoula and Liakopoulou-Kyriakides, 2006)

[d] Wet cells were mixed in 50ml of each gel or immobilized by adsorption on the cut agar (3/3/3 mm, 2.0g) (Ivanova *et al*., 1995)

[e] PolyHIPE disc with volume of 3ml

[f] Shake flask with 100ml medium in 250ml conical flask

8.3.0 Comparison of sulphonated polyHIPE with other types of polyHIPEs

Previous studies have shown that modification of polystyrene-divinylbenzene polyHIPE polymer (PHP) by sulphonation has allowed it to be used as an ion exchange polymeric monolith for the removal of nickel ions from contaminated water (Akay *et al*., 2006) and as a de-emulsifier adsorber for the separation of highly stable water-in-crude oil emulsions (Noor *et al*., 2005). This functionality is due the superior hydrophilicity of sulphonated polyHIPE that facilitates the rapid diffusion of fluid throughout its polymeric structure. This modified polymeric material circumvents problems associated with conventional hydrophobic PHP which exhibits reduced movement and distribution of fluid throughout the matrix. As shown in Section 8.2.1, sulphonated polyHIPEs polymeric (SPHPs) matrices exhibit a much better performance as an immobilized cell support. Therefore, this section will compare the performance of this matrix with another type of polyHIPE matrix, namely vinyl pyridine polyHIPE (TVP-5).

Samples were taken during throughout the operation of the microreactor to determine the rate of α-amylase production and the rate of cell loss. At the end of the experimental run, which was 48h long, the matrices were analyzed by scanning electron microscopy (SEM) to observe the morphology and distribution of cells. A summary of physical characteristics of the modified polyHIPE matrices is shown in Table 8.2.5.

Table 8.2.5: Characteristics of the sulphonated (SPHP)and vinyl pyridine (TVP) polyHIPE matrices used in this study

PHP Code No.	Pore size (D) (μ m)	Interconnect size (d) (μ m)	d/D (μ m)	BET surface area (m^2/g)
TVP-5	24.0±1.05	6.5±1.16	0.30	4.15 ± 0.041
SPHP-6	30.0±0.64	11.0±0.76	0.37	1.63± ±0.29
SPHP-4	36.0±0.50	16.0±0.89	0.44	0.91± 0.09

8.3.1 Comparison based on α-amylase production

Three matrices were inoculated with spores of *B. subtilis* strain 168 (pKTH10) and perfused with LB broth at 37°C for 48 h. Samples were taken every two hours for the determination of released cells and α-amylase activity. At the end of the experiment, the matrices were dehydrated with a series of ethanol concentration followed by critical-point dried with liquid CO_2 and then subject to analysis by SEM.

The analysis of α-amylase production of immobilized *B.subtilis* cells on sulphonated polyHIPEs (SPHP-4 & SPHP-6) matrices after 48h was compared with vinyl pyridine polyHIPE (TVP-5) and shown in Figure 8.2.13. The total α-amylase production throughout growth for each of these matrices is shown in Figure 8.2.14.

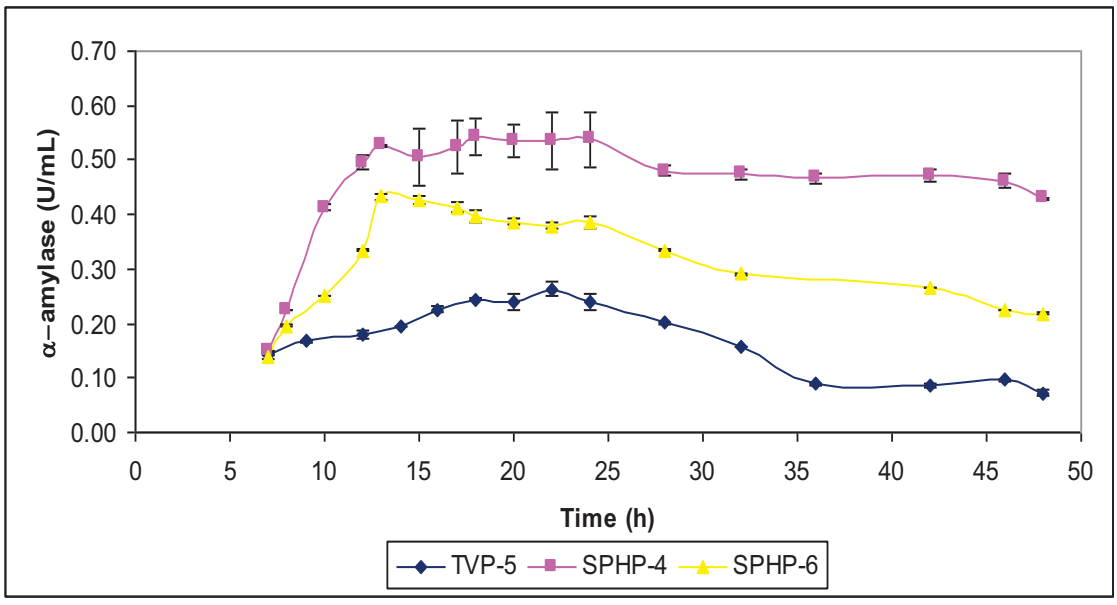

Figure 8.2.13: The time-course of α-amylase production by *B. subtilis* immobilized in sulphonated polyHIPE: SPHP-4 (ϕ = 36.0μm) and SPHP-6 (ϕ =30.0μm) and vinyl pyridine polyHIPE, TVP-5 (ϕ =24.0μm) during incubation for 48h. The nutrient medium flow rate used was 1ml/min.

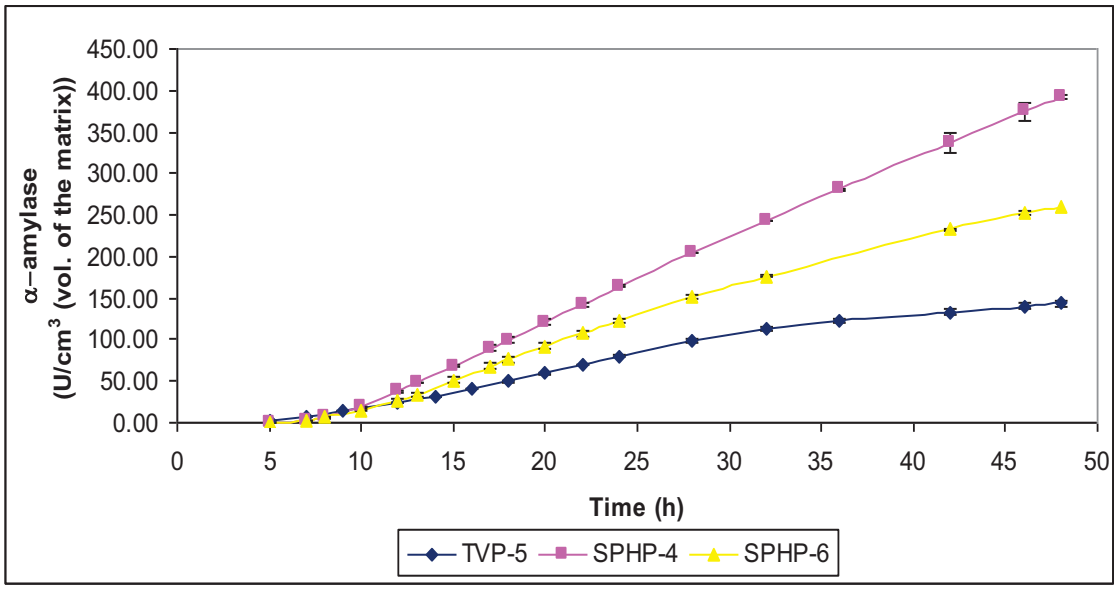

Figure 8.2.14: Comparative α-amylase production by immobilized cells in sulphonated and vinyl pyridine polyHIPEs matrices during incubation for 48h The nutrient medium flow rate used was 1ml/min. The data is based on the total production of α-amylase throughout growth.

By monitoring the production of α-amylase from cells immobilized on the SPHP-4 (ϕ = 36.0μm), SPHP-6 (ϕ = 30.0μm) and TVP-5 (ϕ = 24.0μm), it was possible to compare their performances (Figure 8.2.13). The data clearly show that the SPHP-4 matrix was the most effective – it reach an optimum production rate of ~0.5 U/ml after ~12 hours and maintained a similar rate throughout the remainder of the experiment. The production of α-amylase from *B. subtilis* immobilized on the SPHP-6 matrix also reached a maximum production rate of ~0.45 U/ml after 12 hours, however, the production rate declined to approximately half of this value over the remaining 36 hours of the experiment. In the case of the TVP matrix, production of α-amylase did not peak, at 0.2 U/ml, until 22 hours. This level of production was not maintained and after 48 hour the rate of production had fallen to ~0.05U/ml. A comparison of α-amylase production in the three matrices is given in Figure 8.2.14.

A summary of the results for the three immobilized cell matrices is shown in Table 8.2.6. The highest yield of enzyme and cell dry weight was also obtained by the immobilized cells on the SPHP-4 matrix. There was 2.4-fold and 2.1-fold

higher level of α-amylase production, respectively, by cells immobilized on the SPHP-4 and SPHP-6 matrices when the experimental time was increased from 24h to 48h (Table 8.2.7). Additionally, the amount of enzyme produced by the SPHP-4 matrix was 2.7-fold and 1.5-fold higher than that of the TVP-5 and SPHP-6 matrices (Table 8.2.6).

Table 8.2.6: α-Amylase production by immobilized cells of *B. subtilis* 168(pKTH10*)* in sulphonated and vinyl pyridine polyHIPEs matrices after 48h with a nutrient medium flow rate 1 ml/min

Type of PolyHIPE	Pore size (μm)	Total α-amylase produced (U)	Average yield of α-amylase (U/ml)	CDW (g biomass/ g SPHP)	CDW (mg/cm^3)
TVP-5	25.0 ± 1.05	431.86 ±9.6	0.15 ± 0.003	0.02±0.005	2.0
SPHP-6	30.0±0.64	[a]782.11 ±9.3	0.27± 0.003	0.24±0.01	35.0
SPHP-4	36.0±0.50	[a] 1177.78 ±9.7	0.41 ±0.003	0.38 ± 0.01	47.8

(CDW in mg/cm^3 unit was calculated based on volume of polyHIPE disc).
[a] Total α-amylase produced (U) by immobilized cells on SPHP-6 and SPHP-4 after 24h incubation at flow rate of nutrient medium 1 ml/min were 368.3U and 492.8U respectively

The volumetric productivities of each of the immobilized cell matrices were calculated with respect to the volume of polyHIPE matrices and total volume of the growth medium (Table 8.2.7). The SPHP-4 immobilized cell matrix yielded the highest volumetric productivity of α-amylase from immobilized cells of *B. subtilis* 168(pKTH10) compared to the SPHP-6 and TVP-5 matrices. The volumetric productivity per volume of matrix obtained for SPHP-4 was 1.2-fold and 9-fold higher than that obtained for 24h incubation and batch culture (24h). However, when the volumetric productivities were calculated with respect to the volume of growth medium (Table 8.2.7), productivity was ~1000 lower than that obtained using the volume of the polyHIPE disc. One factor that needs to be considered in subsequent experiments is the flow rate (currently 1 ml/min), as a longer retention time may allow for a higher rate of substrate utilisation.

The specific activities of α-amylase per unit of total culture supernatant protein were determined (Table 8.2.7). Calculated on polyHIPE matrices volume, the specific activity obtained from immobilized cells on the SPHP-6 and SPHP-4

matrices were 1.9-fold and 2.3-fold higher than that for the TVP-5 matrix (Table 8.2.7). The specific activity of the SPHP-4 matrix increased with time; from 0.19 for the 24h culture to 0.23 U/mg/cell/h for the 48h culture (Table 8.2.2).

Table 8.2.7: Comparative analysis results of α-amylase production by immobilized cells in sulphonated and vinyl pyridine polyHIPEs matrices after 48h incubation (with nutrient medium flow rate, 1ml/min)

					Per volume of polyHIPE disc		Per ml of total medium used	
SPHPs Code No.	Pore size of SPHPs (μm)	Incubation time (h)	Yield of α-amylase per ml of medium used (U/ml)	*CDW (g/g PHP)	**Volumetric productivity (U/ml/h)	*Specific α-amylase (U/mg protein of supernatant culture)	**Volumetric productivity (mU/ml/h)	*Specific α-amylase (U/mg protein of supernatant culture)
SPHP-2	42.0±0.61	24	0.14 ± 0.013	0.18±0.05	2.90±0.27	3470 ±320	6.02±0.0006	7.20 ±0.67
SPHP-4	36.0±0.50	24	0.34 ± 0.002	0.33±0.03	6.84±0.03	8210 ±39	14.26±0.0001	17.14±0.08
		48	0.41 ±0.003	0.38 ± 0.01	8.18 ±0.07	19,630 ±162.0	8.52 ±0.0001	20.5 ±0.14
SPHP-6	30.0±0.64	24	0.26 ± 0.005	0.23±0.04	5.12±0.1	6140 ±119	10.66±0.0002	12.80 ±0.25
		48	0.27± 0.003	0.24±0.01	5.43 ±0.06	16,294 ± 195.0	5.66 ± 0.0001	17.0 ±0.20
TVP-5	25.0±1.05	24						
		48	0.15 ± 0.003	0.02±0.005	3.0 ±0.07	8468 ± 188.0	3.12 ± 0.0001	8.82 ±0.20

*Statistical significance was determined with one-way ANOVA where p-value = 0.080 (not significant).

**Statistical significance was determined with one-way ANOVA where $p<0.05$.

Total medium used: 1440 ml for 24h; 2880 ml for 48h

8.3.2 Comparison based on released cells from matrix

The cells released from the various immobilised cell systems were also evaluated and the results shown in Figure 8.2.15. The data clearly show that the TVP matrix released the least cells.

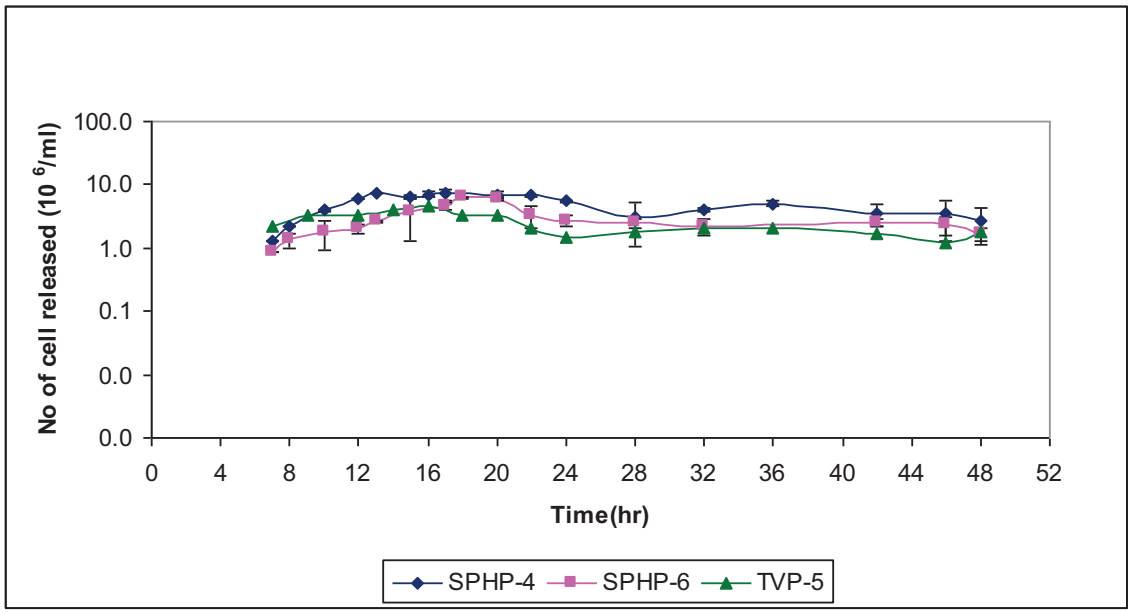

Figure 8.2.15 : Released cells in 10^6/ml from immobilized cells in sulphonated and vinyl pyridine polyHIPEs matrices

8.3.3 Comparison based on cell growth and proliferation

Scanning electron microscopy was used to determine the morphology of the *B. subtilis* cells and their distribution throughout the matrices of the polyHIPE discs. SEM was used to study cells at all levels of the matrix and, as shown in Figure 8.2.16A&B, there was extensive growth of cells on the surface of the SPHP-4 (ϕ = 36μm) and SPHP-6 (ϕ = 30μm) discs. In the case of SPHP-4 (Figure 8.2.16A), the cells were elongated and there were few signs of remaining spores or cell debris. The cells in the SPHP- 6 (Figure 8.2.16B) were similar to those in the SPHP-4 matrix, since they were similarly elongated. However, there was some cell debris, indicating that there might have been a small proportion of the cell undergoing cell lysis. In contrast, the cell in the TVP-5 (ϕ = 24μm) matrix were on average considerably shorter, they were less dense and there was again signs of cell debris (Figure 8.2.16C). In addition, a number of ungerminated spores were still present on the surface of the matrix.

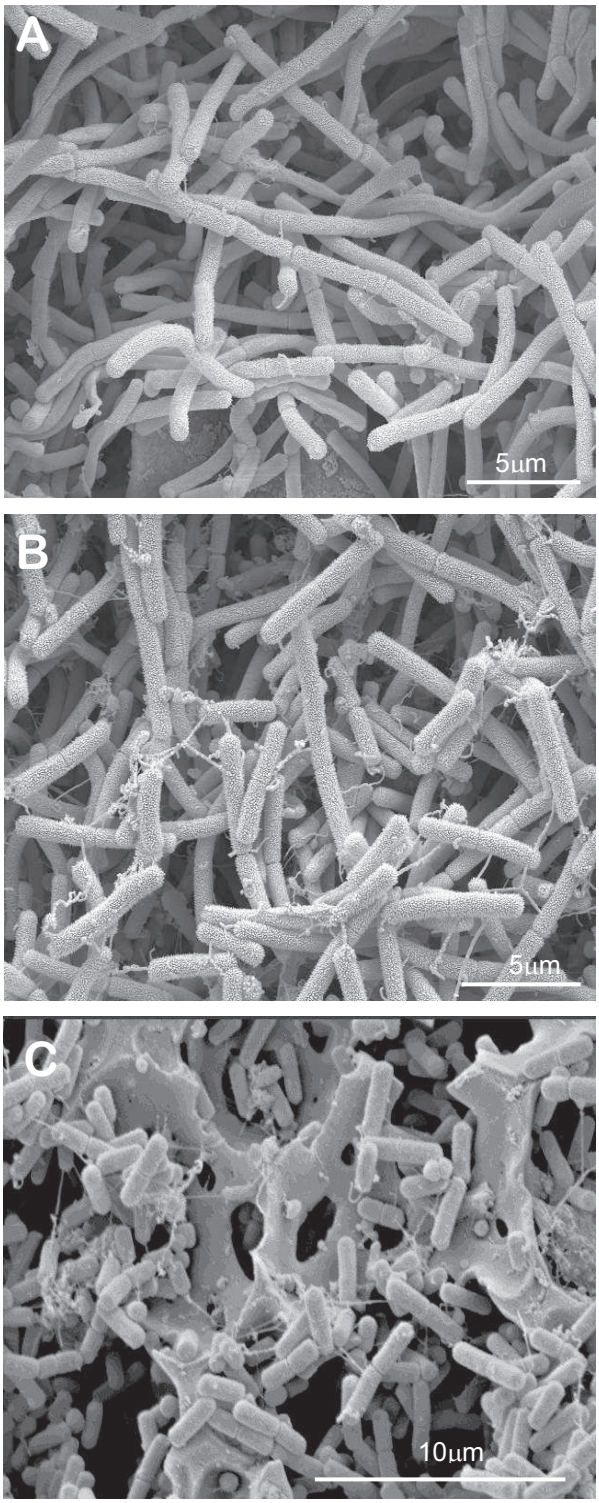

Figure 8.2.16: Analysis of cells *B. subtilis* immobilized on the top surface of TVP or SPHP polyHIPE matrices by SEM after 48h cultivation. (A) SPHP-4 (ϕ = 36µm), (B) SPHP-6 (ϕ = 30µm) and (C) TVP-5 (ϕ = 24µm) at same magnification

When cross-sections of the TVP and SPHP matrices were observed by SEM, it was clear that the SPHP matrices facilitated much better growth within the matrix than the TVP matrix (Figure 8.2.17 and Figure 8.2.18). However, it was clear that there was uneven distribution of cells within all of the matrices, with areas containing a cell high density next to regions containing virtually not cells. Overall the numbers of cells tended to decrease with increasing matrix depth. Although the distribution of cells was heterogeneous, cells were observed throughout the matrices, both in the middle and at the edges (Figure 8.2.17E) In contrast, relatively few cells were found in the cross section of the TVP-5 (ϕ = 24μm), matrix (in Figure 8.2.19F) even when the incubation time was extended to 48h. Furthermore, the distribution of cells in the cross-section of this type of polyHIPE was uneven compared to the first sulphonated polyHIPE matrices (Figure 8.2.19C).

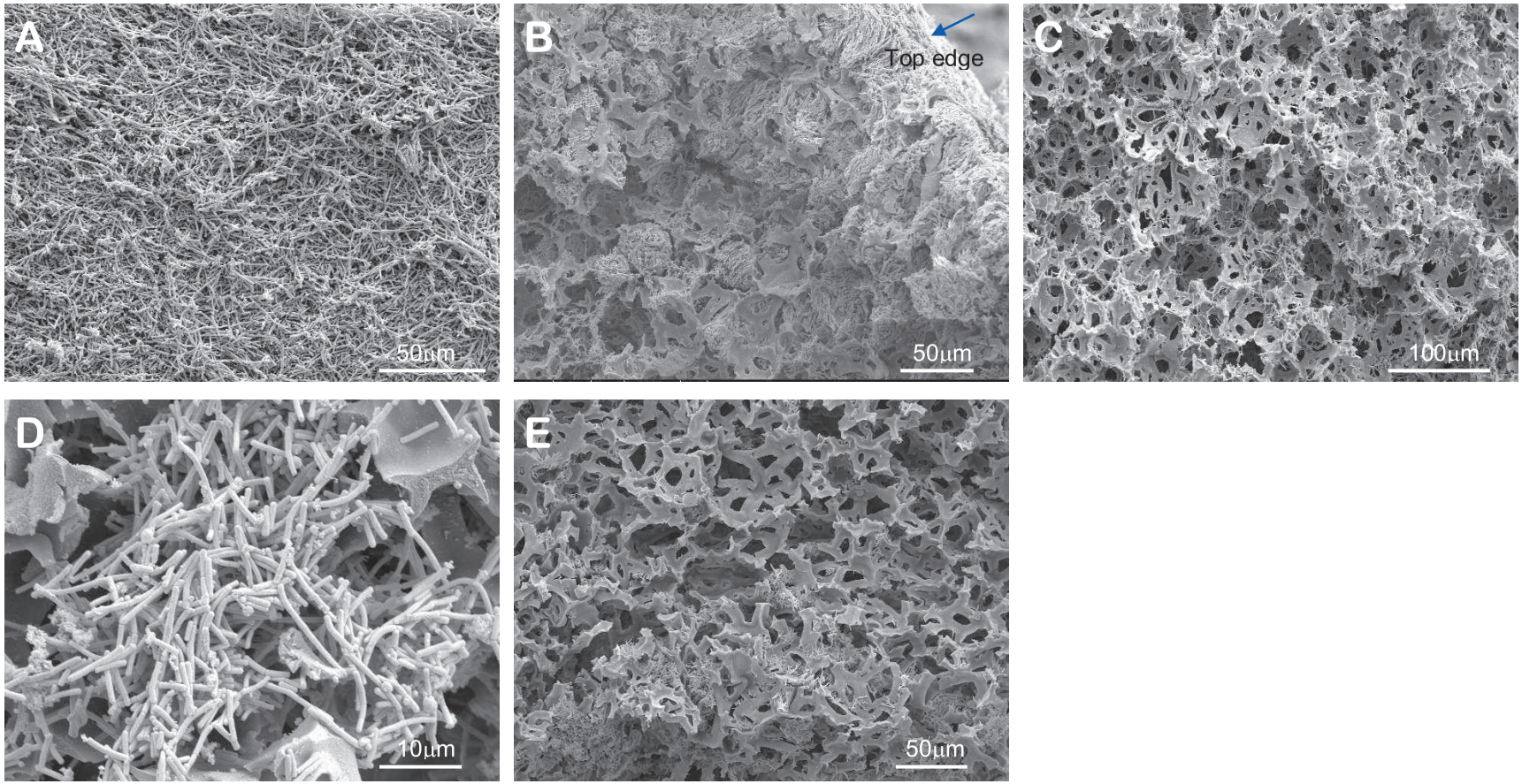

Figure 8.2.17: Scanning electron micrograph of immobilized cells on SPHP-4 matrix after 48h cultivation (A) General view of top surface (x500) (B) cross-section into the matrix from the top edge (C) cross-section in the middle of the matrix, (D) cross-section in the middle of the matrix at higher magnification (x2000) and (E) bottom edge. The terminology of the regions of the matrix is defined and illustrate in Fig. 2.6.

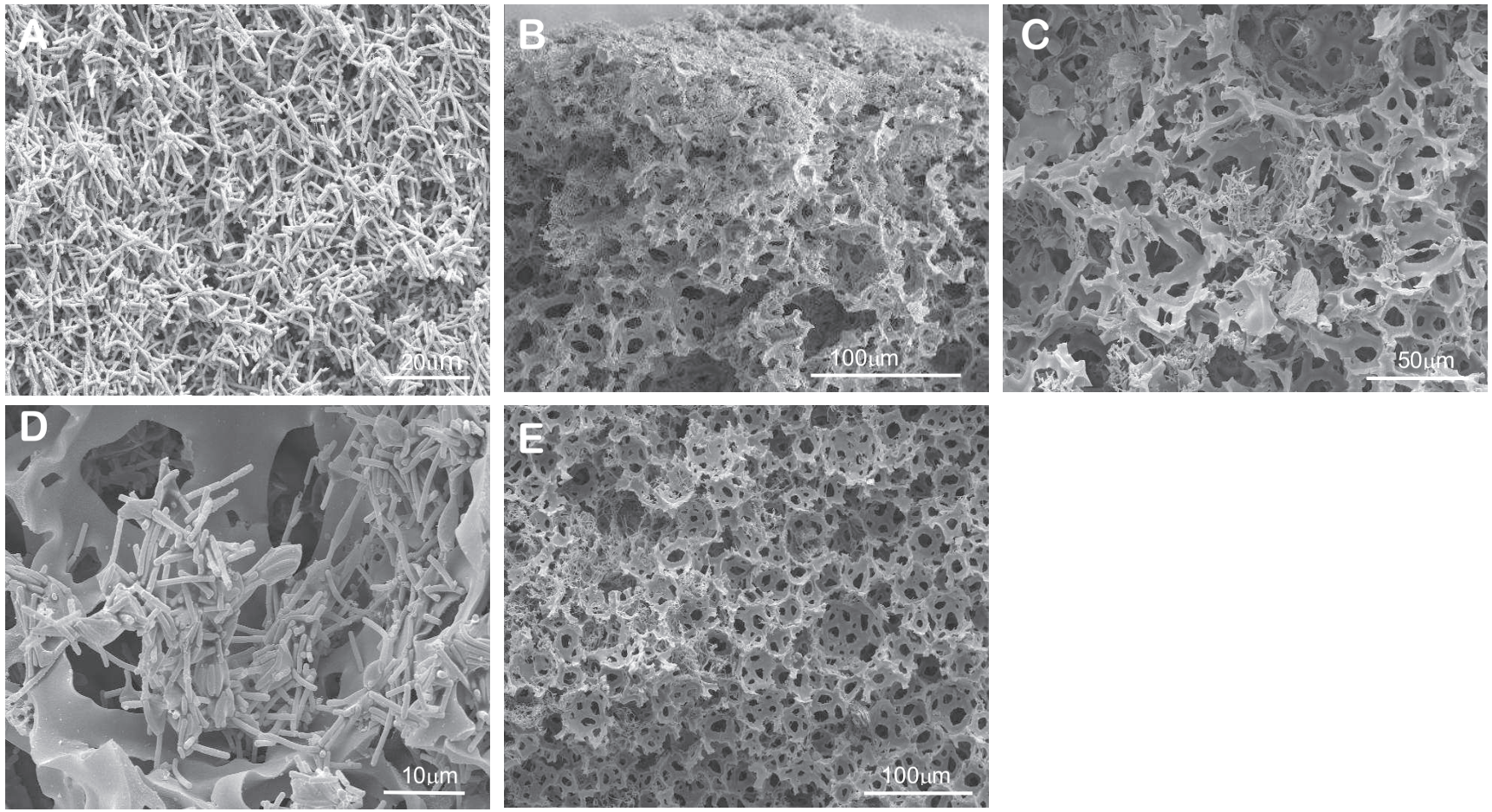

Figure 8.2.18: Scanning electron micrograph of immobilized cells on sulphonated polyHIPE matrix, SPHP-6 after 48h cultivation (A) General view of top surface, (B) cross-section from the top edge, (C) in the middle of the matrix (x500), (D) at high magnification (x2000) and (E) further deep (x250). The terminology of the regions of the matrix is defined and illustrate in Fig. 2.6.

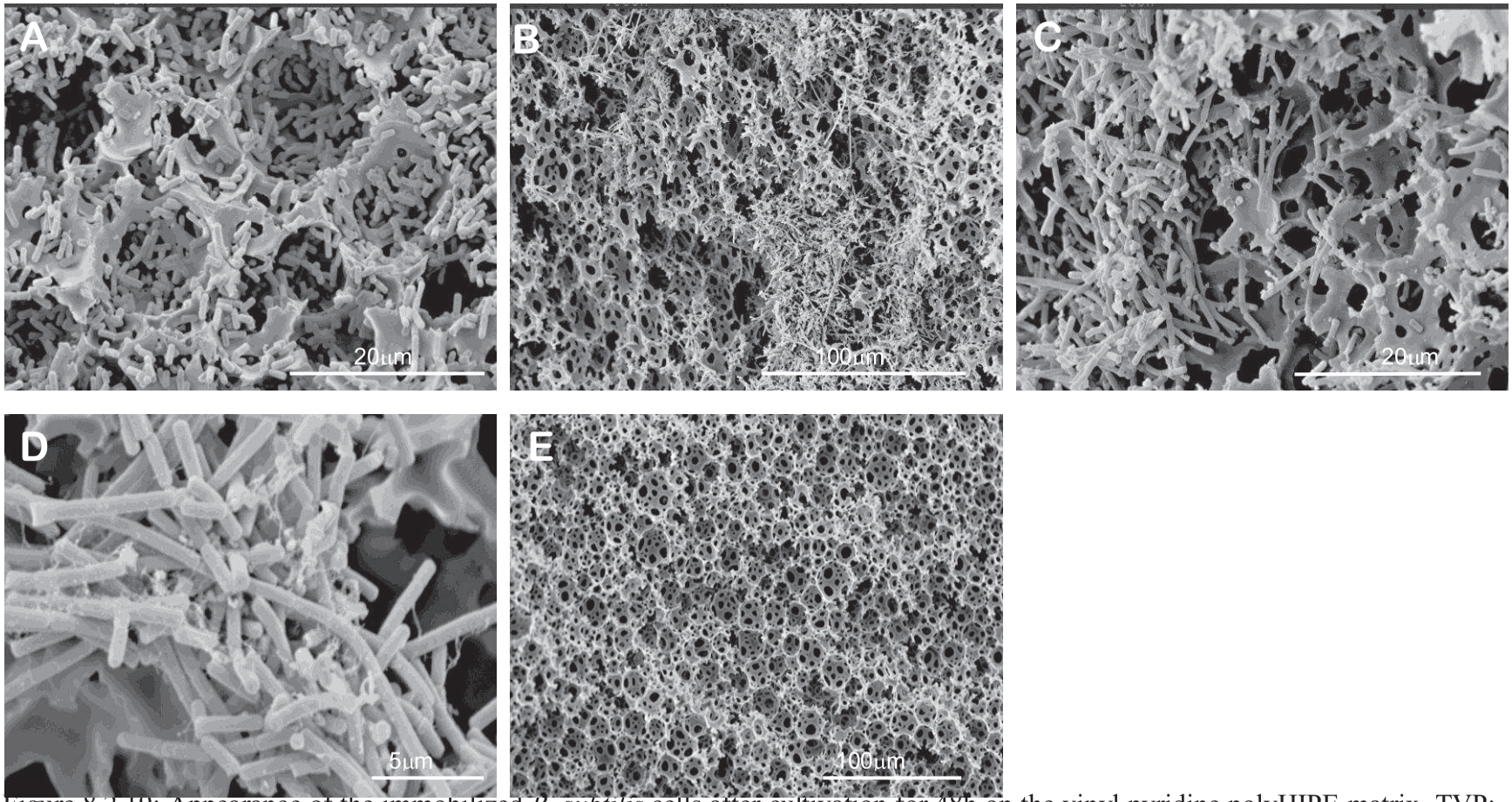

Figure 8.2.19: Appearance of the immobilized *B. subtilis* cells after cultivation for 48h on the vinyl pyridine polyHIPE matrix, TVP: (A) General view of top surface, (B) cross section in the middle of the matrix (x500), (C) cross-section in the middle of the matrix (x2000), (D) cross-section in the middle of the matrix (x5000) and (E) further deep (x250). The terminology of the regions of the matrix is defined and illustrate in Fig. 2.6.

8.3.4 Discussion

Previous studies have shown that the performance of polyHIPE polymeric materials used as microbial cell matrices or as scaffolds for osteoblastic cell was dependent on its physical and chemical characteristics (Akay *et al*., 2005a, Akay *et al*., 2004, Bokhari, 2003, Erhan *et al*., 2004). In this study two chemically different of polyHIPE matrices, with pore sizes in the range of 20 to 40μm, were synthesized and evaluated. These polymeric materials exhibited different levels of hydrophilicity.

As can be seen in Figure 8.2.16 there was an increase in numbers of cells on the top surface of all polyHIPE matrices when the incubation time was extended to 48h (the appearance of cells on the top surface of SPHPs after 24h incubation is shown in Figure 8.2.5); the surface of the two SPHP matrices were completely covered while there were still areas of the TVP-5 matrix that were not completely covered with cells (Figure 8.2.16C). This indicates nutrients and oxygen were available throughout this area of the matrix to support cells growth. However, the accumulation of cells on the top surface could develop into a barrier to the accessibility of nutrient for the cells in the cross section of the polyHIPE matrix.

More cells were detected in the cross section of SPHP-4 matrix (Figure 8.2.17), which has a slightly bigger pore and interconnects than the other two matrices. However, the number of bacterial cell decreased with distance from the upper surface, presumably reflecting a corresponding decline in the available nutrients (Figure 8.2.17C-E). In the case of TVP-5 matrix, relatively few cells permeated through the matrix. These results indicated that the pore and interconnect sizes of the SPHP-4 matrix facilitated greater penetration of cells throughout the interior of its matrix. Therefore, this physical characteristic is important in designing the matrix used as an immobilized cell carrier.

Analysis of the matrices by SEM show that the sulphonated polyHIPEs (SPHP-4 and SPHP-6) exhibited a much better performance as immobilized cell matrices compared to the non-sulphonated polyHIPE (TVP-5) in promoting the growth of the inoculated cells and allowing penetration of cells across the matrix. This is likely to be due to the more hydrophilic characteristic of these matrices

compared with that of TVP-5. This feature improved the permeability of the growth medium throughout this matrix. Consequently, SPHP provided a permissive environment that promoted better growth and proliferation of the immobilized cells throughout the interior section of the matrix. As a result, more cells were entrapped in this matrix and α-amylase production was higher (Figure 8.2.13 and Table 8.2.6). However, more cells were released from the SPHP-4 matrix compared to the other matrices, presumably reflecting it ability to sustain growth further into the matrix.

The productivity of the developed systems for the production of α-amylase increased with time; in the case of the SPHP-4 matrix from 6.84 U/ml/h after 24h to 8.18 U/ml/h after 48h. Future studies should be aimed at improving this level of productivity, which is still significantly lower than planktonic batch cultures using the same culture medium. These studies should focus on optimising the composition of the growth medium and its feed rate. This study clearly shows that the polystyrene-DVB polyHIPE, modified by sulphonation, is suitable for use as an immobilized cells matrix. The matrix is itself immobilised and sealed within a complete novel micro-bioreactor system that is well-instrumented with probes for pH, DO and temperature control. The next challenge is to optimise the microreactor and associated control systems to improve the commercial viability of the process.

In conclusion, the results in this chapter show that:

- The pore size of matrices affected the production of α-amylase by *B. subtilis* and sulphonated polyHIPE matrix with pore size of 36μm (SPHP-4) was shown to allow cells to penetrate throughout the matrix.

- A cell loading concentration of 2 x 10^8 cells/ml resulted in the highest α-amylase productivity, although more cells were released from the matrix

- A high volumetric productivity of α-amylase per volume of occupied matrix was obtained by the immobilized cell cultures (6.84 U/ml/h was obtained by *B. subtilis* immobilized on SPHP-4 (ϕ = 36μm) matrix)

compared to planktonic batch culture. However, this volumetric productivity was relatively low if compared to planktonic batch cultures when it determined on the basis of total nutrient medium used throughout growth. Consequently, the overall yield of α-amylase by immobilized cell cultures was relatively low compared to planktonic batch cultures

- Sulphonated polyHIPEs matrices were observed to give a better performance of growth, proliferation and penetration of cells as well as α-amylase enzymes production compared to non-sulphonated polyHIPE matrices (vinyl pyridine polyHIPE)

9 Effect of nutrient media composition to the immobilised *B. subtilis* on sulphonated polyHIPEs

9.1.0 Introduction

The productivity of bacteria for the production of specific proteins can be improved by optimisation of the growth medium (Dey *et al*., 2001, Longo *et al*., 1999, Konsoula and Liakopoulou-Kyriakides, 2006). Therefore in this study medium composition was varied to study its affect on the starch-degrading enzyme, α-amylase produced by immobilized *B. subtilis* cells (Table 9.1). LB medium used in this study is a general purpose medium that supports a high level of protein secretion in *B.subtilis* (Antelmann *et al*., 2001). The main components of LB medium are tryptone, yeast extract and NaCl. These were independently varied to determine their influence on α-amylase production. All experiments and measurements were performed independently and in triplicate.

Table 9.1: Variations to the components of LB medium (D3)

Different conc. media	Media composition (g/L)		
	Tryptone	NaCl	Yeast extract
D1	5	5	2.5
D2	7.5	7.5	3.75
D3	10	10	5
D4	20	20	10

9.1.1 Effect of LB media concentration to the production of α-amylase

SPHP-4 (ϕ = 36 μm) showed the best performance as an immobilized matrix for the production of α-amylase and was therefore used to evaluate changes in medium composition. SPHP-4 discs were autoclaved and placed into the sealed filter-shaped PTFE microchamber and pre-wetted with sterilized distilled water for 1h followed by nutrient medium for a further hour. The matrices were inoculated with 2 ml of a pre-germinated spore suspension (~2 x 10^8 cells/ml) using the forced-flow technique. After an hour, well-aerated nutrient medium was continuously pumped through the seeded SPHP matrix for 24 hours. The apparatus was maintained in a 37^0C room. Samples were collected for the analysis of α-amylase production and cell loss at various times throughout growth.

Figure 9.1 shows the analysis of α-amylase production by the LB media of different compositions. The data shows that optimum α-amylase production was observed using D4 medium, although this was only slightly higher than that of D3 medium in which each of the components were at half the concentration. Maximum production occurred after 12 hour and remained relatively constant at ~0.5 U/ml. In the case of the D2 medium, the production of α-amylase reached only half the α-amylase production rate of D3 medium (~0.25 U/ml) after 12 hours, but increased slightly to ~0.30 U/ml at 18 hours and remained steadily until the end of experiment. The α-amylase production rate obtained using D1 medium did not reach steady state during the 24 h incubation time, reaching a level of 0.15 U/ml at the end of the experiment. The α-amylase production for each of the LB media variants, based on a nutrient medium flow rate of 1ml/min for 24 hours, per volume of SPHP matrix can be seen in Figure 9.2.

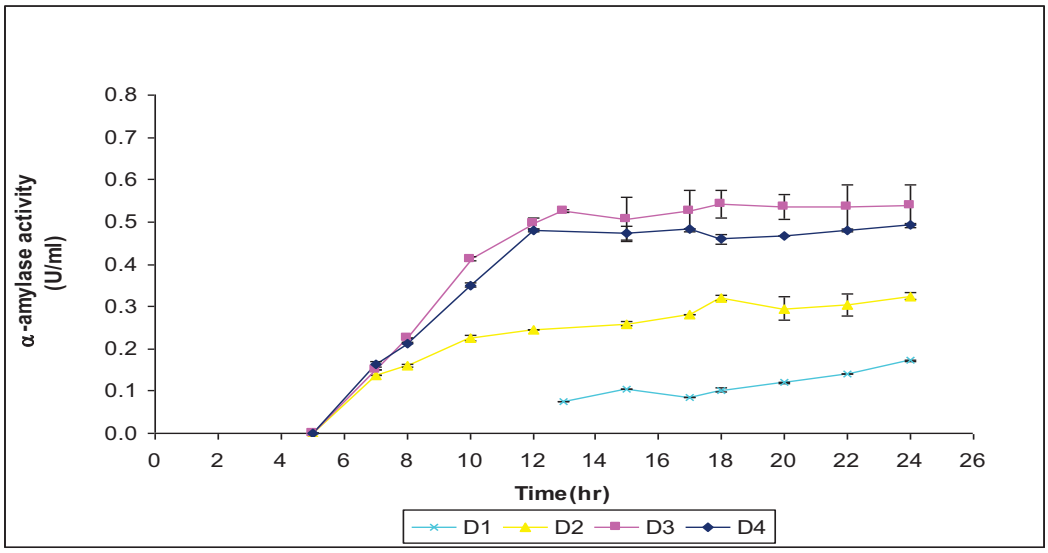

Figure 9.1: The time-course of the production of α-amylase by *B. subtilis* immobilized in sulphonated polyHIPE matrix with pore size of 36.0 ±0.50µm (SPHP-4) for four different composition of Lb medium (D3). (for 24h incubation with 1ml/min of nutrient medium flow rate).

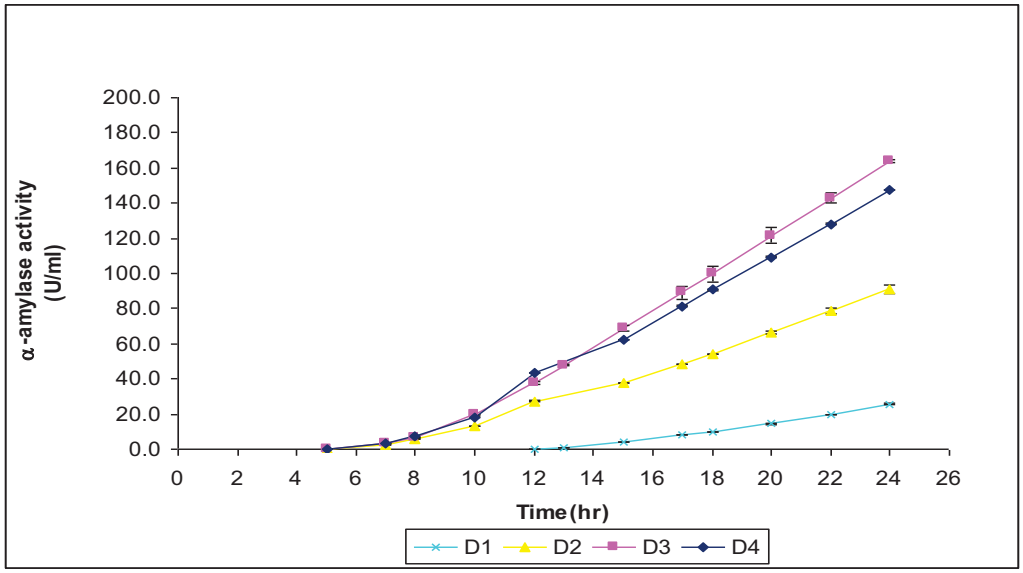

Figure 9.2: Cumulative α-amylase production by cells of *B. subtilis* immobilized on SPHP matrix with pore size of 36.0 ±0.50µm (SPHP-4) with four different composition of Lb medium. (Calculation was based on flow rate of 1ml/min used for 24h incubation).

9.1.2 Effect of LB media concentration on the rate of cell release

The cell released from SPHPs matrices was also observed (Figure 9.3). The cells were determined by counting the number of colonies on the nutrient agar plates

after growth overnight at 37^0C. These results show that the number of cells released for the D3 and D4 media were almost identical. In the case of D1 and D3 media, the cells released were least compared to D3 and D4 media.

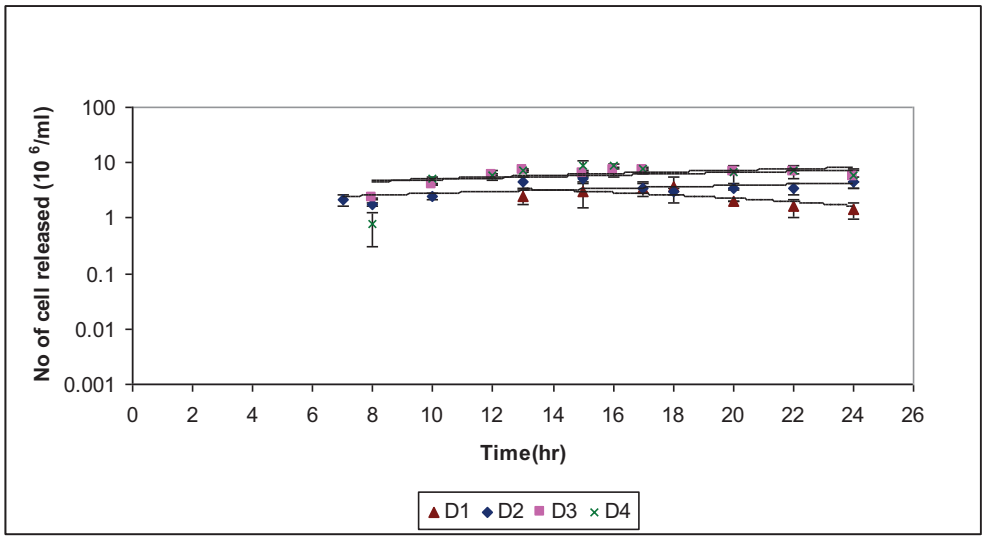

Figure 9.3: Cells released from sulphonated polyHIPE matrices (pore size of 36μm) perfused with four variants of LB medium.

9.1.3 Comparison between immobilized cells and planktonic cell cultures

The yield of α-amylase per total of medium used, volumetric productivity of α-amylase produced (per total of medium used or volume occupied by SPHP matrix) and specific α-amylase production rates (per mg dry cell weight or mg/ml of total protein of supernatant culture) of the LB medium variants were determined (Table 9.2). In order to estimate amount of biomass in the matrices their dry weight was determined at the start and end of the experiment. The data was compared with that obtained from planktonic cultures (Table 9.2).

Total α-amylase production for each medium was calculated on the basis of a flow rate of 1ml/min for 24h (Figure 9.2). D1 and D2 yielded less than 300U of α-amylase, while D3 yielded the highest α-amylase at 500U. When the concentration of LB medium (D3) was doubled (D4), the total α-amylase produced was slightly lower at ~448U). A slightly reduced level of α-amylase production by the immobilized cells in D4 medium might be due to the concentration of NaCl (0.34M) being too high. However, the data for the

planktonic batch cultures showed a different trend, and the α-amylase production by the D4 medium was 1.6-fold higher than that of D3. In fact the yields of α-amylase of all of the planktonic cultures for all of the LB medium variants (D1, D2, D3 and D4) were higher than the yields of immobilized cells (Figure 9.2).

The volumetric productivity of α-amylase of the immobilized cells was significantly higher than that of the the planktonic cultures if calculated on the basis of the volume occupied by the SPHP matrix (Figure 9.2). The volumetric productivity of α-amylase obtained by the immobilized cells with LB medium (D3) was 4.0-fold and 1.8-fold higher, compared to D1 and D2 media, respectively. This volumetric productivity was slightly reduced, from 6.84 U/ml/h to 6.23 U/ml/h, in D4 medium. However, the volumetric productivities of α-amylase per total nutrient medium of immobilized cells on the SPHP matrices were relatively low (<1) compared to that of the planktonic cultures (Figure 9.2). The highest volumetric productivity of α-amylase obtained by planktonic batch culture was with the D4 medium (1.42U/ml/h) and with the D3 medium for the immobilized cells.

The specific α-amylase production rates per mg dry cell weight for the immobilized cells were calculated on the basis of the volume occupied by the SPHP matrix (Figure 9.2). The rates decreased as the nutrient medium was changed from LB medium (D3) to D1 or D2 medium. In the case of the D4 medium, the specific production rate was similar to LB medium. However, based on the amounts of media used, the specific production rates of the immobilised cells were relatively small compared with that of the planktonic cultures (Figure 9.2).

The specific α-amylase production per mg dry cell weight of the planktonic cultures with D1 (22,018 U/g cell) and D2 (21,763 U/g cell) media was higher that that of LB medium (D3; 16,669 U/g cell). In contrast, the specific α-amylase production per mg dry cell weight of the immobilized cells was higher when D4 medium (4206.6 U/g cell) was used.

Table 9.2: Analysis results of α-amylase produced by the immobilized cells on SPHP-4 matrix `after 24h incubation for different LB medium composition and the results are compared with planktonic batch culture. Statistical significance was determined with one-way ANOVA where **p<0.05, **p-value is not significant (p = 0.341).

						Per ml of total medium used (1440ml)			Per volume of polyHIPE disc (3ml)		
	Conc. of Nutrient media	Yield of α -amylase per ml of medium used (U/ml)	**CDW (g/g PHP)	CDW (mg/cm^3)	Total α -amylase produced (U)	**Volumetric productivity (mU/ml/h)	Specific α -amylase production rate (mU/h/mg cell)	**Specific α -amylase (U/mg protein of supernatant culture)	**Volumetric productivity (U/ml/h)	Specific α -amylase production rate (U/h/mg cell)	**Specific α -amylase (U/mg protein of supernatant culture)
Immobilised cells on SPHP-4 matrix	D1	0.05 ± 0.0003	0.11 ±0.04	13.83	77.43 ±2.8	2.24 ± 0.0000	0.22	4.19 ± 0.00	1.71 ±0.007	0.08	2048±13.5
	D2	0.19 ± 0.0051	0.22 ±0.03	25.33	273.4 ±7.28	8.00 ± 0.0002	0.31	10.26 ± 0.28	3.80 ±0.10	0.15	4930 ±90.8
	D3 (LB)	0.34 ± 0.002	0.33 ±0.03	36.67	492.8 ±2.35	14.26±0.0001	0.40	17.14±0.08	6.84 ±0.03	0.19	8210 ±39
	D4	0.31 ± 0.0002	0.29 ±0.02	33.92	448.0 ±0.31	12.82 ± 0.0000	0.38	15.55 ± 0.01	6.23 ±0.007	0.18	7470 ±8.5
	Specific α -amylase production rate (U/mg cell)	D1	D2	D3	D4						
		1866	3597	3946	4207						
						Per ml of total medium used (100ml)					
	Conc. of Nutrient media	Yield of α -amylase per ml of medium used (U/ml)	*** CDW (mg cells/ml)		Total α -amylase produced (U)	**Volumetric productivity (U/ml/h)	Specific α -amylase production rate (U/h/mg cell)	**Specific α -amylase (U/mg protein of supernatant culture)	Specific α -amylase production rate (U/mg cell)		
Planktonic batch culture	D1	12.11 ±0.02	0.55 ±0.002		1211 ±2.8	0.50 ± 0.0011	0.92 ± 0.0021	602.6 ±1.36	22,018		
	D2	17.41 ±0.01	0.8 ±0.03		1741 ±2.1	0.73 ± 0.0009	0.91 ± 0.0010	926.0 ±1.04	21,763		
	D3 (LB)	21.67 ±0.02	1.3 ±0.02		2167 ± 2	0.90 ± 0.0012	0.69 ± 0.0008	1083.5 ±1.19	16,669		
	D4	34.14 ±0.14	2.54 ±0.003		3414 ±19.8	1.42 ± 0.0082	0.56 ± 0.0032	1126.8 ±6.51	13,441		

9.2 The effect of increasing individual components of LB medium to the immobilized cell culture on sulphonated polyHIPEs

9.2.1 Introduction

From previous results, it found that when each of the elements in LB medium was doubled (D4) the production of α-amylase decreased slightly (Figure 9.2). The work in this section was carried out to investigate further which components of the LB medium (NaCl, tryptone or yeast extract have the largest influence (either positive or negative) on α-amylase production. The LB medium variants are shown in Table 9.3. All measurements were performed on three independent experiments and the corresponding data were expressed as average values.

Table 9.3: Variations to the components of LB medium

Media variants	Media composition (g/L)		
	Tryptone	NaCl	Yeast extract
D3 (LB)	10	10	5
D4	20	20	10
D6	10	20	5
D7	10	10	10
D8	20	10	5

9.2.2 Effect of increasing individual components of LB medium to the α-amylase production

A SPHP-4 disc was autoclaved and placed into a sealed filter-shaped PTFE microchamber in the 37^0C room. The disc was pre-wetted with sterilized distilled water for 1h followed by nutrient medium for a further hour. The matrix was inoculated with 2 ml of pre-germinated spores (~2 x 10^8 cells/ml) using the forced-flow technique at a flow rate of 0.55ml/min. After an hour, well-aerated LB medium was continuously pumping into the seeded SPHP matrix for 24 hours.

Samples were collected for analysis of α-amylase production and cell loss at various times throughout growth. The same procedures were repeated for the LB media of different compositions (Table 9.3). Figure 9.4 shows the relationship between α-amylase production and media type over time.

Figure 9.5 shows the total α-amylase produced throughout growth of 24 hours incubation. The results obtained were compared with D3 and D4 (Figure 9.1 and Figure 9.2). Figure 9.4 shows the effect of varying the composition of LB medium with respect to α-amylase production by the immobilized *B. subtilis* cells on the sulphonated polyHIPE matrix (SPHP-4, pore size of 36 μm). The data shows that the maximal α-amylase production (~0.6 U/ml) was obtained using D7 medium (doubled yeast extract concentration). Optimal productivity was reached after 12 h and remained at this level until the end of the experiment. When the concentration of tryptone was doubled (D8 medium), the maximal α-amylase production of ~0.45U/ml was obtained after 13 hours, increasing throughout the remaining growth period to ~0.5 U/ml. Doubling the concentration of sodium chloride (D6 medium) had a very negative effect on α-amylase production which only reached a level of ~0.3 U/ml after 12 hours, increasing ~0.35 U/ml by the end of the experiment. The determination of the total α-amylase produced was made on the basis of a medium flow rate of 1ml/min (Figure 9.5).

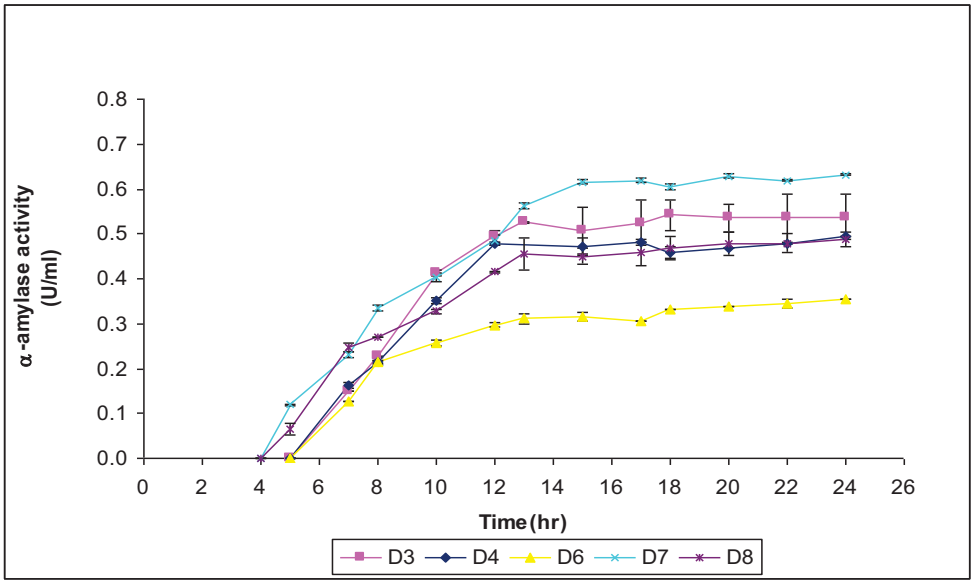

Figure 9.4: The time-course of the production of α-amylase by *B. subtilis* immobilized on sulphonated polyHIPE with pore size of 36.0±0.50µm for five different composition of nutrient media (for 24h incubation with 1ml/min of nutrient medium flow rate).

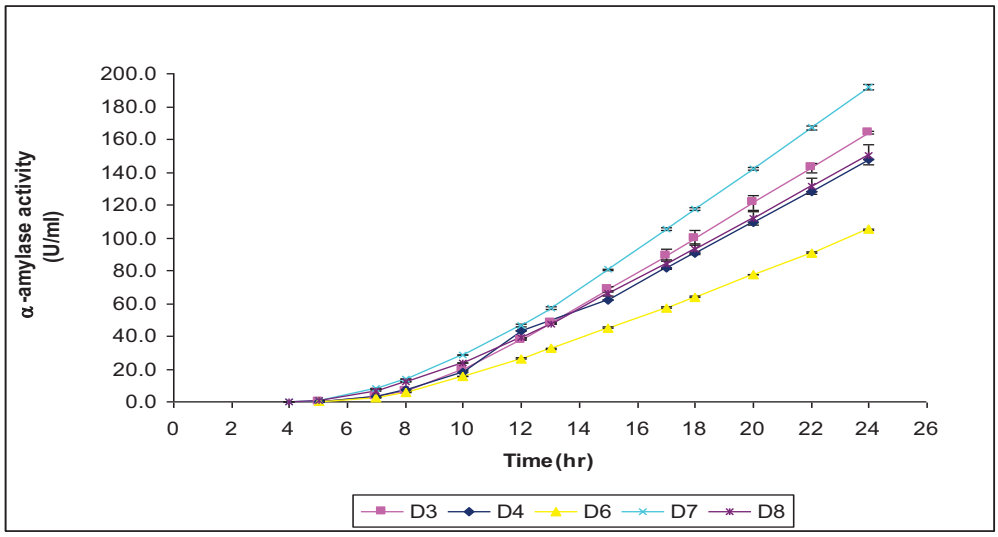

Figure 9.5: Kinetics of extracellular α-amylase production by immobilized cells in sulphonated polyHIPE with pore size of 36.0±0.50µm with five different concentrations of nutrient medias. (The total α-amylase production was calculated on basis of flow rate of 1ml/min for 24h incubation per volume of occupied by matrix)

The yields of α-amylase per ml of medium for all five different compositions of nutrient medias are estimated and shown in Table 9.4**.** The yield of α-amylase from D7 medium (double yeast extract concentration) was 1.2-fold higher than LB medium (D3 medium). The yield of α-amylase from D4 (doubled

medium components) and D8 (doubled tryptone concentration) media were similar to each other and to LB medium (D3). However, the yields for all media used were relatively low (less than 1U/ml) compared to the planktonic culture (Table 9.5). The cell dry weights were similar for all of the media, exception D6, which was almost that of the other media (Figure 9.4).

Table 9.4: Yield of α-amylase produced (per total volume of medium used) and cell dry weight (CDW) by immobilized cells in sulphonated polyHIPE with pore size of 36μm in five different concentrations of nutrient medium (CDW in mg/ml unit was calculated based on volume of polyHIPE disc).

Different conc. of media	Yield of α-amylase per ml of medium used (U/ml)	*CDW (g/g PHP)	CDW (mg/ml)
D3 (Lb)	0.34±0.002	0.32 ±0.03	36.63
D4	0.31 ±0.0002	0.29 ±0.02	35.50
D6	0.22 ±0.001	0.17 ±0.04	21.67
D7	0.40±0.003	0.33 ±0.02	39.17
D8	0.31 ±0.01	0.30 ±0.06	35.50

*Statistical significance was determined with one-way ANOVA where p= 0.027.

9.2.3 Effect of increasing individual components of LB medium to cell release

The release of cells from the SPHPs matrices was also determined by enumerating number of viable cells on nutrient agar plates after growth overnight at 37^{o}C. Generally, D6 medium (double sodium chloride concentration) released the lowest number of cells (Figure 9.6). The release of cell from D7 and D8 media were slightly lower compared to that of LB medium (D3).

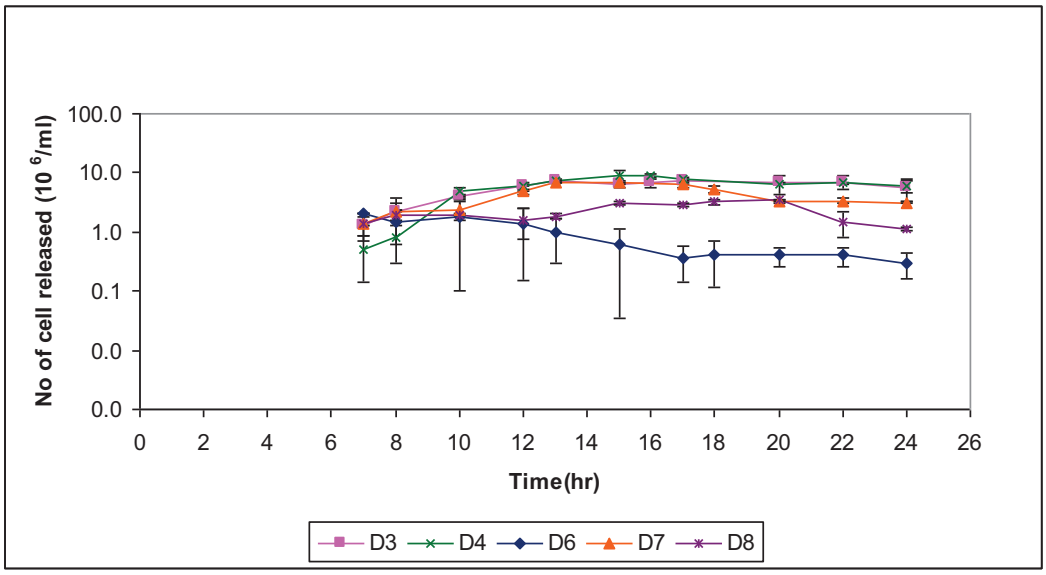

Figure 9.6: Released cells in 10^6/ml from five different concentrations of nutrient medium used in immobilized cells in sulphonated polyHIPE matrices with pore size of 36µm (for 24h incubation with 1ml/min of nutrient medium flow rate).

9.2.4 Comparison of immobilized cells with planktonic batch cultures

Total of α-amylase production, its yield per medium used, volumetric productivity (per total of medium used or volume occupied by SPHP matrix) and specific α-amylase production rates (per mg dry cell weight or mg/ml of total protein of supernatant culture) of immobilized *B. subtilis* fed with the different Lb medium variants are shown in the Table 9.5**.** The data was calculated on the basis of a nutrient medium flow rate of 1ml/min for 24 hours. These resulting data were compared with the data from the planktonic batch cultures. When the concentration of each component of LB medium was doubled (D4), the production of α-amylase by immobilized *B. subtilis* culture decreased slightly, from 492.8 U to 448.0 U. In contrast, the same medium lead to an increase in productivity from the planktonic batch cultures, from ~2167 U to ~3414 U. Moreover, there was a 1.9-fold and 1.6-fold increase in total α-amylase produced by planktonic batch cultures, respectively, the D7 and D8 media were used in place of LB medium. In the case of the immobilized cells, the total α-amylase production on increased slightly (10%) when D7 medium was used to in place of LB medium, and a slight decrease (to 0.9-fold) when D8 medium was used. For the both systems, total α-amylase production decreased by more than 50% when

D6 medium was used. This result is likely to be due to the osmotic stress imposed by the high salt content this medium.

The volumetric productivity of α-amylase produced by immobilized cells was significantly higher than the planktonic batch cultures when it was calculated on the basis of the volume of polyHIPE disc (Table 9.5). The highest volumetric productivities of α-amylase produced by both cultures techniques, immobilized cells and planktonic cultures, were observed when D7 medium was used. The volumetric productivities of α-amylase produced by immobilized cells, its yields and specific α-amylase production rate (per mg cell) for LB medium and its variants were relatively low compared to that of the planktonic batch cultures, when calculated on the basis of total volume of medium used (Table 9.5)**.** The highest specific α-amylase production per mg dry cell weight of the planktonic cultures (17,418 U/g cell) was obtained when the concentration of tryptone was doubled. In contrast, the specific α-amylase production per mg dry cell weight of immobilized cells was higher when D7 medium (4,902 U/g cell) was used. If compared with LB media used (D3), the planktonic cultures (16,669 U/gcell) had of specific enzyme production level that was four times that of the immobilized cells (3,946 U/gcell). The specific α-amylase production rates (per mg dry cell weight) were also calculated (Table 9.5) and found to be similar, although again the D7 medium yielded the highest specific production rates.

Table 9.5: Analysis results of α-amylase produced by the immobilized cells on SPHP-4 matrix after 24h incubation for different Lb medium composition and the results are compared with planktonic batch culture.*Statistical significance was determined with one-way ANOVA where $p<0.05$.

				Per ml of total medium used (1440ml)			Per volume of polyHIPE disc (3ml)		
	Conc. of Nutrient media	*Total α-amylase produced (U)	Yield of α-amylase per ml of medium used (U/ml)	*Volumetric productivity (mU/ml/h)	Specific α-amylase production rate (mU/h/mg cell)	*Specific α-amylase (U/mg protein of supernatant culture)	*Volumetric productivity (U/ml/h)	Specific α-amylase production rate (U/h/mg cell)	*Specific α-amylase (U/mg protein of supernatant culture)
Immobilised cells on SPHP-4 matrix	D3 (Lb)	492.8 ±2.35	0.34 ± 0.002	14.26±0.0001	0.40	17.14±0.08	6.84 ±0.03	0.19	8210 ±39
	D4	448.0 ±0.31	0.31 ± 0.0002	12.82 ± 0.0000	0.37	15.55 ± 0.01	6.23 ±0.007	0.18	7470 ±8.5
	D6	314.83 ±1.6	0.22±0.001	9.11 ± 0.00005	0.42	19.88 ± 0.10	4.37 ±0.02	0.18	8630 ± 47
	D7	576.0 ±4.2	0.40±0.03	16.67 ± 0.0001	0.43	36.36 ± 0.26	8.00 ±0.06	0.20	9575 ±35.2
	D8	451.8 ±17.5	0.31±0.01	13.07 ± 0.0005	0.36	28.52 ± 1.10	6.28 ± 0.24	0.18	9413 ± 371.2
Specific α-amylase production rate (U/mg cell)	D3	D4	D6	D7	D8				
	3946	4207	4844	4902	4242				
				Per ml of total medium used (100ml)					
	Conc. of Nutrient media	Total α-amylase produced (U)	Yield of α-amylase per ml of medium used (U/ml)	*Volumetric productivity (U/ml/h)	Specific α-amylase production rate (U/h/mg cell)	*Specific α-amylase (U/mg protein of supernatant culture)	Specific α-amylase production rate (U/mg cell)		
Planktonic batch culture	D3 (Lb)	2167 ± 2	21.67 ±0.02	0.90 ± 0.0012	0.69 ± 0.0008	1083.5 ±1.19	16,669		
	D4	3414 ±19.8	34.14 ±0.14	1.42 ± 0.0082	0.56 ± 0.0032	1126.8 ±6.51	13,441		
	D6	1173 ±15.6	11.73 ±0.11	0.49 ± 0.0064	0.46 ±0.0060	586.5 ±7.7	10,963		
	D7	4116 ±104.7	41.16 ±0.74	1.72 ± 0.0436	0.67 ±0.0169	1030.0 ±26.1	16,016		
	D8	3414 ±9.9	34.14 ±0.07	1.42 ± 0.0041	0.73 ±0.0021	1138.0 ±3.3	17,418		

9.2.5 Discussion

One of the approaches that can be taken to improve protein production by bacterial cells is to investigate the influence of medium composition. Therefore, in this study, the concentration of the components of LB medium was varied (Table 9.1) to study the production of α- amylase by *B. subtilis* immobilized on a sulphonated polyHIPE matrix. The relative amounts of each of the medium components are likely to affect metabolite formation and, consequently, the pattern of enzyme production (Figure 9.1 or Figure 9.2). Media D1 and D2 yielded significantly lower levels of α-amylase that the original LB medium (D3), while D4 medium, in which each of the components was present at double the original concentration, showed just a small reduction in α-amylase production. The specific α- amylase production per g cell for LB medium (D3) was 2.1-fold and 1.1-fold higher, compared to D1 and D2 media, respectively. These results indicated that D1 and D2 had insufficient nutrients for optimal cell maintenance and enzyme production. In the case of D4, a higher concentration of nutrients in this medium might actually inhibit the metabolism of *B .subtilis*, particularly the high concentration of sodium chloride. A previous study (Alam *et al*., 1989) has reported that in the absence of pH control, additional amounts of yeast extract can lead to an increase in acid production which can limit the growth of *B. subtilis*. Similarly, high medium salinity increases the osmotic pressure on the cell, resulting in a change in metabolism to the production of zwitterionic organic molecules such as glycine betaine, choline or proline which are osmoprotectants.

A number of previous studies have attempted to investigate the influence of immobilization on cell growth and metabolic activity (Duran-Paramo *et al*., 2000, Argirakos *et al*., 1992, Chevalier and De La Noue, 1987, Dobreva *et al*., 1998, Konsoula and Liakopoulou-Kyriakides, 2006, Tonkova *et al*., 1994). The general conclusion is that the cells are responding to stresses in the microenvironment of the immobilization system (Konsoula and Liakopoulou-Kyriakides, 2006). Based on data presented in Table 9.5, the ratios of total α-amylase produced and yield between immobilized cells and plankonic cell cultures were less than one. These results

indicated the low production efficiency of the immobilized cells in comparison to free cell cultures. Oxygen and substrate gradients occurring within the polyHIPE matrices subsequently led to gradients of entrapped cells in polyHIPE matrix. Another reason might be due to the nutrient medium flow rate (1 ml/min) used in the experiments being too high, resulting in the retention time of the nutrients in the matrix being too short for maximise substrate uptake. In other word too much substrate may be retained in the outflow from the system. It was found that the specific enzyme of immobilized cultures (per g biomass) with LB media was 4.2-fold lower than planktonic cultures. The enzyme production rate of the planktonic cultures was significantly higher than that of the immobilized cultures (Table 9.2). This indicates that the growth of planktonic cultures was better than immobilized cells. Additionally, the specific activity of α–amylase (per mg protein of supernatant culture) produced by planktonic culture with LB media (D3) was 1083 U/mg while that of the immobilized cells was only ~17.14 U/mg (Table 9.2). However, the volumetric productivity of immobilized cells (if calculated in basis of volume occupied by SPHP matrix) was 7.6-fold higher (Table 9.2) than the planktonic batch cultures. The sulphonated polyHIPE disc, which has a volume of ~3ml and a depth of ~5cm limits the available space for the cells to proliferate. Consequently, enzyme production is limited by the number of cell that can be maintained in the matrix. Therefore, consideration needs to be given to modifying the design of the immobilized cell microreactor as well as optimizing the medium and its flow rate.

The results indicated that doubling the concentration of yeast extract (D7 medium) had the most significant impact on α-amylase production by *B. subtilis* cells immobilized on a sulphonated polyHIPE matrix. This might be due to the presence of a growth limiting vitamin and other trace nutrients present in yeast extract, of the need for higher concentrations of other nitrogen and carbon sources. This result is similar to that observed for *B. subtilis* FERM-P No. 2040 immobilized in polyacrylamide gel (Kokubu *et al*., 1978). In the case of D8 medium, which contained double the concentration of tryptone, the total and volumetric productivity of α-amylase was similar to that of D4 medium. This might be due to a component of the D8 medium inhibiting the synthesis of α-amylase. This result contradicts the

findings of Konsoula and Liakopoulou-Kyriakides (Konsoula and Liakopoulou-Kyriakides, 2006) who observed that *B. subtilis* cells entrapped in calcium alginate capsule gels yielded maximal α-amylase production when 2% (w/v) tryptone (of 0.5% in LB medium and 1% in D8 medium) was used. The specific α-amylase production per mg biomass of immobilized cell system increased to 1.2-fold and 1.1-fold when LB media was substituted with D7 and D8 media. Doubling the concentration of the media components had promoted cell growth consequently increased enzyme production. Previous studies have reported that the supplementation of a complex medium such as LB medium with various specific growth factors can improve cell growth (Yang *et al*., 2006). However, attempts to optimise a specific growth medium can be extremely time-consuming and have both beneficial and detrimental affects (Yang *et al*., 2006).

The cell dry weight produced on the sulphonated polyHIPE matrix with D6 medium was 50% lower than cell dry weight obtained in LB medium (D3) (Table 9.4). This was likely to be due to the high concentration of sodium chloride in this medium and its affect on osmotic stress. The change in cellular metabolism that results from the need to synthesise osmotic protectants could be at the expense of biomass production.

B. subtilis encodes a lipoprotein called PrsA which is essential for the efficient secretion of specific target proteins and for cell viability (WahlstroÌˆm et al., 2003, Kontinen and Sarvas, 1993, Kontinen et al., 1991, Kontinen and Sarvas, 1988, Wahlstrom et al., 2003). Previous studies have showed that the overproduction of PrsA enhances the secretion of A*my*Q from plasmid pKTH10 (Vitikainen *et al*., 2001). Since PrsA is exposed at the surface of the single membrane in this bacterium, the elevated concentration of sodium chloride in D6 medium may affect the activity of PrsA and the folding and secretion of the α-amylase AmyQ (Tjalsma *et al*., 1999).

When D7 and D8 media were used to grow cells in planktonic culture, the yield of α-amylase was significantly different from that observed by the immobilized cultures. Similarly with the immobilized cell, the D7 medium also supported the highest α-amylase activity and volumetric productivity in planktonic culture. The total α-amylase production was 1.9-fold and 1.6-fold higher, respectively, with the

D7 and D8 media in comparison to LB medium (D3). However, the specific enzyme production of D7 media (per g biomass) was 0.96-fold reduced compare to D3 media. This is likely to be due to the presence of a component in the D7 medium at a concentration that was inhibitory to α-amylase production. These similar media yielded 3.3-fold and 4.1-fold increased of specific enzymes (per g biomass) compared to that immobilized cells. Additionally, the specific α-amylase production rates per mg biomass for planktonic cultures were significantly higher than the immobilized system (Table 9.5), indicating that α-amylase production is related to cell growth and the cells in the planktonic cultures growth better than those immobilized on the sulphonated polyHIPE matrix.

In conclusion, the results in this chapter show that:

- When the composition of the LB medium was varied (D1, D2, D3 and D4), the original medium (D3) performed best in the immobilized cell system while D4 medium, in which the composition of the main components were doubled, performed better with the planktonic batch cultures.

- However, when one of the LB medium components was increased, D7 medium (doubling the concentration of yeast extract) resulted the highest α-amylase activity and volumetric productivity in both systems: immobilized cell and plankonic culture

- The release of cell from D6, D7 and D8 media were slightly lower compared than that of LB medium (D3) with D6 media (double sodium chloride concentration) released the lowest number of cells. The amount of cell loss from these matrices was probably about 1% or less from the cells entrapped in the matrices.

- A high volumetric productivity of α-amylase enzymes per volume occupied of matrix was obtained by the immobilized cell cultures compared to planktonic batch culture. However, this volumetric productivity was relatively

low if compared to planktonic batch cultures when it determined on the basis of total nutrient medium used throughout growth. Consequently, the overall yield of α-amylase by immobilized cell cultures was relatively low compared to planktonic batch cultures

10 Conclusions

In this thesis we have evaluated whether sulphonated polystyrene-divinylbenzene PHP can be use as a matrix for the support of immobilised cells of the Gram-positive bacterium, *Bacillus subtilis*. The performance of this sulphonated PHP as a matrix was then compared with non-sulphonated PHP. The main achievements were as follows:

1. The production of immobilised cell matrices, based on polyHIPE polymers (PHPs), with a controlled range of pore and interconnects sizes.

2. The characterization of PHP matrices (physico-chemical characteristics) for the immobilization of the starch-degrading bacterium, *B. subtilis,* with respect to growth and α-amylase production.

3. The determination of the effects of pore size on the growth, viability, proliferation and enzyme productivity of *Bacillus subtilis* immobilised onto polyHIPE matrices.

4. The determination of the effects of medium composition and cell loading on the growth and enzyme productivity of immobilized *Bacillus subtilis*

5. The comparative productivity of the developed immobilized system with that of a planktonic batch culture for the production of the enzyme α-amylase.

Initially, in Chapter 3, the growth of model organism, *B. subtilis,* was studied in planktonic batch culture. The effect of medium composition on cell growth and its enzyme productivity were investigated by using various LB media concentrations including increasing LB medium component (Tryptone/NaCl/Yeast extract). Reducing the concentrations of the individual components (media D1 and D2) caused a reduction in the yield of α-amylase.

When the concentration of individual components of LB medium was increased, doubling the concentration of yeast extract (D7) improved cell growth and increased α-amylase production, while doubling the concentration of sodium chloride had precisely the opposite effect. Both the vegetative cells and spores of *B. subtilis* had a low affinity towards the hydrocarbon hexadecane, indicating that they preferred a hydrophilic environment. The *in-situ* incorporation of *B. subtilis* spores during the synthesis of polystyrene-DVB PHP showed that the spores were extremely resistance to the harsh environment generated during the polymerisation reaction, as indicated by the observation that some of the inoculated *in situ* spores were able to germinate in the presence of culture medium.

Chapter 5 reviews the characterization of the polystyrene-DVB PHP used for the *in situ* incorporation of *B. subtilis* spores. For this purpose, the target pores and interconnect sizes of polystyrene-DVB PHPs matrix were between 20μm and 5μm. Rates of mixing and dosing parameters were identified that produced a relatively homogeneous polymer with the target pore size and consistent interconnect sizes. Shorter dosing times yielded irregular pore and interconnect structures, while, increasing the mixing time led to a clear reduction in the pore size. However, there is a limit to the amount of energy that could be supplied to the emulsion and further increases in the mixing time only had a small influence on reducing pore size. Chemically modifying polystyrene-DVB PHP by inclusion of vinyl pyridine (TVP) only had a minor influence on the pore and interconnect sizes and reduced the surface area slightly. However, the change and resulting reduction in hydrophobicity resulted in a 6-fold increase in the water uptake capacity compared to the unmodified polystyrene-DVB PHP. This confirmed that the physico-chemical characters of PHP can be modified as desired.

Chapter 6 extends the experimental work on the *in situ* incorporation of *B. subtilis* spores during the synthesis polystyrene-DVB PHP and vinyl-pyridine PHP matrices. These studies identified a number of problems and issues that, ultimately, limited the value of this approach. These limitations included ease of contamination, the failure of the polyHIPE emulsion to polymerize and the presence of residual un-reacted chemicals, as well as toxicity of isopropanol used to wash the polyHIPE. The vinyl-pyridine polyHIPE matrix had a higher spore germination rate compared with polystyrene-DVB PHP. This is likely to be due to

the fact that vinyl-pyridine PHP is more hydrophilic than polystyrene-DVB PHP. Consequently, vinyl-pyridine PHP was used in latter studies. A modification of the micro-chamber was needed to counter the accumulation of nutrient medium and cells within the spaces at the edges and the bottom of the matrices due to the difficulty of sealing these areas in the original microchamber.

Attempts to immobilise viable spores *in situ* during the synthesis of polystyrene-DVB PHP and vinyl pyridine PHP was of limited success, for the reasons outlined above. This led to the development of an immobilization technique in which pre-germinated spores were force-fed into a vinyl pyridine PHP (TVP) matrix sealed into a PTFE microchamber (Chapter 7). However, the vegetative cells were only found on the top surface of the TVP matrix and failed to penetrate deep into this type of polyHIPE. Nevertheless, this system demonstrated that the inoculation of pre-germinated spores was a viable alternative approach and many outgrowing cells were observed on the top surface of this matrix. Although vinyl pyridine polyHIPE matrix is more hydrophilic than polystyrene-divinylbenzen polyHIPE, it still restricted the diffusivity of fluid through the matrix. This suggested the need for an even more hydrophilic structure that was both highly permeable to fluid and biocompatible. Additionally, such a matrix needs to have optimal pore and interconnect sizes, not only for ease of substrate transport but also to allow the penetration of cells.

Chapter 8 discussed the use of polystyrene-DVB PHP modified by sulphonation to improve its hydrophilicity. Three different pore sizes of sulphonated polyHIPEs matrices (42.0±0.61μm, 36.0±0.50μm and 30.0±0.64 μm) were used. The sulphonated polyHIPE matrix with a pore size of 36μm was observed to give better cell growth, with cells penetrating throughout the matrix. As a result, this modified PHP provided a better matrix for bacterial cell growth, proliferation and penetration as well as improved α-amylase production.

The sulphonated PHP matrix was used to evaluate the affect on growth, cell release and α-amylase production of changing the concentration of the LB medium (0.5 dilution, 0.75 dilution and 2x) and the cell loading concentration (2 x 10^8/ml, 2 x 10^7/ml and 2 x 10^6/ml). In the case of the immobilized cell cultures, the best performing medium for the production of α-amylase was the original LB medium, while in the case of the planktonic cultures, the medium with double the

media components provide the highest enzyme yield. The volumetric productivity of immobilized cells per volume occupied by SPHP matrix was 7.6-fold higher than the planktonic batch cultures but its productivity was relatively low (<1) if determined on the basis of total volume of medium used.

Finally (Chapter 9) the effects of increasing the concentration of individual components of LB medium (Tryptone/NaCl/Yeast extract) were determined with respect to α-amylase production and the cell loss. The results indicated that doubling the yeast extract had a positive influence on α-amylase production by immobilized *B. subtilis* cells on the sulphonated polyHIPE matrix and planktonic batch culture. Doubling the concentration of tryptone has virtually no influence on productivity while doubling the NaCl concentration had a negative effect on enzyme productivity. Overall, the relative total α-amylase yield by the immobilized cell cultures was low compared to that on the planktonic cultures.

11 Future work

There are several issues with regards to polyHIPE matrix to be used as immobilised cells matrix and immobilized cells system with using this polymeric matrix that can be brought up as subjects for future work:

i. Chemical modification of polyHIPE in order to produce a matrix that allow strong attachment/interaction of cells to prevent washout of cells
ii. Modification of polyHIPE matrix that has a high surface area to allow more cells attach onto polyHIPE
iii. Optimize flow rate use to pumping nutrient medium to the microreactor to ensure appropriate flow rate applies on the immobilized cells system.
iv. Quantify the unused nutrient medium in the outlet stream thus this information will allow the determination of yield of product to substrate ($Y_{P/S}$)
v. Run a series of microreactors in order to increase the consumption of the supply nutrient media and conversion of substrate to product
vi. Prolong the continuous fermentation experiment to determine the life-span polyHIPE and immobilized cells

References:

Ahimou, F., Paquot, M., Jacques, P., Thonart, P. and Rouxhet, P. G. (2001) 'Influence of electrical properties on the evaluation of the surface hydrophobicity of *Bacillus subtilis*', *Journal of Microbiological Methods,* 45, (2), pp. 119-126.

Akay, G. (2005) 'Bioprocess and chemical process intensification', *Encyclopedia of Chemical Processing*, pp. 181-198.

Akay, G., Aydin, A. F., Calkan, O. F. and Noor, Z. Z. (2006) *CHISA 2006 - 17th International Congress of Chemical and Process Engineering.* Prague,

Akay, G., Birch, M. A. and Bokhari, M. A. (2004) 'Microcellular polyHIPE polymer supports osteoblast growth and bone formation in vitro', *Biomaterials,* 25, (18), pp. 3991-4000.

Akay, G., Birch, M. A., Bokhari, M. A., Byron, V. J., Erhan, E. and Keskinler, B. (2005a) *Sustainable (Bio)Chemical Process Technology - Incorporating the 6th Intenational Conference on Process Intensification.* Delft,

Akay, G., Bokhari, M., Byron, V. J. and Dogru, M. (2005b) 'Development of nano-structured materials and their application in bioprocess-chemical process intensification and tissue engineering', *Chemical Engineering Trends and Developments*, pp. 171-196.

Akay, G., Dawnes, S. and Price, V. J. (2002a) *Microcellular polymers as cell growth media and novel polymers*.

Akay, G., Dogru, M., Calkan, B. and Calkan, O. F. (2005c) 'Flow induced phase inversion phenomenon in process intensification and micro-reactor technology', *Microreactor Technology and Process Intensification*.

Akay, G., Downes, S. and Price, V. J. (2002b) *MICROCELLULAR POLYMERS AS CELL GROWTH MEDIA AND NOVEL POLYMERS*. EP1 183 328.

Akay, G., Erhan, E. and Keskinler, B. (2005d) 'Bioprocess intensification in flow-through monolithic microbioreactors with immobilized bacteria', *Biotechnology and Bioengineering,* 90, (2), pp. 180-190.

Alam, S., Hong, J. and Weigand, W. A. (1989) 'Effect of yeast extract on α-amylase synthesis by *Bacillus amyloliquefaciens*', *Biotechnology and Bioengineering,* 33, (6), pp. 780-785.

Antelmann, H., Tjalsma, H., Voigt, B., Ohlmeier, S., Bron, S., Van Dijl, J. M. and Hecker, M. (2001) 'A proteomic view on genome-based signal peptide predictions', *Genome Research,* 11, (9), pp. 1484-1502.

Argirakos, G., Thayanithy, K. and Wase, D. A. J. (1992) 'Effect of Immobilization on the Production of Alpha-Amylase by an Industrial Strain of *Bacillus-Amyloliquefaciens*', *Journal of Chemical Technology and Biotechnology,* 53, (1), pp. 33-38.

Barbetta, A., Carnachan, R. J., Smith, K. H., Zhao, C. T., Cameron, N. R., Kataky, R., Hayman, M., Przyborski, S. A. and Swan, M. (2005a) 'Porous polymers by emulsion templating', *Macromolecular Symposia,* 226, pp. 203-211.

Barbetta, A., Dentini, M., De Vecchis, M. S., Filippini, P., Formisano, G. and Caiazza, S. (2005b) 'Scaffolds based on biopolymeric foams', *Advanced Functional Materials,* 15, (1), pp. 118-124.

Baron, G. V. and Willaert, R. G. (2004) 'Cell Immobilization in Pre-formed Porous Matrices', in Nedovic, V. and Willaert, R.(eds) *Fundamentals of Cell Immobilization Biotechnlogy.* Springer: Belgium, pp. 229- 244.

Baudet, C., Barbotin, J. N. and Guespin Michel, J. (1983) 'Growth and sporulation of entrapped *Bacillus subtilis* cells', *Applied and Environmental Microbiology,* 45, (1), pp. 297-301.

Berlinger, A., Gliemann, H., Barczewski, M., Durigon, P. E. R., Petri, D. F. S. and Schimmel, T. (2001) 'Influence of sulphonation on polymer and polymer blend surfaces studied by atomic force microscopy', *Surface and Interface Analysis,* 32, pp. 144-147.

Bhumgara, Z. (1995a) 'Polyhipe foam materials as filtration media', *Filtration & Separation,* 32, (3), pp. 245-251.

Bhumgara, Z. (1995b) *A study of the development of polyHIPE foam materials for use in separation process.* thesis. Exeter University.

Bokhari, M., Birch, M. and Akay, G. (2003) 'Polyhipe polymer: a novel scaffold for in vitro bone tissue engineering', *Advances in experimental medicine and biology,* 534, pp. 247-254.

Bokhari, M., Carnachan, R. J., Cameron, N. R. and Przyborski, S. A. (2007a) 'Novel cell culture device enabling three-dimensional cell growth and improved cell function', *Biochemical and Biophysical Research Communications,* 354, (4), pp. 1095-1100.

Bokhari, M., Carnachan, R. J., Przyborski, S. A. and Cameron, N. R. (2007b) 'Emulsion-templated porous polymers as scaffolds for three dimensional cell culture: Effect of synthesis parameters on scaffold formation and homogeneity', *Journal of Materials Chemistry,* 17, (38), pp. 4088-4094.

Bokhari, M. A. (2003) *Bone tissue engineering using novel microcellular polymers.* thesis. University of Newcastle, Newcastle Upon Tyne, UK.

Bokhari, M. A., Akay, G., Zhang, S. and Birch, M. A. (2005) 'The enhancement of osteoblast growth and differentiation in vitro on a peptide hydrogel - polyHIPE polymer hybrid material ', *Journal of Biomaterials (Science Direct),* 26.

Bowen, W. R., Fenton, A. S., Lovitt, R. W. and Wright, C. J. (2002) 'The measurement of Bacillus mycoides spore adhesion using atomic force microscopy, simple counting methods, and a spinning disk technique', *Biotechnology and Bioengineering,* 79, (2), pp. 170-179.

Burdon, K. L. (1955) 'Useful criteria for the identification of *Bacillus Anthracis* and related species', 71, pp. 25-41.

Busby, W., Cameron, N. R. and Jahoda, C. A. B. (2001) 'Emulsion-derived foams (PolyHIPEs) containing poly(Sε-caprolactone) as matrixes for tissue engineering', *Biomacromolecules,* 2, (1), pp. 154-164.

Busby, W., Cameron, N. R. and Jahoda, C. A. B. (2002) 'Tissue engineering matrixes by emulsion templating', *Polymer International,* 51, (10), pp. 871-881.

Byron, V. J. (2000) *The development of microcellular polymers as support for tissue engineering.* thesis. University of Newcastle, Newcastle Upon Tyne, UK.

Cameron, N. R. (2005) 'High internal phase emulsion templating as a route to well-defined porous polymers', *Polymer,* 46, (5), pp. 1439-1449.

Cameron, N. R. and Barbetta, A. (2000) 'The influence of porogen type on the porosity, surface area and morphology of poly(divinylbenzene) polyHIPE foams', *Journal of Materials Chemistry,* 10, (11), pp. 2466-2471.

Cameron, N. R. and Sherrington, D. C. (1996) 'High Internal Phase Emulsions (HIPEs) - Structure, Properties and Use in Polymer Preparation', in *Advances in Polymer Science*. Vol. 126, pp. 162-214.

Cameron, N. R., Sherrington, D. C., Ando, I. and Kurosu, H. (1996) 'Chemical modification of monolithic poly(styrene-divinylbenzene) PolyHIPE® materials', *Journal of Materials Chemistry,* 6, (5), pp. 719-726.

Carnachan, R. J., Bokhari, M., Przyborski, S. A. and Cameron, N. R. (2006) 'Tailoring the morphology of emulsion-templated porous polymers', *Soft Matter,* 2, (7), pp. 608-616.

Castet, J., Craynest, M., Barbotin, J.-N. and Truffaut, N. (1994) 'Improvement of plasmid stability of recombinant *Bacillus-subtilis* cells in continuous immobilized cultures', *FEMS Microbiology Reviews,* 14, (1), pp. 63-67.

Chakravorty, B., Mukherjee, R. N. and Basu, S. (1989) 'Synthesis of ion-exchange membranes by radiation grafting', *Journal of Membrane Science,* 41, (C), pp. 155-161.

Chevalier, P. and De La Noue, J. (1987) 'Enhancement of α-amylase production by immobilized *Bacillus subtilis* in an airlift fermenter', *Enzyme and Microbial Technology,* 9, (1), pp. 53-56.

Christenson, E. M., Soofi, W., Holm, J. L., Cameron, N. R. and Mikos, A. G. (2007) 'Biodegradable fumarate-based polyHIPEs as tissue engineering scaffolds', *Biomacromolecules,* 8, (12), pp. 3806-3814.

Coleman, G. and Elliott, W. H. (1962) 'Studies on alpha-amylase formation by *Bacillus subtilis*', *The Biochemical journal,* 83, pp. 256-263.

Coleman, G. and Grant, M. A. (1966) 'Characteristics of α-amylase formation by *Bacillus subtilis* ', *Nature,* 211, pp. 306-307.

Cortezzo, D. E., Setlow, B. and Setlow, P. (2004) 'Analysis of the action of compounds that inhibit the germination of spores of *Bacillus* species', *Journal of Applied Microbiology,* 96, (4), pp. 725-741.

Cortezzo, D. E. and Setlow, P. (2005) 'Analysis of factors that influence the sensitivity of spores of Bacillus subtilis to DNA damaging chemicals', *Journal of Applied Microbiology,* 98, (3), pp. 606-617.

Dervakos, G. A. and Webb, C. (1991) 'On the merits of viable-cell immobilisation', *Biotechnology Advances,* 9, (4), pp. 559-612.

Dey, G., Mitra, A., Banerjee, R. and Maiti, B. R. (2001) 'Enhanced production of amylase by optimization of nutritional constituents using response surface methodology', *Biochemical Engineering Journal,* 7, (3), pp. 227-231.

Dharani Aiyer, P. V. (2004) 'Effect of C:N ratio on alpha amylase production by *Bacillus licheniformis* SPT 27', *African Journal of Biotechnology,* 3, (10), pp. 519-522.

Dizge, N., Aydiner, C., Imer, D. Y., Bayramoglu, M., Tanriseven, A. and Keskinler, B. (2009a) 'Biodiesel production from sunflower, soybean, and waste cooking oils by transesterification using lipase immobilized onto a novel microporous polymer', *Bioresource Technology,* 100, (6), pp. 1983-1991.

Dizge, N., Keskinler, B. and Tanriseven, A. (2009b) 'Biodiesel production from canola oil by using lipase immobilized onto hydrophobic microporous styrene-divinylbenzene copolymer', *Biochemical Engineering Journal*.

Dobreva, E., Tonkova, A., Ivanova, V., Stefanova, M., Kabaivanova, L. and Spasova, D. (1998) 'Immobilization of *Bacillus licheniformis* cells, producers of thermostable α-amylase, on polymer membranes', *Journal of Industrial Microbiology and Biotechnology,* 20, (3), pp. 166-170.

Dose, K. and Gill, M. (1995) 'DNA stability and survival of *Bacillus subtilis* spores in extreme dryness', *Origins of Life and Evolution of the Biosphere,* 25, (1-3), pp. 277-293.

Driks, A. (1999) 'Bacillus subtilis spore coat', *Microbiology and Molecular Biology Reviews,* 63, (1), pp. 1-20.

Driks, A. (2002b) 'Proteins of the spore core and coat', in Abraham L. Sonenshein, J. A. H., and Richard Losick (ed), *Bacillus Subtilis and Its Closest Relatives: From Genes to Cells* Washington, DC:American Society for Microbiology pp. 527 -535.

Duran-Paramo, E., Garcia-Kirchner, O., Hervagault, J. F., Thomas, D. and Barbotin, J. N. (2000) 'α-Amylase production by free and immobilized *Bacillus subtilis*', *Applied Biochemistry and Biotechnology - Part A Enzyme Engineering and Biotechnology,* 84-86, pp. 479-485.

El-Banna, T. E., Abd-Aziz, A. A., Abou-Dobara, M. I. and Ibrahim, R. I. (2007) 'Production and immobilization of α-amylase from *Bacillus subtilis*', *Pakistan Journal of Biological Sciences,* 10, (12), pp. 2039-2047.

Erhan, E., Yer, E., Akay, G., Keskinler, B. and Keskinler, D. (2004) 'Phenol degradation in a fixed-bed bioreactor using micro-cellular polymer-immobilized *Pseudomonas syringae*', *Journal of Chemical Technology and Biotechnology,* 79, (2), pp. 195-206.

Foster, S. J. and Johnstone, K. (1990) 'Pulling the trigger: The mechanism of bacterial spore germination', *Molecular Microbiology,* 4, (1), pp. 137-141.

Gitli, T. and Silverstein, M. S. (2008) 'Bicontinuous hydrogel-hydrophobic polymer systems through emulsion templated simultaneous polymerizations', *Soft Matter,* 4, (12), pp. 2475-2485.

Griffiths, M. S. and Bosley, J. A. (1993) 'Assessment of macroporous polystyrene-based polymers for the immobilization of *Citrobacter freundii*', *Enzyme and Microbial Technology,* 15, (2), pp. 109-113.

Guo, Y., Lou, F., Peng, Z. Y. and Yuan, Z. Y. (1990) 'Kinetics of growth and α-amylase production of immobilized *Bacillus subtilis i*n an airlift bioreactor', *Biotechnology and Bioengineering,* 35, (1), pp. 99-102.

Haibach, K., Menner, A., Powell, R. and Bismarck, A. (2006) 'Tailoring mechanical properties of highly porous polymer foams: Silica particle reinforced polymer foams via emulsion templating', *Polymer,* 47, (13), pp. 4513-4519.

Hainey, P., Huxham, I. M., Rowatt, B., Sherrington, D. C. and Tetley, L. (1991) 'Synthesis and ultrastructural studies of styrene-divinylbenzene polyhipe polymers', *Macromolecules,* 24, (1), pp. 117-121.

Haq, Z. Lever Brothers Company (New York, NY) (1985) *Porous cross-linked absorbent polymeric materials* 4536521.

Harwood, C. R. (1990) '*Bacillus* ', in Michael C. Flickinger, S. W. D.(ed), *Encyclopedia of Bioprocess Technology: Fermentation, Biocatalysis, and Bioseparation*John Wiley & Sons, Inc., pp. 243- 259.

Harwood, C. R. and Archibald, A. R. (1990) 'Growth, maintenance and general techniques', in Colin R. Harwood, S. M. C.(ed), *Molecular Biological Methods for Bacillus.* Wiley: Chichester : New York.

Harwood, C. R. and Cutting, S. M. (1990) *Molecular Biological Methods for Bacillus*
Wiley: Chichester : New York.

Hayes, C. S. and Setlow, P. (2001) 'Notes: An α/β-type, small, acid-soluble spore protein which has very high affinity for DNA prevents outgrowth of *Bacillus subtilis* spores', *Journal of Bacteriology,* 183, (8), pp. 2662-2666.

Hayman, M. W., Smith, K. H., Cameron, N. R. and Przyborski, S. A. (2004) 'Enhanced neurite outgrowth by human neurons grown on solid three-dimensional scaffolds', *Biochemical and Biophysical Research Communications,* 314, (2), pp. 483-488.

Hayman, M. W., Smith, K. H., Cameron, N. R. and Przyborski, S. A. (2005) 'Growth of human stem cell-derived neurons on solid three-dimensional polymers', *Journal of Biochemical and Biophysical Methods,* 62, (3), pp. 231-240.

Ishihara, Y., Takano, J., Mashimo, S. and Yamamura, M. (1994) 'Determination of the water necessary for survival of *Bacillus subtilis* vegetative cells and spores', *Thermochimica Acta,* 235, (2), pp. 153-160.

Ivanova, V., Stefanova, M., Tonkova, A., Dobreva, E. and Spassova, D. (1995) 'Screening of a growing cell immobilization procedure for the biosynthesis of thermostable α-amylases', *Applied Biochemistry and Biotechnology,* 50, (3), pp. 305-316.

Jeřábek, K., Pulko, I., Soukupova, K., Štefanec, D. and Krajnc, P. (2008) 'Porogenic solvents influence on morphology of 4-vinylbenzyl chloride based PolyHIPEs', *Macromolecules,* 41, (10), pp. 3543-3546.

Karagöz, P., Erhan, E., Keskinler, B. and Özkan, M. (2009) 'The use of microporous divinyl benzene copolymer for yeast cell immobilization and ethanol production in packed-bed reactor', *Applied Biochemistry and Biotechnology,* 152, (1), pp. 66-73.

Karel, S. F., Libicki, S. B. and Robertson, C. R. (1985a) 'Immobilization of whole cells: Engineering principles', *Chemical Engineering Science,* 40, (8), pp. 1321-1354.

Karel, S. F., Libicki, S. B. and Robertson, C. R. (1985b) 'Immobilization of whole cells:Engineering principles', *Chemical Engineering Science,* 40, (8), pp. 1321-1354.

Kempf, B. and Bremer, E. (1998) 'Uptake and synthesis of compatible solutes as microbial stress responses to high-osmolality environments', *Archives of Microbiology,* 170, (5), pp. 319-330.

Kinoshita, S., Okada, H. and Terui, G. (1968) 'On the nature of α-amylase forming system in *Bacillus subtilis*', *Fermentation Technology,* 46, pp. 427-436.

Kirk-Othmer. (2007) *Surfactants.* Wiley-Blackwell.

Kocher, G. S. and Mishra, S. (2010) 'Immobilization of *Bacillus circulans* MTCC 7906 for enhanced production of alkaline protease under batch and packed bed fermentation conditions', *Internet Journal of Microbiology,* 7, (2).

Kokubu, T., Karube, I. and Suzuki, S. (1978) 'α-Amylase production by immobilized whole cells of *Bacillus subtilis*', *European Journal of Applied Microbiology and Biotechnology,* 5, (4), pp. 233-240.

Konsoula, Z. and Liakopoulou-Kyriakides, M. (2006) 'Thermostable alpha-amylase production by *Bacillus subtilis* entrapped in calcium alginate gel capsules', *Enzyme and Microbial Technology,* 39, (4), pp. 690-696.

Kontinen, V. P., Saris, P. and Sarvas, M. (1991) 'A gene (prsA) of *Bacillus subtilis* involved in a novel, late stage of protein export', *Molecular Microbiology,* 5, (5), pp. 1273-1283.

Kontinen, V. P. and Sarvas, M. (1988) 'Mutants of *Bacillus subtilis* defective in protein export', *Journal of General Microbiology,* 134, pp. Pt 8/.

Kontinen, V. P. and Sarvas, M. (1993) 'The PrsA lipoprotein is essential for protein secretion in Bacillus subtilis and sets a limit for high-level secretion', *Molecular Microbiology,* 8, (4), pp. 727-737.

Koshikawa, T., Yamazaki, M., Yoshimi, M., Ogawa, S., Yamada, A., Watabe, K. and Torii, M. (1989) 'Surface hydrophobicity of spores of *Bacillus* spp', *Journal of General Microbiology,* 135, (10), pp. 2717-2722.

Krajnc, P., Leber, N., SÌŒtefanec, D., Kontrec, S. and Podgornik, A. (2005) 'Preparation and characterisation of poly(high internal phase emulsion) methacrylate monoliths and their application as separation media', *Journal of Chromatography A,* 1065, (1), pp. 69-73.

Kulygin, O. and Silverstein, M. S. (2007) 'Porous poly(2-hydroxyethyl methacrylate) hydrogels synthesized within high internal phase emulsions', *Soft Matter,* 3, (12), pp. 1525-1529.

Lamas, M. C., Bregni, C., D'Aquino, M., Degrossi, J. and Firenstein, R. (2001) 'Calcium alginate microspheres of *Bacillus subtilis*', *Drug Development and Industrial Pharmacy,* 27, (8), pp. 825-829.

Lazazzera, B. A. (2000) 'Quorum sensing and starvation: signals for entry into stationary phase', *Current Opinion in Microbiology,* 3, (2), pp. 177-182.

Lépine, O., Birot, M. and Deleuze, H. (2008) 'Influence of emulsification process on structure-properties relationship of highly concentrated reverse emulsion-derived materials', *Colloid and Polymer Science,* 286, (11), pp. 1273-1280.

Liu, S., Chan, C. M., Weng, L. T. and Jiang, M. (2005) 'Surface segregation in polymer blends and interpolymer complexes with increasing hydrogen bonding interactions', *Journal of Polymer Science, Part B: Polymer Physics,* 43, (14), pp. 1924-1930.

Livshin, S. and Silverstein, M. S. (2007) 'Crystallinity in cross-linked porous polymers from high internal phase emulsions', *Macromolecules,* 40, (17), pp. 6349-6354.

Livshin, S. and Silverstein, M. S. (2008a) 'Cross-linker flexibility in porous crystalline polymers synthesized from long side-chain monomers through emulsion templating', *Soft Matter,* 4, (8), pp. 1630-1638.

Livshin, S. and Silverstein, M. S. (2008b) 'Crystallinity and cross-linking in porous polymers synthesized from long side chain monomers through emulsion templating', *Macromolecules,* 41, (11), pp. 3930-3938.

Longo, M. A., Novella, I. S., Garcia, L. A. and Diaz, M. (1999) 'Comparison of *Bacillus subtilis* and *Serratia marcescens* as protease producers under different operating conditions', *Journal of Bioscience and Bioengineering,* 88, (1), pp. 35-40.

Maldonado-Santoyo, M., Cesteros, L. C., Katime, I. and Nuno-Donlucas, S. M. (2004) 'Miscible blends of poly(vinyl phenyl ketone hydrogenated) and poly(styrene-co-4-vinylpyridine)', *Polymer,* 45, (16), pp. 5591-5596.

Mamo, G. and Gessesse, A. (1997) 'Thermostable amylase production by immobilized thermophilic *Bacillus* sp', *Biotechnology Techniques,* 11, (6), pp. 447-450.

Margaritis, A. and Kilonzo, P. M. (2005) 'Production of Ethanol Using Immobilized Cell Bioreactor Systems', in Nedovic, V. and Willaert, R.(eds) *Applications of Cell Immobilization Biotechnology.* Springer: Netherlands, pp. 375-405.

Menner, A., Haibach, K., Powell, R. and Bismarck, A. (2006a) 'Tough reinforced open porous polymer foams via concentrated emulsion templating', *Polymer,* 47, (22), pp. 7628-7635.

Menner, A., Powell, R. and Bismarck, A. (2006b) 'A new route to carbon black filled polyHIPEs', *Soft Matter,* 2, (4), pp. 337-342.

Millar, J. R., Smith, D. G., Marr, W. E. and Kressman, T. R. E. (1963) 'Solvent-modified polymer networks. Part I. The preparation and characterisation of expanded-network and macroporous styrene-divinylbenzene copolymers and their sulphonates', *Journal of the Chemical Society (Resumed)*, pp. 218-225.

Moir, A., Corfe, B. M. and Behravan, J. (2002) 'Spore germination', *Cellular and Molecular Life Sciences,* 59, (3), pp. 403-409.

Nicholson, W. L. and Setlow, P. (1990a) 'Molecular Biological Methods for *Bacillus*', in Colin R. Harwood, S. M. C.(ed), *Molecular Biological Methods for Bacillus.* Wiley: Chichester: New York.

Nicholson, W. l. and Setlow, P. (1990b) 'Sporulation, germination and outgrowth', in Colin R. Harwood, S. M. C.(ed), *Molecular Biological Methods for Bacillus.* Wiley: Chichester : New York.

Noor, Z., Dogru, M., Akay, G. and Larter, S. R. (2005) *7th World Congress of Chemical Engineering, GLASGOW2005, incorporating the 5th European Congress of Chemical Engineering.* Glasgow, Scotland,

Noor, Z. Z. (2006) *Intensification of separation processes using functionalised polyHIPE polymer.* thesis. University of Newcastle, Newcastle Upon Tyne, UK.

Normatov, J. and Silverstein, M. S. (2007) 'Porous interpenetrating network hybrids synthesized within high internal phase emulsions', *Polymer,* 48, (22), pp. 6648-6655.

Ohlson, S., Flygare, S., Larsson, P.-O. and Mosbach, K. (1980) 'Steroid hydroxylation using immobilized spores of Curvularia lunata germinated in situ', *Applied Microbiology and Biotechnology,* 10, (1), pp. 1-9.

Paidhungat, M., Setlow, B., Daniels, W. B., Hoover, D., Papafragkou, E. and Setlow, P. (2002) 'Mechanisms of induction of germination of *Bacillus subtilis* spores by high pressure', *Applied and Environmental Microbiology,* 68, (6), pp. 3172-3175.

Paidhungat, M. and Setlow, P. (2001) 'Localization of a germinant receptor protein (GerBA) to the inner membrane of *Bacillus subtilis* spores', *Journal of Bacteriology,* 183, (13), pp. 3982-3990.

Paidhungat, M. and Setlow, P. (2002) 'Spore Germination and Outgrowth', in Sonenshein, A. L., Hoch, J. and Losick, R.(eds) *Bacillus subtilis and its Closest Relatives: from Genes to Cells.* ASM Press: Washington D.C, pp. 537-549.

Palva, I. (1982) 'Molecular cloning of α-amylase gene from Bacillus amyloliquefaciens and its expression in B. subtilis', *Gene,* 19, (1), pp. 81-87.

Parker, M. S. (1969) 'Some effects of preservatives on the development of bacterial spores', *Journal of Applied Bacteriology,* 32, (3), pp. 322-328.

Pedersen, H. and Nielsen, J. (2000) 'The influence of nitrogen sources on the α-amylase productivity of Aspergillus oryzae in continuous cultures', *Applied Microbiology and Biotechnology,* 53, (3), pp. 278-281.

Perego, P., Converti, A. and Del Borghi, M. (2003) 'Effects of temperature, inoculum size and starch hydrolyzate concentration on butanediol production by Bacillus licheniformis', *Bioresource Technology,* 89, (2), pp. 125-131.

Piggot, P. J. and Hilbert, D. W. (2004) 'Sporulation of *Bacillus subtilis*', *Current Opinion in Microbiology,* 7, (6), pp. 579-586.

Popham, D. L. (2002) 'Specialized peptidoglycan of the bacterial endospore: The inner wall of the lockbox', *Cellular and Molecular Life Sciences,* 59, (3), pp. 426-433.

Prescott, L. M., Harley, J. P. and Klein, D. A. (2004) *Microbiology.* McGraw-Hill Higher Education.

Ramakrishna, S. V., Jamuna, R. and Emery, A. N. (1992) 'Continuous Production of Thermostable α-Amylase by Immobilized *Bacillus* Cells in a Fluidized-Bed Reactor', *Applied Biochemistry and Biotechnology,* 37, (3), pp. 275-282.

Riddle, K. W. and Mooney, D. J. (2004) 'Biomaterials for Cell Immobilization', in Nedovic, V. and Willaert, R.(eds) *Fundamentals of Cell Immobilization Biotechnlogy.* Springer: Belgium, pp. 15-32.

Ronner, U., Husmark, U. and Henriksson, A. (1990) 'Adhesion of *bacillus* spores in relation to hydrophobicity', *Journal of Applied Bacteriology,* 69, (4), pp. 550-556.

Rosenberg, M. (1984) 'Bacterial adherence to hydrocarbons: A useful technique for studying cell surface hydrophobicity', *FEMS Microbiology Letters,* 22, (3), pp. 289-295.

Rosenberg, M., Gutnick, D. and Rosenberg, E. (1980) 'Adherence of bacteria to hydrocarbons: A simple method for measuring cell-surface hydrophobicity', *FEMS Microbiology Letters,* 9, (1), pp. 29-33.

Ryan, S. M., Fitzgerald, G. F. and Van Sinderen, D. (2006) 'Screening for and identification of starch-, amylopectin-, and pullulan-degrading activities in bifidobacterial strains', *Applied and Environmental Microbiology,* 72, (8), pp. 5289-5296.

Saito, N. and Yamamoto, K. (1975) 'Regulatory factors affecting α- amylase production in *Bacillus licheniformis*', *Journal of Bacteriology,* 121, (3), pp. 848-856.

Santos, E. D. O. and Martins, M. L. L. (2003) 'Effect of the medium composition on formation of amylase by *Bacillus* sp', *Brazilian Archives of Biology and Technology,* 46, (1), pp. 129-134.

Scragg, A. H. (1991) 'Batch and continuous growth', in Scragg, A. H.(ed), *Bioreactors in Biotechnology: a practical approach.* Ellis Horwood Limited: Chichester, West Sussex, England, pp. 45.

Sergienko, A. Y., Tai, H., Narkis, M. and Silverstein, M. S. (2002) 'Polymerized high internal-phase emulsions: Properties and interaction with water', *Journal of Applied Polymer Science,* 84, (11), pp. 2018-2027.

Sergienko, A. Y., Tai, H., Narkis, M. and Silverstein, M. S. (2004) 'Polymerized high internal phase emulsions containing a porogen: Specific surface area and sorption', *Journal of Applied Polymer Science,* 94, (5), pp. 2233-2239.

Setlow, B., Loshon, C. A., Genest, P. C., Cowan, A. E., Setlow, C. and Setlow, P. (2002) 'Mechanisms of killing spores of *Bacillus subtilis* by acid, alkali and ethanol', *Journal of Applied Microbiology,* 92, (2), pp. 362-375.

Setlow, B., McGinnis, K. A., Ragkousi, K. and Setlow, P. (2000) 'Effects of major spore-specific DNA binding proteins on Bacillus subtilis sporulation and spore properties', *Journal of Bacteriology,* 182, (24), pp. 6906-6912.

Setlow, P. (2002b) 'Spore germination and outgrowth', in Abraham L. Sonenshein, J. A. H., and Richard Losick (ed), *Bacillus Subtilis and Its Closest Relatives: From Genes to Cells.* Washington, DC:American Society for Microbiology, pp. 537-549.

Setlow, P. (2003) 'Spore germination', *Current Opinion in Microbiology,* 6, (6), pp. 550-556.

Setlow, P. (2006) 'Spores of *Bacillus subtilis*: Their resistance to and killing by radiation, heat and chemicals', *Journal of Applied Microbiology,* 101, (3), pp. 514-525.

Shinmyo, A., Kimura, H. and Okada, H. (1982) 'Physiology of α-amylase production by immobilized *Bacillus amyloliquefaciens*', *European Journal of Applied Microbiology and Biotechnology,* 14, (1), pp. 7-12.

Shuler, M. L. and Kargi, F. (2001) *Bioprocess Engineering: Basic Concepts.* Prentice Hall PTR.

Silverstein, M. S., Tai, H., Sergienko, A., Lumelsky, Y. and Pavlovsky, S. (2005) 'PolyHIPE: IPNs, hybrids, nanoscale porosity, silica monoliths and ICP-based sensors', *Polymer,* 46, (17), pp. 6682-6694.

Sonomoto, K., Hoq, M. M., Tanaka, A. and Fukui, S. (1981) 'Growth of *Curvularia lunata* spores into Mycelial from within various gels, and steroid 11β-Hydroxylation by the entrapped mycelia', *Fermentation Technology,* 59, (6), pp. 465-469.

Sonomoto, K., Hoq, M. M., Tanaka, A. and Fukui, S. (1983) '11β-Hydroxylation of cortexolone (Reichstein compound S) to hydrocortisone by *Curvularia lunata* entrapped in photo-cross-linked resin gels', *Applied and Environmental Microbiology,* 45, (2), pp. 436-443.

Stefanec, D. and Krajnc, P. (2005) '4-Vinylbenzyl chloride based porous spherical polymer supports derived from water-in-oil-in-water emulsions', *Reactive and Functional Polymers,* 65, (1-2), pp. 37-45.

Szczesna-Antczak, M., Antczak, T. and Bielecki, S. (2004) 'Stability of extracellular proteinase productivity by Bacillus subtilis cells immobilized in PVA-cryogel', *Enzyme and Microbial Technology,* 34, (2), pp. 168-176.

Szczesna-Antczak, M., Galas, E. and Bielecki, S. (2001) 'PVA-biocatalyst with entrapped viable Bacillus subtilis cells', *Journal of Molecular Catalysis - B Enzymatic,* 11, (4-6), pp. 671-676.

Tai, H., Sergienko, A. and Silverstein, M. S. (2001) 'High internal phase emulsion foams: Copolymers and interpenetrating polymer networks', *Polymer Engineering and Science,* 41, (9), pp. 1540-1552.

Thaler, W. A. (1983) 'Hydrocarbon-soluble sulfonating reagents. Sulfonation of aromatic polymers in hydrocarbon solution using soluble acyl sulfates', *Macromolecules,* 16, (4), pp. 623-628.

Thwaite, J. E., Laws, T. R., Atkins, T. P. and Atkins, H. S. (2009) 'Differential cell surface properties of vegetative *Bacillus*', *Letters in Applied Microbiology,* 48, (3), pp. 373-378.

Tjalsma, H., Kontinen, V. P., Pragai, Z., Wu, H., Meima, R., Venema, G., Bron, S., Sarvas, M. and Van Dijl, J. M. (1999) 'The role of lipoprotein processing by signal peptidase II in the gram- positive eubacterium *Bacillus subtilis*. Signal peptidase II is required for the efficient secretion of α-amylase, a non-lipoprotein', *Journal of Biological Chemistry,* 274, (3), pp. 1698-1707.

Tonkova, A., Ivanova, V., Dobreva, E., Stefanova, M. and Spasova, D. (1994) 'Thermostable α-amylase production by immobilized *Bacillus licheniformis* cells in agar gel and on acrylonitrile/acrylamide membranes', *Applied Microbiology and Biotechnology,* 41, (5), pp. 517-522.

Trujillo, R. and Laible, N. (1970) 'Reversible inhibition of spore germination by alcohols', *Applied microbiology,* 20, (4), pp. 620-623.

Vieira Grossi, C., de Oliveira Jardim, E., de Araújo, M. H., Lago, R. M. and da Silva, M. J. (2010) 'Sulfonated polystyrene: A catalyst with acid and superabsorbent properties for the esterification of fatty acids', *Fuel,* 89, (1), pp. 257-259.

Vitikainen, M., Pummi, T., Airaksinen, U., Wahlstrom, E., Wu, H., Sarvas, M. and Kontinen, V. P. (2001) 'Quantitation of the capacity of the secretion apparatus and requirement for PrsA in growth and secretion of α-amylase in *Bacillus subtilis*', *Journal of Bacteriology,* 183, (6), pp. 1881-1890.

Wahlstrom, E., Vitikainen, M., Kontinen, V. P. and Sarvas, M. (2003) 'The extracytoplasmic folding factor PrsA is required for protein secretion only in the presence of the cell wall in *Bacillus subtilis*', *Microbiology,* 149, (3), pp. 569-577.

Walsh, D. C., Stenhouse, J. I. T., Kingsbury, L. P. and Webster, E. J. (1996) 'PolyHIPE foams: Production, characterisation, and performance as aerosol filtration materials', *Journal of Aerosol Science,* 27, pp. 629-630.

Warth, A. D. (1978) 'Molecular structure of the bacterial spore', *Advances in Microbial Physiology,* 17, pp. 1-45.

Wei, P., Chen, J., Lu, Y., Liang, X., Chen, H. and Xu, Z. (2010) 'High density cultivation of *Dictyostelium discoideum* in a rotating polyurethane foam-bed bioreactor', *World Journal of Microbiology and Biotechnology,* 26, (6), pp. 1117-1123.

Williams, J. M., James Gray, A. and Wilkerson, M. H. (1990) 'Emulsion stability and rigid foams from styrene or divinylbenzene water-in-oil emulsions', *Langmuir,* 6, (2), pp. 437-444.

Williams, J. M. and Wrobleski, D. A. (1988) 'Spatial distribution of the phases in water-in-oil emulsions. Open and closed microcellular foams from cross-linked polystyrene', *Langmuir,* 4, (3), pp. 656-662.

Wood, J. M. (1999) 'Osmosensing by bacteria: Signals and membrane-based sensors', *Microbiology and Molecular Biology Reviews,* 63, (1), pp. 230-262.

Yang, Y., Biedendieck, R., Wang, W., Gamer, M., Malten, M., Jahn, D. and Deckwer, W. D. (2006) 'High yield recombinant penicillin G amidase production and export into the growth medium using *Bacillus megaterium*', *Microbial Cell Factories,* 5.

Yasuda-Yasaki, Y., Namiki-Kanie, S. and Hachisuka, Y. (1978) 'Inhibition of *Bacillus subtilis* spore germination by various hydrophobic compounds: demonstration of hydrophobic character of the L-alanine receptor site', *Journal of Bacteriology,* 136, (2), pp. 484-490.

Yoo, Y. J., Cadman, T. W., Hong, J. and Hatch, R. T. (1988) 'Kinetics of alpha - amylase synthesis from *Bacillus Amyloliquefaciens*', *Biotechnology and Bioengineering,* 31, (4), pp. 357-365.